THE UNIVERSITY OF MICHIGAN
COLLEGE OF LITERATURE, SCIENCE, AND THE ARTS
Department of Communication Sciences

Technical Report

AN EXPERIMENTAL STUDY OF THE FORMATION AND DEVELOPMENT OF HEBBIAN CELL-ASSEMBLIES BY MEANS OF A NEURAL NETWORK SIMULATION

Marion Finley, Jr.

ORA Project 08333

supported by:

DEPARTMENT OF HEALTH, EDUCATION, AND WELFARE
PUBLIC HEALTH SERVICE
NATIONAL INSTITUTES OF HEALTH
GRANT NO. GM-12236-03
BETHESDA, MARYLAND

administered through:

OFFICE OF RESEARCH ADMINISTRATION ANN ARBOR

March 1967

This report was also a dissertation submitted in partial fulfillment of the requirements for the degree of Doctor of Philosophy in The University of Michigan, 1967.

ACKNOWLEDGEMENTS

I first of all wish to express my profound gratitude to Professors John H. Holland and J. W. Crichton for virtually constant moral support and technical assistance. It was Professor Holland who stimulated me into developing the basic steady-state calculus of Chapter 4 and Professor Crichton who assisted me in much of the arduous programming involved. Moreover, Professor Crichton, by his deep knowledge of the Aristotelian writings on the intellect, added a dimension to my understanding that previously had been lacking.

To Professor Edward L Walker I am indebted for my first contact with neurophysiology. To Professor Anatol Rapoport I owe much of my early interest in neural networks, leading to this particular study. Finally, to Professor Henry H. Swain, I am grateful for what appears to be a genuine and enthusiastic interest in a scientific study such as this.

It would be a gross injustic not to mention my feelings of gratitude and appreciation to Professor Arthur W. Burks for his many good and wise counsels as well as his active financial patronage of my research conducted at the Logic of Computers Group. To the members and staff of that worthy group I extend my cordial appreciations, especially to Mrs. Kuniko Misawa, whose excellent handiwork is displayed herein.

This work was supported by the National Institutes of Health while I was with the Logic of Computers Group at the University of Michigan. I am particularly grateful to the National Institutes of Health for their generous allocation of funds for computer time.

Finally, mere words cannot express my admiration for my wife, Lorol, for bearing with me through the often discouraging days of this work.

TABLE OF CONTENTS

TABLE OF CONTENTS (Continued)

TABLE OF CONTENTS (Concluded)

LIST OF FIGURES

LIST OF FIGURES (Continued)

LIST OF FIGURES (Continued)

LIST OF FIGURES (Concluded)

LIST OF TABLES

ABSTRACT

The primary objective of this study is to derive a structural and dynamic characterization of Hebbian cell-assemblies in terms of a particular class of models of neural networks $\mathfrak{N}$. Within these models, Hebb's postulate of synapse-growth occupies a pivotal position. The networks of the given class of models may, together with any appropriate environments, be simulated by means of a digital computer program. Consequently, hypotheses about the behavior of such networks can be subjected to a rigorous test. The simulated networks, then, are to be used to test the formation and development of cell-assemblies. The advantages of the simulation are two-fold: (1) in some cases, it allows difficult mathematical calculations to be by-passed (e.g., the distance-bias case below); (2) it allows "rolling-back" (via use of auxiliary storage devices such as disk, magnetic tape, etc.) to an earlier point in an experiment, modifying some parameter, then continuing from that point on.

A number of subsidiary goals immediately became apparent, however. First of all, it was found necessary to characterize stable, steady-state behavior of a network $\mathfrak{N}$. Next, the role of negative connections in such a network needed clarification. Finally, the problem of guaranteeing localization of certain neural events arose.

To meet these goals, a steady-state stability calculus relating the essential network parameters N (number of neurons in $\mathfrak{N}$), the threshold curve, and ρ (density of connections in $\mathfrak{N}$) was worked out. This was done first for the case that positive equal connections only are present in $\mathfrak{N}$. This calculus was then modified to include the case that positive and negative connections (inhibitory connections) are present in $\mathfrak{N}$. The inhibitory connections are shown quantitatively to be essential to ensure

the negative feedback necessary to sustain steady-state. Again, relationships for the "mix" of positive versus negative connections and the relationship of these quantities to the threshold curve are given.

Finally, modification of this calculus to include a distance-bias on the connection density ρ was considered. Unfortunately, even for the relatively simple distance-bias selected, the calculations are quite difficult. It was found, however, that calculations from the preceding case (distance-bias absent) could be used as crude initial approximations.

A series of experiments were performed (using the above calculations as a guide in setting the network parameters) with networks of progressively greater complexity. A number of stable networks are exhibited. Then, using one of these stable networks with $N = 400$, $\rho = 55$ (this ρ decomposible into positive and negative components), $R = 6$ (distance-bias radius), simple closed cycles (candidates for cell-assemblies) were formed as a consequence of appropriate training stimuli. An imbalance in the fatigue mechanism of the model was uncovered at this point. This was corrected adequately in the current work, but points to the need for modifying the steady-state calculus to include this mechanism. In the concluding experiment, an embryonic cross-inhibiting pair of such closed cycles was formed by applying alternating periodic stimuli to two disjoint input areas of $\mathcal{M}$.

Hebb's basic theory (especially the synapse-growth law) is thus vindicated in terms of the given models. There certainly appears to be every reason to expect the more advanced portions of his theory (e.g. phase sequences) to be put to the test using the larger and faster computer hardware emerging today.

1. INTRODUCTION

1.1 STATEMENT OF THE PROBLEM

A class of models of neural networks is given purporting to represent, admittedly in an approximate fashion, a fragment of the mammalian cortex. A model may be visualized in an environment together with appropriate sensory and motor apparati. This allows, for example, detection of objects and movement in the environment. The main problem is to determine whether the models presented have the capacity to learn, in the sense that, as a consequence of feedback from the environment to the model, certain internal changes occur in the model with a resulting (eventual) improvement in behavior.

The given class of neural network models has at least one distinctive feature: it is interpreted directly into a computer program. This results in a rigorous expression of (the particular interpretation of) the class of models, from which any specific model is obtained merely by specification of certain parameters. Inasmuch as any program is a formal expression of certain formal operations, analogous to the specification of a list of functions used in the definition of partial recursive functions, some of the advantages found in the study of formal systems are present. On the other hand, there also is the advantage that any analytically derived property of the models may be subjected to a well-defined test in the interpretation afforded by the computer program.

Because of the relative ease with which operations of the models are interpreted into sets of digital computer operations, the computer simulation of such models is lifted out of the realm of a mere programming application. In a sense, the program itself is a model. Study it

— i.e., its behavior — and you are studying the model.

1.2 BASIC PREMISES AND THEORY: RELATION TO NEUROPHYSIOLOGICAL FACT

The original source for the specification of this class of neural net models and of the neural as well as behavioral processes involved in learning stems back to the theory which was developed by D. O. Hebb [9], later modified somewhat by P. M. Milner [10]. The theory, which integrates knowledge of neural events, taking place in time intervals of up to a hundred milliseconds or so, with behavioral events, taking place in time intervals of seconds on up, has as its basis the proposed mechanism of the cell-assembly. Informally characterized, this is a system of cortical (association layer) neurons which are capable of acting as a closed autonomous functional unit for a brief period of time. These neurons are anatomically diffuse, but functionally connected. The functional unity of the cell-assembly results from the initial existence of proper inter-connections among the neurons of the system together with a particular (i.e., selective) sequence of cortical events forcing these neurons to act briefly as a unit. This, in turn, results in a growth of synaptic strength at the connections such that after a period of time the assembly may be activated by appropriate excitatory stimuli.

The cell-assembly is a hypothetical structure; its physiological existence has not been demonstrated — on the other hand, the concept does not conflict with current neurophysiological knowledge. Moreover, the formation of a cell-assembly rests upon three main premises: (a) the initial existence of the proper inter-connections among the neurons of the system, (b) an initial selective sequence of cortical events that forces the neurons of the system to act briefly as a unit, and (c) a law of growth in

synaptic strength between neurons. This latter premise is taken by Hebb as his basic neurophysiological premise. Stated more fully, it reads:

> When an axion of cell A is near enough to excite cell B and repeatedly or persistently takes part in firing it, some growth process or metabolic change takes place in one or both cells such that A's efficiency as one of the cells firing B, is increased [9].

While there is evidence that is very suggestive, the validity of this hypothesis has not yet been demonstrated neurophysiologically; again, it does not conflict with known properties of neurons. It was conclusively demonstrated shortly after the appearance of Hebb's book (for example, Eccles [6]) that some neurons send out inhibitory as well as excitatory connections. Milner [10] argues effectively for the inclusion of inhibitory connections, subject to the same synapse growth law (c) and his suggestion is adopted here.

It should be noted here, that many properties of cortical neurons are inferred from the known properties of peripheral neurons. There seems to be no reason, at this time at least, for not doing this as it may be some time before techniques are evolved allowing the fine, detailed study on the cortical neuron that has been carried out on neurons in the spinal ganglia, etc. This is obviously one area where new knowledge will be of the greatest interest in the study of models such as the one developed here.

There is one other premise which, although not explicit in the above formulation of the cell-assemply, is in some respects the most important of all. That is that the system of neurons under consideration be sufficiently large and the inter-connections among these neurons be sufficiently dense such that the probabilities of existence of "the proper inter-connections" in premise (a) above be of a magnitude such that cell-assemblies may actually come into existence. Here the evidence from neuro-

anatomy is encouraging: the human cortex has of the order of 10^{10} neurons; (peripheral) neurons have been observed with approximately 1500 synaptic endings on them (i.e., 1500 input lines). Moreover, a given cortical neuron (association layer) seems to send out connections to all points in the spherical region surrounding it with radius approximately one millimeter.

Hebb's theory is in some respects a stimulus-response theory, where "response" does not necessarily mean immediate (muscular) response. This is reflected most strongly in premise (b), where the "initial selective sequence of cortical events" refers to the "priming" of the initial skeletal pathway assumed in (a) by massive "training" stimuli together with the stimulus which alone is to activate the assembly later on. The massive "training" stimuli may result from a sensation, e.g., hunger, from some environmental feedback, the action of other, already established assemblies, etc.

Referring back to the statement of the problem given above, the main problem then reduces to that of testing the role of the cell-assembly in learning — i.e., Hebb's theory — via the digital computer simulation of the models involved. One of the objects of this study is to give — in terms of the model — a precise characterization of the formation and development of cell assemblies in some rudimentary learning process. It is hoped that this will serve as the basis of a more detailed and profound study in the future. It will be seen, however, that just to achieve this modest goal, several fundamentally difficult problems must be solved.

A final observation on the character of cell-assemblies and phase sequences of cell-assemblies is in order: That is, that they allow one

to discuss learning and associated problems at a "molar" level (as Hebb puts it) — i.e., in terms of aggregates of neurons, their statistical properties, etc. — just as, for example, in statistical mechanics one works with aggregates of point masses, with little if any attention being paid to the individual bodies of the system.

1.3 THE CORTICAL NEURON AND SYSTEMS OF CORTICAL NEURONS

The advent of the micro-electrode and associated probing techniques in the last fifteen years have allowed physiologists to determine electrical properties of neurons from direct inter-cellular readings. Consequently, a wealth of knowledge has been gained about the electrical behavior of neurons, axonal propagation of pulses, etc. Most of this knowledge has been gleaned from studies on non-cortical neurons, e.g., neurons in the spinal ganglia, etc. A good, though slightly outdated, account of this is given in Eccles [6]. It is assumed that the properties of non-cortical neurons carry over to those of the cortex. Histologically, the cortical neuron is a neuron; while direct electrical studies on the cortex are hard to interpret, they tend to support this assumption.

It is manifestly impossible to simulate the real neuron in all its complexity. In fact, even if it were possible to do so, it would probably be unnecessary, as some of the properties of the neuron most likely are unessential to the problem at hand. As in any science, simplifying assumptions have to be made, albeit with great care, while trying to retain the most essential properties of the object described. The neuron to be simulated in this study is described in the following sections.

1.3.1 Structure

The gross-structure of the physiological neuron is as follows.

The main part of the organ is the cell body or soma, S, which sends out one fiber called the axon, A, which may later branch out quite profusely. A number of axons from other cells impinge on the soma of the body, sometimes on extensions of the soma — which often are quite profuse — called the dendrites, of the given cell. The point of contact of an incoming (afferent) axon with the soma or dendrites is the synapse and is usually characterized by a nodal swelling or button-like ending. There is a very narrow gap between this ending and the cell body, called the synaptic gap. Neurons have been observed with of the order of 1500 synaptic endings on their soma. A given incoming axon may make contact several times with a given soma. The afferent or incoming axons are, in effect, input lines; the axon sent out from the soma, an output line. Thus the neuron is a multiple input, single output device.

There are neurons of different structure than this, but their use in the nervous system seems to be specialized and not of relevance here (e.g., bipolar neurons in the optic nerve). It should be noted that in the cortex there are neurons with very complex dendritic branching and small — if any — axons as well as neurons with dendritic branching and quite long axons.

1.3.2 Input and Output, Threshold

The axon of a neuron is capable of transmitting a pulse of electric potential (called the action potential) with no significant decrease in amplitude throughout its length. The pulse originates in the soma of the nerve cell as a consequence of input-pulses on the incoming fibers (synapses) to the cell and spreads down the cell's axon to its various endings. A cell is said to fire when it sends out such a pulse.

The neuron (and its axon) is a threshold device: As a result of summation of its inputs (at the synapses), depending on the length of the time interval since the last firing, it either fires completely or not at all. "Firing completely" means that the amplitude of the outgoing pulse is independent of the magnitude of the input pulses.

The total input to the cell at a given time is determined by the number of impulses present at the synapses at that time and the level of activity (recall hypothesis (c), 1.2 above) at these synapses. Actually summation of this potential activity over a brief interval of time probably takes place. The inputs thus sum, in a fashion as yet unknow, spatially and temporally. In the model, the inputs (see below) are added. If the summed stimuli exceed the threshold at that time, the neuron fires — if not, it does not fire.

Once the neuron fires, it cannot be made to fire again for a period of time called the absolute refractory period. After that period of time, it maintains a high threshold which gradually decreases to its quiescent or resting value. The time interval, after the absolute refractory period, required for recovery to the quiescent state is called the relative refractory period. Thus, the neuron has the following threshold characteristic:

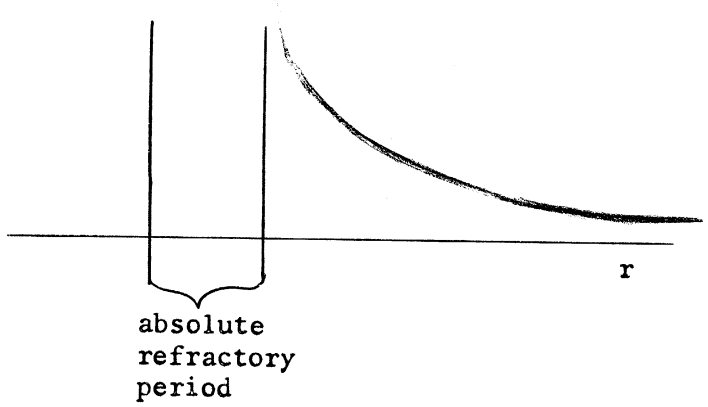

The time interval since the last firing of the neuron is called the recovery state.

In the model, time is quantized, t = 0, 1, 2, ... where a unit of time corresponds approximately to one millisecond. A neuron fires at time t + 1 depending upon

(1) whether it fired at time t. If it did, then it cannot be made to fire until time t + k, where k, a positive integer and a parameter of the system, represents the absolute refractory period.

(2) whether the sum of the inputs exceeds the threhold at time t + 1. If so, it fires at t + 1; otherwise it remains refractory.

(3) a spontaneous firing mechanism which is explained below.

1.3.3 Synapses

The exact nature of transmission across the synaptic gap and summation of the incoming pulses is as yet unknown. Here, it is assumed that each input line has an associated synapse level, λ. This synapse level in turn is used to determine the synapse value, $S(\lambda)$, for that line, usually by a table giving the value of $S(\lambda)$ for each value of λ. If there are n active input lines, then the total input at time t is $\sum_{i=1}^{n} S_i(t)$ where $S_i(t)$ is the synapse value corresponding to the i-th line at time t. Notice that in general there will be negative values of the synapse values: these correspond to inhibitory connections.

According to the hypothesis (c), Section 1.2, the synapse levels are subject to a synapse-growth law as follows: suppose there is a synapse from neuron A to neuron B — i.e., neuron A sends, via its axon, one connection to neuron B. Then, if A fires at time t and B fires at t + 1,

the synapse level from A to B, λ_{AB}, is increased by a uniform amount $\delta\lambda$. If A fires at t and B does not fire at t + 1, λ_{AB} is decreased by $\delta\lambda$; otherwise no change in λ_{AB} is made: symbolically,

$$A(t) \;\&\; B(t+1) \Longrightarrow \lambda_{AB} \rightarrow \lambda_{AB} + \delta\lambda$$

$$A(t) \;\&\; \overline{B(t+1)} \Longrightarrow \lambda_{AB} \rightarrow \lambda_{AB} - \delta\lambda$$

λ ranges in value from 0 to a maximum. In addition to the law stated above, there is a probabilistic mechanism in the model that serves to "slow down" the λ change. Essentially, if λ is to be changed (i.e., either A(t) & B(t+1) or A(t) & $\overline{B(t+1)}$), then a probability particular to that level is consulted: if it exceeds a certain amount, then the change takes place, otherwise no change occurs. This mechanism can be used to bias the direction of synapse-level change.

1.3.4 Fatigue, Spontaneous Firing

In addition to the threshold function, there is a long term mechanism which delays full-recovery, called fatigue. The evidence for this from neuro-physiology, in the case of peripheral neurons, is fairly definite. The fatigue function and its implementation will be discussed at length in a later chapter. The effect of fatigue is one of the subgoals of this study, as is that of spontaneous firing. There is also fairly good evidence that cortical neurons fire spontaneously (see, for example, Sharpless, S. K. and Halpern, L. M. [12]). In the model this is defined as follows: if the recovery state of a neuron exceeds a certain value, then the neuron fires with a certain probability. Spontaneous firing, though not used in this study, may act as a form of drive if it is a function of some "reward" or "punishment", etc., i.e., a non-specific global disturbance. As the mechanisms of fatigue and spontaneous firing can be

defined very exactly in the model, their effects can be studied under tightly controlled conditions.

1.3.5 Systems of Neurons

The mammalian cortex consists of several layers of neurons of different structure. The outer layer, for example, consists of neurons with axons which spread out horizontally over large distances; the inner layers consist of neurons with very complex axonal branching in the immediate vicinity of the cell; axons from within the cortex and perhaps those from subcortical structures descend up through all the layers and back down again, probably with complex branching along the way, etc. (see, e.g., Eccles, ibid., pp. 229-331).

Moreover, there are regions of the cortex, into which sensory input is projected (e.g., the visual cortex) and other regions from which motor control is effected.

These features can be simulated to some degree in the model. First of all, a neighborhood relationship for a group of neurons may be defined that determines the neurons to which the neurons of the given group are connected and the density of connections sent out by these neurons. This neighborhood relationship thus permits structuring several layers of neurons with different connections for the different layers as well as inter-layer connection. For example, in the figure below, layer 1 may have very dense local connections, similarly for layer 2, while layer 3 may be more diffuse, neurons sending out connections over greater distances; layer 1 may connect to layer 2 in an approximate one-one fashion, while layer 2 may send out diffuse connections to layer 3, etc.

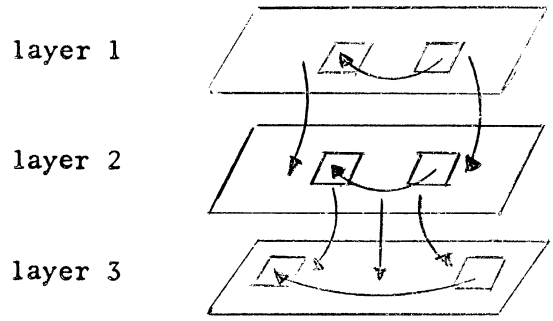

From the discussion so far, it is evident that there are many parameters and functions that can be varied in the given class of models; threshold function, fatigue, spontaneous firing, neighborhood relation, density of interconnections, etc. Moreover, the relationship between the various possible choices may be complicated and subtle. Hence, the great value of the simulation approach: hypotheses, such as those described in 1.5, concerning such relationships can be tested — hypotheses whose validity (in the models) simply may not be rigorously demonstrable a priori.

1.4 PREVIOUS NEURAL NET STUDIES

This study is not the first in its field. Rochester, Holland, et al. [11] experimented first with a "discrete-pulse model," using a simulation program for the IBM 701, then with an "FM model," using a simulation program for the IBM 704. In the first case, they exhibited "diffuse reverberation," a phenomenon somewhat akin to the sustained activity discovered in isolated cat cortex by Burns [1], but could not demonstrate any tendency on the part of the neurons to form cell-assemblies. While the "diffuse reverberation," in the authors' eyes, might serve as a mechanism for short term memory, they felt that additional structure must be imposed upon the net to allow formation of cell-assemblies. They conferred with Milner and followed his suggestion [10] of introducing negative synapse

values into their model. At the same time, taking advantage of the larger and faster IBM 704 computer, they reprogrammed their model so that the detailed firing history of the neurons was lost, being replaced by a frequency of firing for each neuron. This frequency varied with the time, hence the term "FM model." They simulated a net of 512 neurons with six inputs each. In their experiments with this model they observed the formation of cell-assembly-like structures, i.e., sets of neurons such that within each set the connections between the neurons had large, excitatory synapse values while between the various sets themselves the interconnections had large inhibitory synapse values. They also observed phenomena somewhat like the fractionation and recruitment of neurons, as required by Hebb's theory. On the other hand, the cell-assemply-like structures they observed could not arouse one another, as Hebb's theory again requires, that is, their model was too environment-dependent.

In later studies with this model, Holland and Rochester demonstrated binary learning (Holland — personal communication). However, for a variety of reasons, the project was abandoned and not resumed by any of its originators. It was continued, however, at the Logic of Computers Group at the University of Michigan, under the supervision of John H. Holland, by J. W. Crichton [5].

Crichton and Holland [5] proposed a new method of simulating neural nets which took advantage of the increased storage of the IBM 704 computer and which would allow simulation of up to 2000 neurons with about 150 inputs per neuron. This gives rise to the so-called "variable-atom" model, in which all neurons with the same characteristics (i.e., firing history, threshold, fatigue, etc.) are lumped together into an "atom." Computation of the number of active inputs to a neuron is performed by reference to

appropriate Poisson tables.

This model was never simulated on the IBM 704. The availability of an IBM 709 computer, a machine representing a considerable advancement over the IBM 704, possessing much improved input-output equipment and procedures and new powerful operation codes, caused a major change in plans and the model was to be reprogrammed for the IBM 709, taking advantage of its new features. Crichton was joined by Finley at this point.

Crichton and Finley modified the model, programming it for simulation on the IBM 709 [4]. Early experiments with this model revealed the distressing fact that the model was not capable of sustained activity such as Burns observed [1]. Stimulated "slabs" would not maintain activity indefinitely, but in fact died down rather rapidly. Marked epileptic behavior resulted — that is, intense activity alternated with low activity, leading rather quickly to "death," i.e., no activity at all. No modification of network parameters seemed to produce a cure for this behavior and we were forced to re-appraise the whole model. This lead to the discovery that the statistical techniques used in the model contained a fatal flaw, basically that it would not allow a small number of neurons to produce a sufficient stimulus to fire a single neuron. Several modifications of the original technique were tried with little success. This forced us back to basic principles and led to the implementation of a new technique aimed at introducing greater statistical disuniformity into the model. Unfortunately, this model too was discovered by the current author to be defective. The variable atom concept was discarded, being replaced by a straightforward neuron-by-neuron simulation. The latter method, although perhaps slower and more memory consuming than the former, lends itself quite well to detailed statistical analysis.

1.5 Scope of This Study

In Chapter 2, a detailed formal description of the class of models is given. This is followed in Chapter 3 by a summary account of some simple experiments involving networks without cycles (i.e., no feedback). The object of these experiments was to determine how well the behavior of a single isolated neuron of the model would correlate with various patterns of inputs presented to it. In reality, this chapter summarizes results obtained in the early stages of this work. In some respects it is not that relevant to the hard core of the later stages. It is included here primarily for historical reasons. A detailed description may be found in Finley [7].

In Chapter 4, a comprehensive discussion is given of the analysis and operation of networks with cycles (i.e., feedback present). This is easily the most important chapter of this work. The discussion proceeds from the simplest types of networks with cycles (uniform random distribution case) to more complex networks (distance-bias). The important concept of "steady-state behavior" is developed, with an analysis that may be used to determine the threshold curve parameters in terms of other basic network parameters. The role of the simulation as a means of bypassing tedious (if not impossible) mathematical calculations is repeatedly emphasized. Finally, an attempt is made to characterize simple cell-assemblies that might arise as a consequence of certain training stimuli (single periodic stimuli and alternating periodic stimuli).

The discussion of Chapter 4 is a semiformal and heuristic exposition of certain hypothesis. The remaining chapters deal with the experimental verification of these hypotheses

Chapter 5 is a descriptive essay on the experimental methodology

peculiar to experiments involving networks with cycles. Chapter 6 is devoted exclusively to stimulus-free or steady-state behavior of networks with cycles, Chapter 7 to networks with periodic stimuli.

The chief results of Chapter 6 center about successfully producing stable, steady-state behavior in networks with a sufficiently complex cyclic structure that cell-assemblies might be expected to form when patterned external training stimuli are introduced into them. This means that the networks may contain sufficient information capacity to allow cell-assembly formation (development of learned responses) as a result of "training" stimuli from the environment. For appropriate setting of certain network parameters, this is not too hard to accomplish.

Chapter 7 contains two main results. One is the formation of a simple cell-assembly (closed cycle). The essential role of the synapse-growth law is clearly brought out here. The second result is the partial formation of competing cell-assemblies-partial, since computer funds dictated cessation of experimentation. Partial though the evidence is, it seems to suggest that a more complete experiment would be entirely successful.

Several appendices are included that are concerned with some of the behind-the-scenes aspects of the simulation, e.g., random number generation, testing statistical distributions, etc. In point of fact — as is perhaps true of all experimental work — perhaps 90% of the effort involved in this work was concerned with "behind-the-scenes" problems, such as programming special-purpose I/O routines, statistical tests, reprogramming the network simulation routine, etc. Such tasks are the analog in simulation of the design and check-out of physical apparati in, say, Physics or Chemistry.

2. FORMAL DESCRIPTION OF THE MODELS

2.1 INTRODUCTION

In this chapter, the structure and operation of models of the class being considered are defined formally. The notions of run and experiment are clarified and, using the network equations, the abstract prototype for all experiments is given. Recursive equations are given for the various network functions, such as threshold, fatigue, etc. Following this, in the next section, an attempt is made to clarify the role of the various functions and to display possible functional forms for them, though no attempt is made at this point to give formal derivations. Finally, a note is given on the network simulation program, followed by a reference list of symbols used in this chapter.

2.2 THE NETWORK EQUATIONS

A neural network, $\mathfrak{N}$, of the class of models considered in this study, consists of a set of N elements called neurons with a set of specified directed connections between these neurons. "Directed" implies, for example, that neuron A may send a connection to neuron B, but not conversely, i.e., there is a connection A-to-B, but not B-to-A. Such a connection is referred to as the output of A, the input to B. A neuron of the model may have many inputs, but it always has only one output. This output, however, may branch and go to several neurons, including the source neuron, as inputs or go to the environment. All that is external to the network itself but which influences, and is influenced by, the network, is called the environment. In general the environment will supply input to selected neurons of the network and receive output from selected neurons. Included in the concept of environment would be, for example, reflex mechanisms, a simulated biological environment, a human observer,

etc.

Time is quantized in these models, t = 0, 1, 2, 3, ... At any time t, the state of the network, S(t), is determined by the functions (see below) performed by the model; likewise the state of the environment, E(t), is determined. From S(t) plus the input, I(t), to the network at t from the environment is determined the state at time t + 1, S(t+1). Also, S(t) determines the output at t to the environment, O(t). Symbolically,

$$S(t+1) = F\ (S(t), I(t)) \qquad (t = 0, 1, 2, \ldots),$$

where F is the state-transition function for the network. (In general, F is far too complicated to define explicitly, however it is defined implicitly by the network equations given below.) Likewise, E(t+1), the state of the environment of time t + 1, is determined by E(t) and O(t):

$$E(t+1) = F_E(E(t), O(t)) \qquad (t = 0, 1, 2, \ldots).$$

Since $I(t) = g(E(t))$, for some function g, then

$$S(t+1) = F\ (S(t), I(t))$$

$$F\ [S(t), g[F_E(E(t), O(t))]].$$

This is a recursive equation for S(t); S(0) and E(0) form the initial conditions for the network and the environment respectively. Given S(0) and E(0), and a starting signal, the network and environment proceed automatically over the time steps t = 0, 1, 2, ... until a stopping condition, determined in the environment, is reached. Notice that the cycle, network → environment → network, forms a closed feedback loop. The procedure of running the system $\langle$network, environment$\rangle$, given S(0) and E(0), from t = 0 or $t = t_0 (\geq 0)$ down to a terminal time step t_f will be called a run. The sequence of outputs O(0) (or $O(t_0)$), ..., $O(t_f)$ form the behavior of the network. However, the term "behavior" will be used in the broader

sense of reaction of the network to the environment. The specification of a network-environment pair, the initial conditions, and a set of hypotheses about the behavior of the network constitutes an experiment.

Thus, the abstract prototype of all experiments has the following structure:

(Given: Behavioral Hypotheses, S(0), E(0))

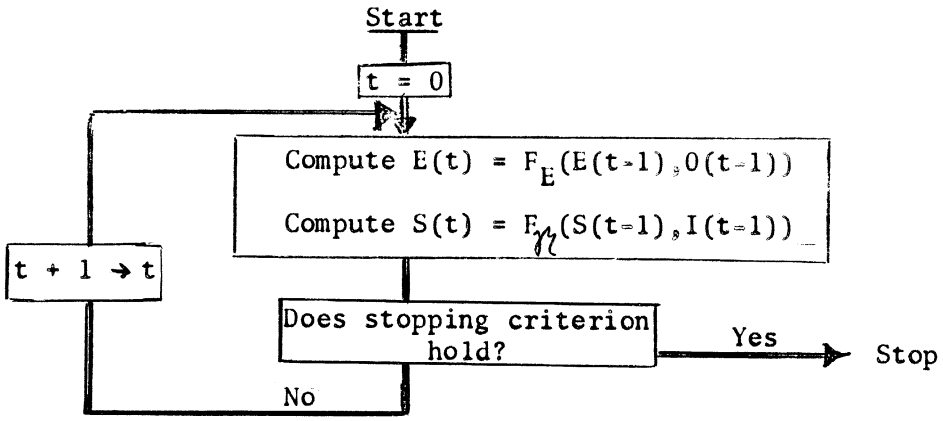

As mentioned, the state-transition function is too complicated to be defined explicitly and must be defined implicitly. This is done as as follows: At any time t, a neuron may fire or not fire. If it fires, it puts a 1 at its output, if not — a 0. The set of neurons that fire at time t, together with input from the environment, will determine the set that fire at t + 1. The condition for the firing of the i-th neuron at time t + 1 is given as a recursion relative to the real-valued functions R, F, S, and I which in turn are defined relative to recursions on $r_i(t)$, $\ell_i(t)$ and $\lambda_{ji}(t)$ by the functions V, ϕ, S, and I. Once these functions are given, then the behavior of the network is determined for all t from the initial states. This condition is

$T_i(t)$: $[\delta_i(t+1) = 1]$ if and only if $[R_i(t) + F_i(t) \triangleq \sum_j S_{ji}(t)\delta_j(t) + I_i(t)]$

$(i = 1, 2, \ldots, N)$

where $\delta_i(t) = 1$ means "neuron i fired at t." Thus, T says that neuron i fired at t + 1 if and only if the condition

$$R_i(t) + F_i(t) \leq \Sigma_j S_{ji}(t)\delta_j(t) + I_i(t)$$

holds. $R_i(t)$ and $F_i(t)$ are the threshold and fatigue values of neuron i at time t respectively. $S_{ji}(t)$ is the weight or synapse value of the directed connection from neuron j to neuron i at time t. For neurons j which do not send connections to neuron i, S_{ji} may be considered as equal to zero. $I_i(t)$ is input to neuron i at t from the environment; it will be referred to as the pre-stimulus to neuron i. R, F, S, and I are all real numbers; R and F > 0, S and I either > or < 0. Negative values of S are called inhibitory inputs, positive values are called excitatory. They are defined recursively as follows:

$$R_i(t) = V(r_i(t))$$

where V, the threshold function, is a real-valued function of $r_i(t)$; $r_i(t)$ is the recovery-state of neuron i at t defined as follows:

$$r_i(t) = \begin{cases} 0 \text{ if } \delta_i(t) = 1 \\ r_i(t-1) + 1 \text{ if } \delta_i(t) = 0 \\ r_{max} \text{ if } \delta_i(t) = 0 \ \& \ r_i(t-1) = r_{max} \text{ or } r_{max}-1 \end{cases}$$

For $r_i(t) = 0, \ldots, r_a$, $V(r_i(t)) = \infty$. r_a is the absolute refractory period; i.e., if $\delta_i(t) = 1$, then neuron i cannot fire again until $t + r_a$. Note that the function V is the same over all neurons of the net.

$$F_i(t) = \phi(\ell_i(t))$$

where ϕ, the fatigue function, is a real-valued function of $\ell_i(t)$; $\ell_i(t)$ is the fatigue-level of neuron i at t defined as follows:

$$\ell_i(t) = \begin{cases} \ell_i(t-1) + \Delta_2 & \text{if } \delta_i(t) = 0 \\ \ell_{max} & \text{if } \delta_i(t) = 0 \text{ and } \ell_i(t-1) = \ell_{max} \\ \ell_i(t-1) - \Delta_1 & \text{if } \delta_i(t) = 1 \\ \ell_{min} & \text{if } \delta_i(t) = 1 \text{ and } \ell_i(t-1) = \ell_{min} \end{cases}$$

where $\Delta_1 > \Delta_2 > 0$. Δ_1 and Δ_2 are extremely important parameters, determined from the system background firing rate, f_b, by the relation

$$f_b = \frac{\Delta_2}{\Delta_1 + \Delta_2} = \frac{F_b}{N}$$

$$S_{ji}(t) = m_{ji} S(\lambda_{ji}(t))$$

where S is the synapse-value function, taking positive, negative, and zero values, m_{ji} is the multiplicity of the connection $j \to i$, while $\lambda_{ji}(t)$ is the synapse-level of the connection $j \to i$ at time t. F_b is the expected number of neurons of $\mathcal{N}$ firing at t when $\mathcal{N}$ is operating in steady-state (see Chapter 4). It is defined as follows:

$$\lambda_{ji}(t) = \begin{cases} \lambda_{ji}(t-1) + 1 \text{ iff } \delta_j(t-1) = 1 \text{ and } \delta_i(t) = 1 \text{ and } \rho_i(t) > U(\lambda_{ji}(t-1)) \\ \lambda_{ji}(t-1) - 1 \text{ iff } \delta_j(t-1) = 1 \text{ and } \delta_i(t) = 0 \text{ and } \rho_i(t) > D(\lambda_{ji}(t-1)) \\ \lambda_{ji}(t-1) \quad \text{otherwise.} \end{cases}$$

$\rho_i(t)$ is a number drawn randomly and independently for all i and t from the open interval (0,1). $U(\lambda)$ and $D(\lambda)$ are the probabilities of change up and change down of synapse-levels respectively; notice that U and D in general vary with λ. If $\lambda = \lambda_{max}$, then $U(\lambda) = 0$; if $\lambda = \lambda_{min}$, then $D(\lambda) = 0$. The condition $\rho_i(t) > U(\lambda_{ji}(t-1))$ says simply that $\lambda_{ji}(t-1)$ is incremented by 1 with probability $U(\lambda_{ji}(t-1))$ at t. As with Δ_1 and Δ_2, U and D are extremely important quantities, and relate to the system background firing rate f_b as follows:

$$f_b = \frac{D(\lambda)}{U(\lambda) + D(\lambda)} = \frac{F_b}{N} \quad \text{(for all } \lambda\text{)}.$$

The law for incrementing or decrementing λ is the implementation in the models of Hebb's synapse growth law.

The multiplicity m_{ji} of the connection $j \to i$ determines the density of the connection $m_{ji} = 0, 1, 2, \ldots, m_{ji} = 0$ corresponds to the case of no connection from j to i. Specification of the set of m_{ji}'s for all i, j determines the connection scheme for a given network.

Thus, with these recursive definitions in mind, the flow-chart given above representing the abstract prototype of all experiments takes on the following more specific form:

(Given: Behavioral Hypotheses, $r_i(0)$, $\ell_i(0)$, $\lambda_{ji}(0)$ for all $i,j = 1, 2, \ldots, N$)

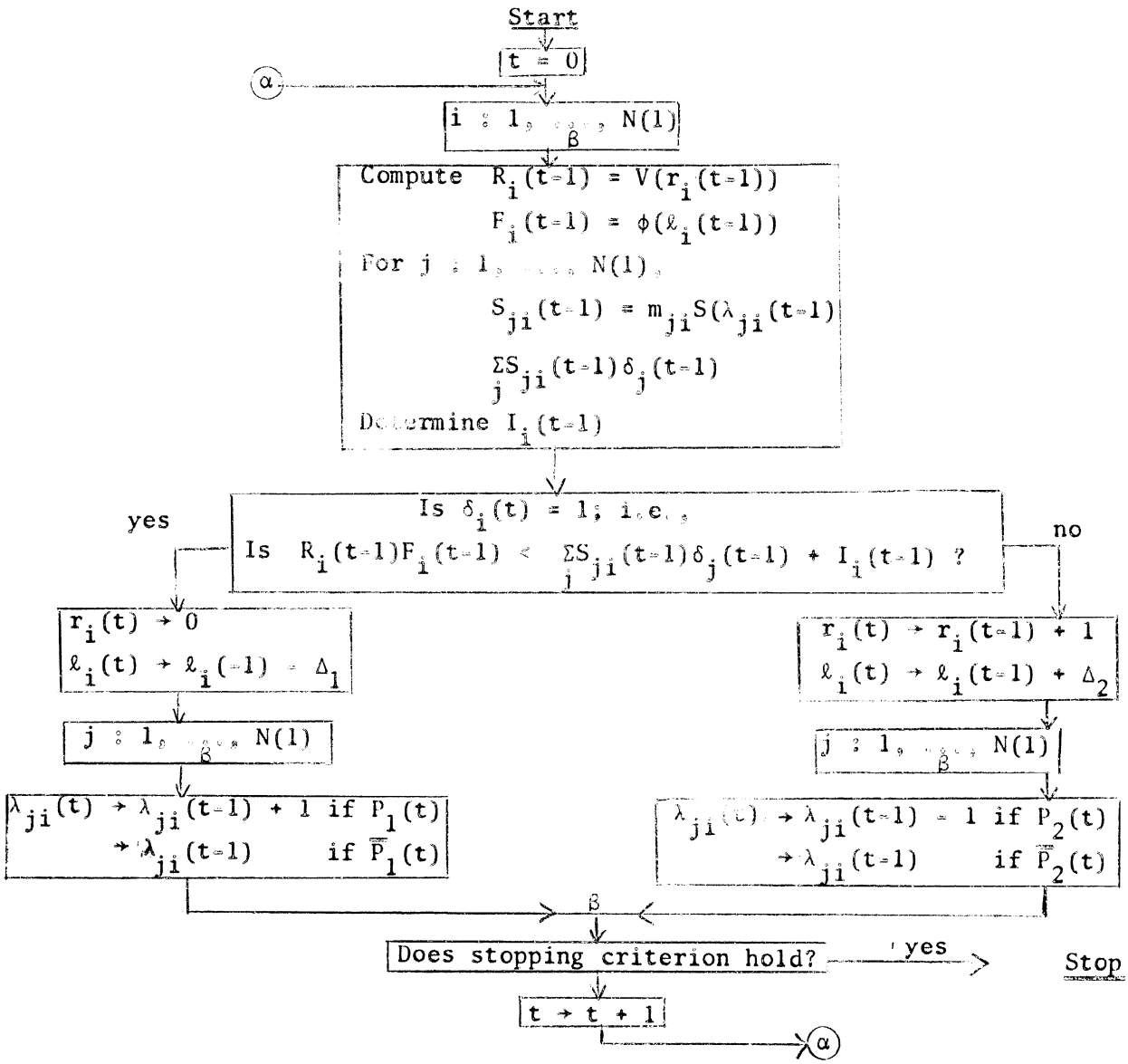

In this diagram, the notation "A→B" means that the value of A is replaced by the value of B; "i = 1, ..., N(1)" means that the computation from the occurrence of this statement down to the point β is first done for i = 1, then repeated for i = 2, i = 3, ..., down to i = N. (This is just a "loop" on the index i in increments of 1.) $P_1(t)$ is the condition for incrementation of $\lambda_{ji}(t)$ given earlier, $P_2(t)$ that for decrementation.

2.3 THE NETWORK FUNCTIONS R, F, AND S

In the preceding section, a formal characterization of the functions R, F, and S was given, with no attention being paid to their specific analytic forms. As was mentioned in the Introduction, the study of these forms is a subgoal of this paper, since prior to this there has not been a rigorous demonstration for any one of these functions assuming a given functional form. Since these functions may be specified as one wills, they in fact are parameters of the network. Given values of these parameters and values of $N = \overline{\overline{\mathcal{M}}}$, m_{ji}, $i,j = 1, \ldots, N$, a specific network is determined.

2.3.1 Control of Firing Rate

From the network equations $T_i(t)$ one can see that the function of the threshold value $V_i(t)$ of a neuron, as modified by the additive quantity $F_i(t)$, is to determine whether or not neuron i of the network fires at t. If the combined input to neuron i is at least as great as the product of $R_i(t)$ and $F_i(t)$, then it fires, otherwise it does not. The function V, which determines R, then controls the firing rate of the neurons of the network $\mathcal{M}$. Immediately after neuron i fires, V is infinite and i cannot fire. After a few time steps (r_α = the absolute refractory period), it "recovers" slightly, that is a very large input stimulus can cause it

to fire, after a few more, less stimulus is required, down to the point where — if it has not yet fired, a minimal stimulus is required to cause it to fire. This point is called the resting or quiescent value of V, V_q. The function ϕ which determines $F_i(t)$ modulates the control of V in the sense that if the firing rate of neuron i is high, then ϕ is large, hence larger stimulus is required to cause i to fire. If the firing rate is low, the magnitude of ϕ is small (close to 1) and less stimulus, depending upon the value of V, is required.

2.3.2 The Threshold Function

From 2.2 one sees that the threshold value, $R_i(t)$, of neuron i is that value which corresponds to the recovery state r_i of neuron i; that is, r_i = the number of time steps since neuron i fired. Each neuron i of the network has associated with it a value of r_i, depending on its immediate firing history. Thus, if $\delta_i(t) = 1$ (i.e., neuron i fired at time t), then $r_i(t) = 0$; if $\delta_i(t-10) = 1$, and $\delta_i(t-9) = 0, \ldots, \delta_i(t-1) = 0$, $\delta_i(t) = 0$ (i.e., neuron i fired at t-10 and did not fire again up to and including time t), then $r_i(t) = 10$. Each time neuron i fires, r_i is set to zero. Each time it fails to fire, it is incremented by 1, i.e., $r_i(t) = r_i(t-1) + 1$. r_i has a maximum value r_m; further incrementation fails to change it — i.e., $r_m + 1$ is the same as r_m. The function $V(r_i(t))$ which gives the value $R_i(t)$ is the same for all neurons of $\mathcal{N}$. Because, at any given time t, these neurons may have distinct values of r(t), they will usually have distinct threshold values.

The absolute refractory period or period of infinite threshold is r_a. That is, if $\delta_i(t) = 1$ (neuron i fires at t), then i cannot fire again until $t + r_a$ (until $r_i = r_a$). The total number of time steps to

quiescence, that is, the resting values of threshold, is r_q. Thus, if neuron i fires at t, it is fully recovered (has reached the resting value) at $t + r_q$. In general in this work, $r_a = 3$, $r_q = 16$, and $r_m = 64$.

There are three important aspects of the threshold curve. The first is its value at $r = r_a$, the second is its quiescent value — i.e., $V_q = V(r_q)$, and the third is its functional form (i.e., exponential, quadratic, linear, etc.) especially in the mid-recovery range $r \simeq r_a + (r_q - r_a)/2$. A procedure for determining the form of V(r) will be given in Chapter 4. Note that the reciprocal of the recovery state for a given neuron i, $1/r_i$, averaged in some appropriate fashion, will correspond to the firing-rate of neuron i. For example, if a neuron fires on the average once every five times, its "average" recovery is $\bar{r} = 5$ and its firing rate $= 1/5 = 1/\bar{r}$.

The threshold curve, then, has the following form, where V_m = the maximum value (for $r = r_a$), V_q = the quiescent value ($r = r_q$):

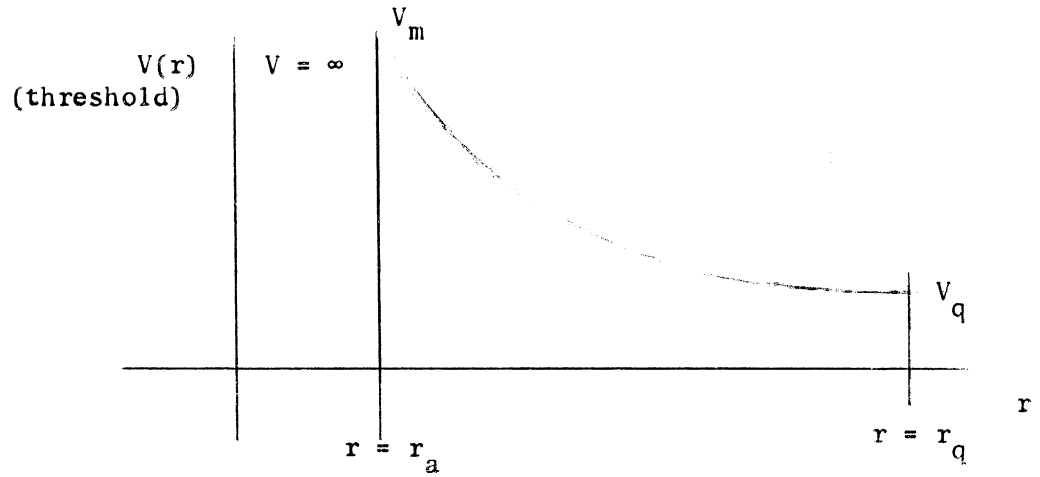

The functional form of this curve, the quantities V_m and V_q as well as the initial values of r for each neuron of the net, will be specified for each experiment. The quantity V_q is important because it defines the least amount of input stimulus (synapse-value) which may fire

the neuron.

2.3.3 The Fatigue Function

As already mentioned, the fatigue value $F_i(t)$ serves to modulate the threshold value $R_i(t)$ of neuron i and hence modulates the firing rate of i. The desired effect of the fatigue function is as follows: given the neuron in a fully recovered state, that is, the threshold value is near V_q and the fatigue value is 0. Suppose inputs are presented to the neuron so as to cause it to fire at a fairly high rate (above the background rate f_b). Then, gradually over a period of a large number of consecutive time steps the fatigue value, i.e., $\phi(\ell)$, of the neuron increases in such a fashion as to force the firing rate of the neuron to drop down to f_b on even lower, keeping it there as long as the given inputs are present. Suppose next the inputs themselves drop off so that at the most they would cause the neuron to fire at f_b. Then, the fatigue value, $\phi(\ell)$ decreases slowly back to 0 so as to preserve approximately the average firing rate of f_b. Intense activity of the neuron, that is, firing at near maximal rates, produces more abrupt increases in ϕ, whereas sudden drop-off in activity, that is, firing at very low rates ($<f_b$) produces a more abrupt decreases in ϕ.

The fatigue value $F_i(t)$ of neuron i is determined by the fatigue function ϕ from the fatigue level $\ell_i(t)$ of neuron i at time t, $F_i(t) = \phi(\ell_i(t))$. The function ϕ is the same for all neurons of the network $\mathcal{N}$. Similar remarks for the variation in threshold values among the neurons of the network apply to the fatigue values as well. The fatigue value is used, as has been indicated, as an additive factor of the threshold value for the given neuron. ϕ is a monotonically decreasing function of ℓ with $\phi \geq 1$. The larger the ϕ, the larger the sum $R + F$. Thus, neuron i may be

fully recovered, $r_i(t) = r_q$, and $R_i = V(r_q(t)) = V_q$, but ϕ may be so large that $R_i(t) + F_i(t) = V_q + \phi(\ell_i(t))$ is much greater than V_m. Fatigue is rendered ineffective by setting $\phi(\ell) = 0$ for all ℓ. Then $R_i(t) + F_i(t)$ always equals $R_i(t)$. Note that the fatigue value has no effect on the absolute refractory period ($\phi + \infty = \infty$).

The quantity ℓ for a given neuron varies incrementally from 0 to ℓ_m with $1/\ell_m$ as the smallest possible increment. The manner of variation is the following: Suppose the neuron has fatigue level ℓ_0 at time t. Then, if the neuron fires at r, ℓ_0 is decremented by a quantity Δ_1, i.e., $\ell_0 \to \ell_0 - \Delta_1$. If it does not fire at t,, then it is incremented by a quantity Δ_2, i.e., $\ell_0 \to \ell_0 + \Delta_2$. This is illustrated below:

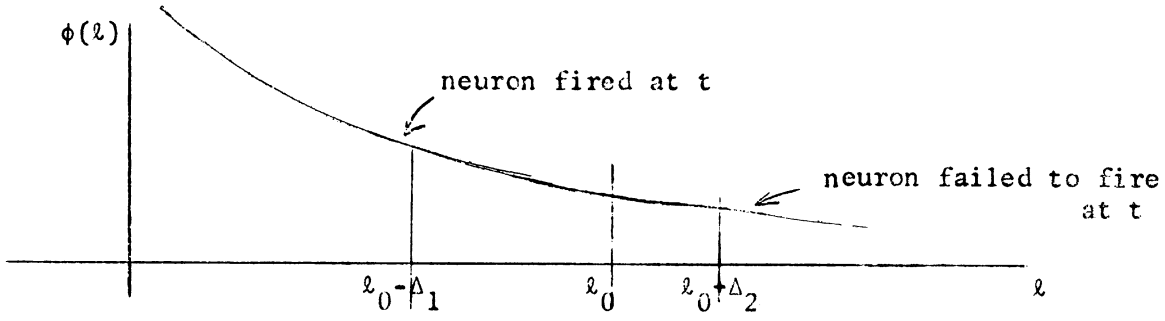

In general, $\Delta_1 > 0$, $\Delta_2 > 0$, and $\Delta_1 > \Delta_2$. Decrementation below 0 and incrementation above ℓ_m have no effect, i.e., $0 - \Delta_1 = 0$, $\ell_m + \Delta_2 = \ell_m$.

Δ_1 and Δ_2 are extremely important numbers since in terms of them is expressed a crucial parameter of the net, namely the firing rate at which a neuron experiences no net change in fatigue level. If a neuron is firing at this rate — call it f_b — then over an interval of length T time steps, say, there is no net change in the ℓ for that neuron. Recalling that f_bT is the expected number of times a neuron will fire in the given interval and $(1-f_b)T$ the expected number of non-firings, this means that

$$\Delta_1 f_b T - \Delta_2(1-f_b)T = 0.$$

Solving for f_b gives

$$f_b = \frac{\Delta_2}{\Delta_1 + \Delta_2} = \frac{F_b}{N}$$

This quantity, f_b, already mentioned, is called the background firing rate or the "nominal system average." It will be treated in detail later on. Note that given f_b, one can determine Δ_1 and Δ_2 (up to a constant multiple $k > 0$ which may be chosen as 1) and, conversely, given Δ_1 and Δ_2, f_b is uniquely determined. f_b plays an important role in Crichton's theory [2].

The functional form of the fatigue curve, the numbers Δ_1 and Δ_2 (or, f_b), as well as the initial value of ℓ for each neuron of the net, will be specified for each experiement. The form of the curve is clearly of the greatest importance since it, together with the numbers Δ_1 and Δ_2, determine the recovery rate of a neuron as well as its fatiguing rate. The desired properties of this curve have been outlined above. The rationale for these will be given in the next chapter. In general, Δ_1 and Δ_2 are functions of ℓ. This allows greater flexibility in creating $\phi(\ell)$. For example, ϕ may be made into a hysteresis function.

In contrast with the case of the threshold, no convenient analysis relating $\phi(\ell)$ to the other network parameters $N = \{\ell_i, \rho$ (see Chapter 4), $V(r)$, etc. was developed in the current work. See Chapter 7 for a further discussion of this.

2.3.4 The Synapse Value Function

Suppose a neuron j sends one directed connection to another neuron i. From 1.3.3, recall that to each such directed connection at time t is associated a positive number, the synapse level, $\lambda_{ji}(t)$. Just as with the recovery states and fatigue levels, λ is used to determine a value,

the synapse value, S, by means of a functional relationship. λ has a range from 0 to λ_m. It is incremented according to the synapse-growth law as follows: suppose the connection $j \to i$ has the synapse level λ_0. Then, if j fired at t - 1 and i fired at t, $\lambda_0 \to \lambda_0 + 1$, with probability $U(\lambda_0)$. Otherwise, $\lambda_0 \to \lambda_0$ — i.e., no change. If $\lambda_0 = 0$, no further decrementation is allowed; if $\lambda_0 = \lambda_m$, no further incrementation is allowed. The statement "$\lambda_0 \to \lambda_0 + 1$ $(\lambda_0 - 1)$ with probability $U(\lambda_0)(D(\lambda_0))$" means that if λ_0 is to be increased (decreased) — depending upon whether j fired at t - 1 and i at t, etc. — then the incrementation takes place with probability $U(\lambda_0)(D(\lambda_0))$. Note that $U(\lambda_m) = 0$ and $D(0) = 0$. The incrementations with probability $U(\lambda_0)$ or decrementations with probability $D(\lambda_0)$ form independent trials, e.g., if the synapse level from j to i is λ_0 and that from k to ℓ also equals λ_0, where both neurons j and k fired at t - 1, and both i and ℓ fired at t (hence λ_{ji} and $\lambda_{k\ell}$ are both candidates for incrementation), then the probability $U(\lambda_0)$ is consulted independently in each case.

The numbers U and D are of great importance, especially in light of the theory developed by Crichton mentioned above. Like the numbers Δ_1 and Δ_2 of the preceding section, U and D are related to the nominal system average, f_b. The reason is quite simple: Assume that the rate of change up of a synapse is proportional to U, say = kU, likewise that the amount of change down is proportional to D, say = kD. f_b is again defined as that firing rate for which no net change in λ between A and B will occur, assuming for the moment that neurons A and B are firing randomly and independently at the rate f_b. If this is the case, then f_b^2 will represent the probability that the firing of A at t - 1 is followed by the firing of B at t ("success"), likewise $f_b(1-f_b)$ is the probability that a firing

of A at t - 1 is followed by a non-firing of B at t ("failure"), $f_b^2 T$ is the expected number of "successes" over a time interval of length T, $f_b(1-f_b)T$ the expected number of "failures." $kUf_b^2 T$ is the expected net increase in the interval of length T; $kDf_b(1-f_b)T$ the net decrease. By assumption, the difference of these is zero and

$$Uf_b^2 = D(1-f_b)f_b$$

or

$$f_b = \frac{D}{U + D} = \frac{F_b}{N} .$$

Recall that the firing or non-firing of a neuron is determined by a comparison of the sum of the synapse values on the active inputs (that is, those connections coming from neurons which fired the preceding time step) with the sum R + F (which is infinite if the neuron has fired at one of the previous $r_a - 1$ time steps). If this sum is less than R + F the neuron does not fire, otherwise it does. No restriction has been placed on synapse values. However, synapse values for small λ's are assumed to be negative, large λ's — positive. The negative synapse values for active input lines correspond to inhibitory inputs to the neuron. S is assumed to be some monotonic increasing function of λ. Since U and D are both functions of λ, it is possible to vary the rate of change of $S(\lambda)$ over the range of λ. This feature may be introduced to tend to "trap" values of λ (hence $S(\lambda)$) in certain ranges. For example, it might be desirable to bias the change of λ away from values corresponding to $S(\lambda) = 0 \pm \varepsilon$ (ε small, positive), etc.

2.4 NOTE ON THE SIMULATION PROGRAM

A diagram representing the operation of the network, given an environment, the initial conditions, and the behavioral hypothesis was given

earlier. A program was written for the IBM 7090 computer which simulates the operations indicated in that diagram. This program consists of four basic parts: (1) the lists which describe the state of the network at each time step. The lists are a block of reference information for (2) below and in turn consist of two parts: (a) a permanent part which is never changed in the course of a run, and (b) a volatile part which may change; (2) the network program which computes at each time step the various functions required by the model, referring to the lists for parameter values and making appropriate changes to the lists; (3) the executive and environment routine, a supervisory program which performs two functions: (a) it monitors pertinent network parameters, running time of the program, etc., and handles the appropriate output editing and (b) simulates the environment of the model — i.e., computes input and output functions, making any necessary changes to lists; (4) input-output editing and other special-purpose routines, usually ancillary to the executive routine.

The network program seldom ever will be varied; the executive and environment routines will vary from experiment to experiment and often from run to run. Parameters in the lists will vary from run to run in general, while those lists particular to a given experiment will vary from experiment to experiment. It is the lists that determine the structure of a given net; i.e., neuron inter-connections, density of connections, etc.

Note that the executive routine contains provisions for experimenter intervention in an experimental run. The experimenter, while watching a real-time display of selected functions of the network, may at any time change the display, modify parameters, store the entire state of the system for future back-up purposes, etc.

Diagrams giving the overall structure of the program and the flow of

control are given below:

Structure of Program

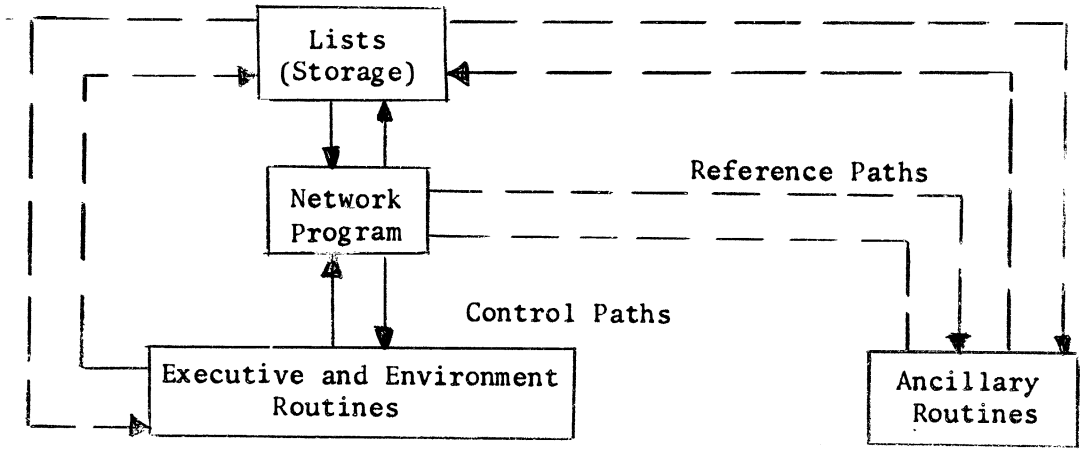

Flow of Control

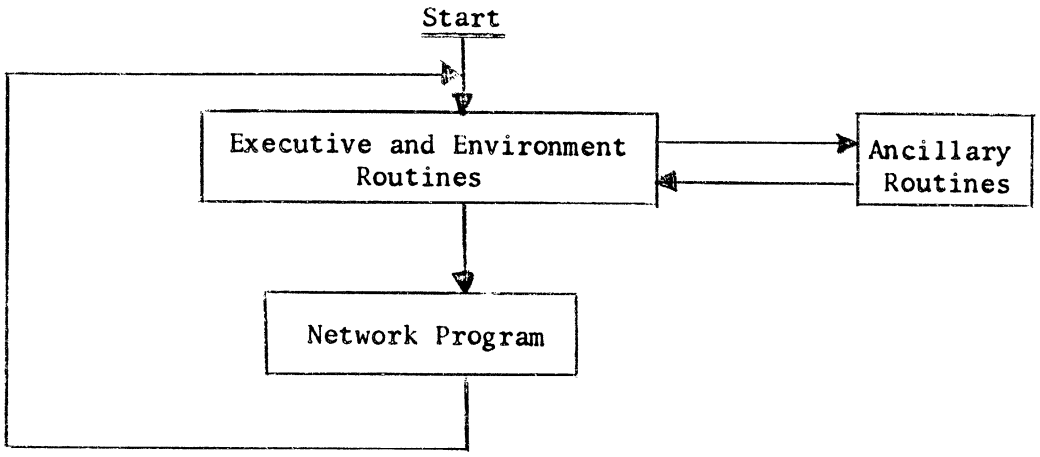

Symbols Used in Section 2.2

$\mathfrak{N}$	a neural network
M	the number of neurons in $\mathfrak{N}$
$S(t)$	state of the network at time t
$E(t)$	state of the environment at time t
$I(t)$	input to the network from the environment at time t
$O(t)$	output from the network to the environment at time t
F_N, F_E	state transition function of the network and the environment, respectively
$\delta_i(t) = 1$	the statement "neuron i fired at time t"
$T_i(t)$	the condition for $\delta_i(t) = 1$
$R_i(t)$	threshold-value of neuron i at time t
$F_i(t)$	fatigue-value of neuron i at time t
$S_{ji}(t)$	synapse-value of the connection from neuron j to neuron i at time t
$I_i(t)$	input to neuron i at time t from the environment
$r_i(t)$	recovery state of neuron i at time t
$\ell_i(t)$	fatigue-level of neuron i at time t
$\lambda_{ji}(t)$	synapse-level of the connection from neuron j to neuron i at time t
$V(r_i(t))$	threshold function, gives $R_i(t)$ as a function of $r_i(t)$, $R_i(t) = V(r_i(t))$
$\phi(\ell_i(t))$	fatigue function, gives $F_i(t)$ as a function of $\ell_i(t)$, $F_i(t) = \phi(\ell_i(t))$
$S(\lambda_{ji}(t))$	synapse-value function, gives $S_{ji}(t)$ as a function of $\lambda_{ji}(t)$, $S_{ji}(t) = S(\lambda_{ji}(t))$

$\rho_i(t)$	random number associated with neuron i at time t
1	fatigue-level change if $\delta_i(t) = 1$
2	fatigue-level change if $\delta_i(t) = 0$
f_b	nominal system frequency or average background frequency
F_b	expected number of neurons of $\{1, \ldots, N\}$ firing at t
$U(\lambda_{ji}(t))$	probability of change for synapse-level $\lambda_{ji}(t)$
$D(\lambda_{ji}(t))$	probability of change down for synapse-level $\lambda_{ji}(t)$
m_{ji}	multiplicity of the connection from neuron j to neuron i

Symbols Used in the Flow-Diagram

$i = 1, \ldots, N(1)$	"loop" to β N times, starting at i = 1, incrementing i by 1 each time; i.e., first i = 1, then i = 2, 3, ..., etc. through i = N
$A \rightarrow B$	replace the value of A by the value of B
$P_1(t)$	the condition for incrementing $\lambda_{ji}(t)$
$P_2(t)$	the condition for decrementing $\lambda_{ji}(t)$

3. CORRELATION EXPERIMENTS, CYCLE-LESS CASE

3.1 INTRODUCTION

In the implementation of Hebb's theory, several questions may be isolated in an attempt to elucidate the nature of the cell-assembly. Perhaps the first of these concerns identification of cell-assemblies, that is, in terms of the given models, what are the criteria for cell-assembly-ness? This question is aimed at a static, structural condition and may be paraphrased as follows: suppose a model is given in which it is suspected that cell-assemblies have formed. How, then, are they identified? The second question (which, causally speaking, should be first) is concerned with the formation of cell-assemblies; i.e., in terms of the given models, how does a cell-assembly like structure come into existence? This question is aimed at dynamic, structural changes and goes hand-in-hand with a third: what are the stability conditions, in the given models, for cell-assemblies? To make this last question more meaningful, the informal description of cell-assembly given in 1.2 is augmented as follows: One may regard a cell-assembly as a union of a large number of reverberatory circuits (in the Lorente de Nó sense of the term), any several of which may be active for a very brief period of time and interrelated so that while any one of the circuits may be rapidly extinguished (within 1/100th of a second in the physiological situation), yet for a much greater period of time (several seconds or longer) the structure as a whole is active in the sense that at least one of the component circuits is active. That is, within a given cell-assembly there are a number of alternate pathways which perform the same function. Therefore, the stability question for such a structure is absolutely crucial. This character of the cell-assembly accounts for the fact that the loss

or damage of part of a fully developed cell-assembly need not impair its overall function, thus for the seemingly small effect in some cases of brain damage upon learning ability and memory. (This is part of Hebb's dual trace memory mechanism and accompanies his postulate of synapse growth since the reverberatory activity would assist to retain memory temporarily while at the same time it would facilitate the long-run growth changes necessary for permanent memory (see [9], pages 60-78, in particular, p. 62).

The cell-assembly is, therefore, not strictly dependent upon individual neurons for its functioning. For its growth and development, it does depend upon the synapse-growth law (Hebb's neurophysiological postulate) and upon the availability of neurons which can be "recruited" to the assembly when they "cooperate" with it and likewise which can be dropped out of the assembly (fractionation) when they fall into disuse.

The ability or non-ability of the models to allow recruitment of neurons to an assembly or fractionation of neurons away from it, then poses a fourth question which is taken as the starting point of this study: do the neurons of the models have the ability to be recruited into an assembly when presented with the same input patterns and, dually, to fall away through disuse? This question leads, as shall be shown in the next section, to simple networks which are extremely useful for studying the behavior of single neurons and small groups of neurons.

Crichton, in the appendix to his thesis [2] has discussed the stability of cell-assembly-like structures, called by him "semi-autonomous subsystems." Some results of his analysis will be used later. Questions of stability and structure of cell-assemblies are considered in Chapter 4. The results of this chapter form the basis of the design of the $U(\lambda)$ and

$D(\lambda)$ tables used in the experiments of Chapters 6 and 7.

3.2 CORRELATION

The behavior of a neuron of the model depends upon its input history (which includes synapse value changes on the input lines) and upon its internal state changes (threshold, fatigue). To determine the response of a given neuron to a particular input pattern, one has to take into consideration the effect of this pattern upon the internal state changes of the neuron and the relationship of this pattern to any other inputs the neuron may have. Basically, therefore, the behavior of a neuron may be regarded as being determined by some function over the totality of its inputs.

Consider now a situation in which recruitment might occur. Let C be an uncommitted neuron of the system and suppose it is presented with a patterned input from a source A of neurons. (A might be, for example, a set of neurons of area 17, reflecting a direct sensory input from the retina.) Lump all the other inputs to C into a group B. Now it might be that A directly affects a system of neurons D, which may form part of a cell-assembly Γ. The synapse values from the neurons of A to C will be, by assumption, low initially.

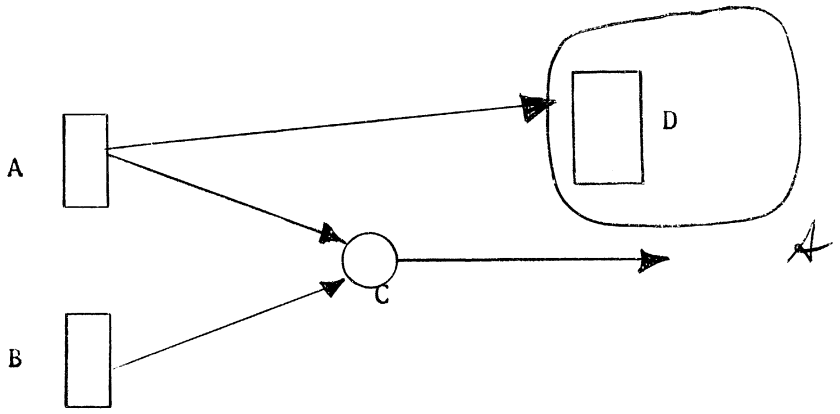

Likewise, the synapse values from A to D are assumed to be high. If, as a result of repeated application of the input from A, the synapse values from A to C rise and become high, then the neuron C is a good candidate for recruitment into the cell-assembly A. Whether it is recruited or not depends, of course, upon its relationship to other neurons of the system, specifically, upon how A's output affects some of the successor neurons to D. It may merely continue to operate in parallel to the assembly A. In fact C could become part of a system of neurons which would tend to suppress, via inhibitory connections, an antagonistic assembly B. In any case, the question of when C would "correlate" with A in its firing arises. Here "correlate" means that the synapse values of A to C are high and that C tends to follow the same firing pattern as do the neurons of A. Therefore, whether C correlates with A or not depends critically upon the relationship between the firing patterns of A and B. The conditions under which correlation occurs are essential to the formation of cell-assemblies, as shown by the experiments of Chapter 7.

3.3 EXPERIMENTAL CONFIGURATIONS FOR CORRELATION STUDY

3.3.1 Overview

The general configuration of neurons that is to serve as the basis for the first part of this study is the following:

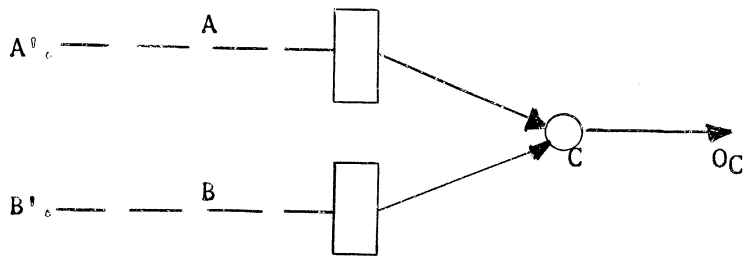

A and B are sets of neuron, C is a single neuron. Each neuron of A and B sends a connection to C. There are no other connections between neurons of A and B and C — i.e., no cycles. The neurons of A and B are assumed to be driven from stimulus sources A' and B'. From the patterns on the input lines A to C and B to C and the initial states of C, the output 0_C may be determined.

The sizes of the sets A and B, the particular patterns which they supply to C, the initial states, the net parameters — all these are to be specified by the particular experiment at hand. Thus, A and B may consist of a single neuron each or A may have N neurons and B have none, etc. One can readily see then how it is possible to study the behavior of A as a function of a wide range of possible inputs and at the same time study the response of C "in isolation," as it were, given different settings of the basic net parameters.

A model situation of concern in this chapter is that in which group A essentially provides "back-ground noise" to C, while group B provides patterned inputs of various types. One example of this is the case in which the neurons of B fire within a periodic envelope as follows:

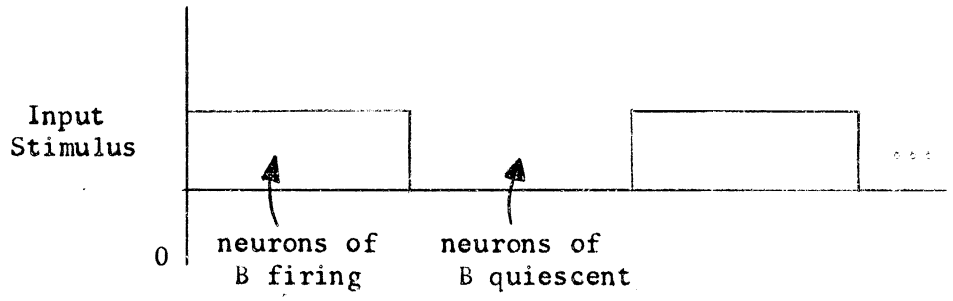

Questions such as what are the lengths of the "on" and the "off" periods in relation to neuron parameters, what are suitable firing rates of the neurons of B in the "on" and the "off" periods, etc., immediately arise and become of the greatest importance. The next step would be to have

both A and B providing similar patterns such as this but out of phase, then to ask how C depends upon the phase difference, etc.

3.3.2 Network Structure

The models of interest consist of $N = 2M + 1$ neurons (where N is the size of the network). The N neurons are partitioned into two groups of M neurons each and one group of one neuron. The former two groups will be designated by A and B respectively, the single neuron by C. Each neuron of A and B respectively sends exactly one directed connection to neuron C. C, therefore, has 2M inputs. The output of C goes to the environment. The environment provides the neurons of A and B with inputs of the following type: Letting $\alpha_1, \ldots, \alpha_M$ be the neurons of A and $\alpha_{M+1}, \ldots, \alpha_{2M}$ be those of B, then to each α_i is associated a probabilistic stimulus $X_{\alpha_i}(t)$. At time t, independently of $X_{\alpha_i}(t+k)$ for all $k = \pm 1, \pm 2, \ldots$, and with probability f_{α_i}, $X_{\alpha_i}(t) = 1$; with probability $1 - f_{\alpha_i}$, $X_{\alpha_i}(t) = 0$. If $X_{\alpha_i}(t) = 0$, neuron α_i is not effected. If $X_{\alpha_i}(t) = 1$, α_i is provided with an input stimulus ($I_{\alpha_i}(t)$ in the network equations $T_{\alpha_i}(t)$) which is always greater than $R_{\alpha_i}(t) + F_{\alpha_i}(t)$ unless, of course, α_i is absolutely refractory (i.e., if $\delta_{\alpha_i}(t-1) = 1$ or $\delta_{\alpha_i}(t-2) = 1$). α_i has no other inputs. Notice that the probability f_{α_i} approximates the actual firing rate of α_i: $f_{\alpha_i} \cdot T$ is the expected number of firings of α_i over a time interval of length T. Specification of the probabilistic vector $X_{\alpha_i}(t)$, $i = 1, \ldots, 2M$, then determines the "vector" of firing frequencies f_{α_i} of the neurons α_i which comprise the total input set to neuron C. In any particular experiment, the vector $X_{\alpha_i}(t)$ must be specified in complete detail.

The connection-scheme, complete with the input vector $X_{\alpha_i}(t)$, has

the following form:

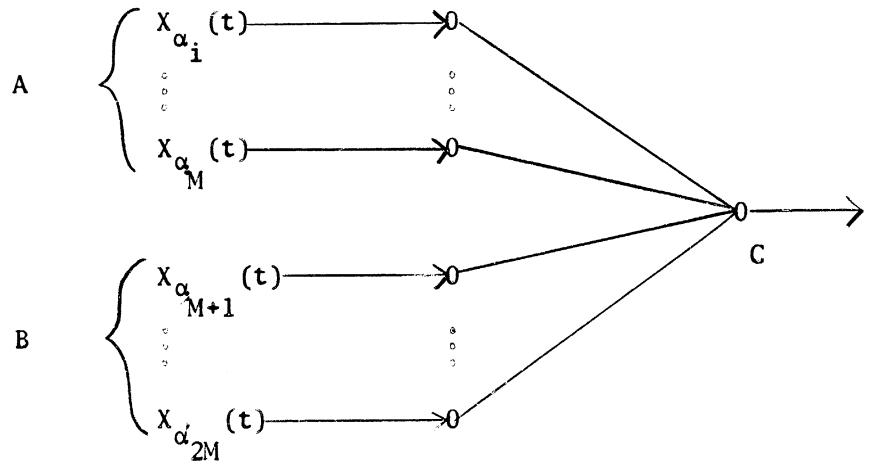

The distinction between A and B is only for the purpose of allowing two subvectors of $X_{\alpha_i}(t)$, $i = 1, \ldots, 2M$ to be applied, i.e., $X_{\alpha_i}(t), \ldots, X_{\alpha_M}(t)$ and $X_{\alpha_{M+1}}(t), \ldots, X_{\alpha_{2M}}(t)$. (Note: This network is obtained by specifying the m_{α_i}'s, $i = 1, \ldots, 2M$, to be 1's and all others to be zero out of the set of N^2 possible interconnections within the given set of N neurons.)

3.3.3 Network Functions, Initial Conditions, Environment

The threshold, fatigue, and synapse-value functions together with the parameters associated with them, such as Δ_1, Δ_2, U and D, etc., were varied with the experiments performed.

The initial conditions comprise specification of the following values:

1. $\lambda_{\alpha_i}(0)$, $i = 1, \ldots, 2M$
2. $r_{\alpha_i}(0)$, $i = 1, \ldots, 2M$ and $r_C(0)$
3. $\ell_{\alpha_i}(0)$, $i = 1, \ldots, 2M$ and $\ell_C(0)$
4. $I_{\alpha_i}(0)$, $i = 1, \ldots, 2M$

The $I_{\alpha_i}(0)$'s are assumed to be all equal and constant over all time, and so large that except when the α_i are absolutely refractory, they always cause α_i to fire when $X_{\alpha_i} = 1$. Thus, the initial values $r_{\alpha_i}(0)$ and $\ell_{\alpha_i}(0)$ are not so important. Yet the initial values of r_C and ℓ_C clearly are important for, for example, if $\ell_C(0)$ is at the minimum, then neuron C starts out fully fatigued and may fail to respond to initial inputs for some period; whereas if it is fully rested, that is $\ell_C(0)$ is near the maximum, then C will most likely respond to the initial inputs.

The function of the environment in these experiments is, at each time step, to operate the probabilistic vector $X_{\alpha_i}(t)$, $i = 1, \ldots, 2M$ and to observe the output of neuron C.

3.4 Summary of Experiments

3.4.1 Experimental Hypothesis

Consider the network of the preceding section. Relabel the 2M neurons of A and B as $A_1, A_2, \ldots, A_M$ and $B_1, B_2, \ldots, B_M$ respectively. The corresponding stimulation rates will be f_{B_i} and f_{A_i} respectively for $i = 1, 2, \ldots, M$. In general, the neurons of each group will be fired at the same rate, i.e., $f_{A_i} = f_A$ and $f_{B_i} = f_B$ for $i = 1, 2, \ldots, M$.

Divide the interval $(0, \infty)$ into subintervals U_k of length ℓ $[2k\ell, (2k+1)\ell]$ $(k = 0, 1, 2, \ldots)$ and the complementary subintervals, $U_k^* = [(2k+1)\ell, (2k+2)\ell]$ $(k = 0, 1, 2, \ldots)$;

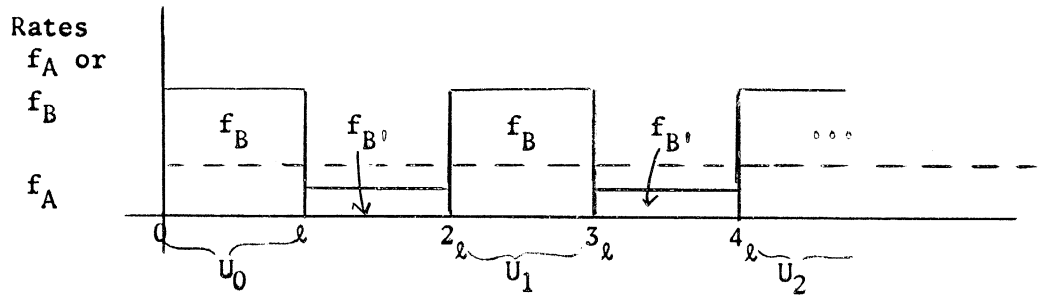

In intervals U_k, $f_B > f_A$; in intervals U_k^*, $f_B < f_A$. The average of f_B over one cycle (interval of lenth 2ℓ) is, in general, $f_B/2 = f_A = f_b$. The neurons of A are stimulated then randomly and independently at rate $f_A = f_b$; the neurons of B are stimulated randomly and independently at rate $f_B > f_A$ for $t \in U_k$, $k = 0, 1, \ldots$ and at rate $f_B < f_A$ in the intervals U_K^*, $k = 0, 1, \ldots$. The intervals U_k are called the "high" or "on" periods of stimulation of B; the U_k^* — the "low" or "off" periods.

Correlation Hypothesis

For appropriate selections of the network functions V, ϕ, and S together with certain initial conditions, neuron C will tend to correlate with group B in the sense that as t becomes sufficiently large,

$$\lambda_{\overline{BC}}(t) >> \lambda_{\overline{AC}}(t)$$

and for $i = 1, \ldots, M$.

$$\delta_{B_i}(t) = 1 \text{ implies that } \delta_C(t+1) = 1 \quad \text{a.a.}$$
$$\delta_{B_i}(t) = 0 \text{ implies that } \delta_C(t+1) = 0 \quad \text{a.a.}$$

where $f_B > f_A$ for t in the intervals U_k, $f_B < f_A$ otherwise. $f_A = f_b$ is the background rate of the system. $\lambda_{\overline{AC}}$ and $\lambda_{\overline{BC}}$ represent averages of the λ_{A_iC} and λ_{B_iC} respectively. "a.a." means "almost always" — i.e., with very high probability, but not probability one. This leaves room for occasional occurrences of the complementary events

$$\delta_{B_i}(t) = 1 \text{ and } \delta_C(t+1) = 0,$$
$$\delta_{B_i}(t) = 1 \text{ and } \delta_C(t+1) = 0.$$

The hypothesis merely states that group B eventually gains control over neuron C while group A loses control. Group B may be regarded as the information bearing lines, group A a continuous source of background noise. Hopefully, C will correlate with the information bearing source and not with the noisy one. For example, over the rapid staccatto of

a pneumatic hammer operating out-of-doors, a human being might well hear a periodic knocking on the door.

3.4.2 Some Theoretical Considerations

In the appendix to his thesis [2], Crichton discusses the stability of systems of neurons which he calls "semi-autonomous subsystems." These are networks of neurons which may correspond in a limited way to the cell-assemblies of Hebb's theory. In his development, he makes a number of assumptions, two of which are relevant to the experiments of this chapter: (1) the neurons of the system fire aperiodically, randomly and independently of one another, and (2) all neurons tend in their firing to a common average rate f_b. This f_b he calls the "nominal system average." From his arguments he derives some bounds on the threshold curve (to be discussed later) and some important relationships between the fatigue increments, Δ_1 and Δ_2, and the probabilities of synapse-level change, $U(\lambda)$ and $D(\lambda)$. These have already been used in Chapter 2. The gist of his argument is this; that the role of the fatigue function must be to drive the neurons of the system to the frequency f_b; thus, if a neuron falls below f_b in its firing rate, then the fatigue should decrease so as to bring the rate back down to f_b. Firing at the rate of f_b, there is no net change in fatigue. This last condition implies that $f_b = \Delta_2/(\Delta_1+\Delta_2)$ since then $Tf_b\Delta_2 - T(1-f_b)\Delta_1$ must be zero, where T is the length of the time-interval under consideration (see 2.3.3). Similarly, the condition for no net change in synapse-level becomes $f_b = D(\lambda)/(U(\lambda)+D(\lambda))$.

One further relation that he gives is useful: Consider two neurons A and C with a connection going from A to C, where A and C fire aperiodically at the rates f_A and f_C respectively. The expected rate of increase in λ_{AC} per time step is $f_A \cdot f_C$, and the expected rate of decrease is

$f_A(1-f_C)$. Recalling that $D/(U+D) = f_b$ from which $U/D = (1-f_b)/f_b$, it follows that $U = K(1-f_b)$, $D = Kf_b$ for some constant $K > 0$. U and D correspond to the rate of increase and the rate of decrease of a connection and $f_A f_C K(1-f_b)$ to the expected rate of increase in λ_{AC} per time step, $f_A(1-f_C)Kf_b$ to the rate of decrease in λ_{AC} per time step. Therefore, the expected net rate of increase in λ_{AC} per time step is

$$f_A f_C K(1-f_b) - f_A(1-f_C)Kf_b = Kf_A(f_C-f_b) \qquad (F)$$

This is positive, i.e., λ_{AC} is increasing, if $f_C > f_b$ (f_A, f_C, and f_b are all assumed positive or zero), negative, i.e., λ_{AC} is decreasing, if $f_C < f_b$ and zero if $f_A = 0$ or $f_C = f_b$. This relation (F) Crichton gives as the fundamental formula for trends in synapse-levels.

These relationships provided very useful guides and were used in the correlation experiments. However, a few points should be noted: (1) In the current experiments, the assumption of independence of firing of the neurons does not hold. As N increases, however, one would expect it to become more plausible. The validity of Crichton's analysis therefore increases with N in the present situation. (2) Although his theory yields fruitful relations between Δ_1, Δ_2, $U(\lambda)$, and $D(\lambda)$ and is useful in analyzing trends in synapse-levels, yet, beyond the bound mentioned it says nothing about the form of the threshold, fatigue, and synapse-value functions. The analysis of Chapter 4 does yield information about the former.

3.4.3 Summary of Experimental Results

Just the general conclusions obtained together with one prototype experiment will be mentioned here. For further details the reader is referred to Finley [7].

The hypothesis was successfully demonstrated for a variety of

functions V, ϕ, and S (U(λ) and D(λ)). Several observations are noteworthy, however:

(a) The rate of decay of fatigue was, in general, too fast. It appeared that a slight hysteresis effect would be desirable. This would allow "trapping" neurons in lower fatigue states (higher fatigue values). For all the correlation experiments, Δ_1 and Δ_2 were not functions of ℓ, as they were defined in Chapter 2. The correlation experiments directly inspired the modification to make them so.

(b) The synapse-levels required a fairly strong positive bias (reflected on the values of U(λ) and D(λ)) to allow proper growth of the λ_{B_iC}'s. The setting of this "bias" (via setting U and D) is very critical. Below a certain setting, the synapse levels λ_{B_iC} tended rather rapidly to values giving negative synapse values, while the λ_{A_iC} become larger ($S(\lambda_{A_iC})$ more excitatory) — the very opposite behavior predicted by the hypothesis. In this case, the recruitment of neurons, an essential property of the networks to guarantee cell-assembly formation, would be impossible (see Chapter 7). Once again, inclusion of a "trapping" feature seemed desirable.

(c) The results seemed excessively dependent upon the form of the threshold curve.

The results of one of the correlation experiments are summarized in Figure 3.1 together with the network functions and parameters.

At this point it was decided that, rather than pursue experiments with these cycle-less networks any further, it would be of greater profit to introduce cycles into the networks and increase the network sizes substantially. Immediately a wide range of problems arise of a far more difficult and subtle nature than any encountered in the correlation experiments. The remaining chapters of this work are devoted to networks with cycles.

Figure 3.1. Sample Correlation Experiment.

For this experiment, M = 16, $f_B = 1/6$, $f_A = 1/13$, U = 0.5402, D = 0.04502, $\Delta_1 = 3/4$, $\Delta_2 = 1/16$. The curves $V(r)$, $\phi(\ell)$, and $S(\lambda)$ used are given below. Results: After 10,000 time steps, the firing rate of C approximated f_B; $\overline{S_A} = S(\lambda_{\overline{AC}})$ tended to $\frac{1}{2} S_B = \frac{1}{2} S(\lambda_{BC})$.

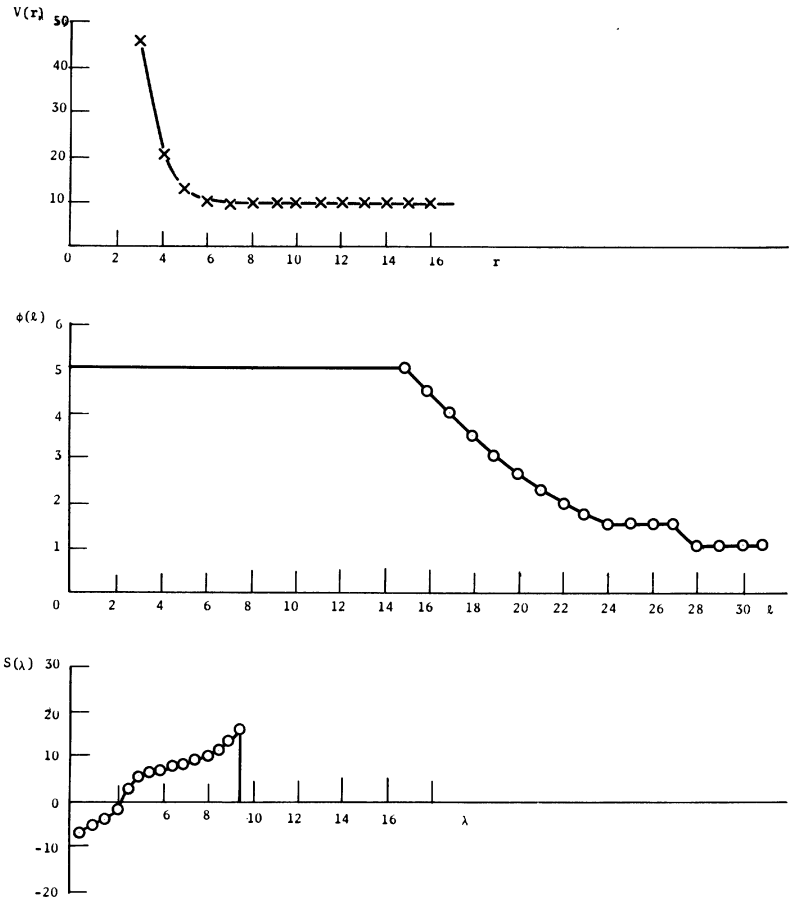

4 NETWORKS WITH CYCLES

4.1 Forword

Consider a network $\mathcal{N}$ in which the output of a neuron may act as input to several neurons, perhaps cycling back as input to itself. In general, such a closed path in which the terminal and initial vertices coincide will entail a chain of k intervenining neurons, where $r_a \leq k \leq K$. The lower bound is determined by the absolute recovery period, since an output of a neuron $i \in \mathcal{N}$ will have no effect if it returns to i in fewer than r_a time steps. The upper bound is determined by the density of connections in $\mathcal{N}$ and the size of $\mathcal{N}$, $N = |\mathcal{N}|$.

The intention is to introduce into $\mathcal{N}$ sufficient cyclic complexity that it will allow formation of closed, self-reexciting chains of neurons. Such chains of neurons, sometimes called reverberatory circuits, were suggested by Lorente de No as a mechanism for memory. This suggestion was partially adopted by Hebb [9] to explain the formation and operation of the cell-assembly (Hebb's "dual trace" mechanism, see Chapter 3, Section 3.1).

However, once such complexity is present, several major problems have to be resolved before cell-assembly formation can be studied. These problems center about the notion of stability, more specifically of stable, background behavior of $\mathcal{N}$. The first part of this chapter (Sections 4.2 and 4.3) is devoted to the development of this concept. Some problems that arise on this development are: (1) The choice of a network density function $\rho = \rho(r)$ giving the expected number of connections received by a neuron of $\mathcal{N}$ within a disk of radius r. In the first case considered (uniform random distribution case), $r = \infty$. In the second (distance-bias case), $0 < r < \infty$, the proper choice of r is a subproblem. (2) Given

the density function $\rho = \rho(r)$, develop an analysis relating the threshold curve and other network parameters of $\mathcal{N}$ so that stable-steady-stable behavior is guaranteed. (3) Modify this analysis to determine the effects on stable behavior of external stimuli.

It will be seen that a fairly complete steady-state calculus can be developed for the case ρ is not a function of distance. This calculus covers the case in which negative (inhibitory) connections are present in $\mathcal{N}$. In fact, it is later shown that such connections are absolutely necessary to ensure the desired stability conditions.

For the distance-bias case, development of a steady-state calculus presents formidable obstacles. However, the uniform random calculus may be applied fruitfully as an approximation. In both cases, ultimate "proof" rests on the simulation.

The latter part of the chapter (Sections 4.5 and 4.6) is concerned with (1) development of the concept of cell-assembly, (2) structural identification of a cell-assembly, and (3) dynamic characterization of cell-assemblies. Finally, an attempt is made to explore the interaction of two cell-assemblies.

The developments of this chapter are semiformal and heuristic in nature. In fact, they constitute something of an existential hypothesis of the form: "There exist networks $\mathcal{N}$ (with certain parameters specified) with such-and-such properties." The existence proof is then thrown back onto the simulation. While the conceptual developments may be heuristic, the simulation is not. As mentioned in Chapter 1, Section 1.1, a computer program itself constitutes a type of formal system, allowing rigorous testing of hypothesis such as the one above.

At the end of the chapter (Section 4.6), a brief summary of the main

results is given. A list of terms and symbols introduced in this chapter is appended at the end of the summary. Chapters 6 and 7 contain the experimental verification of the claims of this chapter.

4.2 Distributions of Connections

In the notation of Chapter 3, Section 3.2, networks $\mathcal{N}$ of N neurons shall be considered in which for any pair of neurons (j,i), the multiplicity m_{ji} of the connection from neuron j to neuron i, i.e., $j \to i$, is assigned initially by some rule. The set $\{m_{ji} \mid i, j = 1, 2, \ldots, N\}$ of all such m_{ji}'s constitutes a distribution of connections over the network. If $m_{ji} = 0$, there is no connection $j \to i$; if $m_{ji} = 1$, there is exactly one connection $j \to i$; if $m_{ji} = k$, neuron j sends exactly k connections to neuron i, etc. Exactly how this assignment is carried out is to be discussed in the next few sections, for the moment it is only assumed that it can be done. What is important is that an assignment scheme can be devised that will introduce a great variety of cyclic structure into the models, especially if the total number of connections and the number of neurons of $\mathcal{N}$ are large.

As, in general, different neurons will receive and emit different numbers of connections, some averaging process must be used to estimate the count of the number of connections a neuron receives or emits; this will constitute the expected number of connections received or emitted by a given neuron. As will be evident shortly, these two quantities will be identical, allowing definition of an extremely important parameter of connections received or emitted by a neuron of the network. ρ will be called the network density parameter or simply the density.

It is now necessary to examine the two theoretical models of networks

with cycles used in this study together with the associated connection-assignment schemes, then to contrast briefly the resulting networks. The first models to be examined are those of networks with uniform random distributions of connections, in which any neuron of $\mathcal{N}$ has the same probability of being connected to any other neuron in $\mathcal{N}$. The second class of models are those of networks with a distance bias on the distribution of connections, allowing neurons to be connected or not depending upon the distance between them. It will be seen that the latter class of models offers some definite advantages for this work, as well as great difficulties for attempts at analytic study. Note that as in the case of the models of Chapter 3, the problem of assigning the initial state of the networks must be examined very carefully, i.e., the initial assignments of the λ_{ji}'s, the r_i's the ℓ_i's and likewise the selection of the network functions V, S, and ϕ.

4.2.1 Networks with Uniform Random Distributions of Connections

In this section the class of networks with uniform random distributions of connections are characterized. From this characterization an efficient algorithm is extracted for evaluating the distribution $\{m_{ji}\}$ for any particular network $\mathcal{N}$. Note that a network with uniform random distribution of connections conforms to one's intuitive picture of a randomly connected network of neurons.

The Underlying Model (Urmodel)

Suppose a network, $\mathcal{N}$, of N neurons is given and a total of M connections are given to distribute over $\mathcal{N}$. Let the ordered pairs of neurons of $\mathcal{N}$, i.e., the elements of $\mathcal{N} \times \mathcal{N}$ be numbered from 1 to N^2. Associate with the pair of index ν a counter C_ν which is set to zero initially. Now perform M trials as follows: select a number ν at random

with probability $1/N^2$ from the given set and increment the counter C by 1 each time ν is selected. The number in the counter C_ν corresponding to the ordered pair (j,i) is interpreted as the number of connections neuron j sends to neuron i. This is a sampling with replacement model where essentially a random draw of an ordered pair out of an urn of N^2 such pairs is made, assigning a connection and putting it back. After M such samplings, the distribution of the number of connections assigned to pairs is binomial, i.e., the probability P_k that a given pair receive exactly k connections is given by the binomial probability $B_k(M,1/N^2) = \binom{M}{k}(\frac{1}{N^2})^k(1-\frac{1}{N^2})^{M-k}$ which, if the mean of the distribution $\rho_o = M/N^2$ is moderate in magnitude, while M is large and $1/N^2$ is small, may be approximated by the Poisson probability $p_k(\rho_o) = e^{-\rho_o}\frac{\rho_o{}^k}{k!}$.

Variant of Urnmodel

This model may be viewed somewhat differently as follows: scan through the list of ordered pairs, letting P_ν denote the number of pairs and F_ν the number of connections remaining after processing the ν-th pair as described below. For $\nu = 1$ (the first pair), $P_1 = M^2$ and $F_1 = M$. Now, for each ν, make F_ν throws with probability $1/P_\nu$ of "success" where success means that a connection is assigned to pair ν. Then reduce F_ν by the number of connections assigned C_ν and proceed on to the next pair, $\nu + 1$ with $F_{\nu+1} = F_\nu - C_\nu$. Now, it is easy to see by induction that the expected value of the C_ν, $E(C_\nu)$, equals $\rho_o = M/N^2$. For $\nu = 1$, C_1 is by definition M/N^2. For $\nu = \ell$ observe that the expectation of $C_{\ell-1}$ is $F_{\ell-1}/P_{\ell-1} = F_{\ell-1}/N^2 - (\ell-1) = \rho_o$ by the induction hypothesis. Now

$$F_\ell = F_{\ell-1} - \frac{F_{\ell-1}}{N^2-(\ell-1)} = \frac{F_{\ell-1}[N^2-(\ell-1)] - F_{\ell-1}}{N^2-(\ell-1)} = \frac{F_{\ell-1}[N^2-\ell]}{N^2-(\ell-1)} = \rho_o(N^2-\ell)$$

and $E(C_\ell) = F_\ell/N^2 - \ell = \rho_o$. Therefore, again ρ_o connections are expected

to be assigned per pair ν and the M connections are expected to be distributed binomially over the network (or, to a very good approximation, Poisson).

The advantage to this variant of the urmodel is that the random sampling of neuron pairs has been replaced by a systematic scansion of the ordered pairs of [illegible]. However, per pair ν, F_ν samplings must be done. These considerations lead to the following:

Approximation to the Urmodel

Again scan the ordered pairs, however this time performing M experiments per pair with probability $1/N^2$ of success (connection is assigned). The expected number of connections assigned per pair is still M/N^2; however, the total number M' of connections is a random variable whose expectation is M, i.e., $E(M') = M$. Once more an expected binomical distribution of connections over neurons results. The procedure is readily translated into a reasonably efficient programmable algorithm with the mean ρ_0 of the connections a neuron expects to receive from another neuron as parameter. Only $p_k(\rho_0)$ $(= e^{-\rho_0} \frac{\rho_0^k}{k!})$ that are numerically significant are calculated. A random number generator is used to simulate drawing a number, n, at random from the unit interval $0 \leqq n \leqq 1$, selecting $0, 1, \ldots, k$ connections depending upon whether $p_0(\rho_0)$, $p_0(\rho_0) + p_1(\rho_0)$, $\ldots$ $p_0(\rho_0) + p_1(\rho_0) + \ldots + p_k(\rho_0)$ exceed n or not (see Chapter 5, Sections 5.1 and 5.2).

Flow Charts

To bring out more graphically the structure of the three different algorithms outlined above, the corresponding flow charts are given in the next few pages. The same conventions are observed as in the flow chart given in Chapter 2, Section 2.2, representing the prototype of all experiments, q.v.

Flowchart 4.1 Algorithm for the Urmodel. The ordered pairs $(j,i) \in \mathcal{U}$ are numbered from $\nu = 1$ to N^2. For each ν, the counter C_ν contains at the termination of the algorithm the number of times the ν-th connection was selected. The C_ν's are assured to have been set to zeroes initially.

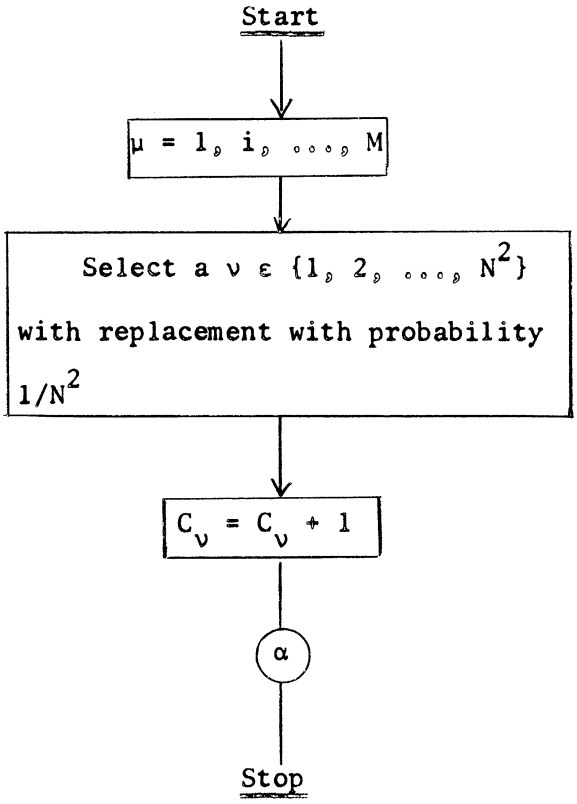

Flowchart 4.2 Algorithm for Variant of Urmodel. Ordering and indexing of connections as in Flowchart 4.1. Note that $E(C_\nu) = \rho_0$ for all $\nu \in \{1, 2, \ldots, N^2\}$ (see text for proof). The sequence $\{1, 2, \ldots, \nu\}$ is a variable length sequence beginning with $\{1, 2, \ldots, N^2\}$ and ending with $\{1\}$. The C_ν's are set to zero initially.

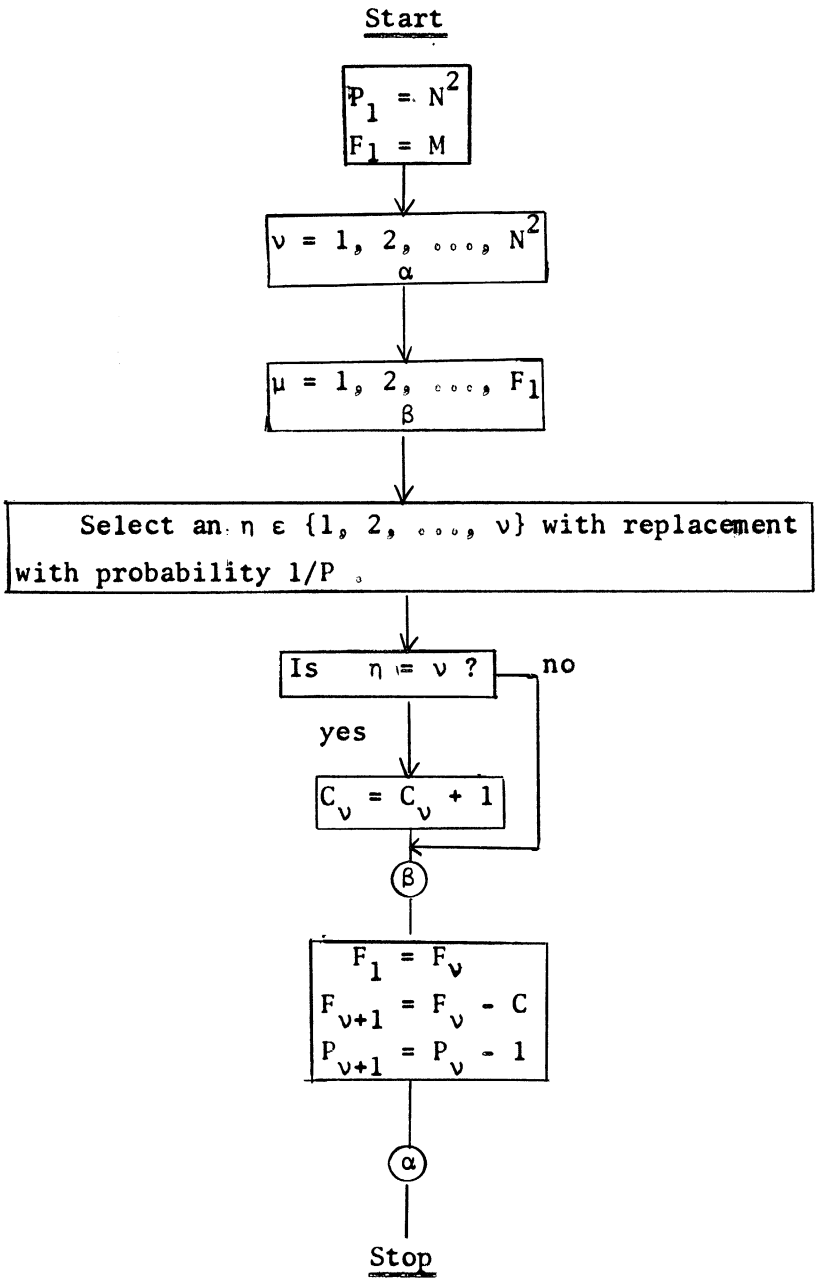

Flowchart 4.3 Ideal Algorithm for Connection-Assignment Procedure.

ν and C_ν are as in Flowcharts 4.1 and 4.2. The actual number of connections assigned is a random variable M' with $E(M') = M$. See text. The C_ν's are set to zeroes initially.

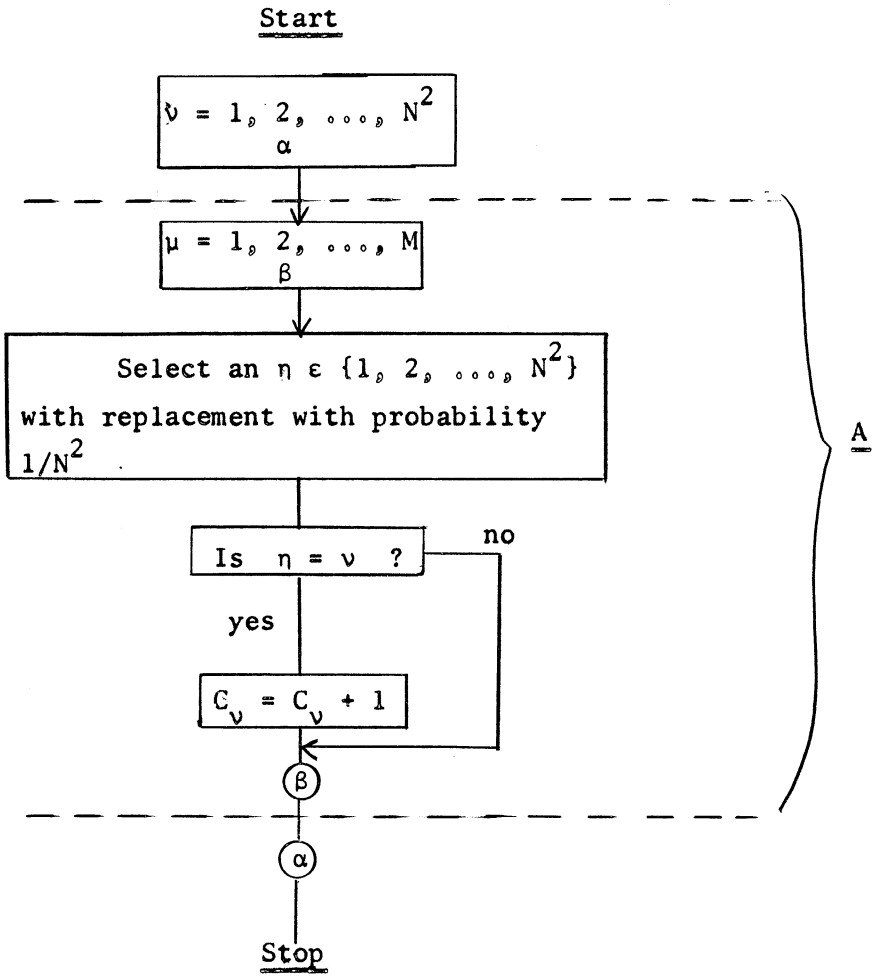

Flowchart 4.4 Implementation of Subprocedure A of Flowchart 4.3. The ideal selection procedure of Flowchart 4.3 is replaced by this procedure. See text for the definitions of the $p_K(\rho_0)$. In any given case, a K_{max} must be specified, assuming that the $p_\ell(\rho_0)$ are negligible for $\ell > K_{max}$. Consequently, for the algorithm to work, $\sum_{\ell=0}^{K_{max}} p_\ell(\rho_0)$ must equal unity. Drawing of the random number $n \in (0,1)$ is affected by the generator of Appendix B.

(For a given pair (j,i) ε [illegible] whose index is ν)

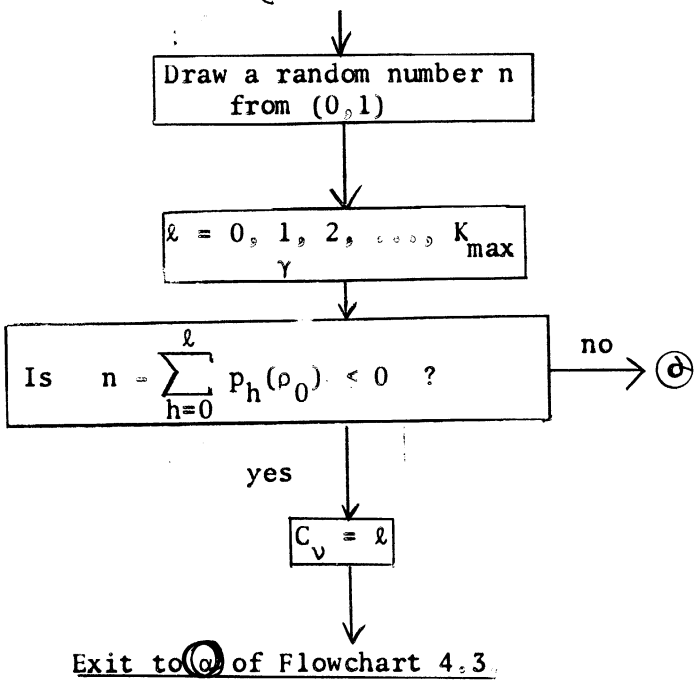

The Network Density ρ

In terms of the above discussion, define the quantity $\rho = N \cdot \rho_0$, that is, the expected number of connections a neuron receives from the whole net, as the network density parameter, or simply the density. By symmetry, this is also the expected number of connections a neuron emits to the entire network.

Uniform Random Distributions

By now it is clear that, whichever of the above procedures be adopted, in no way is any subset of neurons of $\mathcal{N}$ favored or not favored. The probabilities and expectations apply uniformly over all neurons of $\mathcal{N}$. Another way of phrasing this is that there is no bias on the density parameter ρ. Were this not the case, that is, if the definition of the assignment scheme included some definite criterion for including or excluding certain neurons of $\mathcal{N}$ (from the point of view of being connected to a given neuron), then in some sense a neighborhood structure would have been imposed over the network, resulting in some form of geometry over $\mathcal{N}$. This idea is explored in the next section, but first a few more observations about the uniform case are in order.

Connections between Subsets of $\mathcal{N}$

Of great interest in the sequel will be questions of the following type: given two subsets A and B of $\mathcal{N}$, what is the expected number of connections A receives from B and conversely? This is easily resolved in the present situation: Denote the cardinality of a set S by $\overline{\overline{S}}$ and assume that $\overline{\overline{A}}$ and $\overline{\overline{B}}$ are given. Let $\lambda(A \to B)$ and $\lambda(B \to A)$ denote respectively the expected number of connections B receives from A and conversely. The expected number of connections sent out to the network from A is $\overline{\overline{A}}\rho$, where ρ is the network density. Consequently, the expected number of

connections that an arbitrarily picked neuron of $\mathcal{N}$ receives is $A\rho/N$ since $\mathcal{N}$ is a random network. Therefore, the expected number of connections received by the entire subset B is $(\bar{A}\rho/N)\bar{B}$ minus the overlap $(\overline{A\cap B}\rho/N)\bar{A}$ (as these would be counted twice otherwise) and

$$\lambda(A\to B) = (\bar{A}\rho/N)\bar{B} - (\overline{A\cap B}\rho/N)\bar{A} = \frac{\bar{A}\rho}{N}[\bar{B}-\overline{A\cap B}]. \tag{I}$$

Similarly,

$$\lambda(B\to A) = \frac{\bar{B}\rho}{N}[\bar{A}-\overline{A\cap B}]$$

A second and related question now is also easily answered: suppose A and B are subsets of neurons randomly and independently distributed over $\mathcal{N}$, their exact magnitudes not known, but where $\bar{A}$ and $\bar{B}$ represent the expected sizes of A and B respectively. What form do $\lambda(A\to B)$ and $\lambda(B\to A)$ take now? Clearly, the basic formulas (I) above still hold, now the cardinality of the intersection $A\cap B$ may be estimated by $(\overline{AB}/N^2)N$ since the probability that a neuron of $\mathcal{N}$ lie in both A and B is $(\bar{A}/N)(\bar{B}/N) = \overline{AB}/N^2$ and N such neurons exist. Therefore

$$\lambda(A\to B) = \bar{A}(\bar{B}-\overline{A\ B})\rho/N$$
$$= \lambda_0(A)(\bar{B}-\frac{\overline{AB}}{N}) = \lambda_0(A)\bar{B}(1-\frac{\bar{A}}{N}).$$

Similarly, (II)

$$\lambda(B\to A) = \lambda(B)\bar{A}(1-\bar{B}/N)$$

where $\lambda(S)$ is the expected number of connections that an arbitrarily chosen neuron of $\mathcal{N}$ receives from $S\subseteq\mathcal{N}$.

Comment about Notation and Derivations

Perhaps the obvious has been belabored in this section, especially in deriving formulas (I) and (II) which are, after all, rather trivially deduced from elementary probability theory, but these procedures tend very often to be taken for granted. Hence, it was the intention here to

make them explicit so that the principles underlying later calculations may be quite clear. It also is of interest to contrast the marked simplicity of the uniform distribution case with the distance-bias case to be discussed in the next section.

An apology is definitely in order to the mathematically sophisticated reader for the mixing of symbol fonts to denote objects that belong to the same class of objects, e.g., $\mathcal{M}$, A, B, etc. to denote sets. However, the guiding maxim has been that one, familiar to all programmers, that goes: "use symbols that are convenient and have mnemonic value." In this paper, the intention is to apply mathematical analysis where possible and to the extent that it is fruitful, not on developing a mathematical theory per se.

4.2.2 Networks with Distance-Bias

In the previous section, networks were considered with connections distributed in a very simple way with the result that certain neurons may not be isolated a priori and the claim made that they do not receive or transmit connections from or to certain other neurons of the network. In a word, there is no provision for neighborhoodness in those models. Suppose then that a network $\mathcal{M}$ has a function $d = d(j,i)$ defined over it so that for any two pairs of neurons (j,i), d is the distance between j and i. Furthermore, assume that the connections are assigned to neuron pairs (j,i) with probabilities $\rho(j,i)$ that are functions of the distance $d(j,i)$. If the $\rho(j,i)$ are, say, inverse square functions of the $d(j,i)$, $\rho(d) = K/d(j,i)^2$, then the density of connections is the greatest for small $d(j,i)$ and the smallest for large $d(j,i)$. Considering the universality of inverse square laws in the physical sciences, this does not

seem to be an unnatural assumption. Some special assumptions must be made as $d(j,i)$ tends to zero, of course, but as shall be seen later (Section 4.3.4), this presents no real problem although it does it does pose some interesting questions about the density of connections in actual cortical networks in the immediate vicinity of a neuron, perhaps to be tested by future neuro-physiological experiments.

The distribution yielding $\rho(d) = K/d(j,i)^2$ does not necessarily insulate distal parts of $\{i\}$; it merely lowers the probabilities of two neurons in separate, but distal, areas being connected. The favoritism excluded in the case of uniform distributions is therefore allowed; neighborhoodness is defined.

In general, $\rho(d)$ will be a monotone decreasing function of d, tending to 0 as $d \to \infty$. One possibility, to be discussed in more detail in Section 4.3.4, is to set $\rho(d) = \rho =$ constant for $d \leq R$ for some fixed R and $\rho(d) = 0$ for $d > R$, using the basic technique of Section 4.2.1 for determining the connections received by a neuron within the neighborhood with radius R. This gives a distribution that is "flat" — i.e., uniform and random in the neighborhood $d \leq R$ of a given neuron and zero elsewhere. The advantage to such a distribution is that $\{i\}$ may be regarded from the point of view of Section 4.2.1 in sufficiently small regions. Clearly, this procedure may be generalized to that in which the distribution is uniform in the neighborhood $d \leq R$ with density ρ_1, uniform in the neighborhood $R < d \leq R_2$ with density ρ_2, uniform in the neighborhood $R_2 < d \leq R_3$ with density ρ_3, etc. The latter type of distribution may be used as an approximation to the inverse-square distribution by appropriate settings of the disk $d \leq R$ and the annuli $R_{k-1} < d \leq R_k$, $k = 1, 2, \ldots$ together with the corresponding densities ρ_k.

Connections between Subsets of

Just as in the case of networks with uniform random distributions of connections, it is necessary to calculate the expected number of connections, $\lambda(B \to A)$ that a subset A of receives from another subset B. It will be seen that this is no longer such a simple chore.

Pass over for the moment to the continuous case as an approximation to the discrete networks of the model. Consider to be a closed and bounded subset of the real plane E_2 and let d be the usual metric over E_2. Of course, the discrete case may always be re-obtained by appropriate choice of grid size. Let A and B be subsets of and assume the intersection $A \cap B = 0$. A and B are of arbitrary shapes. The density function $\rho(d)$ now takes the form $\rho(w,z)$, the expected number of connections received at point w from a unit of area about point z. Then, if $w \in A$, $z \in B$, the expected number of connections received from an element of area about the point $z \in B$ by an element of area about the point w is

$$\Delta A(w)\rho(w,z)\Delta B(z)$$

and from all of B is,

$$\Delta A(w) \int_{z \in B} \rho(w,z)dB(z)$$

and, therefore, all of A expects to receive:

$$\lambda(B \to A) = \int_{w \in A} dA(w) \int_{z \in B} \rho(w,z)dB(z). \qquad \text{(III)}$$

For arbitrary configurations of A and B, such an integral will be tedious to evaluate. In fact, integrals of form (III) are similar to those arising in physics in attempting to evaluate the electrostatic force field about a charged body of arbitrary shape, the difficulties encountered in their calculations are expected to be similar. Approximations to (III) shall be considered later (Section 4.3.4) for particularly simple forms of A and B. Moreover, the simple disk-type distribution will be seen

to be perfectly adequate for the present study, thereby avoiding some of the computational problems of the inverse-square type of distribution.

4.2.3 Brief Contrast of Uniform and Distance-Bias Distribution

It has already been remarked that in the case of networks with uniform distributions of connections, there is no notion of neighborhoodness except in the trivial sense that any neuron of a network $\mathcal{N}$ is equally like to be a neighbor of any other neuron. This means that no localization of phenomena may be expected if the assignment scheme is reasonably random. Yet, with all the physiological results of Burns [1] and others in mind, as well as the considerations of Hebb's theory, localization is intuitively exactly the sort of thing required in the models. Therefore, rather naturally the distance-bias case arises in which activity may occur in one part of the network without immediately affecting another (distal) part. It will be seen, both experimentally and theoretically, in the sequel, just how important this consideration really is. Because of their inherent simplicity, however, networks with uniform distributions are chosen as the starting point. The results obtained will be used as a basis for analyzing networks with distance-bias of the simple disk type outlined above.

4.3 Stimulus-Free Behavior in Networks with Cycles

In Chapter 3, the response of certain networks to various types of stimulus patterns was studied. As there was no feedback among the neurons of those networks, they were completely stimulus dependent and there was no question of stimulus-independent activity. In the case of networks with cycles, however, whichever of the two basic types discussed above be chosen, it is entirely possible that a network, once certain neurons have

been made to fire at t = 0, maintain an activity independently of external stimuli for a large number of consecutive time steps; the number of neurons firing at time t, F(t), does not become zero until t becomes very large. This, of course is due to the feedback present in such models.

The following considerations illustrate the nature of this feedback together with several other important factors of interest at this time.

4.3.1 Steady-State Behavior

The sequence of firings of neurons of $\mathcal{M}$, F(0), F(1), F(2), ..., F(t), F(t+1), ... will be called the behavior of $\mathcal{M}$ that occurs as a consequence of F(0) neurons being caused to fire at t = 0. It is necessary to determine how this behavior depends upon the initial set of neurons fired, F_0, and the network parameters r_i, l_i, i = 1, ..., N, λ_{ji}, i,j = 1, ..., N together with the network functions V, S, and ϕ.

Example of a Simple Cycle

Suppose F_0 consists solely of one neuron i_1 and also that the assignment of connections over $\mathcal{M}$ is such that there is a cycle $i_1 \to i_2 \to i_3 \to \cdots \to i_k \to i_1$ of neurons of $\mathcal{M}$. Assume, for simplicity, that these neurons have no other inputs. What happens after stimulation of i_1 depends critically upon the parameters and functions listed above. For example, if $\lambda_{i_1 i_2}$ is such that the synapse value from i_1 to i_2 is less than the effective threshold of i_2, then i_2 will not fire at t = 1 and F(1) will, of course, be zero. Likewise for i_2 to i_3, ..., i_{k-1} to i_k. On the other hand, if the synapse-values and effective threshold values are appropriately set, then the firing of i_1 at t = 0 will cause i_2 to fire at t = 1, ..., i_{k-1} firing at t = k - 2 will cause i_k to fire at t = k - 1.

The firing of i_k at $t = k - 1$ now will cause i_1 to fire at $t = k$ provided that the effective threshold of i_1 has recovered sufficiently from the firing at $t = 0$. Similarly, i_1 will cause i_2 to fire at $t = k + 1$ if i_2 has recovered sufficiently, etc. Hence, for appropriate initial settings of the recovery and fatigue states, the synapse-levels, and the functions V, S, and ϕ, a "pulse" may be caused to circulate around the closed cycle $i_1 \rightarrow i_2 \rightarrow \ldots \rightarrow i_k \rightarrow i_1$. If the length k of the cycle is equal or greater than the fatigue period, it will continue to circulate indefinitely, but if k is short with respect to the fatigue period (the usual case), the fatigue values of the neurons will increase until at some point the firing of one of the neurons is suppressed and the pulse is extinguished.

This simple example illustrates the basic ideas very well: the choice of network parameters and functions must be made judiciously to insure that pulses may circulate about in a network with cycles.

Cycles of Subsets

Now let $\mathcal{N}$ be a network with density ρ (which may be a function of distance) and $\rho > 1$. There may then be many cycles involving any particular neuron and the situation is not as simple as above. However, the same general conclusions may be drawn as follows:

Let F(t) denote the subset of neurons of $\mathcal{N}$ that fire at time t, where F(0) is the set of neurons caused to be fired at $t = 0$. Let S_1 be the subset of neurons of $\mathcal{N}$ that receive one or more connections from F(0), $F(1) \subseteq S_1$. Whether or not a neuron of S_1 fires, i.e., is a neuron of F(1) as well, depends upon its effective threshold and the total number of inputs it receives from F(0). Likewise, if S_{k+1} is the subset of neurons of $\mathcal{N}$ that receive one or more connections from F(k), then a neuron in S_{k+1} fires, i.e., is in F(k+1), as determined by

its effective threshold and total input. Therefore, the following general process is obtained:

$$\begin{array}{l} F(0) \to S_1 \\ \quad \cup \\ \quad F(1) \to S_2 \\ \quad\quad \cup \\ \quad\quad F(2) \to S_3 \\ \quad\quad\quad \cup \\ \quad\quad\quad F(3) \to \cdots \end{array}$$

where the notation $F(k) \to S_{k+1}$ means that S_{k+1} is the subset of receiving connections from $F(k)$. The successive S_i's need not be mutually disjoint: in general, $S_k \cap S_j \neq 0$ for $j,k = 0, 1, 2, \cdots$. However, since a neuron cannot fire in its absolute refractory period, the $F(i)$'s will be disjoint up to at least the r_a-1'th successor:

$F(i) \cap F(i+1) = 0 = F(i) \cap F(i+2) = \cdots = F(i) \cap F(i+r_a-1)$ for $i = 1, 2, \cdots$;

but it may occur that

$$F(i) \cap F(j) \neq 0 \text{ for } j \geq i + r_a.$$

To avoid $\bar{F}(t)$ going to zero as t increases, the initial choice of the λ_{ji}'s, r_i's, etc. must be made very carefully. Assuming such a choice is possible (see next section), the successor sets S_i will exhaust after some number k_0 time steps. Likewise, tracing the successor sets $F(i)$, after a certain number k_1 time steps, every neuron of would be expected to occur in some $F(i)$.

This does not mean that an exact cycle of subsets $F(0) \to F(1) \to F(2) \to \cdots F(k) \to F(0)$ will be obtained, since, for example, $F(\ell)$ may overlap $F(0)$ for some $0 < \ell < k$ and the neurons in successive $F(i)$'s become very shuffled. However, it may be that after $F(k)$ fires,

a large part of the original F(0) fires plus some new neurons, say F(0)'. Likewise, F(0)' may cause a set F(1)' to fire where F(1) ∩ F(1)' ≠ 0, etc. A quasi-cyclic firing of subsets would be obtained:

$$F(0) \to F(1) \to \cdots F(k) \to F(0)' \to F(1)' \to \cdots F(k)' \to F(0)'' \to F(1)'' \to \cdots$$

Exactly how far this quasi-cyclic sequence deviates from the purely cyclic one depends upon the size of $\mathcal{N}$ and the density ρ, the network parameters and function settings, in particular the threshold curve and the distribution of positive versus negative connections in

Implication of a Stable, Steady-State Behavior

These considerations point to the possibility of a stable, steady-state behavior, that is, a sequence F(0), F(1), ..., F(t), ... where the expected values of the $\overline{F}(t)$ are the same for all time, i.e., $E(\overline{F}(t)) = \text{constant} = F_b$ for all t. Each neuron of $\mathcal{N}$ will then fire at an expected rate f_b, the background rate of the network.

Motivation for Considering Steady-State Behavior

The concept of stable, steady-state behavior is intimately connected with the basic objective of this study, namely, the formation and development of cell-assemblies. A cell-assembly is to come into existence, as a result of appropriately applied stimulus to the network, via the mechanism of the synapse-level growth law. A cell-assembly may be regarded as a learned response to the given stimulus. The precise physical identification of a cell-assembly is a difficult matter and forms the goal of Sections 4.4, 4.5, and 4.6 below. For now it is sufficient to note that a given cell-assembly is identified structurally by means of conditions on the synapse-levels of connections among the neurons of the assembly as well as between the neurons of the assembly and the remainder of the network; letting C be the neurons of the assembly, then the structure of C

is determined by a set T_C of conditions on λ_{ji} for all $j,i \in C$ and on λ_{kl} for $k \in C$, $l \notin C$, or $k \notin C$ and $l \in C$.

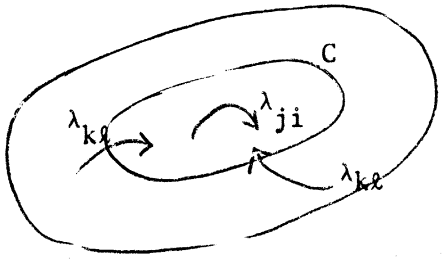

Since permanent learning of the model resides in the synapse-levels, the primary condition on steady-state behavior is that it not perturb existing synapse-levels so that the conditions T_C no longer obtain, therefore possibly disrupting an existing cell-assembly, nor that it give rise to any new cell-assemblies. In other words, steady-state should act to preserve the status quo of the network, structurally speaking. This is essentially the reason behind the derivation of the equation

$$f_b = D(\lambda)/[U(\lambda) + D(\lambda)]$$

in Section 2.3.4 which relates the nominal system average or background firing rate f_b of $\mathcal{N}$ to the probabilities $U(\lambda)$ and $D(\lambda)$. Since the firing rate of a neuron is determined by the threshold and fatigue functions, these two functions must be adjusted to preserve an overall firing rate of f_b. Thus, for a network to operate at steady-state with a background firing rate f_b, conditions are imposed on all the network functions V, ϕ, and S.

The next question is: what should F_b be? The answer to this brings out yet another facet of steady-state behavior. It is clear that F_b cannot be 0: Suppose a network $\mathcal{N}$ has been quiescent for several hundred time steps, say, $F(t) = 0$ for $t = 0, 1, \ldots, 200$. All neurons will be completely recovered with respect to threshold and fatigue: for all $i \in \mathcal{N}$, $r_i = r_{max}$ and $\ell_i = \ell_{max}$. For simplicity, assume all synapse-

levels are set to a common value λ_0 so that $S(\lambda_0)$ is moderately positive and that $V_q = S(\lambda_0)$ (quiescent value of threshold).

If a stimulus is presented at t = 201 to a subset Σ_0 of $\mathcal{N}$ causing all neurons of Σ_0 to fire, then every neuron of $\mathcal{N} - \Sigma_0$ that receives connections from Σ_0 will fire at t = 202. Denote the set of such neurons by Σ_1. In general, Σ_1 will be larger than Σ_0. Likewise, Σ_1 will cause a set Σ_2 of neurons to fire at t = 203, $\Sigma_2 \subset \mathcal{N} - \Sigma_0 - \Sigma_1$. Again, Σ_2 will be larger than Σ_1, etc. The sets Σ_i, i = 0, 1, 2, ... will continue to grow in cardinality until $\mathcal{N} - \Sigma_0 - \Sigma_1 - \Sigma_2 - \ldots$ is exhausted; there exists a k_0 such that

$$\overline{\overline{\Sigma}}_0 \leq \overline{\overline{\Sigma}}_1 \leq \ldots \leq \overline{\overline{\Sigma}}_{k_0}$$

and a k_1, $k_0 < k_1$ such that

$$\overline{\overline{\Sigma}}_{k_0} \geq \overline{\overline{\Sigma}}_{k_0+1} \geq \ldots \geq \overline{\overline{\Sigma}}_{k_1}.$$

The numbers k_0 and k_1 depend upon N, ρ, the threshold curve and Σ_0. Generally, $k_1 = r_{max}$.

This is an extreme case; the same principle holds true, however, if the synapse-levels vary over a range of values (provided there are some positive values, of course). The presence of negative connections merely tends to increase k_1.

Therefore, the following general principle may be stated; steady-state behavior in a network $\mathcal{N}$ must be such that large groups of highly recovered neurons do not come into existence. Otherwise, the possibility of a violent oscillation or a series of such oscillations in F(t) exists. Worse still, such oscillations, as the example shows are usually fatal; F(t) goes to 0.

These violent oscillations are undesirable from many points of view; first of all, they may be fatal. Secondly, if they arise as a consequence

of application of stimulus to the network (presumably operating up to that time in steady-state), they could act to make $\mathcal{N}$ insensitive to future stimulus. In this case, $\mathcal{N}$ is deprived of opportunities for further learning.

The condition of violent oscillations in a network $\mathcal{N}$ will be referred to as "epilepsy" in analogy with the neuro-pathological condition found in human beings. It is interesting to note the similarities of the sequences $\{\underline{F}(t)\}$ with an electroencephalogram of a patient undergoing an epileptic seizure.

To summarize: the functions of steady-state behavior are two: (1) to preserve the status quo of any existing structures and, likewise, not to give rise to any new structures in the network, (2) to preserve a distribution of neurons over recovery states so that large groups of highly recovered neurons do not evolve. From these, certain conclusions may be drawn, to be made more precise in the sequel; (3) F_b $(=E(\overline{\overline{F}}(t))$ must not be too small; (4) $\overline{\overline{F}}(t)$ cannot vary too far from F_b; (5) a single application of a moderate sized stimulus to a network operating in steady-state must not produce epilepsy.

It will be seen that the effect of stimulus upon a network operating in steady-state is similar to modulation of a carrier wave by an information bearing signal in AM radio transmission.

Notice that the symbol F(t) is now used to denote the set of neurons firing at, now for the cardinality of this set (strictly, $\overline{\overline{F}}(t)$). Since it will always be clear from context which is meant, only F(t) will be written from now on.

4.3.2 The Threshold Curve and Steady-State Analysis

The purpose of this section is to display the role of the threshold

curve in determining steady-state behavior. A simple computational scheme is given whereby the behavior of a given network with uniform random distribution of connections may be predicted as a function of the size N, density ρ, distribution of synapse values, the form of the threshold curve V(r), and the number of neurons firing at t = 0, F(0). This scheme allows computation of the expected value of F(t+1) as a function of F(t), t = 0, 1, 2, ... While it is tedious to perform the calculations of the F(t)'s by hand for more than about twenty time steps, yet within this relatively short time span, tendencies toward oscillatory or stable behavior are readily discerned. Using the network parameter values thus obtained for a stable case, the actual behavior of the corresponding model may be tested and compared with the predicted behavior. Gross deviations of the experimentally obtained behavior from the predicted would indicate either statistical anomalies in the model or the malfunction of some network function. An example of the first case would be a skewing in the connection distribution. In the second case, the calculations might indicate that a given network should be stable, but the experimentally obtained behavior might develop fatal oscillations after, say, several thousand times steps. While a statistical deficiency in the model might explain this, the long period of stable behavior suggests the cumulative effect of some network function such as fatigue or the synapse-level growth law that has little effect on behavior over relatively short time intervals, but might well have a deleterious effect over longer intervals, if not properly adjusted initially.

The scheme is presented first in its simplest form in which the distribution of synapse-values over connections is uniform, i.e., all the S_{ji}'s are equal. It is then modified to comprise progressively more

complicated distributions. The importance of negative synapse-values as a source of negative feedback is emphasized. This scheme is modified in Section 4.3.4 to treat networks with distance-bias.

Consider a network $\mathcal{N}$ of size N and density ρ, ρ not a function of the distance. Let V(r) be the threshold function of $\mathcal{N}$ where r_a and r_q are the absolute refractory period and the quiescent value of the recovery respectively. Let the initial assignments of the $\lambda_{ji}(0)$'s be $\lambda_{ji}(0) = \lambda_0$ = constant for all $j,i = 1, 2, 3, \ldots, N$ such that $S_{ji}(0) = S(\lambda_{ji}(0)) = S(\lambda_0) = V_0$ where $V_0 > 0$. The threshold curve is expressed in terms of V_0 : $V(r_i) = m(r_i)V_0$, $i = 1, 2, \ldots, N$. The fatigue function is assumed to be constant for the moment, $\phi(\ell_i(t)) \equiv 0$ for $i = 1, \ldots, N$. $V(r_i)$ is then the effective threshold of neuron i. The quiescent value V_q will be taken as V_0, $V(r_q) = V_0$. In other words, a fully recovered neuron may be fired by a single synapse of level λ_0.

Define $R_r(t)$ as the set of neurons of $\mathcal{N}$ that have recovery state r at time t; $R_0(t)$ will be the set of neurons that fire at t, $R_0(t) = F(t)$. The set $\hat{R}_{r_q}$ will be regarded as the union of all the R_r's for $r \geq r_q$ since a neuron need not fire when it recovers to r_q, $\hat{R}_{r_q} = R_{r_q} \; R_{r_q+1} \; \cdots \; R_{r_m}$. The set

$$\mathcal{R}(t) = \{R_r(t) \quad r = 0, 1, \ldots, r_q\}$$

is the distribution of neurons over recovery states at time t. Given $\mathcal{R}(0)$, one may computer successively the expected values of $\mathcal{R}(1), \mathcal{R}(2), \ldots, \mathcal{R}(t), \mathcal{R}(t+1), \ldots$ as follows:

Suppose $R_0(t)$ neurons fire at time t. The expected number of neurons of $\mathcal{N}$, $N_k(t)$, that receive at least k connections, $k > 0$, from $R_0(t)$ may be computed from the equation:

$$\overline{\overline{N}}_k(t) = N\Pi_k(\lambda(t)) \qquad \text{where} \qquad \lambda(t) = \frac{\overline{\overline{R}}_0(t)}{N}\rho.$$

$\lambda(t)$ is the expected number of connections received by a neuron of from $R_0(t) \subseteq \mathcal{N}$ and $\pi_k(\lambda(t))$ is the probability that such a neuron receive at least k connections from $R_0(t)$, i = 0, 1, 2, ...,

$$\pi_k(t) = \sum_{\ell=k}^{\infty} e^{-\lambda(t)} \frac{[\lambda(t)]^{\ell}}{\ell}.$$

From the threshold curve and R(t), for ℓ = 1, 2, ..., one can determine the subsets $M_i(t) \subseteq \mathcal{N}$ of neurons requiring at least k connections to fire. The probability that a neuron lie in $N_k(t)$ and $M_k(t)$, i.e., that it receive at least k connections from $R_0(t)$ and require at least k connections to fire may be approximated for large N by

$$\frac{\overline{\overline{N}}_k(t) \circ M_k(t)}{N^2}$$

and the expected size of $N_k(t) \cap M_k(t)$ is

$$N \circ \frac{\overline{\overline{N}}_k(t) \circ \overline{\overline{M}}_k(t)}{N^2} = \frac{\overline{\overline{N}}_k(t) \circ \overline{\overline{M}}_k(t)}{N} = \pi_k(\lambda(t))\ \overline{\overline{M}}_k(t)$$

Then, the expected set of neurons firing at t + 1 is given as

$$R_0(t+1) = \bigcup_{k=1}^{\infty} N_k(t) \cap M_k(t)$$

and the new R_r's, $r \geq 1$, are given by

$$R_r(t+1) = R_{r-1}(t) - R^*_{r-1}(t) \qquad \text{(expected values)}$$

where $R^*_r(t)$ is the set of neurons of $R_r(t)$ that are expected to fire at t,

$$R^*_r(t) = R_r(t) \cap N_k(t)$$

In the preceding section it was noted that in steady-state behavior, the expected value of F(t) is constant for all t, F(t) = constant = F_b. Gross deviation in F(t) from F_b tend to produce fatal oscillations. The problem is to design the threshold curve so that such deviations do

not occur under conditions of no stimulus to the network. This is now readily done using the scheme developed above.

Suppose the initial distribution $\mathcal{R}(0)$ is such that

$$\bar{\bar{R}}_0(0) = F_b = \bar{\bar{R}}_1(0) = \bar{\bar{R}}_2(0) = \cdots = \bar{\bar{R}}_{r_q}(0) = \cdots = \bar{\bar{R}}_{r_m}$$

Now make the following assumptions:

(1) the parameters ρ and $R_{r_q}(0)$ are chosen such that

$$\pi_k(\lambda(0))\bar{\bar{R}}_{r_q}(0) = F_b \quad ; \quad \lambda(0) = \frac{\bar{\bar{R}}_0(0)}{N}\rho = \frac{F_b}{N}\rho.$$

Notice the set $R_{r_q}(t)$ is identical to $M_1(t)$.

(2) the threshold curve is such that

$R^*_{k(r)} = 0$ for $r = r_a, r_a+1, \ldots, r_q-1$, $k(r)$ = values determined by the curve.

From (1) it follows that $\bar{\bar{R}}_0(1) = \pi_k(\lambda(0))\bar{\bar{R}}_{r_q}(0) = F_b$.

Moreover,

$$\lambda(1) = \frac{\bar{\bar{R}}_0(1)}{N}\rho = \frac{f_b}{N}\rho = \lambda(0).$$

From (2) it follows that

$$\bar{\bar{R}}_r(1) = F_b, \; r = 1, 2, \ldots, r_q-1 .$$

and that

$$\bar{\bar{R}}_{r_q}(1) = \bar{\bar{R}}_{r_q}(0).$$

Therefore, by (1) again,

$$\bar{\bar{R}}_0(2) = \pi_k(\lambda(1))R_{r_q}(1) = F_b$$

and by (2),

$$\bar{\bar{R}}_r(2) = F_b, \quad r = 1, 2, \ldots, r_q-1$$

with

$$\bar{\bar{R}}_{r_q}(2) = \bar{\bar{R}}_{r_q}(1) = \bar{\bar{R}}_{r_q}(0).$$

By induction, it is clear that for $t = 0, 1, 2, \ldots,$

$$\bar{\bar{R}}_0(t) = F_b \quad \text{(expected number of neurons firing at t)}$$

and

$$\bar{\bar{R}}_r(t) = F_b, \; r = 1, 2, \ldots, r_q - 1$$

where

$$\bar{\bar{R}}_{r_q}(t) = \bar{\bar{R}}_{r_q}(0).$$

To summarize: pick a threshold curve with the property that the only fireable neurons at time t will be those in $\hat{R}_{r_q}(t)$. Choose ρ, N, and $\hat{R}_{r_q}(0)$ so that precisely F_b neurons of $\hat{R}_{r_q}(t)$ are expected to fire at time t. Figures 4.1, 4.2, and 4.3 illustrate the concepts of this section.

There is an interesting consequence of this analysis: since the expectations of

$$\bar{\bar{R}}_0(t), \bar{\bar{R}}_1(t), \ldots, \bar{\bar{R}}_{r_q-1}(t)$$

are equal to F_b, then

$$r_m \times F_b = N.$$

From Figure 4.1, it is seen that a neuron is expected to fire in the recovery range $r_q \leq r \leq r_m$. The expected firing rate is $N/F_b = r_m$. It is convenient to regard this expectation as another variable $\hat{r}_q$ and take $N/F_b = \hat{r}_q$, where $\hat{r}_q$ relates to the actual limit on recovery by the bounds $r_q \leq \hat{r}_q \leq r_m$. The purpose behind this is that it allows greater freedom is setting the bounds r_q and r_m used in determining $\hat{R}_{r_q}(t) = M_1(t)$. Therefore, in place of the quality above, the following shall be used for relating F_b and N:

$$\hat{r}_q = \frac{N}{F_b}.$$

This analysis is based on the computation of expected values. As such, it proved a very effective guide to correct setting of network

parameters. In practice, of course, there is a variation in the $\bar{\bar{R}}_r(t)$, for $r = 0, \ldots, \hat{r}_q$, and neurons of $M_2(t)$, $M_3(t)$, ... may fire. Within certain limits in the variance of $F(t)$, no harm will result. It is important to note, however, that no mechanism has yet been presented for damping out significant transient deviations of $F(t)$ from F_b. In other words, to obtain steady-state with the techniques given thus far, the network parameters have to be very precisely tuned with little room for variation. This will be the subject of the following Section 4.3.3.

A sample steady-state calculation follows. In general it was found sufficient to perform the calculations for about thirty time steps; that is, if the calculations to that point had not produced violent oscillations, then the simulated network would be stable.

Sample Stability Calculation

This calculation is given in some detail in order that the techniques used in Chapters 5 and 6 may be perfectly clear. Consider the threshold curve of Figure 4.4. $r_a = 3$, $r_q = 16$, $r_m = 19$ and $\hat{r}_q = r_m$, and $V_0 = 1$. There are eight distinct sets $M_k(t)$, $k = 1, 2, \ldots, 8$. The network is assumed to contain 400 neurons, $N = 400$. Since there are twenty basic units of recovery (all the recovery classes are expected to have equal cardinality in steady-state), F_b will be chosen as

$$F_b = \frac{N}{\hat{r}_q} = \frac{400}{20} = 20.$$

For this network, $\rho = 6$ and the number of neurons that are forced to fire at $t = 0$ is twenty, $F(0) = 20$. These neurons are assumed to come from $\hat{R}_{r_q}(0)$.

The calculations are presented in Table 4.1. They are carried out to $t = 30$. Notice that a few neurons enter R_0 from M_2, the predominant part, of course, coming from M_1. The values of $\pi_k(\lambda(t)$ are taken from

standard tables of the cumulative Poisson distribution.[1] For the range of $\lambda(t)$ involved here, $\pi_k(\lambda(t))$ is negligible for $k > 2$.

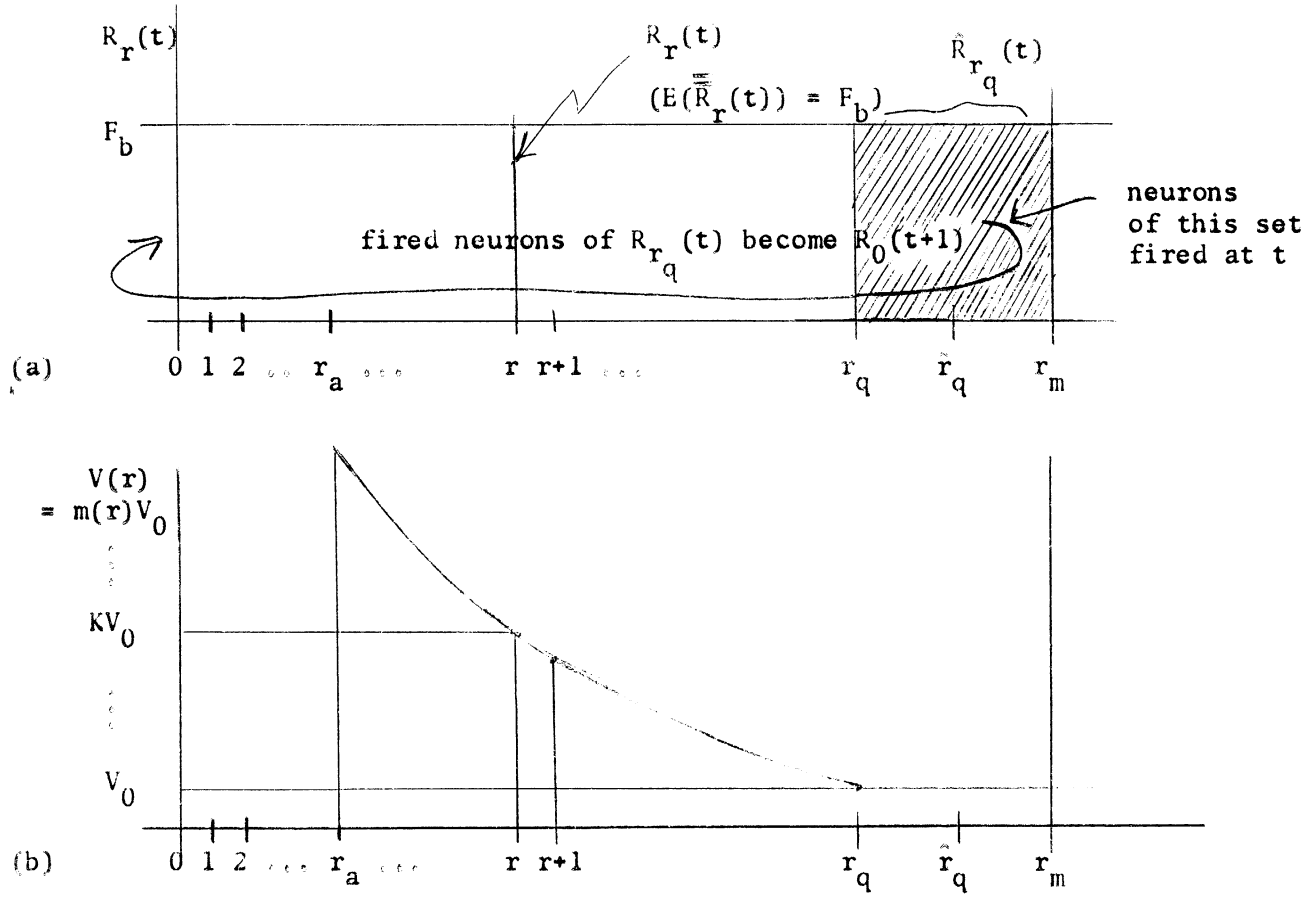

Figure 4.1. Graph of R(t) (a) vis-a-vis V(r) (b). Interpretation: Graphs (a) and (b) are drawn relative to the same scale on the abscissa. In (a), the ordinate F_b represents the expected size of the $R_r(t)$'s. In (b), V(r) is assumed to be infinite for $0 \leq r \leq r_a - 1$. V(r) is expressed in terms of multiples of V_0. In the current discussion, it is assumed that

$$V(r) \geq V_0, \quad r = 0, 1, \ldots, r_m.$$

[1] Burington, R. S. and May, D. C., Handbook of Probability and Statistics with Tables, Handbook Publishers, Inc., Sandusky, Ohio, pp 263-266.

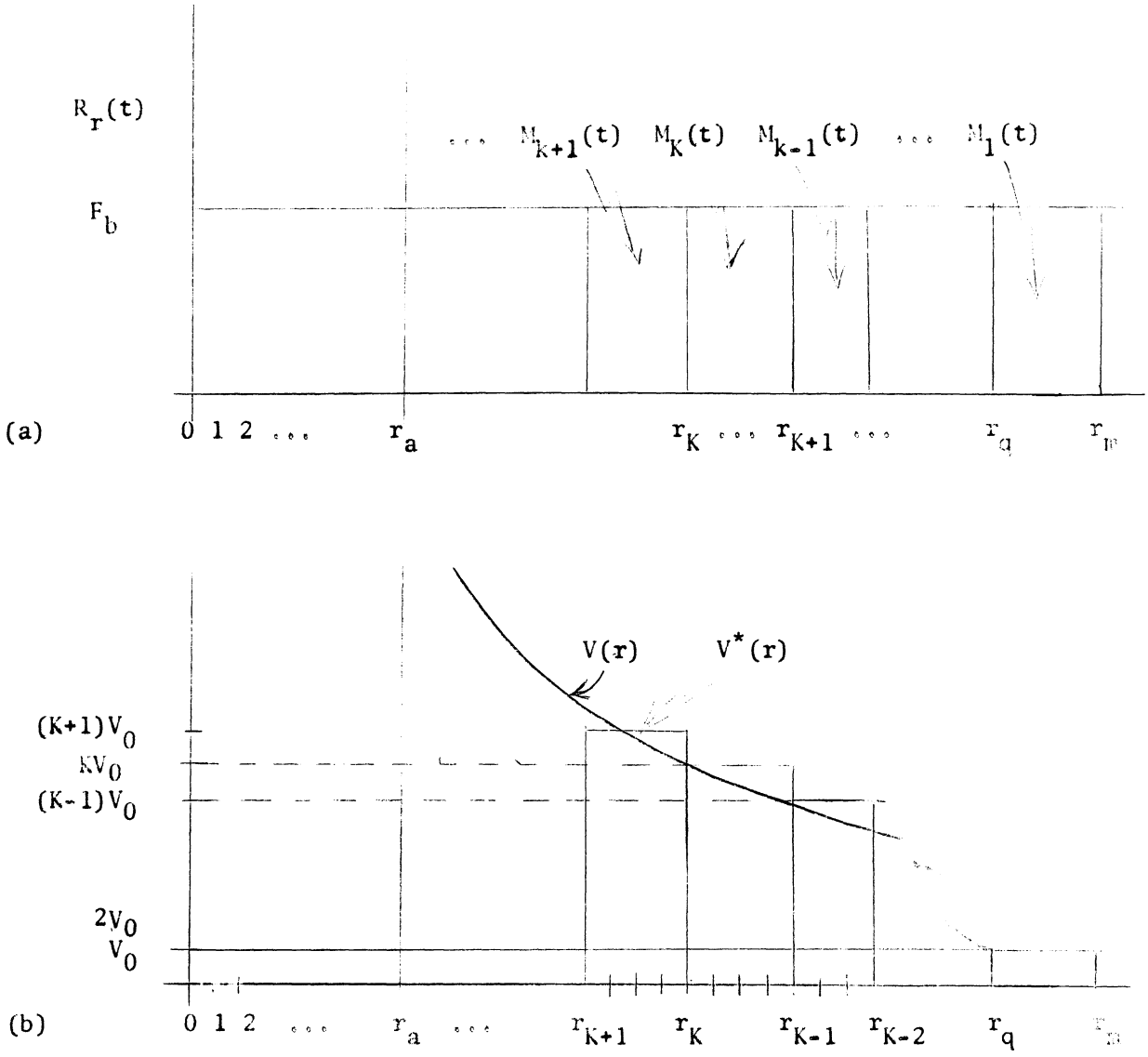

Figure 4.2. Graph of $\mathcal{R}(t)$ with the $M_k(t)$ (a), vis-a-vis $V(r)$, (b). Interpretation: In (b), a continuous curve $V(r)$ is approximated by a step-function $V^*(r)$ so that $V^*(r) = kV_0$, k an integer, for $r \in [r_{k+1}, r_k] \subseteq [0, r_m]$, $k = 1, 2, \ldots$. The corresponding points in (a) determine the boundaries of $M_k(t)$; $\bar{\bar{M}}_k(t) = (r_{k+1} - r_k)F_b$ (expected value).

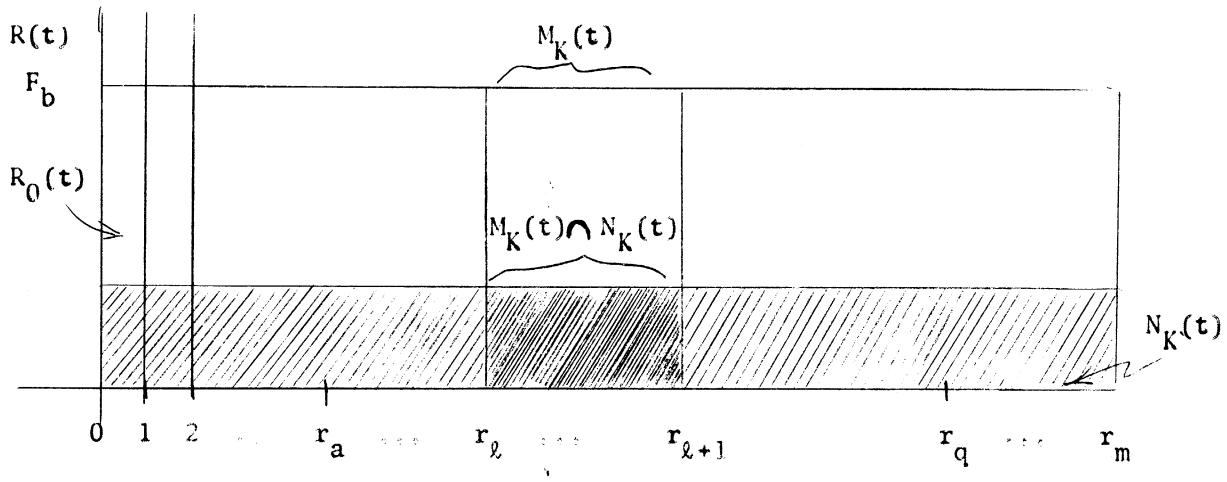

Figure 4.3. Stylized Graph Indicating Relationship of $M_k(t)$ and $N_k(t)$ vis-a-vis $R(t)$. Interpretation: The set $N_k(t)$ spans recovery sets $R_r(t)$, therefore it is shown at the hatched area above. The ordinate does not indicate the cardinality of the $R_r(t) \cap N_k(t)$, rather represents a stylized set boundary.

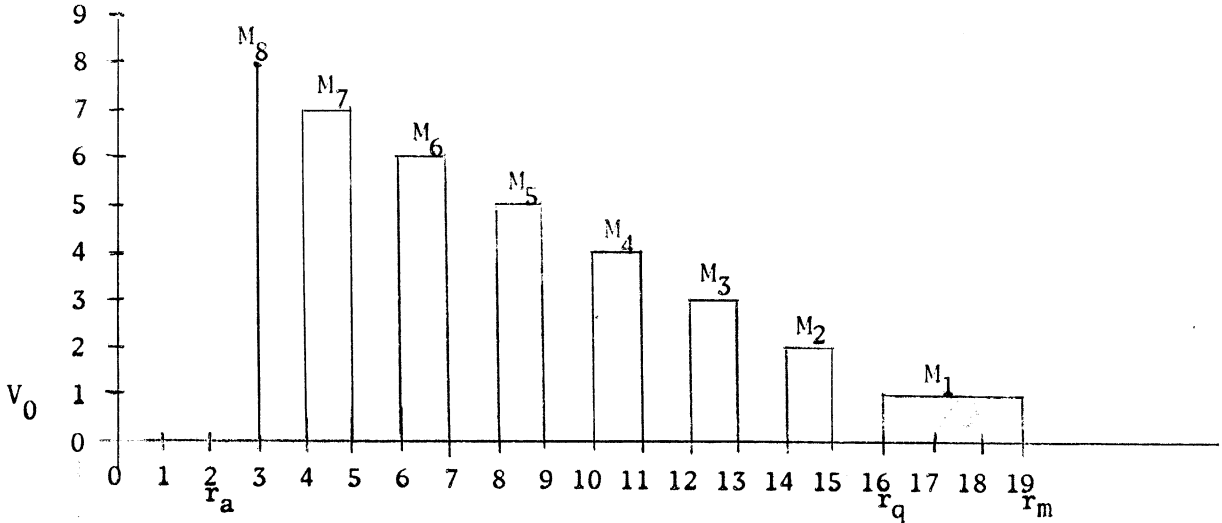

Figure 4.4. Threshold Curve for Sample Calculation. Interpretation: Initially, neurons are distributed randomly and independently over recovery states so that $E(\bar{\bar{R}}_r(0) = 20$, $r = 0, 1, \ldots, r_m$ and $E(\bar{\bar{R}}_{r_q}(0) = 80$. Clearly, $E(\bar{\bar{M}}_8(0)) = 20$, $E(\bar{\bar{M}}_7(0) = E(\bar{\bar{M}}_6(0)) = \ldots = E(M_2(0) = 40$ and $E(\bar{\bar{M}}_1(0)) = 80$.

Table 4.1. Sample Steady-State Calculation

t	λ	R_0	R_1	R_2	R_3	R_4	R_5	R_6	R_7	R_8	R_9	R_{10}	R_{11}	R_{12}	R_{13}	π_2	M_2	π_1	M_1
0	.3	20	20	20	20	20	20	20	20	20	20	20	20	20	20	-	40	-	80
1	.345	23	20	20	20	20	20	20	20	20	20	20	20	20	20	.04	40-2+20-19=39	.26	80-21+19=78
2	.375	25	23	20	20	20	20	20	20	20	20	20	20	20	20	.05	39-2+20-18=39	.29	78-23+18=73
3	.375	25	25	23	20	20	20	20	20	20	20	20	20	20	20	.06	39-2+20-18=39	.31	73-23+18=69
4	.345	23	25	25	23	20	20	20	20	20	20	20	20	20	20	.06	39-2+20-18=39	.31	69-21+18=66
5	.285	19	23	25	25	23	20	20	20	20	20	20	20	20	20	.04	39-2+20-18=39	.26	66-17+18=67
6	.27	18	19	23	25	25	23	20	20	20	20	20	20	20	20	.02	39-1+20-19=40	.25	67-17+18=68
7	.255	17	18	19	23	25	25	23	20	20	20	20	20	20	20	.02	40-1+20-19=40	.24	68-16+19=71
8	.255	17	17	18	19	23	25	25	23	20	20	20	20	20	20	.02	40-1+20-19=40	.22	71-16+19=74
9	.255	17	17	17	18	19	23	25	25	23	20	20	20	20	20	.02	40-1+20-19=40	.22	74-16+19=77
10	.27	18	17	17	17	18	19	23	25	25	23	20	20	20	20	.02	40-1+20-19=40	.22	77-17+19=79
11	.285	19	18	17	17	17	18	19	23	25	25	23	20	20	20	.02	40-1+20-19=40	.24	79-19+19=79
12	.315	21	19	18	17	17	17	18	19	23	25	25	23	20	20	.02	40-1+20-19=40	.25	79-20+19=78
13	.33	22	21	19	18	17	17	17	18	19	23	25	25	23	20	.04	40-2+20-19=39	.26	78-20+19=77
14	.345	23	22	21	19	18	17	17	17	18	19	23	25	25	23	.04	39-2+20-19=38	.27	77-21+19=75
15	.36	24	23	22	21	19	18	17	17	17	18	19	23	25	25	.05	38-2+23-18=41	.29	75-22+18=71
16	.345	23	24	23	22	21	19	18	17	17	17	18	19	23	25	.05	41-2+25-18=46	.30	71-21+18=68
17	.33	22	23	24	23	22	21	19	18	17	17	17	18	19	23	.05	46-2+25-21=48	.29	68-20+21=69
18	.35	21	22	23	24	23	22	21	19	18	17	17	17	18	19	.04	48-2+23-23=46	.27	69-19+23=73
19	.315	21	21	22	23	24	23	22	21	19	18	17	17	17	18	.04	46-2+19-23=40	.26	73-19+23=77
20	.33	22	21	21	22	23	24	23	22	21	19	18	17	17	17	.04	40-2+18-21=35	.26	77-20+21=78
21	.33	22	22	21	21	22	23	24	23	22	21	19	18	17	17	.04	35-1+17-17=34	.27	78-21+17=74
22	.35	21	22	22	21	21	22	23	24	23	22	21	19	18	17	.04	34-1+17-16=34	.27	74-20+16=70
23	.285	19	21	22	22	21	21	22	23	24	23	22	21	19	18	.04	34-1+17-16=34	.26	70-18+16=68
24	.27	18	19	21	22	22	21	21	22	23	24	23	22	21	19	.02	34-1+18-16=35	.25	68-17+16=67
25	.255	17	18	19	21	22	22	21	21	22	23	24	23	22	21	.02	35-1+19-17=36	.24	67-16+17=68
26	.24	16	17	18	19	21	22	22	21	21	22	23	24	23	22	.02	36-1+21-17=39	.22	68-15+17=70
27	.24	16	16	17	18	19	21	22	22	21	21	22	23	24	23	.02	39-1+22-18=42	.21	70-15+18=73
28	.24	16	16	16	17	18	19	21	22	22	21	21	22	23	24	.02	42-1+23-70=44	.21	73-15+20=78
29	.255	17	16	16	16	17	18	19	21	22	22	21	21	22	23	.02	44-1+24-21=46	.21	78-16+21=83
30	.285	19	17	16	16	16	17	18	19	21	22	22	21	21	22	.02	46-1+23-22=46	.22	83-18+22=87

4.3.3 Negative Feedback

The logic of the computational scheme presented above for determining steady state hinges upon the set $\hat{R}_{r_q}$ remaining constant in expected size, i.e., $E(\hat{\bar{R}}_{r_q}) = \text{constant} = R$ for all t. Should $\hat{R}_{r_q}(t)$ decrease below R for a few consecutive time steps, F(t) correspondingly would decrease below F_b. As F(t) decreases, $\hat{\bar{R}}_{r_q}(t)$ gradually increases. Unless F(t) went to zero, F(t) would then increase. Since $\hat{\bar{R}}_{r_q}(t)$ might increase to a value greater than R, F(t) may increase to a value greater than F_b. This again would tend to deplete $\hat{R}_{r_q}(t)$ and again F(t) would be expected to decrease.

Within a certain variance in F(t), this is precisely the behavior one would expect: F(t) tends to oscillate about its mean F_b. However, under certain circumstances, a transient deviation in F(t) may be amplified so that fatal oscillations occur. Suppose as $\hat{\bar{R}}_{r_q}(t)$ decreases in one of the "ebb" periods, hence resulting in a decrease of F(t), the sets $R_{r_q-1}(t), R_{r_q-2}(t), \ldots, R_{r_q-1}(t)$ corresponding to the sets of neurons that fired during a previous "ebb" periods. (τ_1 is the length of the transient decrease of F(t) from F_b). Then, $\hat{\bar{R}}_{r_q-1}(t), \ldots, \hat{\bar{R}}_{r_q-1}(t)$, are less than their expected values. This tends to decrease $\hat{R}_{r_q}(t)$ even further. Likewise, as $\hat{R}_{r_q}(t)$ increases in one of the "flow" periods, resulting in an increase of F(t), the sets $R_{r_q-1}(t), \ldots, R_{r_q-2}(t)$ may correspond to sets of neurons that fired during a previous flow period (τ_2 is the length of the transient increase of F(t) and F_b during that period). $\hat{\bar{R}}_{r_q-1}(t), \ldots, \hat{\bar{R}}_{r_q-2}(t)$ are greater than their expected values, and $\hat{\bar{R}}_{r_q}(t)$ increases above R.

Thus, a transient deviation in F(t) from F_b may result in successive undamped amplifications of the deviation, eventually leading to fatal oscillations. Whether this occurs or not depends upon the phase

relationship between $\hat{R}_{r_q}(t)$ and the sets $R_{r_q-1}(t)$ and the sets $R_{r_q-1}(t), \ldots, R_{r_q-\tau_1}(t)$ or $R_{r_q-1}(t), \ldots, R_{r_q-\tau_2}(t)$; if $\bar{\bar{R}}_{r_q}(t)$ is increasing, but, $R_{r_q-1}(t), \ldots, R_{r_q-\tau_1}(t)$ correspond to a previous "ebb", the effect of the increase in $\bar{\bar{R}}_{r_q}(t)$ may be cancelled out. Similarly if $\bar{\bar{R}}_{r_q}(t)$ is decreasing. This phase, of course, is a function of τ_1 and τ_2. In general, however, the transients do not appear to cancel out. The chief reason for this is that the lengths τ_1 and τ_2 are not constant. Thus, for one transient "ebb", say, $\tau_1 = \tau^*$, but for the next "ebb" $\tau_1 = \tau^* + 3$. The next time the corresponding fired sets arrive at r_q, the decrease in $\bar{\bar{R}}_{r_q}(t)$ is even greater than before, causing a further increase in τ_1, say $\tau_1 = \tau^* + 5$, etc. Likewise, during transient "flows", as F(t) increases above F_b, it robs the sets $R_{r_q-1}(t)$, $R_{r_q-2}(t)$, ... of more than the expected number of neurons required for steady-state. This prolongs the transient, increasing τ_2, and incidentally making the following "ebb" the more severe, since fewer neurons will be available to fire.

The principles of the above paragraphs are illustrated by a continuation of the computation of Table 4.1. Notice that the oscillations become more and more severe until F(t) goes to zero at t = 91. Interestingly enough, as will be discussed in Chapter 5, the corresponding simulated network turned out to be stable. This is related to the fact that both N and ρ were relatively small, ρ not a function of the distance, and fatigue was present.

To conclude: while the scheme of Section 4.3.2 will tolerate small deviations in F(t), there is the definite possibility that a small transient deviation will eventually result in fatal oscillations. We wish now to examine some mechanism or combination of mechanisms that will counteract the effect of such transients. That is, we wish to implement

Table 4.2. Sample Steady-State Calculation (continued)

t	λ	R_0	R_1	R_2	R_3	R_4	R_5	R_6	R_7	R_8	R_9	R_{10}	R_{11}	R_{12}	R_{13}	π_2	M_2	π_1	M_1
31	.345	23	19	17	16	16	16	17	18	19	21	22	22	21	21	.02	46=1+22=21=46	.25	87=22+21=86
32	.404	27	23	19	17	16	16	16	17	18	19	21	22	22	21	.05	46=2+21=22=43	.29	86=25+22=83
33	.45	30	27	23	19	17	16	16	16	17	18	19	21	22	22	.061	43=3+21=20=41	.33	83=27+20=76
34	.45	30	30	27	23	19	17	16	16	16	17	18	19	21	22	.075	41=3+22=19=41	.36	76=27+19=68
35	.404	27	30	30	27	23	19	17	16	16	16	17	18	19	21	.075	41=3+22=18=42	.36	68=24+18=62
36	.345	23	27	30	30	27	23	19	17	16	16	16	17	18	19	.061	42=3+21=18=42	.33	68=24+18=60
37	.285	19	23	27	30	30	27	23	19	17	16	16	16	17	18	.05	42=2+19=19=40	.29	60=17+19=62
38	.255	17	19	23	27	30	30	27	23	19	17	16	16	16	17	.02	40=1+18=19=38	.25	62=16+19=65
39	.225	15	17	19	23	27	30	30	27	23	19	17	16	16	16	.02	38=1+17=18=36	.22	65=14+17=69
40	.225	15	15	17	19	23	27	30	30	27	23	19	17	16	16	.02	36=1+16=17=34	.20	69=14+17=72
41	.225	15	15	15	17	19	23	27	30	30	27	23	19	17	16	.02	34=1+16=16=33	.20	72=14+16=74
42	.24	16	15	15	15	17	19	23	27	30	30	27	23	19	17	.02	33=1+16=15=33	.20	74=15+15=74
43	.255	17	16	15	15	15	17	19	23	27	30	30	27	23	19	.02	33=1+17=15=34	.21	74=16+15=73
44	.255	17	17	16	15	15	15	17	19	23	27	30	30	27	23	.02	34=1+19=15=37	.22	73=16+15=72
45	.255	17	17	17	16	15	15	15	17	19	23	27	30	30	27	.02	37=1+23=16=43	.22	72=16+16=72
46	.255	17	17	17	17	16	15	15	15	17	19	23	27	30	30	.02	43=1+27=18=49	.22	72=16+18=74
47	.255	17	17	17	17	17	16	15	15	15	17	19	23	27	30	.02	49=1+30=22=56	.22	74=16+22=80
48	.285	19	17	17	17	17	17	16	15	15	15	17	19	23	27	.02	56=1+30=26=59	.22	80=18+26=88
49	.345	23	19	17	17	17	17	17	16	15	15	15	17	19	23	.02	59=1+27=29=56	.25	88=22+29=95
50	.465	31	23	19	17	17	17	17	17	16	15	15	15	17	19	.05	56=3+23=28=48	.29	95=28+28=95
51	.585	39	31	23	19	17	17	17	17	17	16	15	15	15	17	.08	48=4+19=24=39	.37	95=35+24=84
52	.615	41	39	31	23	19	17	17	17	17	17	16	15	15	15	.11	39=4=17=19=33	.44	84=37+19=66
53	.51	34	41	39	31	23	19	17	17	17	17	17	16	15	15	.125	33=4+15=15=29	.46	66=30+15=51
54	.345	23	34	41	39	31	23	19	17	17	17	17	17	16	15	.095	29=3+15=13=28	.40	51=20+13=44
55	.210	14	23	34	41	39	31	23	19	17	17	17	17	17	16	.05	28=1+15=13=29	.29	44=13+13=44
56	.36	24	14	23	34	41	39	31	23	19	17	17	17	17	17	.02	29=1+16=13=31	.19	44=23+13=34
57	.18	12	24	14	23	34	41	39	31	23	19	17	17	17	17	.04	31=1+17=14=33	.31	34=11+14=37
58	.12	8	12	24	14	23	34	41	39	31	23	19	17	17	17	.018	33=1+17=15=34	.18	37= 7+15=45
59	.075	5	8	12	24	14	23	34	41	39	31	23	19	17	17	.005	34 +17=15=36	.11	45= 5+15=55
60	.075	5	5	8	12	24	14	23	34	41	39	31	23	19	17	.005	36 +17=16=37	.095	55= 5+16=66

Table 4.2. Sample Steady-State Calculation (concluded)

t	λ	R_0	R_1	R_2	R_3	R_4	R_5	R_6	R_7	R_8	R_9	R_{10}	R_{11}	R_{12}	R_{13}	π_2	M_2	π_1	M_1
61	.09	6	5	5	8	12	24	14	23	24	41	39	31	23	19	.005	37 +17-17=37	.095	66- 6+17=77
62	.105	7	6	5	5	8	12	24	14	23	24	41	39	31	23	.005	37 +19-17=39	.095	77- 7+17=87
63	.12	8	7	6	5	5	8	12	24	14	23	24	41	39	31	.005	39 +23-17=45	.095	87- 8+17=96
64	.18	12	8	7	6	5	5	8	12	24	14	23	24	41	39	.005	45- 1+31-19=56	.11	96-11+19=104
65	.3	20	12	8	7	6	5	5	8	12	24	14	23	24	41	.018	56- 1+39-22=72	.18	104-19+22=107
66	.465	31	20	12	8	7	6	5	5	8	12	24	14	23	24	.04	72- 3+41-30=80	.26	107-28+30=109
67	.69	46	31	20	12	8	7	6	5	5	8	12	24	14	23	.08	80- 6+34-35=73	.37	109-40+35=104
68	.96	64	46	31	20	12	8	7	6	5	5	8	12	24	14	.16	73-12+23-32=52	.5	104-50+32=84
69	1.0	67	64	46	31	20	12	8	7	6	5	5	8	12	24	.26	52-14+14-21=31	.63	84-53+21=42
70	.51	34	67	64	46	31	20	12	8	7	6	5	5	8	12	.264	31- 8+24-12=35	.63	42-26+12=28
71	.21	14	34	67	64	46	31	20	12	8	7	6	5	5	8	.095	35- 3+12-12=32	.40	28-11+12=29
72	.105	7	14	34	67	64	46	31	20	12	8	7	6	5	5	.02	32- 1+ 8-22=17	.19	29- 6+22=45
73	.075	5	7	14	34	67	64	46	31	20	12	8	7	6	5	.005	17 + 5-11=11	.095	45- 5+11=51
74	.075	5	5	7	14	34	67	64	46	31	20	12	8	7	6	.005	11 + 5- 8=8	.095	51- 5+ 8=54
75	.075	5	5	5	7	14	34	67	64	46	31	20	12	8	7	.005	8 + 6- 5=9	.095	54- 5+ 5=50
76	.075	5	5	5	5	7	14	34	67	64	46	31	20	12	8	.005	9 + 7- 5=11	.095	50- 5+ 5=50
77	.075	5	5	5	5	5	7	14	34	67	64	46	31	20	12	.005	11 + 8- 6=13	.095	50- 5+ 6=51
78	.075	5	5	5	5	5	5	7	14	34	67	64	46	31	20	.005	13 +12- 7=18	.095	51- 5+ 7=53
79	.075	5	5	5	5	5	5	5	7	14	34	67	64	46	31	.005	18 +20- 8=30	.095	53- 5+ 8=56
80	.075	5	5	5	5	5	5	5	5	7	14	34	67	64	46	.005	30 +31-12=49	.095	56- 5+12=63
81	.09	6	5	5	5	5	5	5	5	5	7	14	34	67	64	.005	49 +46-20=78	.095	63- 6+20=77
82	.105	7	6	5	5	5	5	5	5	5	5	7	14	34	67	.005	78 +64-31=111	.095	77- 7+31=101
83	.165	11	7	6	5	5	5	5	5	5	5	5	7	14	34	.005	111- 1+67-45=132	.095	101-10+45=136
84	.24	16	11	7	6	5	5	5	5	5	5	5	5	7	14	.005	132- 1+34-63=102	.11	136-15+63=184
85	.585	39	16	11	7	6	5	5	5	5	5	5	5	5	7	.02	102- 2+14-66=58	.21	184-37+66=213
86	.975	65	39	16	11	7	6	5	5	5	5	5	5	5	5	.11	58- 6+ 7-32=27	.44	213-59+32=186
87	1.77	118	65	39	16	11	7	6	5	5	5	5	5	5	5	.245	27- 7+ 5-11=14	.61	186-111+11=86
88	1.2	79	118	65	39	16	11	7	6	5	5	5	5	5	5	.53	14- 7+ 5- 3=9	.83	86-72+ 3=16
89	.21	14	79	118	65	39	16	11	7	6	5	5	5	5	5	.34	9- 3+ 5- 2=9	.70	16-11+ 2=7
90	.015	1	14	79	118	65	39	16	11	7	6	5	5	5	5	.02	9 + 5- 4=10	.19	7- 1+ 4=10
91	0	0	1	14	79	118	65	39	16	11	7	6	5	5	5	-	10 + 5- 5=10		10 + 5=15

some source of negative feedback in the model.

Negative-Feedback Mechanisms

(a) The Fatigue Mechanism

Since the fatigue function effectively raises the threshold of a neuron firing at a rate above F_b, or conversely lowers it if the firing is at a rate below F_b, we might expect some assistance from this direction. That is, the neurons of an "ebb" period tend to fall below F_b, those in a "flow", above F_b. Conceivably, the fatigue might be sensitive enough to lower or raise the corresponding threshold quickly enough that large oscillations do not occur. However, the fatigue is designed to be effective over longer time intervals than are involved here and to take effect rather slowly; it is a cumulative, relatively long range function. What is needed here is a function that will be effective over relatively short time periods, in fact, fractions of a recovery period. The fatigue mechanism, therefore, is rejected for this purpose, although it will be useful over longer time intervals.

(b) Negative Connections

In the analysis of Section 4.3.2, it was assumed that the synapse-levels were all set to a common value λ_0, corresponding to a positive synapse value. This, of course, can be weakened to a distribution of positive synapse values (synapse-levels) about the mean $S(\lambda_0)(\lambda_0)$. It is now of interest to observe the effect of the presence of negative synapse-values on the network's behavior. It will be seen that this provides the negative-feedback desired.

To illustrate the principle involved, consider the simple scheme of Figure 4.5. S_1 and S_2 are two subsets of a network $\mathcal{N}$. Suppose the synapse values from neurons of S_1 to those of S_2 are as shown below

Figure 4.5. Illustration of Effect of Negative Connections.

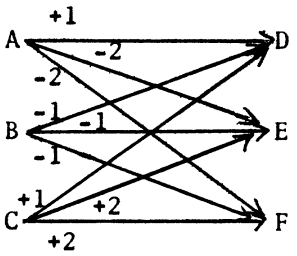

(Assume a net stimulus of +1 synapses is sufficient to fire D, E, or F at t+1.)

If A, B, C fire at t, then D only fires at t+1.

If B and C fire at t, then E and F fire at t+1.

If C fires at t, then D, E, and F fire at t+1.

Table 4.3. Sample Stability Calculations for Periodic Stimulus Case

t	λ	R_0	R_1	R_2	R_3	R_4	R_5	R_6	R_7	R_8	R_9	R_{10}	R_{11}	R_{12}	R_{13}	M_2	M_1
-	.3	20	20	20	20	20	20	20	20	20	20	20	20	20	20	40	80
1	.405	27	20	20	20	20	20	20	20	19	20	19	20	19	20	39	77
2	.405	27	27	20	20	20	20	20	20	20	19	20	19	20	19	39-2+20-19=37	77-25+19=71
3	.375	25	27	27	20	20	20	20	20	20	20	19	20	19	20	37-2+19-19=35	71-23+19=67
4	.345	23	25	27	27	20	20	20	20	20	20	20	19	20	19	35-2+20-19=34	67-21+19=65
5	.285	19	23	25	27	27	20	20	20	20	20	20	20	19	20	34-1+19-19=33	65-18+19=66
6	.27	18	19	23	25	27	27	20	20	20	20	20	20	20	19	33-1+20-19=33	66-17+19=68
7	.36	24	18	19	23	25	27	20	20	20	20	20	20	20	20	33-1+19-19=32	68-16+19=71
8	.35	22	24	18	19	23	25	27	20	20	20	20	20	20	20	32 +20-19=32	71-21+19=69
9	.3	20	22	24	18	19	23	25	27	20	20	20	20	20	20	32 +20-19=32	69-19+19=69
10	.285	19	20	22	24	18	19	23	25	27	20	20	20	20	20	33-1+20-19=32	69-18+19=70
11	.285	19	19	20	22	24	18	19	23	25	27	20	20	20	20	32-1+20-19=32	70-18+19=71
12	.285	19	19	19	20	22	24	18	19	23	25	27	20	20	20	32-1+20-19=32	71-18+19=72
13	.39	26	19	19	19	20	22	17	18	19	23	25	27	20	20	32-1+20-19=32	72-18+19=73
14	.375	25	26	19	19	19	20	22	17	18	19	23	25	27	20	32-2+20-19=31	73-23+19=69
15	.345	23	25	26	19	19	19	20	22	17	18	19	23	25	27	31-2+20-19=30	69-21+19=67
16	.3	20	23	25	26	19	19	19	20	22	17	18	19	23	25	30-1+27-19=37	67-19+19=67
17	.27	18	20	23	25	26	19	19	19	20	22	17	18	19	23	37-1+23-19=40	67-19+19=69
18	.255	17	18	20	23	25	26	19	19	19	20	22	17	18	19	40-1+23-24=38	69-16+24=77
19	.375	25	17	18	20	23	25	19	19	19	19	20	22	17	18	38-1+19-22=34	77-17+22=82

$$S(\lambda_{AD}) = +1,\ S(\lambda_{AE}) = +2,\ S(\lambda_{AF}) = +2$$
$$S(\lambda_{BD}) = +1,\ S(\lambda_{BE}) = +2,\ S(\lambda_{BF}) = +1$$
$$S(\lambda_{CD}) = +1,\ S(\lambda_{CE}) = +2,\ S(\lambda_{CF}) = +2$$

and suppose at the times steps of interest, +1 or more synapses will be required to fire a neuron of S_2. If neurons A, B, and C fire at t, only one neuron of S_2, namely D will fire the next time step. If neurons B and C fire, then E and F fire at t + 1. Finally, if neuron C alone fires, then D, E, and F fire at t + 1. This suggests the following general conclusion: for certain distributions of synapse values over connections, the presence of negative connections suppresses firing of certain neurons at t + 1 if $F(t) > F_b$ and "frees" certain neurons for firing at t + 1 if $F(t) < F_b$. If $F(t) = F_b$, then $F(t+1) = F_b$. Thus, the desired homeostatic mechanism is obtained. It remains to express it quantitatively for the general case of networks with uniform random distributions of connections.

Suppose the network density ρ is given as a sum

$$\rho = \sum_{-s_0}^{s_1} \rho_s = \rho_{-s_0} + \rho_{-s_0+1} + \ldots + \rho_{-1} + \rho_0 + \rho_1 + \ldots + \rho_{s_1}$$

where s_0 and s_1 are positive integers and ρ_s is the expected number of connections received (or emitted) by a neuron of $\mathfrak{N}$ with synapse-value s. For now, s will be assumed to be an integer, although the analysis can be modified to comprise fractional s. A synapse-value assignment scheme can be designed to yield this decomposition of ρ into $s_0 + s_1 + 1$ independent distributions of synapse-values s, $s = -s_0 + 1, \ldots, -1, 0, +1, \ldots, s_1$.

The analysis of Section 4.3.2 requires the probability $\pi_k(\lambda(t))$, the probability that a neuron receive $\geq k$ connections from $R_0(t)$, the set of neurons firing at t. With positive and negative valued connections

present, π_k becomes a function of all the λ's, $P_k^* = \pi_k(\lambda_{-s_0}(t), \lambda_{-s_0+1}(t), \ldots, \lambda_{-1}(t), \lambda_1(t), \ldots, \lambda_{s_1}(t))$ where, as before, $\lambda_s(t) = \bar{\bar{R}}_0(t)\frac{\rho_s}{N}$, $s = -s_0, \ldots, s_1$. P_k^* is the probability that the sum of all incoming synapses to the given neuron is $\geq k$. Again, $P_k^* \cdot \bar{\bar{M}}_k(t)$ is the expected number of neurons of $M_k(t)$ that will fire at time step t. Since 0-valued connections do not affect the firing of a neuron and the different synapse-value distributions are assumed to be independent, the presence of 0-valued connections will be ignored in the analysis. The role of these connections will be discussed in Chapters 6 and 7.

Let A_k^s and A_k^{*s} denote the following events:

A_k^s : "a given neuron receives exactly k connections with synapse-value s."

A_k^{*s} : "a given neuron receives $\geq$ k connections with synapse-value s."

Clearly, $A_k^{*s} = \bigcup_{j=k}^{\infty} A_j^s$.

Denote the probability of an arbitrary event A by P(A). Since the events A_k^s, $k = 0, 1, 2, \ldots$, are mutually exclusive, by the law of total probability

$$P(A_k^{*s}) = P(\bigcup_{j=k}^{\infty} A_j^s) = \sum_{j=k}^{\infty} P(A_j^s).$$

By the multiplication law, for arbitrary A_k^{*s} and A_ℓ^{*t}

$$P(A_k^{*s} A_\ell^{*t}) = P(A_k^{*s})\, P(A_\ell^{*t}).$$

We now give estimates for the probabilities P_k^* for various values of k, s_0 and s_1.

<u>k = 1</u>

The sum of incoming synapses to a given neuron is +1 or greater if

the event E occurs where

Eq. 4.3.1 $$E = \bigcup_{\ell=1}^{\infty} E_\ell$$

where E_ℓ represents the event "the neuron receives $\geq \ell$ positive synapses and $\leq \ell-1$ negative synapses." The E_ℓ's are given by expressions of the form:

$$E_1 = A_1^{*1} \cdot A_0^{*2} \cdots A_0^{*s_1} \cdot A_0^{-1} \cdots A_0^{-s_0}$$

$$E_2 = [A_2^{*1} \cdot A_0^{*2} \vee A_1^{2} A_0^{*1}] \cdot A_0^{*3} \cdots A_0^{*s_1} \cdot [A_0^{-1} \vee A_1^{-1}] A_0^{-2} \cdots A_0^{-s_0}$$

$$E_3 = [A_1^{*1} \cdot A_2^{*2} \vee A_3^{*1}] \cdot A_0^{*3} \cdots A_0^{*s_1} [[A_0^{-1} \vee A_1^{-1} \vee A_2^{-1}] A_0^{-2} \vee A_1^{-2} A_0^{-1}] \cdots A_0^{-s_0}$$

$$E_4 = [A_2^{*2} \vee A_1^{*2} A_2^{*1} \vee A_4^{*1}] \cdots A_0^{*s_1} [[A_0^{-1} \vee A_1^{-1} \vee A_2^{-1} \vee A_3^{-1}] A_0^{-2} \vee [A_0^{-1} \vee A_1^{-1}] A_1^{-2}] \cdots A_0^{-s_0}$$

Attention will be restricted in this discussion to two cases: $s_0 = s_1 = 1$ and $s_0 = s_1 = 2$. For the former,

Eq. 4.3.2 $$E \subseteq [A_1^1 A_0^{-1}] \vee [A_2^1 (A_0^{-1} \vee A_1^{-1})] \vee [A_3^{*1} (A_0^{-1} \vee A_1^{-1} \vee A_2^{-1})]$$

For the latter,

Eq. 4.3.2 $$E = \bigcup_{i=1}^{6} E_i$$

where

$$E_1 = A_0^{-1} A_0^{-2} [A_1^{*2} \vee A_1^{*1}]$$

$$E_2 = A_1^{-1} A_0^{-2} [A_1^{*2} \vee A_2^{*1}]$$

$$E_3 = [A_0^{-1} A_1^{-2} \vee (A_0^{-1} \vee A_1^{-1} \vee A_2^{-1}) A_0^{-2}] A_1^{*2} A_1^{*1}$$

$$E_4 = [[A_0^{-1} \vee A_1^{-1} \vee A_2^{-1} \vee A_3^{-1}] A_0^{-2} \vee [A_0^{-1} \vee A_1^{-1}] A_1^{-2}] [A_2^{*2} \vee A_1^{*2} A_2^{*1} \vee A_4^{*1}]$$

$$E_5 = [[A_0^{-1} \vee A_1^{-1} \vee A_2^{-1} \vee A_3^{-1} \vee A_4^{-1}] A_0^{-2} \vee [A_0^{-1} \vee A_1^{-1} \vee A_2^{-1}] A_1^{-2} \vee A_0^{-1} A_2^{-1}] \times [A_2^{*2} A_1^{*1} \vee A_1^{*2} A_3^{*1} \vee A_5^{*1}]$$

$$E_6 = [[A_0^{-1} \vee A_1^{-1} \vee A_2^{-1} \vee A_3^{-1} \vee A_4^{-1} \vee A_5^{-1}] A_0^{-2} \vee [A_0^{-1} \vee A_1^{-1} \vee A_2^{-1} \vee A_3^{-1}] A_1^{-2} \vee [A_0^{-1} \vee A_1^{-1}] [A_3^{*2} \vee A_2^{*2} A_2^{*1} \vee A_1^{*2} A_4^{*1} \vee A_6^{*1}]$$

Then, for $s_0 = s_1 = 1$, by the law of total probability and Boole's inequality and noting that $P(A_0^{*s}) = P[\bigcup_{k=0}^{\infty} A_k^{*s}] = 1$,

Eq. 4.3.4 $$P_1^* = P(E) = P(A_1^1)P(A_0^{-1}) = P(A_2^1)[P(A_0^{-1}) + P(A_1^{-1}) + P(A_3^{*1})[P(A_0^{-1}) + P(A_1^{-1}) + P(A_2^{-1})].$$

For $s_0 = s_1 = 2$,

Eq. 4.3.5 $$P_1^* = P(E) = P(\bigcup_{i=1}^{6} E_i) \leq \sum_{i=1}^{6} P(E_i),$$

where the E_i are those of Equation 4.3.3. Some observations concerning the computation of P_1^* for various values of the λ_s's, especially for the case $s_0 = s_1 = 2$, will be made later. It is interesting to note that

$$P(A_k^{*s}) = \pi_k(\lambda_s) \quad s = -s_0, \ldots, s_1$$

since

$$P(A_k^{*s}) = P(\bigcup_{j=k}^{\infty} A_j) = \sum_{j=k}^{\infty} P(A_j^*).$$

$k = 2$

The sum of incoming synapses to a given neuron is +2 or greater if the event E occurs where

Eq. 4.3.6 $$E = \bigcup_{i=2}^{\infty} E_1$$

where E_1 represents the event "the neuron receives $\geq \ell$ positive and $\leq \ell - 2$ negative synapses." The E_1's are given by expressions of the form

$$E_2 = [A_1^{*2} \circ A_0^{*1} \vee A_2^{*1} A_0^{*2}] \ldots A_0^{*s} A_0^{-1} A_0^{-2} \ldots A_0^{-s_0}$$

$$E_3 = [A_1^{*2} \circ A_1^{*1}] \ldots A_0^{*s_1}[A_0^{-1} \vee A_1^{-1}] A_0^{-2} \ldots A_0^{-s_0}$$

$$E_4 = [A_2^{*2} \circ A_0^{*1} \vee A_1^{*2} A_2^{*1} \vee A_4^{*1} A_0^{*2}] \ldots A_0^{*s_1} \circ [[A_0^{-1} \vee A_1^{-1} \vee A_2^{-1}] A_0^{-2} \vee A_0^{-1} \circ A_1^{-2}] \circ A_0^{-3} \ldots A_0^{-s_0}$$

$$\vdots$$

Attention will be restricted to the case $s_o = s_1 = 2$. For this case, E may be approximated by

$$E = \bigcup_{i=2}^{8} E_i$$

where

$$E_2 = (A_1^{*2} \vee A_2^{*1})\, A_0^{-1}A_0^{-2}$$

$$E_3 = A_1^{*2}A_1^{*1}(A_0^{-1} \vee A_1^{-1})A_0^{-2}$$

$$E_4 = (A_2^{*2}\vee A_1^{*2}A_2^{*1}\vee A_4^{*1})\,[(A_0^{-1}\vee A_1^{-1}\vee A_2^{-1})A_0^{-2}\vee A_0^{-1}A_1^{-2}]$$

$$E_5 = (A_2^{*2}A_1^{*1}\vee A_1^{*2}A_3^{*1}\vee A_5^{*1})\,[(A_0^{-1}\vee A_1^{-1}\vee A_2^{-1}\vee A_3^{-1})A_0^{-2}\vee(A_0^{-1}\vee A_1^{-1})(A_0^{-2}\vee A_1^{-2})]$$

$$E_6 = (A_3^{*2}\vee A_2^{*2}A_2^{*1}\vee A_1^{*2}A_4^{*1}\vee A_6^{*1})\,[(A_0^{-1}\vee\ldots\vee A_4^{-1})A_0^{-2}\vee(A_0^{-1}\vee\ldots\vee A_2^{-1})A_1^{-2}\vee A_0^{-1}A_2^{-2}]$$

$$E_7 = (A_3^{*2}A_1^{*1}\vee A_2^{*2}A_3^{*2}\vee A_1^{*2}A_5^{*1})\,[(A_0^{-1}\vee\ldots\vee A_5^{-1})A_0^{-2}\vee(A_0^{-1}\vee\ldots\vee A_3^{-1})(A_0^{-2}\vee A_1^{-2})$$
$$\vee(A_0^{-1}\vee A_1^{-1})(A_0^{-2}\vee A_1^{-2}\vee A_2^{-2})]$$

$$E_8 = (A_4^{*2}\vee A_3^{*2}A_2^{*1}\vee A_2^{*2}A_4^{*1})\,[(A_0^{-1}\vee\ldots\vee A_6^{-1})A_0^{-2}\vee(A_0^{-1}\vee\ldots\vee A_4^{-1})(A_0^{-2}\vee A_1^{-2})$$
$$\vee(A_0^{-1}\vee A_1^{-1}\vee A_2^{-1})(A_0^{-2}\vee A_1^{-2}\vee A_2^{-2})\vee A_2^{-1}A_3^{-2}]$$

Then, for P_2^* we get

$$P_2^* = P(E) = P\left(\bigcup_{i=2}^{8} E_i\right)$$

Eq. 4.3.8

$$\leq \sum_{i=2}^{8} P(E_i).$$

For λ_s ($s = 2, -1, 1, 2$) in the range .1 to 1.0, Equation 4.3.8 will be approximated by

Eq. 4.3.8(a)
$$P_2^* = P(E) = P(A_0^{-1})P(A_0^{-2})(P(A_1^{*2}) + P(A_2^{*1}))$$
$$+ P(A_1^{-1})P(A_0^{-2})(P(A_1^{*2})P(A_1^{*1}) + P(A_2^{*2}))$$
$$+ P(A_0^{-1})P(A_1^{-2})(P(A_2^{*2}) + P(A_4^{*1}))$$
$$+ P(A_2^{-1})P(A_0^{-2})(P(A_2^{*2}) + P(A_4^{*1}))$$

For λ_1 and λ_2 in the range 0.6 to 2.5 and λ_{-1} and λ_{-2} in the range 1.2 to 5.0, Equation 4.3.8 will be approximated by

Eq. 4.3.8(b)
$$P_2^* = P(E) \cong P_5 + P_6 + P_7 + P_8$$

where

$$P_5 = [P(A_2^2)P(A_1^1)+P(A_1^2)P(A_3^1)+P(A_5^1)][(1-P(A_4^{*-1}))P(A_0^{-2})+(1-P(A_2^{*-1}))(1-P(A_2^{*-2}))]$$

$$P_6 = [P(A_3^2)+P(A_2^2)P(A_2^1)+P(A_1^2)P(A_4^1)+P(A_6^1)]$$

$$\times [(1-P(A_5^{*-1}))P(A_0^{-2})+(1-P(A_3^{*-1}))P(A_1^{-2})+P(A_0^{-1})P(A_0^{-2})]$$

$$P_7 = [P(A_3^2)P(A_1^1)+P(A_2^2)P(A_3^1)+P(A_1^2)P(A_5^1)]$$

$$\times [(1-P(A_6^{*-1}))P(A_0^{-2})+(1-P(A_4^{*-1}))(1-P(A_2^{*-2}))+(1-P(A_2^{*-1}))(1-P(A_3^{*-2}))]$$

$$P_8 = [P(A_4^{*2})+P(A_3^{*2})P(A_2^{*1})+P(A_2^{*2})P(A_4^{*1}))] \times [(1-P(A_7^{*-1}))P(A_0^{-2})+(1-P(A_5^{*-1}))$$

$$\times (1-P(A_2^{*-2}))+(1-P(A_3^{*-1}))(1-P(A_3^{*-2}))+P(A_0^{-1})P(A_3^{-2})]$$

In Equation 4.3.8(b), an attempt has been made to eliminate the overlap of events $E_5, \cdots, E_8$ by replacing $A_j^{*\ell}$ by A_j^{ℓ} where appropriate. Events E_2, E_3, E_4 are ignored since, for the given range of λ_s ($s = -2, -1, 1, 2$), the $P(A_j^{\ell})$'s and $P(A_j^{*\ell})$'s are negligible.

$k = 3, 4$ and $s_0 = s_1 = 2$

Precisely the same reasoning as for the preceding cases may be carried out for this case. We give only the approximations for P_3^* and P_4^* for λ_s in the range .1 to 1.0:

Eq. 4.3.9
$$\begin{cases} P_3^* = P(A_0^{-1})P(A_0^{-2})[P(A_2^{*2})+P(A_3^{*1})+P(A_1^{*2})P(A_2^{*1})]+P(A_1^{-1})P(A_0^{-2})P(A_2^{*2}) \\ P_4^* = P(A_0^{-1})P(A_0^{-2})[P(A_2^{*2})+P(A_4^{*1})]. \end{cases}$$

From Equations 4.3.8(a) and 4.3.8(b) emerges the following general principle: to compute P_k^* ($k = 1, 2, 3, \cdots$), examine the expansion of $P(E) = P(\bigcup_{i=1}^{\infty} E_i)$. For a given range of the λ_s's ($s = -s_0, \cdots, s_1$), only a few of the E_i are such that $P(E_i)$ is not essentially 0. For these E_i, attempt to reduce the overlaps as much as possible: that is, attempt to make the E_i's mutually exclusive so that the law of total probability

applies (Note that Boole's inequality

$$P(\bigcup_i E_i) \leq \sum_i P(E_i)$$

provides a useful upper bound).

The effect of negative connections upon P_k^* can typically be seen from examination of the expressions $P_5, P_6, \ldots, P_8$ comprising Equation 4.3.8(b). Each P_i consists of two factors, one a sum of products of the general form $P(A_j^s)P(A_\ell^t)$ or $P(A_j^{*s})P(A_\ell^{*t})$, s, t positive, the other a sum of products of the form $P(A_j^{-s})(1-P(A_\ell^{*t}))$. For small λ_{-s} and small j, ℓ, the latter is moderate in size, decreasing as λ_{-s} increases. At the same time, for small λ_s, the former is small, increasing as λ_s increases. Since $\lambda_s(t) = \bar{\bar{R}}_0(t)\frac{\rho_s}{N}$ varies directly with the number of neurons fired at t, ρ_s and N being fixed parameters of the network, this suggests that the parameters N, ρ, ρ_s, $s = -s_0, \ldots, s_1$, may be adjusted so that as $\bar{\bar{R}}_0(t)$ increases above a certain amount F_b, P_k^* decreases and as $\bar{\bar{R}}_0(t)$ decreases below F_b, P_k^* increases. This gives exactly the negative feedback characteristics desired. This reasoning holds as long as $\bar{\bar{R}}_0(t)$ does not vary too greatly from F_b. For larger variations of $R_0(t)$, higher order terms ignored above come into play and eventually the P_k^* may increase again with increasing $\bar{\bar{R}}_0(t)$ or decrease with decreasing $\bar{\bar{R}}_0(t)$.

In Figures 4.6 and 4.7, sample calculations are given for P_1^* and P_2^* using the network parameters for one of the network of Chapter 6. Notice that for this network, to obtain the desired negative feedback, F_b should be set to approximately 35 (or correspondingly, if F_b is set to any other value, the ρ_s's should be adjusted to yield the same results).

(a) P_1^*

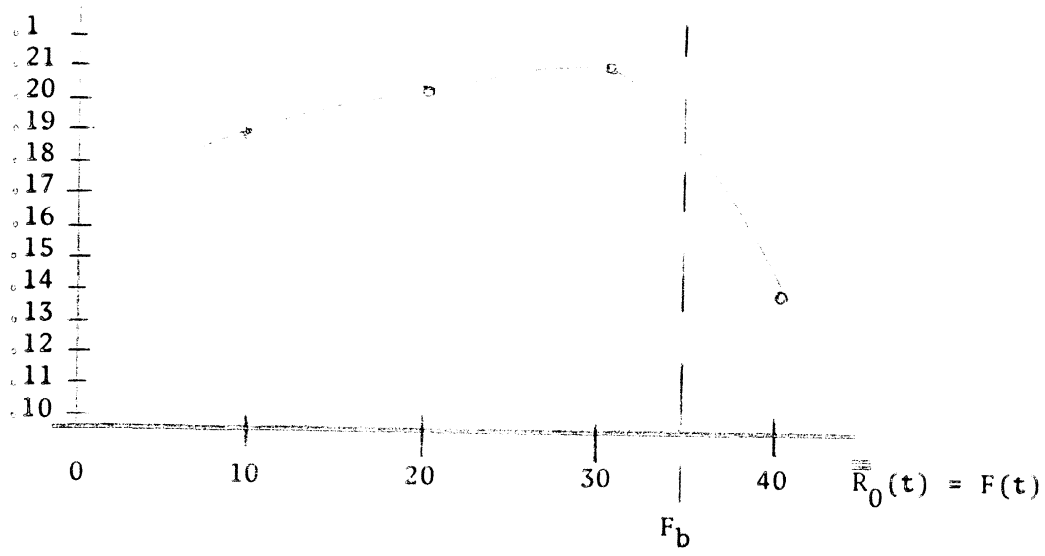

(b) P_2^*

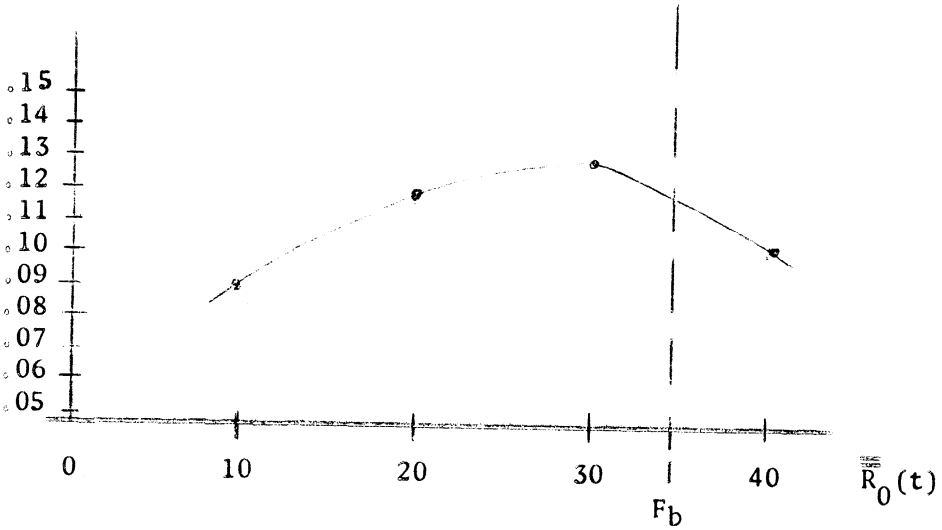

Figure 4.6. Variation of P_1^* and P_2^* as a Function of $R_0(t)$. P_1^* and P_2^* are plotted as functions of R(t) in (a) and (b) respectively. Equations 4.3.5 and 4.3.8(a) for the case $s_0 = s_1 = 2$ were used. $N = 400$, $\rho_1 = \rho_2 = 7$ and $\rho_{-1} = \rho_{-2} = 14$, $\rho = \rho_{-2} + \rho_{-1} + \rho_1 + \rho_2 = 42$ (exclusive of the ρ_0 term used in Chapter 6).

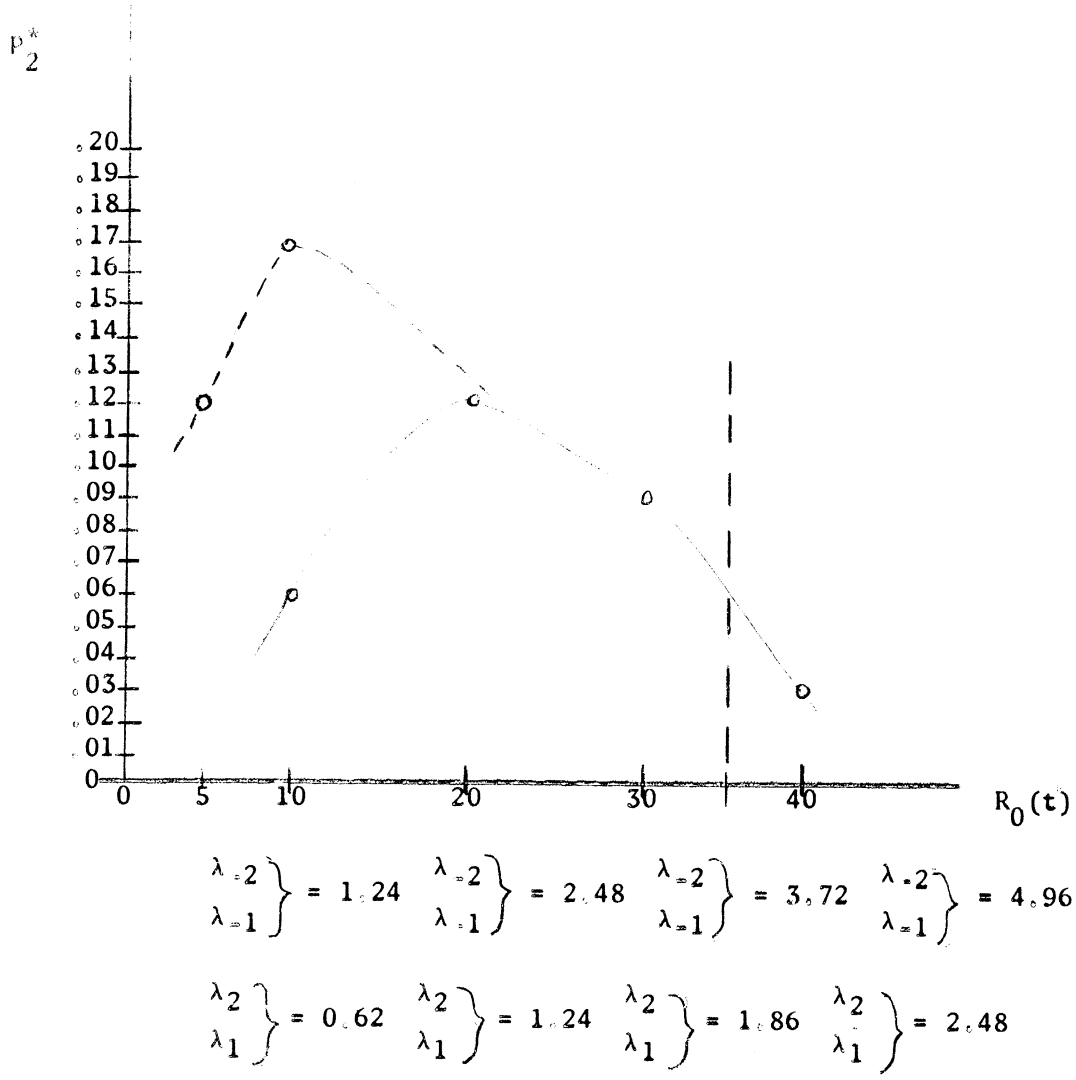

Figure 4.7. Variation of P_2^* as Function of $R_0(t)$. P_2^* is plotted as a function of $R_0(t)$. Equation 4.3.8(b) for the case $s_0 = s_1 = 2$ was used. $N = 113$, $\rho_1 = \rho_2 = 7$, $\rho_{-1} = \rho_{-2} = 14$, $\rho = \rho_{-2} + \rho_{-1} + \rho_1 + \rho_2 = 42$. For each value of $\bar{\bar{R}}_0(t)$, the values of λ_s ($s = -2, -1, 1, 2$) are also given. The dotted curve represents a continuation of the computation, but using Equation 4.3.8(a). At the point $\bar{\bar{R}}_0(t) = 10$, the results of both equations were added to give the value $P_2^* = .17$.

Conclusion

A mechanism involving negative synaptic connections has been devised that tends to surpress variations of $\bar{R}_0(t)$ from F_b. Letting $\delta R_0(t) = R_0(t) - F_b$, it works as follows. For a certain range of $|\delta R_0(t)|$, if $\delta R_0(t) > 0$, then $R_0(t+1)$ is decreased, i.e., $R_0(t) - R_0(t+1) > 0$. If $\delta R_0(t) < 0$, then $R_0(t+1)$ is increased, i.e., $R_0(t) - R_0(t+1) < 0$. Whether this occurs or not depends upon the "mix" of positive versus negative connections, that is upon $\rho = \sum_{s=-s_0}^{s_1} \rho_s$, and the value of F_b.

The analysis of Equation 4.3.2 remains unchanged, except that the probabilities $\pi_k(\lambda(t))$ are replaced by the probability

$$P_k^* = \pi_k(\lambda_{-s_0}(t), \ldots, \lambda_{s_1}(t)).$$

Throughout this section, and indeed the entire chapter, statements such as the following appear: "event A occurs if quantity X remains within certain bounds (is not too large, is not too small)" and more precise quantitative information is not given. In general, such information is not easy to derive and one is forced to be more qualitative than quantitative. This unfortunate situation, however, is considerably relieved by the simulation itself. For example, for the statement above, "for a certain range of $\delta R_0(t)$, etc." can be modified, on the basis of experimental findings alone, to the following: "if $\delta R_0(t)$ is no greater than approximately $F_b/2$, then ... . For larger variations, generally fatal oscillations develope."[1] Thus, much awkward and unwieldy analysis can be

---

[1] Recall that $F_b = E(F(t))$ is the expected number of neurons of $\mathcal{L}$ that fire at t and $1/\hat{r}_q$ is the expected frequency of firing of neurons in steady-state. F_b and $1/\hat{r}_q$ are related by $F_b = N/\hat{r}_q$. The statement concerning the absolute variation $\delta R_0(t)$ could be replaced by one in terms of the relative variation: $\delta^* R_0(t) = \frac{F(t)-F_b}{N} = \frac{1}{r(t)} - \frac{1}{\hat{r}_q}$ where $r(t) = \frac{N}{F(t)}$

by passed by the simulation Once initial trends are established by the analysis, and estimates obtained for the network parameters, a series of control experiments may be executed to further refine the initial estimates.

4.3.4 Networks with Distance Bias

Geometry of Networks with Distance-Bias

Specification of a particular distance-function d = d(j,i) over a network $\mathcal{N}$ implies the existence of some geometry over $\mathcal{N}$ and conversely. For a criterion to determine which are the desirable geometries for $\mathcal{N}$ it is necessary to recall briefly the fundamental objective of this study: to study the formation and development of cell-assembly-like structures in the given class of networks $\mathcal{N}$. The outstanding feature of these networks is the absence of any particular a priori structure. Rather structure is to evolve through the synapse-growth law, in response to certain conditions or patterns of stimulus. This seems to imply a basically uniform locally isotropic geometry. Such a geometry places the responsibility for development of structure squarely upon the shoulders of the synapse-growth law and the stimulus, without the assistance of any intrinsic spatial variations. Therefore, excluded are such spatial anomalies as "warps" (arising in non-Eudidean geometries) or poles and essential singularities (arising in complex function theory).

In the ideal case, several geometries appear to be plausible: (a) the infinite two-dimensional plane with the usual Eudidean metric, (b) ordinary three-dimensional Eudidean space, (c) the surface of a cylinder extending to infinity in either direction of its central axis together with the appropriate metric, (d) the surface of a sphere. (Geometrics (b) and (d) will not be considered here, primarily because of

difficulties arising in their implementation). These geometries all have the desired qualities of isotropy and uniformity: (a), (b), and (c) may be taken as approximations to fragments of the cortical association layer. (c) in fact may be regarded as an infinite strip in the plane folded so that its edges coincide. For this, the simple Eudidean metric may be retained.

For the simulation, of course, it is necessary to reduce the infinite unbounded geometries to finite bounded ones. From (a), a simple square may be taken; from (c), a finite cylinder. The continuous geometry must then be approximated by a finite, discreet geometry. Points of these geometries are neurons of the model.

Unfortunately, reduction of the infinite geometries (a) and (c) to finite bounded geometries violates the principle of isotropy needed, for the spaces are not uniform at their boundaries. For sufficiently large networks (N = very large) this perhaps poses no serious problems, since then the space of may be considered essentially infinite. However, for N relatively small (N = 200 - 900) as in the present study, the presence of boundaries may cause serious anomalous perturbations of the behavior of . Consider, for example, the square of Figure 4.8. Suppose, along one of its boundaries, E, f_o neurons fire at $t = t_0$. The width of the "swath" along the boundary (Area 1 of Figure 4.8) is a function of $\rho(d)$. If f_0 chanced to be sufficiently large, by the reasoning of tion 4.3.3 (assuming negative corrections present), few, if any, neurons in Area 1 would fire at $t_0 + 1$. Let Area 2 be the set of neurons not in Area 1, but receiving connections from Area 1. By the same reasoning, the firing of neurons of Area 2 at $t_0 + 1$ might be increased if f_0 were not too large (limits determined by synapse value distribution). Suppose

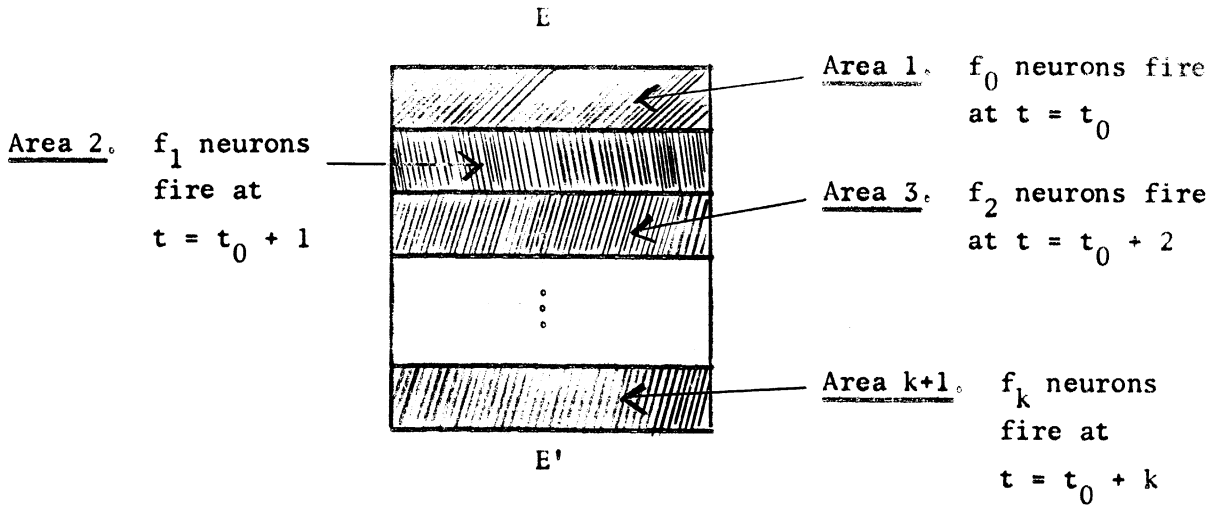

Figure 4.8. An Example of a Boundary Problem. See text for explanation.

f_1 neurons fire at $t_0 + 1$ in Area 2. Likewise, at $t_0 + 2$, most neurons that fire will be in Area 3, since the neurons of Area 2 would be inhibited while most of those of Area 1 are refractory or inhibited. Similarly for $t_0 + 3$, $t_0 + 4$, ..., $t_0 + k$. In effect, a "wave" has been sent across the network, leaving an abnormally large number of highly refractory neurons in its wake. In particular, the number of neurons fireable at $t_0 + k + 1$ may be nil. Thus, the possibility arises of violent oscillations in F(t).

Admittedly, this is an extreme case. However, less violent but equally undesirable effects may be obtained. For example, if f_0 above were of moderate magnitude, the wave sent out from E may reflect off the opposite side E^1 and come back to E, reflect off E, back to E^1, etc., creating a standing wave phenomenon. The behavior of the network would be locked into a particular pattern, with the result that the network's response to stimulus would be erratic. That is, stimulus may produce no

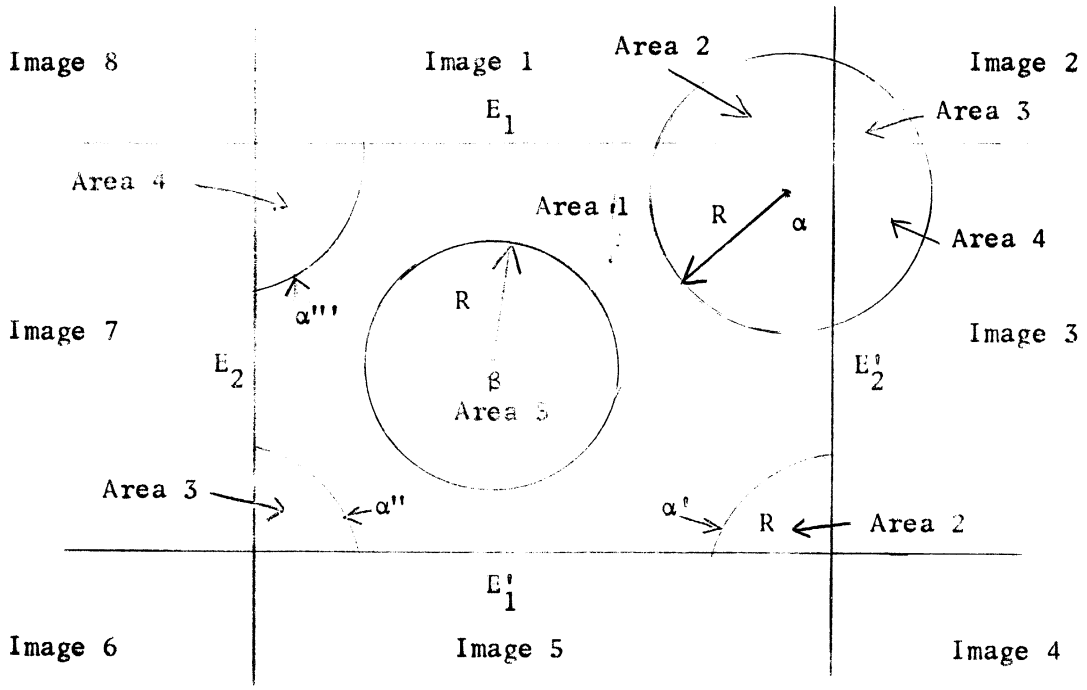

Figure 4.9. Quasi-Torus

effect or may cause fatal oscillations. (This is especially true if the number k is less than $\hat{r}_q$. If $k >> \hat{r}_q$, such phenomenon as the above would appear to be less likely to occur since the wave would tend to break up as it travels from E toward E^1.)

The difficulties arising from bounded geometries may be resolved by the "quasi-torus." Consider the geometry of Figure 4.9. The edges E_1 and E_1^1 are identified, making the square a cylinder. Then, E_2 and E_2^1 are identified, bending the cylinder into a torus. Throughout this process, however, the Eudidean metric of the square is preserved. It is as though the square were iterated on all sides (Images 1 - 8 on the figure). For example, point α has neighbors with a circle of radius R within areas 1, 2, 3, 4 as shown. These areas may be considered on the one hand as the intersect of circles with centers at the virtual images

α', α'', and α''' respectively with the square E_1 E_1' E_2 E_2'. On the other hand, they may be considered as the intersections of the circle with center at α with the images 1, 2, 3 respectively. The point 3 has its neighbors within a circle of radius R in Area 5 as shown. This preservation of the metric in the iterated cells distinguishes the geometry from the actual toroidal geometry, although some essential aspects of the torus remain, e.g., in Figure 4.10 the lines A, A' intersecting E_1' wrap around at E_1, likewise B, B' intersecting E_2 wrap around at E_2. Note that the points $B \cap E_2'$ and $B \cap E_2$ are identical as are $A' \cap E_1'$ and $A' \cap E_1'$, $A \cap E_1'$ and $A \cap E_1'$, etc.

The geometry of the quasi-torus is finite and isotropic, the metric is particularly simple, and boundary problems do not exist. It may be regarded as a crude approximation to the highly convoluted cortical geometry, or it may be regarded merely as a convenient artifact which preserves the basic property of isotropy and allows exploration of Hebb's thesis. Again, as $N \to \infty$, the geometry tends to that of the infinite plane. Throughout the remainder of this paper, all discussions of networks with distance-bias will assume this quasi-toroidal geometry as the underlying space.

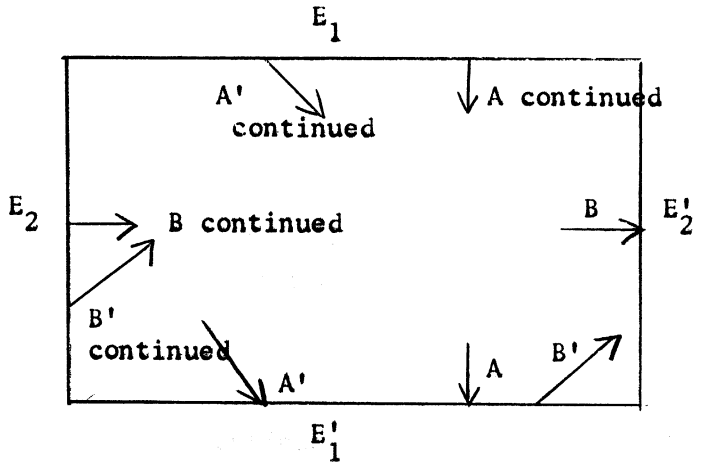

Figure 4.10. Properties of the Quasi-Torus.

Steady-State in Networks with Distance-Bias

The characterization of steady-state behavior in networks with uniform random distributions of connections took the following simple form: "the expected number of neurons firing per time step is F_b." From this condition the conditions of Sections 4.3.2 and 4.3.3 on the threshold curve and synapse-value distribution were derived. Conceivably, on the basis of the principles outlined in those sections, a complete mathematical stability theory could be developed for neural networks with uniform random distributions of connections. Unfortunately, a comparable theory for networks with distance-bias seems to be beset by a multitude of difficult problems from the outset. Consequently, the role of the simulation as a means of by-passing tedious mathematical analysis is all the greater for such networks. However, certain useful principles still may be developed and used as guides to designing effective experiments.

The statement "the expected number of neurons firing per time step is F_b" by itself is not an adequate condition for steady-state in networks with distance-bias. For consider the situation depicted in Figure 4.11, F_b neurons fire at t_0, but these neurons are entirely contained in the circular area A. Suppose $F_b = \bar{A}$. Then, at $t_0 + 1$, neurons in the annulus A', determined by $\rho = \rho(d)$, will fire. At $t_0 + 2$, neurons in the annulus A" plus a few in A' will fire, etc. This yields a series of gradually dissipating, expanding concentric rings of activity with a refractory core in $A \cup A' \cup A'' \cup \ldots$. Several ills might occur in this situation: (1) $\mathcal{M} = (A \cup A' \cup A'' \cup \ldots)$ may be essentially exhausted, that is, not enough fireable neurons are available to maintain stable-steady-state. F(t) would then tend to zero. (2) Enough neurons in the compliment $\bar{\mathcal{M}} = (A \cup A' \cup A'' \cup \ldots)$ are left to maintain activity,

but the neurons in $A \cup A' \cup A'' \cup \ldots$ become hyper-recovered. This violates the second function of steady-state listed in Section 4.3.1. Consequently, the danger of violent, possibly fatal, oscillations arises, and some qualification on the condition is needed. What is needed clearly is some condition on the spatial distribution of neurons firing in steady-state.

The following provides the necessary spatial distribution of neurons: the F_b neurons are distributed randomly and independently over $\mathfrak{M}$ like, for example, the flying-bomb hits on London in World War II, bacteria on a Petri-plate[1], etc. Let F_A = the expected number of neurons firing in area A, then

Eq. 4.3.10 $$F(A) = \frac{F_b}{N} \overline{\overline{A}} = (1/\hat{r}_q) \cdot \overline{\overline{A}}$$

since $\frac{1}{\hat{r}_q} N = F_b$; $1/\hat{r}_q$ is the probability that a neuron of $\mathfrak{M}$ will fire at t. If N is sufficiently large so that the geometry may be regarded as continuous, this is equivalent to saying that

$$F(A) = \frac{1}{\hat{r}_q} A \quad (\text{"A" the area of A})$$

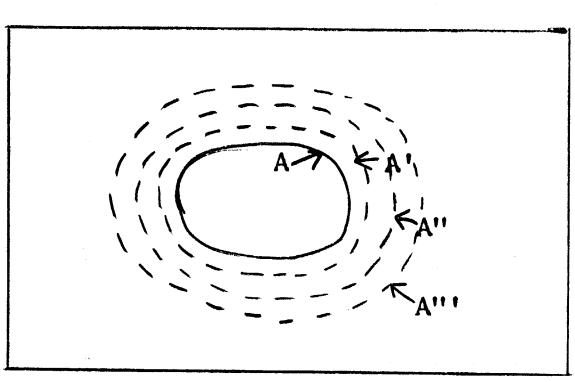

Figure 4.11. Anomalous Steady-State in a Network with Distance-Bias

[1] See, for example, Feller, W. An Introduction to Probability Theory and Its Applications, Vol. I, Wiley, pages 150-152.

and

Eq. 4.3.10(b) $$dF(A)/dA = 1/\hat{r}_q .$$

In other words, $1/\hat{r}_q$ may be regarded as the rate of change in firing per unit area.

Equation 4.3.10(a) will therefore be accepted as a necessary condition for steady-state in networks with distance-bias. It is, of course, an approximation, since, in principle, the firing pattern at t + 1 can always be uniquely determined from the firing pattern at t. The conditions for the firing of a neuron of $\mathcal{N}$ at t are sufficiently complex and variable that it may be regarded as a "random" event (the usual condition for applications of elementary probability theory). The equation essentially limits the expected activity of neurons in any given area. F(A) is an expectation, therefore the question of its variance arises, just as it did in Section 4.3.3 for F(t). Again, as the example above shows, too large a variance can lead to catastrophic results. Recalling the moral stated at the conclusion of Section 4.3.3, it will be assumed that var F(A) remains within certain bounds, these bounds being determined by the simulation.

Conventions of Distance-Measure

The quasi-toroidal geometry of $\mathcal{N}$ takes the following specific form: Let $N = e^2$, the network being laid out as a square on a two-dimensional grid with e neurons per side (see Figure 4.10). Neuron i will have coordinates (x_i, y_i) where x_i is the number of units from (0,0) to the projection of i on the x-axis, y_i the number of units from (0,0) to the projection of i on the y-axis. Given another point (neuron) j, the problem is to define uniquely d(j,i), the distance from i to j. If j has coordinates (x_j, y_j), it would be tempting to define d(j,i) as

$$d(j,i) = [(x_i - x_j)^2 + (y_i - y_j)^2]^{1/2}$$

since an Eudidean metric has been promised. However, a glance at Figure 4.12 indicates that this definition is inadequate: The point j has copies j^1 in the iterated squares 1 - 8. Of these, the points j^1 in squares 3, 4, and 5 are such that the $d(j^1,i)$'s are equally valid candidates for d(j,i).

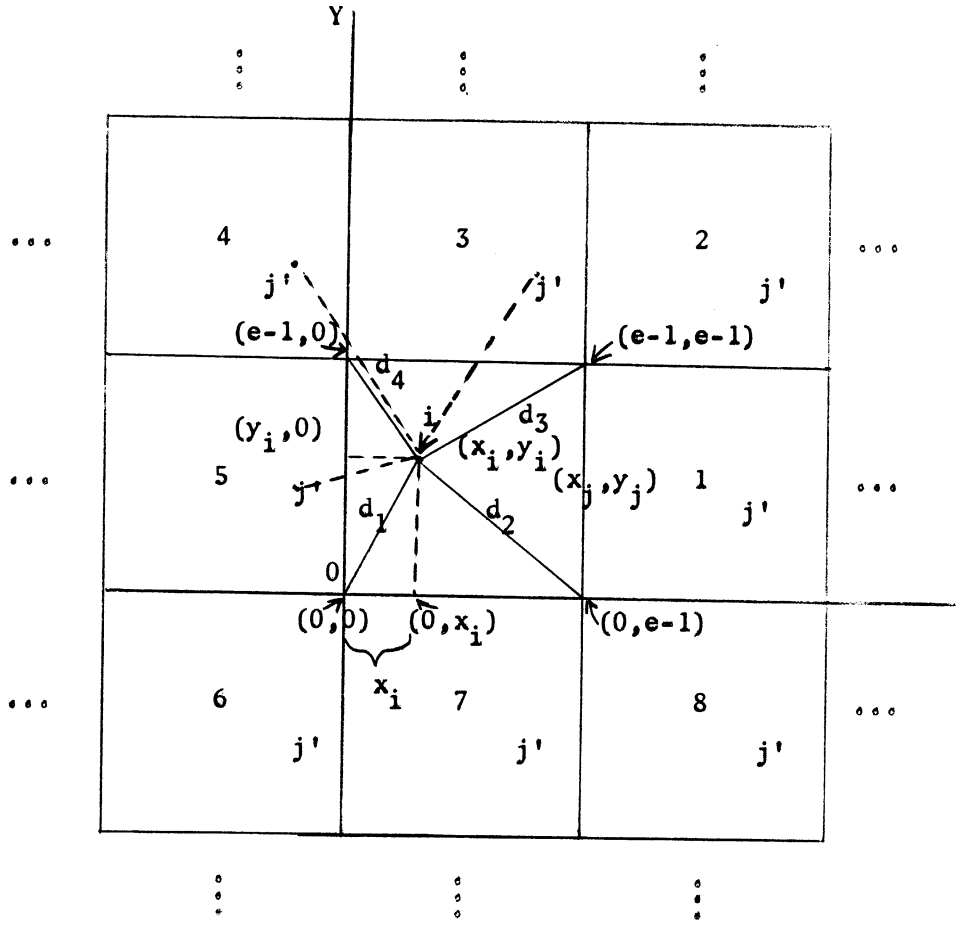

Figure 4.12. Distance Measure on the Quasi-Torus

Therefore, some method of choosing the minimum of all possible d(j,i)'s is required.

For simplicity, suppose one of the points has been mapped into the origin. For d(0,i), d_1, d_2, d_3 and d_4 are candidates. Set

$$d_x = \min(x_i, e - 1 - x_i)$$

$$d_y = \min(y_i, e - 1 - y_i)$$

Then, it is easy to see that the required distance is $d(0,i) = (d_x^2+d_y^2)^{1/2}$. In the figure, $d(0,i) = d_4$.

For arbitrary points (x_i,y_i) and (x_j,y_j), the mapping takes the form

$$(x_j,y_j) \to (0,0)$$

$$(x_i,y_i) \to (x_i-x_j, y_i-y_j)$$

Should $x_i - x_j$ or $y_i - y_j$ become negative, e - 1 is added:

$$(x_i,y_i) \to (x^1,y^1)$$

where $x^1 = x_i - x_j$ if $x_i - x_j \geq 0$

$= x_i - x_j + e - 1$ if $x_i - x_j < 0$

$y^1 = y_i - y_j$ if $y_i - y_j \geq 0$

$= y_i - y_j + e - 1$ if $y_i - y_j < 0$

and x^1,y^1 are used in the definition of d_x and d_y.

Disk Distribution

The specific form of $\rho = \rho(d)$ to be used throughout the remainder of the present work whenever distance is involved is the following (recall Section 4.2.2 above):

Given any neuron $e \in$, the expected number of connections received by i from is

$$\rho(r_i) = \text{constant} = \rho_0 \neq 0 \text{ for } 0 \leq r_i \leq R$$

$$\rho(r_i) = 0 \text{ for } R < r_i$$

where r_i is a radius emanating from neuron i (see Figure 4.13). The basic scheme for assigning connections is modified so that no connections are obtained outside the disk C_R of radius R with center at i. This means that i receives connections equiprobably from the neurons of C_R and none from $\mathcal{M} - C_R$. For N sufficiently large,

$$\overline{\overline{C}}_R = \text{area of } C_R = 2\pi R^2$$

and Equation 4.3.10(a) becomes

$$F(C_R) \cong \frac{1}{r_q} 2\pi R^2 .$$

The numbers R and ρ_0 are constant for a given network ; $\rho_0 = \sum_{-s_0}^{s_1} \rho_s^0$.

The Difficulty

Ideally, a calculus similar to that of Sections 4.3.2-3 should be developed for networks with distance-bias. Unfortunately, an attempt to modify that calculus to treat networks with distance-bias on the distribution of connections immediately leads to a computational impasse. The probabilities $\pi_k(\lambda(t))$ or P_k^* must be modified to account for the distance variation of $\rho = \rho(d)$, hence of the λ_s's, $s = -s_0, \ldots, s_1$. To do this, the geometric structures as well as the respective cardinalities

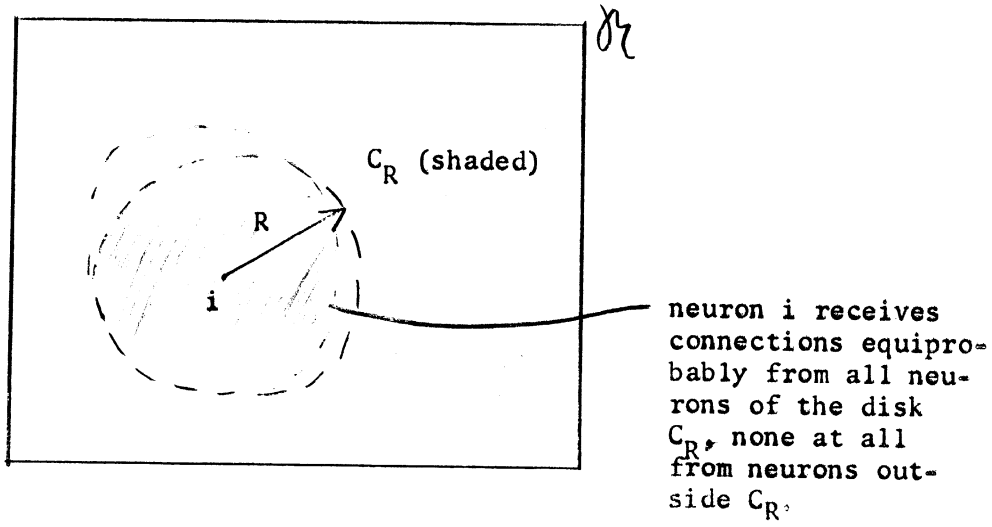

Figure 4.13. Example of a Disk Distribution

of the sets $R_0(t)$, $R_1(t)$, ..., $R_{r_q}(t)$ would have to be specified. Next, the expected number of connections received by each $R_r(t)$, $r_a \leq r \leq r_q$, from $R_0(t-1)$ would have to be estimated. The latter process gives rise to integrals of the type discussed in Section 4.2.2. Figure 4.14 illustrates the variation in the expected number of connections received by a neuron from simple configurations (using crude approximations to the area integrals). While these estimates assist in understanding the effects of distance-bias on the connection probabilities π_k or P_k^*, they are not really useful for the present purposes. There are, however, some useful techniques for estimating the threshold curve and for setting the parameters ρ, R, $\hat{r}_q$ and F_b.

(a) Connections Received from a Disk of Radius h.

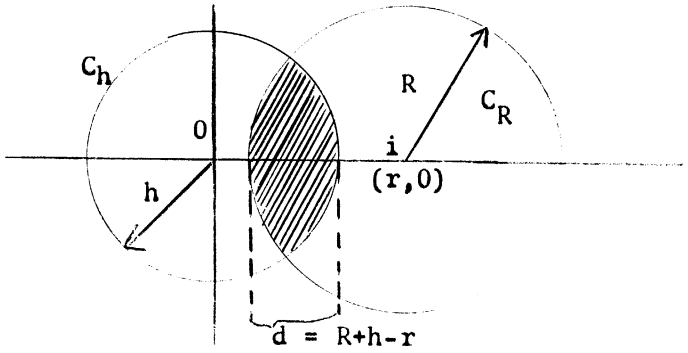

Receiving neuron i at (r,0)

(b) Connections Received from a Line Segment.

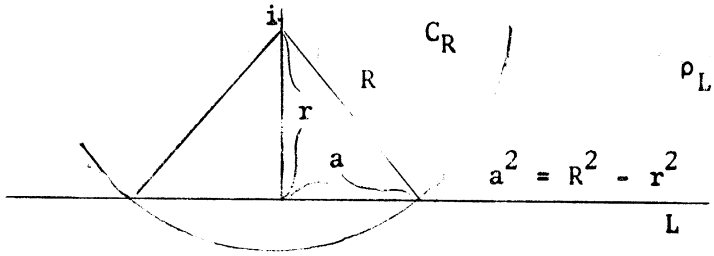

$\rho_L = 2K(R^2-r^2)^{1/2}$

(c) Connections Received from a Box with Circular Ends.

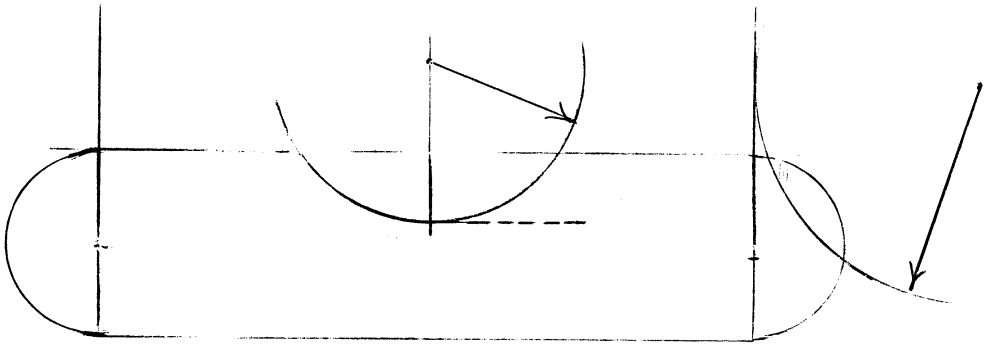

For i in Area 1, $\rho_B = K\frac{1}{2}(1+d^2)$

For i in Area 2, use approximation (a)

These ignore the corner effects (C_R intersects both a circle and the box).

Figure 4.14. Estimates of Expected Number of Connections Received by a Neuron i from Simple Geometric Structures. The basis for the estimates given above is that the expected number of connections ρ_A received by a neuron $i \in A$, is proportional to the area of A (in (b), to the length of a line segment). This holds since $\rho(r)$ is uniform for $0 \leq r \leq R$. The general inference from the estimates below is that ρ_A varies quadratically with the distance from i to the boundary of A.

Given a network $\mathcal{N}$, with $\overline{\overline{\mathcal{N}}} = N$, distance-bias function $\rho = \rho(r)$ as above, $F_b = \frac{1}{\hat{r}_q} N$ the expected number of neurons firing per time step in $\mathcal{N}$. Perform the steady-state calculations of Sections 4.3.2 - 4.3.3 for the neighborhood $C_R \subset \mathcal{N}$. For this, from Section 4.3.10

$$F_b^R = \frac{1}{\hat{r}_q} \overline{\overline{C}}_R = \frac{2\pi R^2}{\hat{r}_q}$$

and the λ_s's are given by

$$\lambda_s = \rho_s^0 \frac{F_b^R}{\overline{\overline{C}}_R} = \rho_s^0 \cdot \frac{1}{\hat{r}_q} = \rho_s^0 \frac{F_b}{N} \quad (s = -s_0, \ldots, s_1)$$

since $\hat{r}_q = \frac{N}{F_b}$. In other words, this is equivalent to treating $\mathcal{N}$ itself as though it were a network with uniform random distribution of connections with density

$$\rho_0 = \sum_{s=-s_1}^{s_2} \rho_s^0 .$$

This calculation, of course, ignores the effect of neurons in $\mathcal{N} - C_R$ upon those of C_R. Depending upon the distribution of synapse-values over synapse-levels (giving the decomposition $\rho^0 = \sum_{s=-s_0}^{s_1} \rho_s^0$), the resulting threshold curve would tend to produce either overdamped or underdamped behavior initially in $\mathcal{N}$. At this point, refuge is again taken in the simulation, the calculations above being used as a guide for setting V(r), then a family of curves derived from V(r) may be tested experimentally, gradually homing in on the one that best satisfies the basic conditions laid down in this chapter for steady-state and stability.

In Chapter 6, it will be seen that this procedure is not as haphazard as it appears and that many of the principles that apply to networks with uniform random distributions of connections carry over with only

slight modification to networks with distance-bias.

4.3.5 Synapse-Level Drift

In the preceding discussions, the synapse-values have been assumed to be set to discrete integral values $-s_0$, $-s_0+1$, ..., s_1. If the network is operating in steady-state, the analysis of Chapter 2, Section 2.3.4, guarantees only that the expected change in synapse-levels is zero. In practice, the levels will "drift" from their initial settings since locally some neurons may be firing at rates greater or lesser than F_b for brief periods of time. If the network is operating in a true steady-state and if all the network functions are properly adjusted, this "drift" should ultimately take the form of a multi-modal distribution of synapse-values about the means $-s_0$, $-s_0+1$, ..., s_1. As usual, the problem of variance arises and, as usual, the burden of the proof will be on the simulation. A drift in synapse-levels in a particular direction would indicate an imbalance in the network functions. For example, the threshold curve might be set for a steady-state firing rate of $1/\hat{r}_q$, while the synapse-level balancing equation is set for a rate of $1/r'_q$,

$$\frac{D(\lambda)}{U(\lambda) + D(\lambda)} = 1/r'_q$$

and $1/\hat{r}_q > 1/r'_q$. In this case, a net increase in synapse-levels (values) would be expected.

4.4 Networks Under a Single Periodic Stimulus

4.4.1 Stimulus and Stability

In the preceding section, computational guidelines were laid down for determining the network parameters N, ρ, r_q, etc., and the threshold function V(r) that will yield stable steady-state behavior in a given

network $\mathcal{N}$. The criteria for such behavior are outlined at the end of Section 4.3.1. Of the five conditions given there, the fifth has not yet been accounted for, namely "a single application of a moderate sized stimulus to a network operating in steady-state must not produce epilepsy." An analysis of this statement and its consequences forms the basis for the present discussion.

Consider a network $\mathcal{N}$ operating in steady-state. This means that there is a distribution $\mathcal{R}(t)$ of neurons over recovery states that is stationary in the sense that the expected values of the $\overline{\overline{R}}_r(t)$ remain constant (in fact all equal to F_b) for all time. The negative synapse-values provide the necessary feedback control mechanism to damp out the effects of transient variations in $F(t)$ from F_b, the bounds on such variations to be determined empirically. The origins of these transient variations were attributed to the random fluctuations of the $\overline{\overline{R}}_r(t)$ from their mean F_b that are inherent to any random process.

Suppose, however, that a subset $\Sigma_0 \subset \mathcal{N}$ is selected as an input set. At certain time step t_0 the neurons of Σ_0 are provided with an external stimulus S_0. In general, the neurons of Σ_0 will be distributed uniformly over $\mathcal{N}$ (in the case of uniform random connection distributions) or over some subregion of $\mathcal{N}$ (in the case of distance-bias). Likewise, neurons of Σ_0 will be distributed randomly over recovery-states. Since a neuron of Σ_0 fires at t_0 if S_0 plus the incoming stimulus to the neuron at t_0 exceeds its effective threshold, for a given S_0, the expected number of neurons of Σ_0 that will fire at t_0 is F_0 where

(a) (uniform random distribution)

$$F_0 = \left(\frac{\overline{\overline{\Sigma}}_0}{N} \; \frac{\overline{\overline{M}}^*_{s_0}}{N}\right) \cdot N = \frac{\overline{\overline{\Sigma}}_0 \cdot \overline{\overline{M}}^*_{s_0}}{N}$$

where $M^*_{s_0}$ is defined as

$$M^*_{s_0} = \bigcup_{k=1}^{[s_0]} M_k .$$

(b) (distance-bias)

$$F_0 = \left(\frac{\bar{\Sigma}_0}{A}\right) \cdot \left(\bar{\bar{M}}^*_{s_0} \frac{\bar{\bar{A}}}{N}\right) \cdot \frac{\bar{\bar{A}}}{N} = \bar{\bar{\Sigma}}_0 \cdot \bar{\bar{M}}^*_{s_0} \cdot \frac{\bar{\bar{A}}}{N}$$

where A is the region of $\mathcal{N}$ containing Σ_0, $\Sigma_0 \subset A \subset \mathcal{N}$. In (b), it is assumed that neurons are distributed uniformly over recovery states over area: if $\bar{\bar{R}}_r$ neurons of $\mathcal{N}$ are in recovery state r, then the expected number in this state in an area A is $\bar{\bar{R}}_r \frac{\bar{\bar{A}}}{N}$. Notice that (a) and (b) are equivalent if $A = \mathcal{N}$ ($\bar{\bar{A}} = N$).

The basic reasoning of Sec. 4.3.3 may now be applied to the case that F(t) undergoes a variation of approximate magnitude $F_b + F_0$ at t_0. (In general, the subset of Σ_0 that fires at t_0 and $R_0(t)$ will overlap. Consequently, the actual expected variation is $F_b + F_0 - \frac{F_0 * F_b}{N}$ or $F_b + F_0 - F_0 F_b \frac{\bar{\bar{A}}}{N^2}$ depending upon the absence or presence respectively of distance-bias. The error term is, of course, frequently negligible.) If F_0 lies below a certain bound F_{max}, the network will remain stable. Empirically and computationally, a safe bound was found to be

$$F_{max} \cong F_b/2$$

although larger variations were tolerated.

Should F_0 exceed F_{max}, depending upon the distribution of synapse-values over connections, F(t) will be driven too far above or below F_b for the behavior to remain stable and fatal oscillations would be expected to occur.

The steady-state calculus of Sections 4.3.2.-3 may be applied to

---

Recall again that $F_b = E(F(t))$ is the expected number of neurons of $\mathcal{N}$ that fire at t in steady-state.

study the effects of stimulating Σ_0 and to obtain estimates of f_{max}. Each subset $M_k \subset M^*_{s_0}$ has to be reduced at t_0 by the expected number that fire in M_k, otherwise the calculation proceeds as before. An example of this calculation will be given in Section 4.4.3.

4.4.2 Periodic Stimulus

The basic thesis of Hebb is that cell-assemblies and phase sequences of cell-assemblies come into existence through the repeated application of a training stimulus pattern. Once the assembly is formed, via the synapse-growth law, it responds to a brief application of this pattern and tends not to respond at all to different patterns. "Response" means arousal of activity in the assembly that continues for a brief period of time independently of external stimulus, a combination of effects of fatigue and external inhibitory stimulus damping out the response. More specifically, a subset of neurons of the assembly will operate briefly at rates greater than the background rate $1/\hat{r}_q$. For this subset, the distribution $\mathcal{R}(t)$ is no longer stationary, since for a brief period of time the mean of the $\bar{R}_r(t)$ differs from its steady-state value and not all the $\bar{R}_r(t)$'s are equal. Eventually, the effects mentioned above drive $\mathcal{R}(t)$ back to its stationary form. It is the purpose of this section to examine the effects upon the behavior and structure of $\mathcal{M}$ of the application of stimulus with the simplest type of pattern, namely simple periodicity.

Suppose a set of neurons Σ_0 (as defined in 4.4.1) is stimulated with stimulus S_0 every τ_0 steps at $t = t_0 + m\tau_0$, $m = 0, 1, 2, \ldots$. At $t_0 + \tau$, the set

$$\Sigma'_\tau = \Sigma_\tau \cup \Sigma''_\tau$$

will fire where Σ''_τ is the component due to the steady-state (i.e., the F_b neurons firing at $t = t_0$) and Σ_τ is the component due to the combined effects of the neurons of Σ_0 that fired at t_0 and the steady-state). The expected number of neurons firing at $t_0 + \tau$ is

$$f^1_\tau = F_b + F_\tau$$

where $F_\tau = \overline{\Sigma}_\tau$. This decomposition of Σ'_τ into Σ_τ Σ''_τ holds only for small τ. As τ grows, the effects of Σ'_0 (unless epilepsy were produced) become dissipated. It is important to realize that F_τ need not remain positive, $\tau < \tau_0$. There are three cases: (1) F_τ remains positive; (2) F_τ becomes negative; (3) F_τ goes to zero. In general, if τ is large (3) indicates that the stimulus has dissipated. (1) indicates the presence of a path of connections from Σ'_0 to Σ'_1 to Σ_2 ... to Σ'_τ (abbreviate $P(\Sigma'_0 \rightarrow \Sigma'_\tau)$) such that $\Sigma'_{\tau-1}$ assists in firing $\Sigma'_{\tau'}$, $0 < \tau' \leq \tau$. Such a path will be designated as an effective connection path from Σ_0 to Σ'_1, $P_E(\Sigma'_0 \rightarrow \Sigma'_\tau)$. (2) and (3) may or may not imply a $P_E(\Sigma'_0 \rightarrow \Sigma'_\tau)$. In the case of (2), however, $F_b + F_\tau$ has become so large that $\overline{R}_{r_q}(t)$ is decreased below its steady state value so that $F(t_0+\tau) = F'$ decreases below its steady-state value F_b. This raises again the danger of violent oscillations. For now, merely assume this does not occur and there exists a $P_E(\Sigma'_0 \rightarrow \Sigma'_\tau)$.

At subsequent applications of the stimulus (assuming the same subset $\Sigma'_0 \subset \Sigma_0$ fires each time) at $t_0 + m\tau_0$, an effective path $P_E(\Sigma'_{m\tau_0} \rightarrow \Sigma'_{m\tau_0+\tau})$ will exist. These paths will, in general, at least partially coincide after repeated applications of the stimulus if the stimulus is sufficiently "strong": i.e., $\overline{\Sigma}_0 \cong F_{max}$, $\tau_0 << r_q$, S_0 large. (While this statement is not, perhaps, a priori evident, again the appeal will be made to the stimulation, which will bear it out. The role of distance-bias is

vital in this argument and will be discussed in 4.4.4. below.)

An important characteristic of the stimulus must now be introduced. If $\tau_0 << \hat{r}_q$, repeated applications of the stimulus will result in fatiguing the neruons of Σ_0, so that eventually they respond but sporadically to it. Therefore, consider that the stimulus is applied periodically every τ_0 time steps for $t = t_0$ to $t = t_1$, then it is turned off from $t = t_1$ to $t = t_2$, then turned on again. Assume, as in Chapter 3, that the lengths t_ℓ of these "on-off" periods are equal: $t_1 - t_0 = t_2 - t_1 = \cdots = t_\ell = \text{constant}$. Set t_ℓ so that the neurons of Σ_0 just begin to fatigue by $t_0 + t_\ell$, and completely recover with respect to fatigue by $t_1 + t_\ell$, etc. The case is very similar to that of the synchronous periodic inputs of Chapter 3. Assume, therefore, that a path

$$P_E = P_E(\Sigma_0^\ell \to \Sigma_\tau^\ell)$$

develops, $\tau \leq \tau_0$, possibly over several "on-off" cycles. Notice that the synapse growth law is involved in this development since the neurons of $\Sigma_{\tau'-1}^\ell$ will be repeated assisting those of $\Sigma_{\tau'}^\ell$ in firing at a rate greater than $1/\hat{r}_q$, therefore causing an increase in the λ_{ji}'s, $j \in \Sigma_{\tau'-1}^\ell$, $i \in \Sigma_{\tau'}^\ell$.

The question arises now: Will the path P_E eventually close back on itself? That is, will an effective path $P_E(\Sigma_\tau^\ell \to \Sigma_{\tau_0}^\ell)$ develop? Since $\Sigma_{\tau_0}^\ell = \Sigma_0^\ell$, this means that a closed cycle $C(\Sigma_0^\ell) = P_E(\Sigma_0^\ell \to \Sigma_0^\ell)$ of length τ_0 has evolved. $C(\Sigma_0^\ell)$ will form a candidate for a cell-assembly in the model.

To demonstrate an affirmative response to the question with the current model will form the bulk of the empirical effort of Chapters 6 and 7. However the following intuitive argument might illuminate the problem somewhat:

If ρ is sufficiently large (and R not too small if distance-bias is involved), then there almost certainly exists at least one chain of neurons from $i_0 \in \Sigma_0'$ to $i_1 \in \Sigma_1'$ ... to $i_{\tau_0-1} \in \Sigma_{\tau_0-1}$ back to i_0 again. That is, there exists a $P_E(\Sigma_0' \to \Sigma_{\tau_0}')$. However, it is unlikely that this chain would be "effective" in the sense that

(1) $S(\lambda_{ji}) > 0$ $\quad j = i_{\ell-1}$, $i = i_\ell$ for $\ell = 1, \ldots, \tau_0 - 1$ and $i_{\tau_0} \equiv i_0$.

(2) the $S(\lambda_{ji})$ above are such that, in general, neuron $i_{\ell-1}$ assists in the firing of neuron i_ℓ ($\ell=1, \ldots, \tau_0$). That is, i_ℓ should not fire independently of $i_{\ell-1}$. As a transient mechanism or artifact for increasing $S(\lambda_{\ell-1,\ell})$, this might be acceptable: however, as a permanent feature, it is clearly not desirable.

These conclusions hold because of the distribution of synapse-values over connections. Each link $i_{\ell-1} \to i_\ell$ of the chain has a definite probability of having a positive or a negative synapse-value. Therefore, the probability that <u>all</u> the $S(\lambda_{ji})$'s are positive decreases rapidly with the length τ_0 of the chain.

At this point — easily the most crucial of this thesis — the synapse growth law emerges in its fullest importance: Since the neurons of Σ_0 fire every τ_0 time steps (except in the off period) and since the connection along a $P_E(\Sigma_0' \to \Sigma_{\tau_0}')$ already exists, in particular, a link $i_{\tau_0-1} \to i_0$ exists, any chance firings of i_{τ_0-1} at time steps $t_0 + m(\tau_0-1)$ ($m > 0$) will <u>fortiori</u> be followed by firings of i_0 at $t_0 + m\tau_0$. Gradually, then, over sufficiently long time intervals,

$$\lambda_{i_{\tau_0-1}, i_0}$$

will be expected to increase, thus making the link $i_{\tau_0-1} \to i_0$ effective, assuming for the moment that $S(\lambda_{i_{\tau_0-1}, i_0})$ is not strongly inhibitory

(very negative). As this link becomes effective, the link $i_{\tau_0-2} \rightarrow i_{\tau_0-1}$ will likewise become so. The latter, of course, depends on the preceding links gradually becoming effective. Therefore, what must happen is that "both ends are worked against the middle" and the path P_E becomes effective. The role of the repeatedly applied stimulus is to "lock-in" the cycle, so to speak via the synapse-growth law.

The process of making the link $i_{\tau_0-1} \rightarrow i_{\tau_0}$ effective, in other words, the process of drawing neuron i_{τ_0-1} into the cycle $C(\Sigma_0')$, is an example of the phenomenon referred to by Hebb as "recruitment". Neuron i_{τ_0-1} is recruited into the cycle $C(\Sigma_0')$. Since a number of chains $i_0 \rightarrow i_1 \rightarrow \cdots \rightarrow i_{\tau_0-1} \rightarrow i_0$ may exist, recruitment need not be a one time only occurrence. The longer the training period, presumably the more the neurons that will be recruited into $C(\Sigma_0')$. Conversely, certain of the chains $i_0 \rightarrow i_1 \rightarrow \cdots \rightarrow i_{\tau_0-1} \rightarrow i_0$ may cease to be effective and a neuron i_{τ_0-1} may drop out of $C(\Sigma_0')$. This corresponds to Hebb's fractionation phenomenon.

Fractionation and recruitment depend some what upon the initial value of $\lambda_{i_{\tau_0-1}, i_0}$. If $S(\lambda_{i_{\tau_0-1},i_0})$ is strongly inhibitory (i.e., near the maximum negative value), the increasing trend in $\lambda_{i_{\tau_0-1},i_0}$ would be less likely to occur, since i_{τ_0-1} would tend to assert a strong inhibitory effect upon i_0. This tends to aid fractionation. If $S(\lambda_{i_{\tau_0-1},i_0}) = \sigma$ and $-\sigma_1 \leqq \sigma$ where σ_1 is a small positive number, the inhibition exerted by i_{t_0-1} upon i_0 may be negligible and the preceding argument stands: recruitment might occur.

This main point of this section is now the following: once the lock-in described above is accomplished and an effective cycle $C(\Sigma_0')$ is formed, the stimulus need not be applied in as strong a fashion as during

the training period. For example, assuming the neurons of $C(\Sigma_0')$ are not unduly fatigued, a single stimulus might go around the cycle $C(\Sigma_0')$ several times before being extinguished. Notice that $C(\Sigma_0')$ may consist of several neurons in each level ℓ and there may actually be several paths in the link $\Sigma'_{\ell-1} \rightarrow \Sigma'_{\ell}$. Starting at $i_0 \in \Sigma_0'$ each time, the stimulus may actually circulate through different paths from Σ_0' to Σ'_{τ_0-1}. Thus, the structure of $C(\Sigma_0')$ is not inflexibly rigid. $C(\Sigma_0')$ would be a self-sustaining cycle since, once activity is initiated (Σ_0 stimulated), it is maintained for a brief period of time (the stimulus circulates through $C(\Sigma_0')$ a number of times before being extinguished).

These properties of $C(\Sigma_0')$ — if they can be demonstrated empirically — appear to qualify $C(\Sigma_0')$ as a cell-assembly in Hebb's original sense [9]. Success in empirically exhibiting a $C(\Sigma_0')$ would appear to give some hope to the field of machine learning.

4.4.3 Stability Calculations

The calculations of 4.3.2-3 may be readily modified to treat simple periodic stimulation of a subset $\Sigma_0 \subset$ [illegible]. First, at $t = t_0$ when the stimulus is first applied, the subsets R_r of $M^*_{s_0}$ are reduced by the appropriate expected amounts, that, together with the neurons of $R_{r_q}(t_0)$ that would have fired at t_0 anyhow in steady-state, from $R_0(t_0)$. Then the calculation proceeds as usual until $t_0 + \tau_0$, at which point R_{τ_0} is reduced by the number in Σ_0 that fired at t_0, $\bar{\bar{\Sigma}}_0'$, this number being added to the number that would have fired anyhow at t_0, thus forming $F(t_0+\tau_0)$. Continue in a similar manner for $t_0 + \tau_0 + 1, \ldots$.

Table 4.3 shows this calculation for the network of Figure 4.4 and Table 4.1: $N = 400$, $\rho = 6$, $\bar{\bar{\Sigma}}_0 = 10$ and $\bar{\bar{\Sigma}}_0' = 7$, $\tau_0 = 6$, $S_0 = 6$. Notice

that $\bar{\bar{R}}_0(t)$, $\bar{\bar{R}}_1(t)$, ..., $\bar{\bar{R}}_5(t)$ are increasing.

4.4.4 Distance-Bias

In section 4.4.2, it was observed that distance-bias played an important role in the formation of an effective path $P_E(\Sigma_0' \rightarrow \Sigma_\tau')$, $\tau \leq \tau_0$. This is, in fact, an example of "localization" alluded to earlier in the chapter. Consider the network $\mathcal{N}$ of Figure 4.15. There, R = ∞ (uniform random distribution) and the neurons of Σ_0 are equi-probably connected to any other neuron of $\mathcal{N}$. The path from Σ_0' to Σ_τ' may be any one of several paths at successive intervals $t_0 + m\tau_0$, and a definite effective path $P_E(\Sigma_0' \rightarrow \Sigma_\tau')$ may or may not occur.

Consider now the network of Figure 4.16. There, R is finite and $\Sigma_0 \subset C_R$. The neurons of Σ_0 are spaced regularly along the 5 x 5 subgrid of $\mathcal{N}$. The spacing of the neurons is such that the neurons of Σ_1' fired by Σ_0' will fire again after the next application of stimulus at $t_0 + \tau_0$, etc. Likewise, the neurons of Σ_1' will tend to fire the same set Σ_2' at succeeding time steps $t_0 + 2 + m\tau_0$. Gradually, of course, the successor-

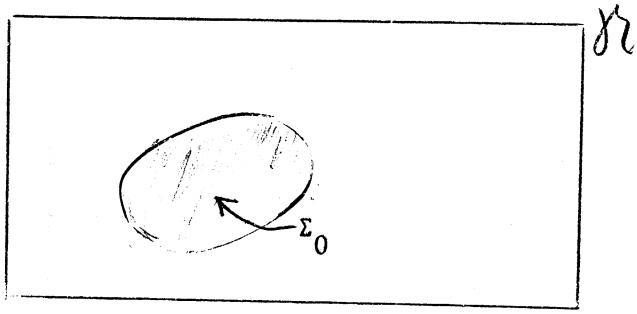

Figure 4.15. Non-Localization Property of Networks with Uniform Random Distribution of Connections. A neuron i ϵ Σ_0 is equi-probably connected to any other neuron of $\mathcal{N}$. Localization (in any uniform, regular sense) is not possible.

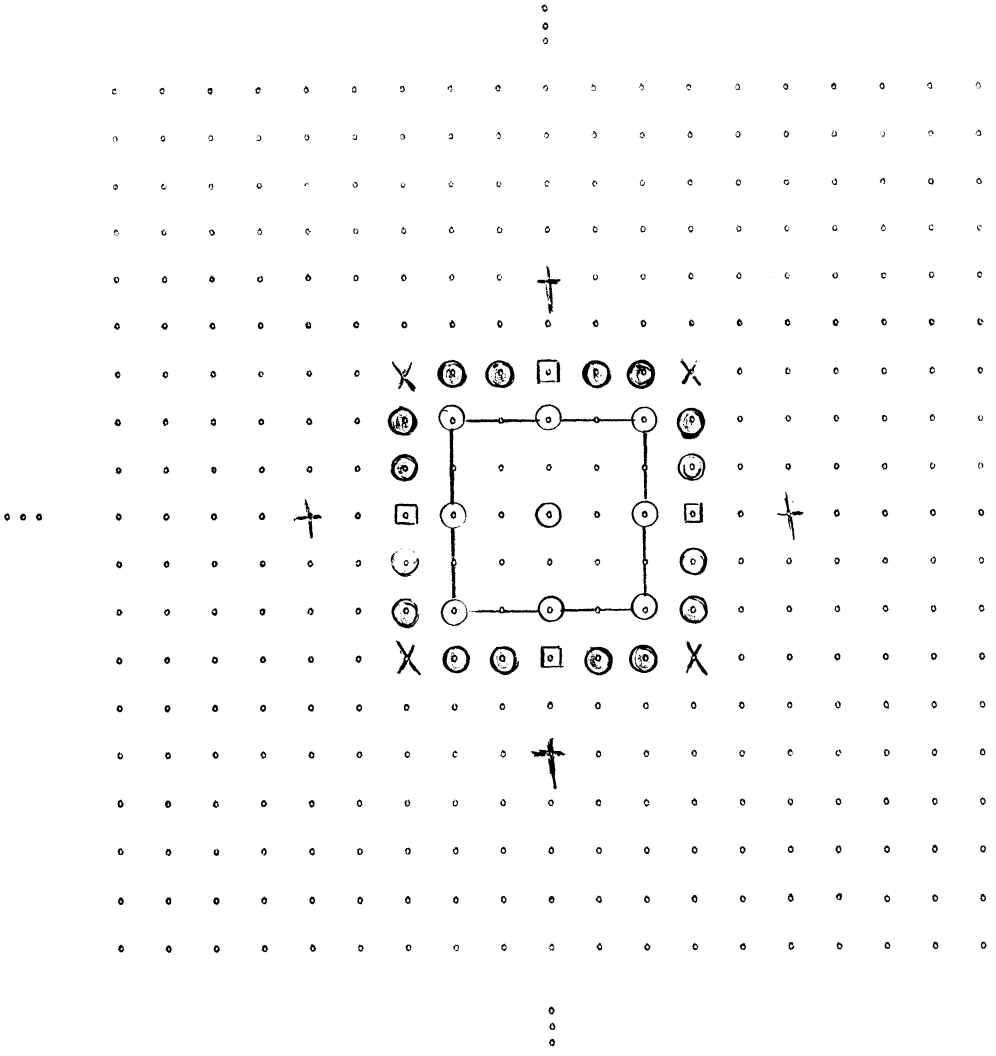

Figure 4.16. Example of an Input Set Σ_0 in a Network $\mathfrak{N}$ with Distance-Bias. In this network, R = 6. A is the shaded area, $\Sigma_0 \subset A$ the encircled neurons. Every neuron of $A - \Sigma_0$ lies in $\bigcap_{i \in \Sigma_0} C_R(i)$, i.e., may receive connections from any neuron of Σ_0. Neurons in the exterior of A, $\mathfrak{N} - A$, receive connections from Σ_0 as follows:

- Neurons in the squares may receive connections from any neuron of Σ_0.
- Neurons in the solid circles may receive connections from all but one neuron of Σ_0.
- Neurons marked with X or the dagger may receive connections from all but three neurons of Σ_0.

sets Σ_τ spread out over $\mathcal{N}$. If R is small, it could happen that Σ_0 would be insulated from Σ_{τ_0-1} and closure would never occur. If the spacing of the neurons of Σ_0 were too close, a core of refractory neurons could result with the consequences outlined in section 4.3.4. The setting of $\rho = \sum_{s=-s_0}^{s_1} \rho_s$ is clearly equally critical.

In conclusion, the distance-bias mechanism is very convenient for ensuring development of the initial path segment $P_E(\Sigma_0'' \to \Sigma_\tau')$. However, it introduces pitfalls all its own and greatly compounds the number of variables available.

4.5 Networks Under Two Alternating Periodic Stimuli

4.5.1 Alternating Cell-Assemblies

In the preceding section, a heuristic argument was given to show the possible formation of a closed self-re-exciting cycle $C(\Sigma_0)$. It was duly noted that such a model constitutes a candidate for a Hebbian cell-assembly. Given that a cycle $C(\Sigma_0)$ may be formed and that it indeed is a cell-assembly, folloiwng the natural development of Hebb's theory, it is natural to ask:

(1) Is it possible to form additional distinct cell-assemblies in $\mathcal{N}$ (as a result of applying distinct stimulus patterns)? This is far from a trivial question, at least for the relatively small N = $\overline{\mathcal{N}}$ used in this work, since conceivably one $C(\Sigma_0)$ could exhaust $\mathcal{N}$ of neurons available for recruitment into new cell-assemblies.

(2) If the answer to (1) is affirmative, then how will these cell-assemblies relate one to another? Specifically, how will activity (circulating stimulus) in one affect activity in another? This is not meant to imply that there necessarily be a relationship between two

arbtrarily chosen cell-assemblies of a network. There may or may not be such a relationship. However, if the cell-assemblies are "proximate", it is reasonable to assume that such a relationship does exist. "Proximate" means that, given cell-assemblies $C(\Sigma_0)$ and $C(\Sigma_0^*)$, some segments of their respective paths lie within a distance R^* from each other. If $R^* < R$, R the distance-bias radius, $C(\Sigma_0)$ may have an immediate effect upon $C(\Sigma_0^*)$ and conversely. If $R < R^* < 2R$, the possible effect will be delayed one time step, etc. Clearly, in the current model, the larger the R, the less probable the possible influence of one cycle upon the other becomes. In the physiological situation, V fibres or other long-distance axoms might yield the short graph distances requires to be "proximate", while entailing long geometric distances.

A special case of (2), to be considered in detail below, is:

(2') How do cell-assemblies arising from negatively correlated stimuli relate to each other? The hypothesis will be made below that they will become mutually cross-inhibiting.

From (2) then flow all the questions concerning the structure of Hebb's theory of learning, i.e., concerning the arousal of cell-assemblies, alternation of activity in cell-assemblies, the development of phase-sequences of cell-assemblies and phase cycles, etc. To adequately discuss all these questions, to provide the necessary analysis and empirical evidence that would be needed, simply exceed the bounds of this paper.[1] All is not lost, however, since the advanced concepts of Hebb's theory

[1] To say nothing of the bounds imposed by the existing computer hardware. The maximum N used effectively in experimentation was 400. One would want for exploration of the more advanced part of theory at least $N = 1000$, preferably $N \geq 10{,}000$.

seem ultimately to reduce to the effects of proximate cell-assemblies upon each others namely: activity in one cell-assembly should tend to arouse activity in a proximate cell-assembly. These cell-assemblies presumably come into existence through sequences of (spatially and temporally) patterned stimuli of some type. For a complete discussion of how this might occur, the reader is referred to Chapter 5, Perception of a Complex: The Phase Sequence, of Hebb [9]. For now, merely assume that there exist two proximate cell-assemblies, $C(\Sigma_0)$ and $C(\Sigma_0^*)$, and it is desired to study the possible mechanisms by which one may arouse the other.

An important facet to this question is that there appears to be, from the development given by Hebb, a temporal restriction on the arousal of the one cell-assembly by the other. In fact, in general, the temporal relation of cortical events takes great importance in his theory. Specifically, assume that, say, activity in $C(\Sigma_0)$ is not to start activity in $C(\Sigma_0^*)$ until a certain time interval has passed. Presumably, this time interval would be related (a) to the stimuli applied to Σ_0 and Σ_0^*, (b) to the rate of fatigue of neurons of $C(\Sigma_0)$.

In effect, then, $C(\Sigma_0)$ has to suppress activity in $C(\Sigma_0^*)$ for a period of time, the degree of suppression gradually decreasing as the activity in $C(\Sigma_0)$ is damped by fatigue. Conversely, it is interesting to ask, after $C(\Sigma_0^*)$ starts becoming active, will it tend to suppress activity in $C(\Sigma_0)$ for a period of time, then allow it to build up again as fatigue takes effect? Therefore, a "multi-vibrator" effect may be possible: after a training period in which $C(\Sigma_0)$ and $C(\Sigma_0^*)$ are stimulated in certain patterns, alternating between one and the other, a brief stimulus applied to one will set up activity that will "oscillate" back and forth between the two for a period of time. If this effect were possible in the given model, it would appear that the model would suffice for deeper study of

the theory. For phase sequences involve a generalization of this type of behavior from that of two cell-assemblies to larger numbers, all intricately interrelated by arousing and suppressing one another at appropriate instants in time. For this reason, the study of this alternation of activity in cell-assemblies will conclude the present work.

Note that the role of inhibitory connections (negative synapse-values) is absolutely vital here. For $C(\Sigma_0)$ to suppress $C(\Sigma_0^*)$ when the former is active implies the development during the training period of strong inhibitory connections from $C(\Sigma_0)$ to $C(\Sigma_0^*)$ and conversely. To the author's knowledge, this point is not explicitly recognized by Hebb [9], although, of course, it certainly is implicit. Milner [10] made the general role of negative synapse values explicit. The development of this mutual or cross inhibition again depends critically upon the synapse-growth law; this time in reverse: Neurons that are active (say in $C(\Sigma_0)$) are trying to fire neurons in $C(\Sigma_0^*)$ that are fatigued and will not respond. Consequently, the corresponding synapse-values drop. Not all synapse-values from $C(\Sigma_0)$ to $C(\Sigma_0^*)$ must become negative however. A few must remain positive so as to help start $C(\Sigma_0^*)$ up again as the activity in $C(\Sigma_0)$ is damped out. The arousal of $C(\Sigma_0^*)$ may depend upon the presence of some "superordinate" structure as well as upon the decrease in inhibition from $C(\Sigma_0)$. For a simple example, a subset $\Xi \subset \eta$ may be supplying both structures $C(\Sigma_0)$ and $C(\Sigma_0^*)$ with a light stimulus at all times, becoming effective on the one only when the inhibition from the other decreases, etc.

Notice that distance-bias on the distribution of connections is truly indispensible at this point. In fact, recalling the highly diffuse character of the hypothetical assemblies described by Hebb, in the long

run one probably would want a more general distance-bias function than the one adopted here. This would approximate even better to real networks and tend to make (as desired by the theory) the network or less susceptible to local damage (slicing, tranma, etc.).

In conclusion, success in demonstrating an alternation of activity in cell-assemblies as suggested above would strengthen Hebb's original attempt to build a "molar" calculus in which human behavior could be more adequately related to basic underlying neurophysiological phenomena. This calculus would form a bridge between detailed neurophysiological knowledge on the one hand and the far grosser body of psychological knowledge on the other.

4.5.2 Alternating Period Stimuli

Given a network $\mathcal{N}$ with distance-bias $\rho = \rho(r)$, $0 \leqq r \leqq R$, let $\Sigma_0 \subset A \subset \mathcal{N}$ and $\Sigma_0^* \subset A^* \subset \mathcal{N}$ be two distinct input sets,

$$A \cap A^* = 0.$$

Suppose A and A^* are separated by a distance d_0,

$$d(j,i) = d_0 \text{ for all } j \in A,\ i \in A^*.$$

d_0 will be taken sufficiently large to minimize the direct effects of stimultation of Σ_0 upon Σ_0^* and conversely, yet sufficiently small that the paths $(\Sigma_0' \to \Sigma')$ and $(\Sigma_0^{*\prime} \to \Sigma_\tau')$ will interact (activity in one affecting activity in the other). A good choice of d_0 was found to be

$$\frac{R}{2} < d_0 \leqq R.$$

As in section 4.4.2, attention will be restricted to the case in which the stimulus has the simplest possible pattern, alternating simple periodicity: Suppose Σ_0 is stimulated with stimulus S_0 once every τ_0 time steps in intervals I_m, $m = 0, 1, 2, \ldots$, and Σ_0^* is stimulated with

stimulus S_0^* once every Σ_0^* time steps in intervals I_m^*, m = 0, 1, 2, ...
where I_m and I_m^* alternate as follows:

$$I_m = [t_0 + m(t_1+t_1^*+\ ),\ t_0 + t_1 + m(t_1+t_1^*+\ )],\ m = 0, 1, 2, \ldots$$

$$I_m^* = [t_0 + t_1 + m(t_1+t_1^*+\ ),\ t_0 + t_1 + t_1^* + m(t_1+t_1^*+\ )],\ m = 0, 1, 2, \ldots$$

t_ℓ and t_ℓ^* are the lengths of the intervals over which S_0 and S_0^* are applied respectively. δ is delay whose function will be discussed below. The overall stimulus pattern is then

$$\ldots\ I_{m-1}\ I_{m-1}^*\ \delta\ I_m\ I_m^*\ \delta\ I_{m+1}\ I_{m+1}\ \delta\ \ldots$$

starting at time t_0. The "on" period of one stimulus is the "off" period for the other (see Figure 4.17).

t_ℓ and t_ℓ^*, as in section 4.4.2, shall be chosen so that by the next application of the respective stimuli, the neurons shall be recovered with respect to fatigue from the effects of the preceding stimuli. They must, however, be long enough that the paths $P(\Sigma_0' \rightarrow \Sigma_\tau')$ and $P(\Sigma_0^{*\prime} \rightarrow \Sigma_\tau')$ may eventually close. Likewise, the delay δ is chosen to allow the neurons of Σ_0 its respective successor — sets to recover with respect to fatigue before the next stimulus cycle begins. This is especially important for smaller networks (N = 400) and relatively large input sets and areas ($\bar{\Sigma}_0 = \bar{\Sigma}_0^* = 9$, $\bar{A} = \bar{A}^* = 25$) since during one complete stimulus period $I_m I_m^*$ a relatively large number of neurons will tend to become hyperrefractory (high fatigue values, $\phi(\ell_i)$ large). If δ were zero, the next simulus sequence might find too many neurons too highly fatigued to react as desired. Moreover, the presence of a relatively large number of hyperrefractory neurons raises again, as discussed in 4.3.3, the danger of underdamped or overdamped behavior. At the best, either of these phenomena tend to make fewer neurons available for recruitment.

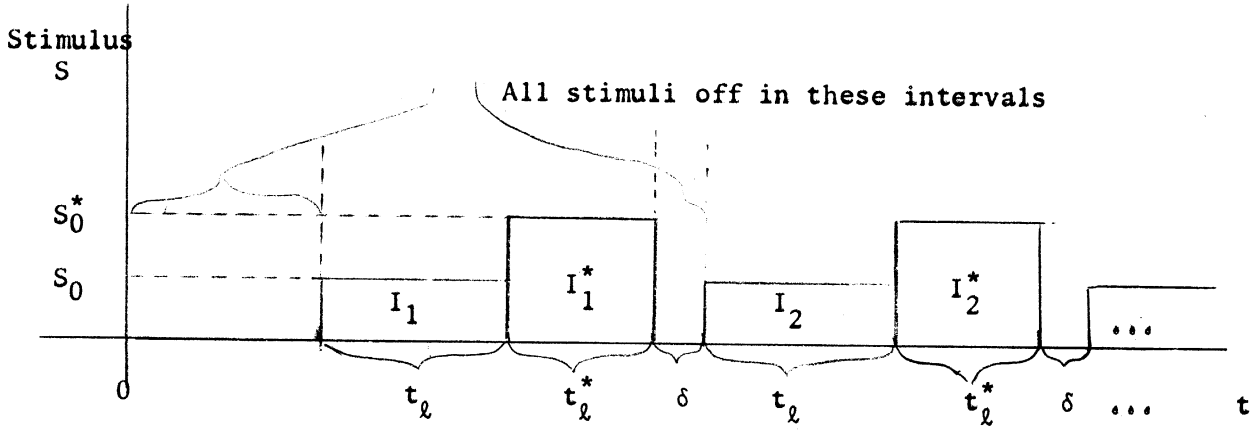

Figure 4.17. Alternating Stimulus Envelopes for Σ_0 and Σ_0^*. Stimulus S_0 is applied to Σ_0 every τ_0 time steps in I_1, I_2, ... Stimulus S_0^* is applied to Σ_0^* every τ_0^* time steps in I_1^*, I_2^*, ... S_0 is shown as less than S_0^* only to aid in discriminating between the envelopes I_m and I_m^*. $S_0 = S_0^*$ or $S_0 > S_0^*$ might equally well have been chosen depending upon the given experiment.

Suppose now that a $C(\Sigma_0)$ already exists, having been obtained by prior training as suggested in section 4.4. Then, the alternating stimulus sequence is turned on (keeping the same period τ_0 for Σ_0 that was used to form $C(\Sigma_0)$ of course). Two questions arise: (1) Will a self-re-exciting cycle $C(\Sigma_0^*)$ develop? (2) Will cross-inhibition between $C(\Sigma_0)$ and $C(\Sigma_0^*)$ develop? The reasoning of 4.4 may be applied to convince oneself of an affirmative answer to (1). Since $C(\Sigma_0)$ and $C(\Sigma_0^*)$ are proximate (and N is small), they certainly will influence one another — connections will go from one cycle to the other. Since a majority of the neurons of $C(\Sigma_0)$, say, will be highly fatigued after an interval I_m, the neurons of $C(\Sigma_0^*)$ will have little effect upon them and the corresponding synapse-values will drop. Likewise, neurons of $C(\Sigma_0^*)$ will tend

to be fatigued after an interval I_m^* and will be little affected by neurons of $C(\Sigma_0)$, etc. Thus, an affirmative answer to (2) may be expected.

Once again, for a demonstration of these claims, appeal is made to the simulation. Unfortunately, lack of time and money for computer usage forced cessation of the experimental work before the additional assembly $C(\Sigma_0^*)$ had actually evolved. However, as will be seen in Chapter 7, the results obtained tend to confirm the claims made in every way; in particular, cross-inhibition appeared to be developing.

4.6 Summary

The main results of this chapter are summarized below:

(1) A steady-state calculus is developed for networks with uniform random distributions of connections. Letting ρ be the network density, this calculus relates the threshold curve $V(r)$ with the expected number of neurons firing at time t in steady-state as follows:

$$E(F(t+1)) = F_b = \pi_1(\lambda(t))\bar{R}_{r_q}(t)$$

where

$$\lambda(t) = \frac{R_0(t)}{N}\rho$$

and $R_0(t)$ is the act of neurons firing at $t - 1$, $\hat{R}_{r_q}(t)$ the set of neurons of $\mathcal{N}$ whose recovery states r exceed $\hat{r}_q$. The assumption of steady-state reduces this to:

$$E(F(t)) = F_b = \pi_1(\lambda(0))\bar{\bar{R}}_{\hat{r}_q}(0).$$

Neurons of $\mathcal{N}$ are assumed to be distributed randomly and uniformly over recovery states $r = 0, i, 2, \ldots, r_q$ at $t = 0$; i.e., $E(R_r(0)) = \text{constant} = F_b$ for $r = 0, 1, 2, \ldots, r_q$.

(2) In general, positive and negative synapse-values will be present in $\mathcal{N}$, giving a decomposition of ρ into corresponding components:

$$\rho = \sum_{-s_0}^{s_1} \rho_s = \rho_{-s_0} + \rho_{-s_0+1} + \ldots + \rho_{-1} + \rho_0 + \rho_1 + \ldots + \rho_{s_0},$$

where $-s_0, -s_0+1, \ldots, -1, 0, 1, \ldots, s_1$ are synapse-values ($s_0 > 0$), ρ_s the expected number of connections received by a neuron of $\mathfrak{N}$ with weight s. It was shown that for some settings of the ρ_s, the negative connections suppress firing of certain neurons a t + 1 if $F(t) > F_b$ and "frees" certain neurons for firing at t + 1 if $F(t) < F_b$. A general procedure for calculating the ρ_s's to obtain this effect was given.

This form of negative feedback seems to ensure homeostasis, i.e., in steady-state, transient deviations in F(t) from F_b will not build up into undamped, possibly fatal, oscillations.

(3) The steady-state calculus was extended to networks with distance-bias, $\rho = \rho(r)$ for $r \leqq R$ ("disk" distribution). The expected number of connections received by a neuron $i \in \mathfrak{N}$ from neuron $j \in \mathfrak{N}$ is ρ if $d(i,j) \leqq R$, zero otherwise. A type of closed geometry (quasi-toroidal) is used over $\mathfrak{N}$.

(4) An attempt was made to characterize (simple) cell-assemblies as closed cycles of subsets, $C(\Sigma_0)$, arising from a patterned stimulation of Σ_0. The synapse-values from the successor-set Σ_i to Σ_{i+1} of $C(\Sigma_0)$ tend to high, excitatory values, while all others (e.g. the "back" values from Σ_{i+1} to Σ_i) tend to small or even negative values. $C(\Sigma_0)$ is responsive only to the particular pattern which created it.

(5) The case of alternation of activity of cell-assemblies was discussed. In the case that two negatively correlated stimuli are applied to input areas Σ_0 and Σ_0^* respectively, the hypothesis was defended that the resulting cell-assemblies $C(\Sigma_0)$ and $C(\Sigma_0^*)$ will be cross-inhibitory.

Symbols and Terms Introduced in Chapter 4

$\overline{\overline{A}}$ - the cardinality of the set A

A_K^S - the event "a neuron receives exactly K connections with synapse-value S" (Section 4.3.3)

A_K^{*S} - the event "a neuron receives K or more connections with synapse-value S" (Section 4.3.3)

alternating periodic stimulus ——— a stimulus applied periodically first to one subset $\Sigma_0 \subseteq \mathcal{N}$ over an interval I_m of t_ℓ time steps, then applied periodically (usually at a different rate) to another subset $\Sigma_0^* \subseteq \mathcal{N}$ over an interval I_m^* of t_ℓ^* time steps. The stimulus (of magnitude S_0) is applied every τ_0 time steps in intervals I_m, (of magnitude S_0^*) every τ_0^* time steps in intervals I_m^*. After a lag of δ time steps, this sequence is repeated, etc. (Section 4.5.2 and Fig. 4.15).

behavior of $\mathcal{N}$ ——— the sequence F(0), F(1), F(2), ..., F(t-1), F(t), F(t+1), ... of neurons of $\mathcal{N}$ firing at t (Section 4.3).

C_R — a disk of radius R centered at a neuron of $\mathcal{N}$ from which the neuron is expected to receive $\rho = \rho_R$ connections. The neuron receives no connections from $\mathcal{N} - C_R$ (Section 4.3.4).

$C(\Sigma_0')$ — a closed cycle of subsets $\Sigma_0' \to \Sigma_1' \to \Sigma_2' \to \cdots \to \Sigma_{\tau_0-1}' \to \Sigma_{\tau_0}' \equiv \Sigma_0'$ arising from periodic stimulation of the subset $\Sigma_0' \subseteq \mathcal{N}$ (Section 4.4). (Note: In later discussions, the prime is dropped. Σ_0' literally means the neurons of Σ_0 that fire when the stimulus is applied.)

d(j,i) — the distance from neuron $j \in \mathcal{N}$ to neuron $i \in \mathcal{N}$ (Section 4.2.2).

distance-bias distribution ——— a distribution of connections over $\mathcal{N}$ in which the probability that a neuron i receive a connection from neuron j is a function of d(j,i) (Section 4.2.2).

E, E_i – compound events used to determine the probability that a neuron receive K(K=1, 2, ...) positive connections from $\mathcal{N}$ in the case that negative connections are present in $\mathcal{N}$ (Section 4.3.3).

$E(X)$ – the expectation or expected value of the random variable X.

epilepsy – the condition of violent fluctuations in F(t), usually with the result that F(t) goes to zero (Section 4.3).

$F(t)$ – the number of neurons of $\mathcal{N}$ firing at t. Also the <u>set</u> of neurons of $\mathcal{N}$ firing at t. (This dual usage should occasion no confusion since the context will always indicate which meaning is intended.) (Section 4.3.1).

F_b – E(F(t)) when $\mathcal{N}$ is operating in stable, steady-state (Section 4.3).

F_τ – the number of neurons of $\mathcal{N}$ firing τ time steps after stimulation of Σ_0 directly due to the stimulus (Section 4.4.2). $F_\tau = \overline{\overline{\Sigma}}_\tau$.

F'_τ – the total number of neurons of $\mathcal{N}$ firing τ time steps after stimulation of Σ_0 (Section 4.4.2). <u>Note</u>: $F'_\tau = F_b + F_\tau = \overline{\overline{\Sigma}}'_\tau$.

fatal oscillations ——— (see epilepsy) violent oscillations in F(t), leading to F(t) going to zero (Section 4.3).

I_m, I_m^* – the intervals within which an alternating periodic stimulus is applied (Section 4.5.2 and Figure 4.15).

$M_k(t)$ – a subset of neurons of $\mathcal{N}$ at time t requiring at least k connections to fire (Section 4.3.2).

N – the number of neurons of $\mathcal{N}$, $N = \#\mathcal{N}$.

$N_k(t)$ – the set of neurons of $\mathcal{N}$ at time t receiving at least k connections from $R_0(t)$ (Section 4.3.2).

negative feedback ——— a homeostatic mechanism by which the steady-state behavior of $\mathcal{N}$ is forced to be stable — i.e., $E(F(t)) = F_b$ and the oscillations of F(t) "not too violent" (Section 4.3.3).

"on-off" simulus envelope ——— a sequence of intervals in which a single periodic stimulus is alternately "on" (being applied) for t_ℓ time steps, the "off" (not being applied) for t_ℓ time steps (Section 4.4.2).

oscillations ——— variations of F(t) from F_b (Section 4.3).

$P(\mathcal{E})$ – probability of the event $\mathcal{E}$.

P_k^* – the probability that the sum of all incoming synapses to a neuron of $\mathcal{N}$ be $\geq k$ (negative feedback present) (Section 4.3.3).

$P_E(\Sigma_0' \to \Sigma_\tau')$ ——— an effective path from $\Sigma_0' \subseteq \mathcal{N}$ to $\Sigma_\tau' \subseteq \mathcal{N}$ (Section 4.4.2).

periodic stimulus ——— a stimulus first applied to a subset $\Sigma_0 \subseteq \mathcal{N}$ every τ_0 time steps over an interval of t_ℓ time steps ("on"), then suppressed ("off") for t_ℓ time steps, this basic sequence is then repeated, etc. (Section 4.4.2).

quasi-toroidal geometry ——— the geometry in which networks $\mathcal{N}$ of the model are embedded in order to obtain a distance metric (Section 4.3.4).

r_m – the maximum value of the recovery-state.

r_q – the recovery state corresponding to the quiescent value of V(r) (Section 4.3.2).

$\hat{r}_q$ — the expected value of r for neurons operating in steady-state: $r_q \leqq \hat{r}_q \leqq r_m$ (Section 4.3.2).

R — radius of the disk C_R (Section 4.3.4).

$R_r(t)$ — the subset of neurons of $\mathcal{N}$ with recovery state r at time t (Section 4.3.2).

$\hat{R}_{r_q}(t)$ — the total subset of neurons having recovery state $r \geqq r_q$ at time t (Section 4.3.2).

$\mathcal{R}(t)$ — the distribution of neurons of $\mathcal{N}$ over recovery states at time t (Section 4.3.2).

S_t — the subset of neurons of $\mathcal{N}$ receiving connections from F(t-1) (subset of neurons firing at t-1). S_t is called the successor-set to F(t-1) (Section 4.3.1).

stability — the condition of the input-free behavior of $\mathcal{N}$ in which F(t) does not oscillate "too violently" about its mean F_b (Section 4.3).

steady-state behavior of ——— a behavior of $\mathcal{N}$ that satisfies the stability criterion (Section 4.3).

successor-set ——— see S_t above.

uniform random distribution of connections ——— a connection distribution over neurons of $\mathcal{N}$ in which any neuron of $\mathcal{N}$ is equiprobably connected to any other neuron of $\mathcal{N}$ (Section 4.2.1).

δ — the lag between successive applications of alternating simuli (see "alternating periodic stimulus" above) (Section 4.5.2 and Fig. 4.15).

$\delta R_0(t)$ — $\bar{\bar{R}}_0(t) - E(\bar{\bar{R}}_0(t)) = \bar{\bar{R}}_0(t) - F_b$ (Section 4.3.3).

$\Delta A(w)$ — element of area in a continuous two-dimensional neural network about the point w (Section 4.2.2).

λ_0 – mean value of synapse-levels (Section 4.3.3).

$\lambda(t)$ – the expected number of connections received by a neuron of $\mathcal{N}$ from $R_0(t) \subseteq \mathcal{N}$ at time t (Section 4.3.2).

λ_{AB}, $\lambda_{A\to B}$ – the synapse-level from neuron A to neuron B.

$\pi_k(\lambda(t))$ – the probability that a neuron of $\mathcal{N}$ receive at least k connections from $R_0(t)$ at time t (Section 4.3.2).

ρ – the network density parameter (Section 4.2.1). $\rho = N\rho_0$.
ρ_0 = expected number of connections received by a neuron of $\mathcal{N}$ from any other neuron of $\mathcal{N}$.

ρ_s – in the case of negative feedback, the density of synapse-values with value s (Section 4.3.3). In the case of negative feedback, $\rho = \sum_{s=-s_1}^{s_2} \rho_s$.

$\rho(r)$, $\rho(j,i)$, $\rho(d)$ – densities as function of distance (Section 4.3).

Σ_0 – a subset of $\mathcal{N}$ to which external stimulus is to be applied (Section 4.4).

Σ_0^* – the alternate input subset to Σ_0 in the case of alternating periodic stimulus.

Σ_τ, Σ'_τ, Σ''_τ —— subsets of $\mathcal{N}$ evolving τ time steps after stimulation of Σ_0 (Section 4.4.2) (See F_τ, F'_τ above) $\Sigma'_\tau = \Sigma_\tau \quad \Sigma''_\tau$.

τ – number of time steps after stimulating Σ_0 (Section 4.4.2).

τ_0 – interval between successive applications of the stimulus to Σ_0 (Section 4.4).

τ_0^* – interval between successive applications of the stimulus to Σ_0^* (Section 4.5.2).

5. METHODOLOGY OF EXPERIMENTS

5.1 Introduction

In the next two chapters, experimental results obtained using networks with cycles are presented. These results constitute the empirical verification of the claims advanced in Chapter 4. These claims, stripped of complicating qualifications, reduce to the following three:

(1) It is possible to produce stable, stimulus-free behavior in networks with cycles (with or without distance-bias) by means of appropriate (a) threshold curve setting, (b) initial distribution of neurons over recovery states, and (c) distribution of synapse-values over connections. This behavior will remain stable under perturbation by a moderate external stimulus.

(2) It is possible to produce in some networks with cycles closed cycles $C(\Sigma_0)$ as a result of periodic stimulation of a certain input set Σ_0, the stimulation occurring in a sequence of "on-off" envelopes (the "training" period). $C(\Sigma_0)$ will consist of a sequence of subsets,

$$\Sigma_0 \rightarrow \Sigma_1 \rightarrow \Sigma_2 \rightarrow \ldots \rightarrow \Sigma_{\tau_0-1} \rightarrow \Sigma_{\tau_0} \equiv \Sigma_0$$

with the property that for $j \in \Sigma_k$, $i \in \Sigma_{k+1}$, $k = 0, 1, 2, \ldots, \tau-1, \tau(\equiv 0)$, the synapse value $S(\lambda_{ji})$ tends to be strongly excitatory and for $j \in \Sigma_k$, $i \in \Sigma_\ell$, $\ell \neq k+1$, $S(\lambda_{ji})$ tends to be moderately positive, zero, or even inhibitory. $C(\Sigma_0)$ is a candidate for a cell-assembly and is a "learned" response of the network to the given stimulus.

(3) It is possible to produce in some networks with cycles a pair of mutually cross-inhibiting cycles $C(\Sigma_0)$ and $C(\Sigma_0^*)$ where

$$C(\Sigma_0) = \Sigma_0 \rightarrow \Sigma_1 \rightarrow \ldots \rightarrow \Sigma_{\tau_0-1} \rightarrow \Sigma_{\tau_0} = \Sigma_0$$

$$C(\Sigma_0^*) = \Sigma_0^* \rightarrow \Sigma_1^* \rightarrow \ldots \rightarrow \Sigma_{\tau_0^*-1}^* \rightarrow \Sigma_{\tau_0^*}^* = \Sigma_0^*$$

and the values of the connections between neurons of the two cycles tend to inhibitory values.

Substantiation of claim (1) and related topics will be the object of Chapter 6. Investigation of claims (2) and (3) is deferred to Chapter 7.

An important assumption pervades the following two chapters: simulated networks closely approximate the abstract (ideal) networks discussed in Chapter 4. That this need not be the case is shown by the following example: The random drawing of a random number n, used in determining the connection distribution for a network $\mathcal{N}$, is implemented by a pseudo-random number generator. Pseudo-random number generators for digital computers are known to have many pitfalls, often producing "skewed" distributions of n. It is, therefore, essential to determine just how closely the resulting simulated distribution approximates the theoretical distribution. Such matters as this are relegated to Appendix B, and it will be assumed that, for all practical purposes, the theoretical and the simulated models coincide.

The material is presented in these chapters in parallel with the development of Chapter 4. Networks with uniform random distributions of connections are examined first, then networks with distance-bias are considered. Both cases are subdivided into two subcases: (1) negative feedback is absent (synapse-values all positive) and (2) negative feedback is present (positive and negative synapse-values are present). This order of presentation is a departure from the actual historical order. In the latter, networks with uniform random distributions of connections were considered first for the steady-state case, then for the cycle-of-subsets case. Lack of success in producing cycles of subsets, together with some considerations such as those given in Chapter 4, led to

the introduction of distance-bias distributions into the networks of the model. The sequence above was repeated for networks with distance-bias: steady-state experimentation, then cycles-of-subsets experimentation. The almost immediate success of the latter led to a lengthy experiment, described in Chapter 7, culminating in an alternating cycles (cell-assemblies) experiment. Since the steady-state experiments for both cases (uniform random and distance-bias distributions) shared many things in common, they are presented as a unit. Similarly for the cycle-of-subsets experiments.

Before giving the description of the experiments, a brief review is given in the next section of the experimental methodology followed in this work. This is done since it is essential that the reader understand the nature of the advantages and the disadvantages offered by the simulation which forms the basis of this work.

Finally, at the end of both chapters, the main experimental results are recapitulated in a summary.

5.2 Methodology

The general methodology used in Chapters 6 and 7 — not dissimilar to that of experimental physics or chemistry — is the following. First, a hypothesis about the behavior of a network is made, given certain parameters values, etc. This hypothesis is defended by the calculus of Chapter 4, as much as this is possible, it being recognized that the initial setting of the parameters is only approximate. The experiment is performed (run) resulting either in "failure" (hypothesis not confirmed for the given parameter settings) or in "success" (hypothesis is confirmed for the given parameter settings). If the result was "failure",

the experiment is repeated by varying in a systematic way the parameters Successive failures, of course, do not invalidate the hypothesis for all possible combinations of parameter values, rather only for the values (or range of values) tested. Likewise, "success" merely provides a set of parameters that work, success is not guaranteed for all possible combinations of parameter values, although it might be implied for a range of parameter values, etc.

Actual experiment must be tempered with reality, especially since the experimental apparatus used[1] is extremely expensive and relatively inaccessible. In the ideal case, a set of parameters might be varied over a large spectrum of values. In practice this would yield for too many possible behaviors than would be profitably analyzed in the span of a lifetime, even if the experimental apparatus were available for such extensive use. Here the skill and intuition of the experimenter enter in an essential way in reducing the number of unnecessary or redundant runs, and in making meaningful inferences from incomplete data. The latter act takes two forms: (a) The networks used are so large and complicated that a detailed monitoring of the complete state of a network at each time step is impractical, resulting in an astronomical volume of computer output. Therefore, values of state variables of the network must be sampled in an economical and, to the experimenter, significant fashion. (b) The expense and relative inaccessibility of the experimental apparatus often dictate reducing the range of parameters to be tested. The experimenter must then examine his incomplete set of data and infer that an untried setting of parameters might yield success. This type of inference is,

[1] The IBM 7090 computer with an IBM 1410 satellite subsystem at The University of Michigan Computing Center.

of course, potentially very dangerous, and must be carefully defended a priori with whatever analytical tools are present. Usually strong "trends" are present in this situation, making the reference more plausible.

The parameters of interest in the sequel are:

(1) $N = |\mathcal{N}|$, the size of $\mathcal{N}$. Generally $N = 400$, however there were several runs involving $N = 200$ and one involving $N = 900$.

(2) ρ, the connection density (uniform random case). Typical values were $\rho = 6$, $\rho = 12$, $\rho = 24$.

(2') ρ and R, if distance-bias is present, where R is the radius of the neighborhood disk C_R. A typical setting was $\rho = 55$, $R = 6$.

(3) The initial distribution of synapse-values over connections.

(4) The threshold curve $V(r)$. In this study, $r_a = 3$, $r_m = 19$. $\hat{r}_q$ varied with the experiment.

(5) The fatigue curve $\phi(\ell)$ and the associated tables of values $\Delta_1(\ell)$ and $\Delta_2(\ell)$. The fatigue function was taken as an additive component of the effective threshold, instead of multiplicative as in Chapter 3.

(6) The synapse-value curve $S(\lambda)$ and the associated tables of probabilities $U(\lambda)$ and $D(\lambda)$.

Since the network-generating program was rather time-consuming, the parameters N, ρ, and R (if distance-bias were present) were varied as little as possible. Internal computer storage determined an absolute upper bound on N of approximately 1000 neurons; however, such factors as ease of analysis, time required to simulate one time step, etc. dictated a moderate value of N. $N = 400$ was taken as a compromise. It is large enough that the statistical assumptions of the theory should hold true,

yet not so large as to make running true exhorbitant or analysis of results any more tedious than necessary.

The initial distribution of synapse-values over connections likewise tended to be fixed, although a set of experiments was devoted exclusively to a study of the effects of varying this parameter. Similarly for $S(\lambda)$ and the tables of $U(\lambda)$ and $D(\lambda)$.

By far the most varied parameter was the threshold curve. For a given N, ρ, the calculus of Chapter 4 gives information about the form of $V(r)$ needed to guarantee stability. However, especially in the cases of negative feedback and distance-bias, the calculations are unwieldy and at best yield a first crude estimate for $V(r)$ (or for ρ, but it is easier to vary $V(r)$ as noted). Consequently, finer "tuning" of the network may be necessary by varying $V(r)$ slightly. It is important to note that the calculations were used primarily as a guide to obtaining an initial estimate of the network parameters. Then, calculations were abandoned and experimentation begun. The modus operandi was to avoid (if possible) much tedious calculation and place the burden of success upon the simulation. The analytical theory, of course, remains important as an aid to the understanding of the models; only the excessively tedious calculations are bypassed.

The fatigue curve $\phi(\ell)$ and its associated tables of values $\Delta_1(\ell)$ and $\Delta_2(\ell)$ were seldom varied, except in a final series of control runs. As noted in Chapter 4, this function was not really adequately analyzed in this work. That is, no general calculus similar to that of Chapter 4, section 4.3, was developed. Although not an impossible task, the modification of the analysis of section 4.3 to consider the effective threshold $V(r) + \phi(\ell)$ will have to await a future work.

6. STIMULUS-FREE BEHAVIOR IN NETWORKS WITH CYCLES

6.1 EXPERIMENTAL OBJECTIVES AND PROCEDURES

6.1.1 Objectives

The objectives of the experiments described in this chapter are twofold:

(1) to exhibit networks that maintain stable, input-free behavior (steady-state).

(2) to derive experimentally stable networks that are adequate for the cell-assembly experiments of Chapter 7.

(1) is the avowed purpose made in claim (1), Chapter 5, Section 5.1. The implication of (2) is that some networks may maintain steady-state behavior, but not yield the desired closed cycles of subsets (cell-assemblies) when subjected to periodic stimulation. This might occur if the network is too small or if the threshold curve is too "steep". In the first case, a sufficiently large fund of neurons might not be available for recruitment into the paths $P_E(\Sigma_0 \rightarrow \Sigma_\tau)$ so that they never close into a cycle $C(\Sigma_0)$. In the second case, V(r) might be so large in the vicinity of $r = \tau_0$ (τ_0 the stimulus rate as in Chapter 4, Section 4.4) that the set Σ_{τ_0-1} cannot fire neurons of Σ_0 ($\equiv \Sigma_{\tau_0}$), their threshold values being too high. Again, $P_E(\Sigma_0 \rightarrow \Sigma_{\tau_0-1})$ would never close into $C(\Sigma_0)$.

The implications of "adequate" stable, steady-state behavir, therefore, are that (a) N is sufficiently large and (b) V(r) is steep enough to maintain stable steady-state behavior but not so steep that $P_E(\Sigma_0 \rightarrow \Sigma_{\tau_0-1})$ will never close into a cycle. (a) raises the dilemma of running time, since the larger the N, the longer — hence, the most costly — the experimental runs. It was blatantly assumed that N = 400 was adequate. This assumption will be defended in Chapter 7, but also the possibility that this value of N may be too small will be examined.

Similarly, (b) raises the dilemma of parameter variations yielding many runs, hence again the issues of expense and time.

As mentioned in 5.1 the historical procedure was to perform a series of steady-state experiments, varying the network parameters until a network displaying a very stable[1] behavior was obtained. Then this network would be subjected to periodic stimulus and judged for adequacy. If inadequate, a new series of steady-state runs would be performed with a new set of parameters. If adequate, a series of closed cycles (cell-assembly) experiments would be initiated, etc. Since a sufficient number of problems arose in the steady-state experiments per se, they are treated as a unit in this chapter. Chapter 7 is devoted to the closed cycles experiments.

6.1.2 Outline of General Experimental Procedure

The experimental procedure used may be divided into three phases: initialization or set-up, run-in, and detailed long-run testing. These are described below:

Phase I Initialization or Set-up

1. Given N and ρ (N, ρ, and R if distance-bias is to be present), the corresponding network $\mathcal{N}$ is generated. The neurons of $\mathcal{N}$ are then uniformly distributed over recovery states $r = 0, 1, \ldots, r_m$ (r_m was taken as 19 throughout the study), yielding

$$E(\bar{\bar{R}}_r(0)) = \frac{N}{r_q}, \quad r = 0, 1, \ldots, r_m$$

2. Synapse-levels $\lambda_{ji}(0)$ are assigned, according to a given

[1] The empirical criteria for "very stable" behavior are derived from Chapter 4 and will be described in section 6.1.2 below.

distribution, to all connections $j \to i$ determined by the connection assignment scheme used in 1 above; i.e., the connections are "weighted". In the early experiments described below, the $\lambda_{ji}(0)$'s were set all equal to a value giving a synapse-value of +1. Later, the $\lambda_{ji}(0)$'s were distributed over ranges of λ giving both positive and negative synapse-values (Chapter 4, section 4.3.3).

3. The neurons of $\mathcal{N}$ are distributed, according to a given distribution, over fatigue states ℓ, $\ell = 0, 1, \ldots, \ell_{max}$. In most experiments described below, $\ell_i(0)$ was set to ℓ_{max} (complete recovery with respect to fatigue), $i = 1, 2, \ldots, N$.

4. The functions $V(r)$, $\phi(\ell)$, and $S(\lambda)$ and the tables $U(\lambda)$, $D(\lambda)$, $\lambda = 0, 1, \ldots, \lambda_{max}$ and $\Delta_1(\ell)$, $\Delta_2(\ell)$, $\ell = 0, 1, \ldots, \ell_{max}$ are specified.

5. A subset $\Sigma_0 \subset \mathcal{N}$ is selected to fire at $t = 0$, $E(\Sigma_0) = \frac{N}{\hat{r}_q}$. Usually, a random sample of neurons of $\mathcal{N}$ was selected so that a fixed "starting" stimulus S_0 would be expected to cause $N/\hat{r}_q$ neurons to fire at $t = 0$. Apart from this "starting" stimulus at $t = 0$, no further stimulus was applied in the steady-state experiments.

Phase II: Run-In

The firing of Σ_0 of step 5, Phase I, properly begins the run-in phase of experimentation. In this phase, the network is allowed to operate over a time interval $[0,T]$ until one of three conditions arise:

(1) $F(t)$ goes to zero, $0 < t \leq T$.

(2) The observer interrupts the run for reasons to be mentioned below.

(3) $t = T$ (end of run interval is reached). Typically, T was chosen as 100, 200, or 400.

If (1) occurred, the network was either overdamped or underdamped

and some parameter (usually, V(r)) modification is necessary. The appropriate parameter is revised and the run-in trial is repeated starting with step 5, Phase I again.

(2) usually occurs only if it obvious to the observer that the behavior of $\mathcal{N}$ is grossly overdamped or underdamped, anticipating that F(t) would go to zero soon anyway. This did not occur too often, since the observer did not always have direct access to the experimental apparatus.

In case (3), the network's behavior was labelled temporarily as "stable" since $F(t) \neq 0$, $t = 0, 1, \ldots, T$. During the course of the run-in (3), a number of network parameters are sampled at the discretion of the experimenter. These include:

(a) F(t) for each t;

(b) $\mathcal{R}(t)$ for each t (distribution of neurons over recovery states at time t).

(c) $\mathcal{F}(t)$ for each t (distribution of neurons over fatigue states at time t).

(d) Samples of $\lambda_{ji}(t)$ for selected time steps t.

(e) The "firing pattern" at t for each or selected t. This is a "picture" of the network, showing the neurons firing at t.

The outputs (a) - (e) of the run-in were then studied. If F(t) remained bounded, $E(F(t)) = F_b$, in particular if no underdamped oscillations appeared to be developing, the network was cleared for further testing from t = T + 1 on (Phase III). The distributions of $\lambda_{ji}(t)$ were checked (when samples were obtained) for sudden or peculiar changes from the distributions at t = 0. This is primarily a test to ensure that no sets of neurons are operating at too high or too low firing rates.

If oscillations appeared to be forming, or if some other anomaly appeared to be present, one of two courses might be followed: (a) if the anomaly appeared to be not too serious, the run-in might be continued from $t = T + 1$ an additional T time steps (subject to conditions (1) - (3) above). "Not too serious" means that hints were present suggesting that the anomaly might be purely transient in nature. (b) If the anomaly appeared not to be of a transient character, the appropriate parameter (usually V(r)) was changed and the run-in repeated from step 5, Phase I.

Phase III: Long-Run Testing

Once past the hurdle of Phase II, the network was subject to further running from $t = T_0 + 1$ on, T_0 being the terminal time step of Phase II ($T_0 = T$ or $T_0 = 2T$, etc., depending upon the option followed in Phase II). The same outputs (a) - (e) of Phase III are obtained as desired by the experimenter. If, for t sufficiently large, the behavior of $\mathcal{N}$ appeared stable with no non-transient anomalies present, the network was judged to be "very stable" and passed on as a candidate for the cell-assembly experiments. "Sufficiently large" means anywhere in the limits t = 400 to t = 1000.

Notice that "very stable" is a purely empirically inferred condition. "Very stable" means essentially that

(1) F(t) does differ sharply from F_b except in a purely random, transient fashion — i.e., undamped oscillations are not building up, $E(F(t)) = F_b$. In particular, F(t) never goes to 0.

(2) No sub-rosa accumulation of neurons with high fatigue values occurs. This could lead to a pocket of hyper-refractory neurons, the evils of which have already been expounded in Chapter 4.

(3) No accumulative large deviations of the λ_{ji}'s occur with the effect of either damping out F(t) or producing underdamped F(t)'s. This could occur, for example, if the synapse-level growth law were too fast, i.e.,

$$\frac{D(\lambda)}{U(\lambda) + D(\lambda)} < \frac{1}{\hat{r}_q} .$$

The occurrence of any one of the anomalies mentioned in (1) - (3) is grounds for modification of parameters and return to Phase II.

Notice that Phases II and III take advantage of the modularity present in forming a network in steps 2 - 4 of Phase I. In fact, the parameters of these steps may be varied at any time step, it not being essential to always back up to step 5 of Phase I. For example, throughout the course of Phase III, it might appear that V(r) allows a slight underdamping, the cumulative effects of which could produce fatal oscillations. The experimenter may, if he wishes, interrupt the run at a certain point, insert a new threshold curve, and continue from that point on. Moreover, as a matter of course, the entire state of the network was "saved" periodically on magnetic tape for future back-up or retrieval purposes. Thus, a library of experiments (at different time steps) was built up for future reference or modification.

6.1.3 Hypothesis

The specific hypothesis being tested in this chapter is: (Stable, Steady State Hypothesis) Given a network $\mathcal{N}$ with specified parameters N, ρ, R (if distance-bias is present), V(r), $\phi(\ell)$, U(λ), D(λ), $\Delta_1(\ell)$, $\Delta_2(\ell)$, $\mathcal{N}$ maintains stable, steady-state behavior as a result of a selected subset $\Sigma_0 \subset \mathcal{N}$ being stimulated at t = 0, $E(\Sigma_0) = F_b = \frac{N}{\hat{r}_q}$.

Phase II may provisionally affirm the hypothesis or may completely invalidate it. In the former case, more complete confirmation awaits Phase III. In the latter case, parameter modification is indicated (Phase I). The hypothesis may also be rejected in Phase III, if non-transient anomalies arise.

6.2 NETWORKS WITH UNIFORM RANDOM DISTRIBUTIONS OF CONNECTIONS

6.2.1 Series I — Networks with Positive Connections Only

In this section, experimental results are given for networks in which the initial distributions of $\lambda_{ji}(0)$'s were such that the corresponding synapse-values, $S(\lambda_{ji}(0))$, were positive. The primary purpose of these experiments was to demonstrate the validity of the basic theory of Chapter 4 (4.3.2) without the complication of negative feedback. Several experiments (variants of the basic experiments below) included negative feedback; however, they were performed before the principles of Chapter 4, 4.3.3, were well understood. Their description is, therefore, included in this section.

Basic Experiment I

The basic claim of the theory developed in Chapter 4, Section 4.3.2, is the following: Given a network $\mathcal{N}$ with density $\rho(\rho \neq \rho(R))$, $S(\lambda_{ji}(t)) = 1$, $R(t)$ such that $\bar{R}_r(t) = N/(r_m+1)$, then $\mathcal{N}$ will maintain a stable, steady-state behavior provided $V(r)$ is chosen so that the expected number of neurons of $\hat{R}_{r_q}(t)$ firing at t is $F_b = N/(\hat{r}_q)$. The assumption is that few, if any, neurons of the $R_r(t)$ for $r < r_q$ fire at t. A simple calculus relates $\hat{R}_{r_q}(t)$, ρ, N, F_b, and $F(t)$, namely

$$F_b = E(F(t+1)) = E(\bar{R}_0(t+1)) = \pi_k(\lambda(t))\hat{R}_{r_q}(t)$$

where

$$\pi_k(\lambda(t)) = \sum_{j=k}^{\infty} e^{-\lambda(t)} \frac{\lambda(t)^j}{j!}$$

and

$$\lambda(t) = \frac{\overline{\overline{R_0}}(t)}{N} \cdot \rho.$$

To test this basic hypothesis, the threshold curve V(r) of Figure 6.1 was chosen. Since $V(r) = \infty$ for $r = 0, 1, 2, \ldots, r_q = 15$ and $V(r) = 1$ for $r = r_q+1 = 16, 17, 18, r_m = 19$, perforce no neurons of $R_r(t)$ for $r < r_q$ may fire. The remaining network parameters were: $N = 400$, $\rho = 6$, $\lambda_{ji}(0) = \lambda_0$ such that $S(\lambda) = 1$, $\phi(\ell) \equiv 1$, $U(\lambda) = .72$, $D(\lambda) = .052$ for all λ where

$$\frac{D(\lambda)}{U(\lambda) + D(\lambda)} = \frac{1}{16} = \frac{1}{r_q}.$$

$\overline{\overline{\Sigma}}_0 = 27$ neurons were stimulated at $t = 0$, i.e., $F(0) = 27$. $\mathcal{R}(0)$, of course, was initialized so that $\overline{\overline{R_0}}(0) = \overline{\overline{R_1}}(0) = \ldots \overline{\overline{R}}_{r_m}(0) = \frac{N}{(r_m+1)} = 20$. It was expected that neuron $i \in \mathcal{M}$ would fire for r_i lying between $r_q = 16$ and $r_m = 19$, perhaps distributed around a mean $\hat{r}_q$ of 17, $E(\hat{r}_q) = 17$. The result — surprising at first to the author, but typical of the networks described in this section — was that after approximately $r_m/2$ time steps, F(t) repeated itself every 17 time steps:

$$F(t+17) = F(t) \qquad \text{for all } t > 10 \cong \frac{r_m}{2}$$

and

$$\hat{r}_q = 17 \text{ (exactly)}.$$

This effect was termed "periodicity". Discussion of it will be delayed until Section 6.2.3. It will suffice for now to observe that it is not a desirable behavior pattern, since, from the point of view of information theory, such rigid periodicity suggests that no information is present, where "no information" would be taken to mean that no neurons are available for recruitment into cell-assemblies. Consequently, it

Figure 6.1. Summary of Results for Basic Experiment I and Variant.

(a) Threshold curve V(r) and other parameters.

(b) EEG ("electroencephalogram") for Experiment I. F(t) is given for selected time intervals.

(c) EEG for Experiment I, Variant.

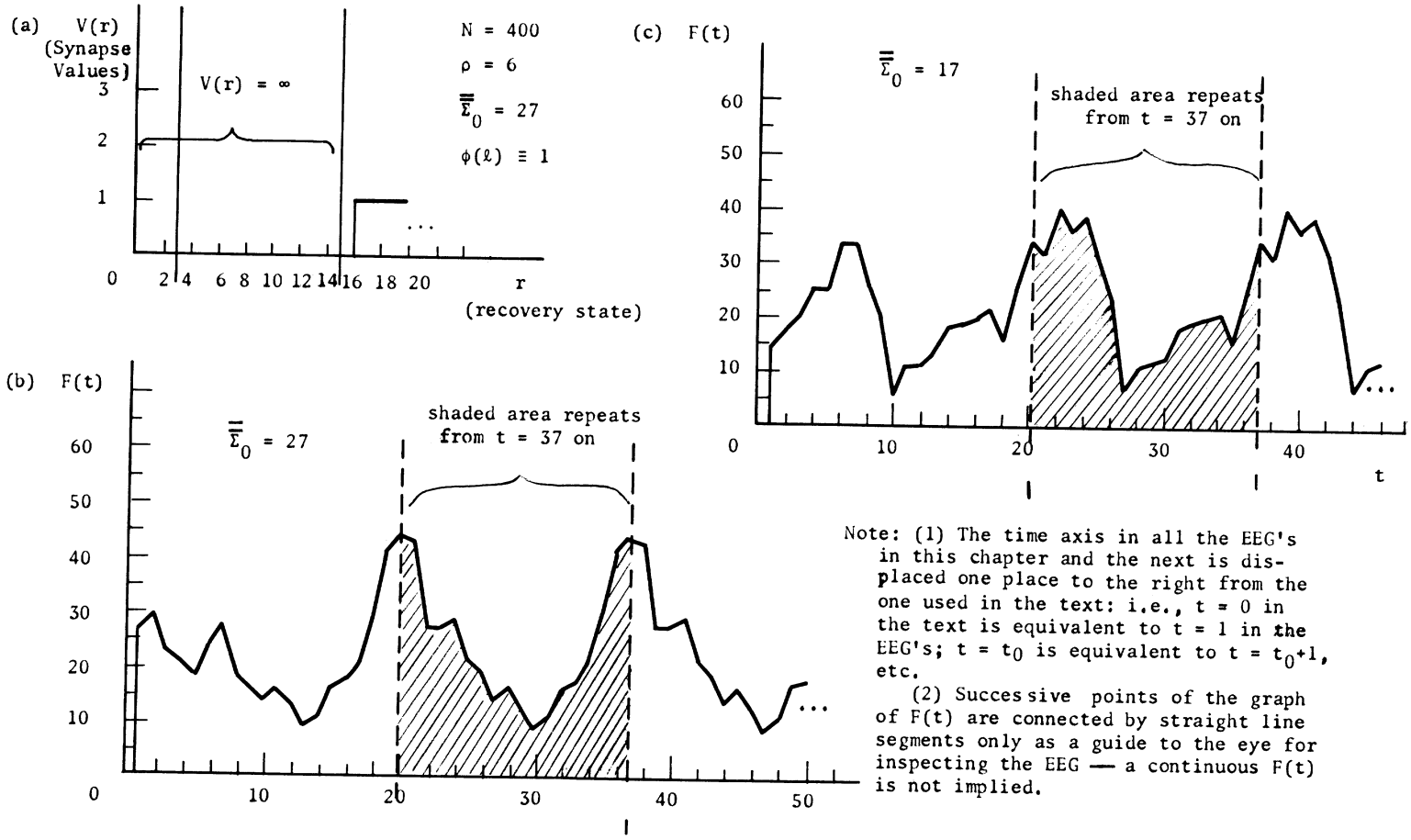

Note: (1) The time axis in all the EEG's in this chapter and the next is displaced one place to the right from the one used in the text: i.e., t = 0 in the text is equivalent to t = 1 in the EEG's; t = t_0 is equivalent to t = t_0+1, etc.

(2) Successive points of the graph of F(t) are connected by straight line segments only as a guide to the eye for inspecting the EEG — a continuous F(t) is not implied.

became a subgoal of this work to eliminate this type of behavior pattern of possible. It is interesting to note that the introduction of distance-bias (with negative feedback) automatically seemed to eliminate it.

Figure 6.1 contains a summary of the results of this experiment, including an "electroencephalogram" or EEG, i.e., F(t) plotted as a function of t.

The experiment was repeated for a different value of $\bar{\bar{\Sigma}}_0$, $\bar{\bar{\Sigma}}_0 = 14$. The results were quite similar to those above: F(t) displayed periodicity with period $\hat{r}_q = 17$. The corresponding EEG is given in Figure 6.1.

Variations of Basic Experiment I

Two interesting variations of the basic experiment were performed next. In the first, the synapse-levels, $\lambda_{ji}(0)$'s, were distributed uniformly over the range $32 \leq \lambda_{ji}(0) \leq \lambda_{max} = 63$ corresponding to the synapse-value range $0 \leq S(\lambda_{ji}(0)) \leq S(\lambda_{max}) = 32$. In the second, the $\lambda_{ji}(0)$'s were distributed uniformly over the entire range of λ, $0 \leq \lambda_{ji}(0) \leq \lambda_{max}$, giving a uniform distribution of synapse values over equal positive and negative ranges. In both cases, $\bar{\bar{\Sigma}}_0 = 18$.

The results of the first variation were precisely similar to those of the basic experiment: periodicity with period $\hat{r}_q = 17$. F(t), however, did not begin repeating itself until t = 27: i.e., for $t \geq 27$, $F(t+17) = F(t)$. The second case, however, was grossly overdamped and F(5) went to zero. The respective λ-distributions and EEG's are indicated in Figure 5.2. It is of worth to note that the more complex λ-distribution of the first variation above stretched out the interval in which F(t) was not periodic. This point will be considered in 6.2.3 below.

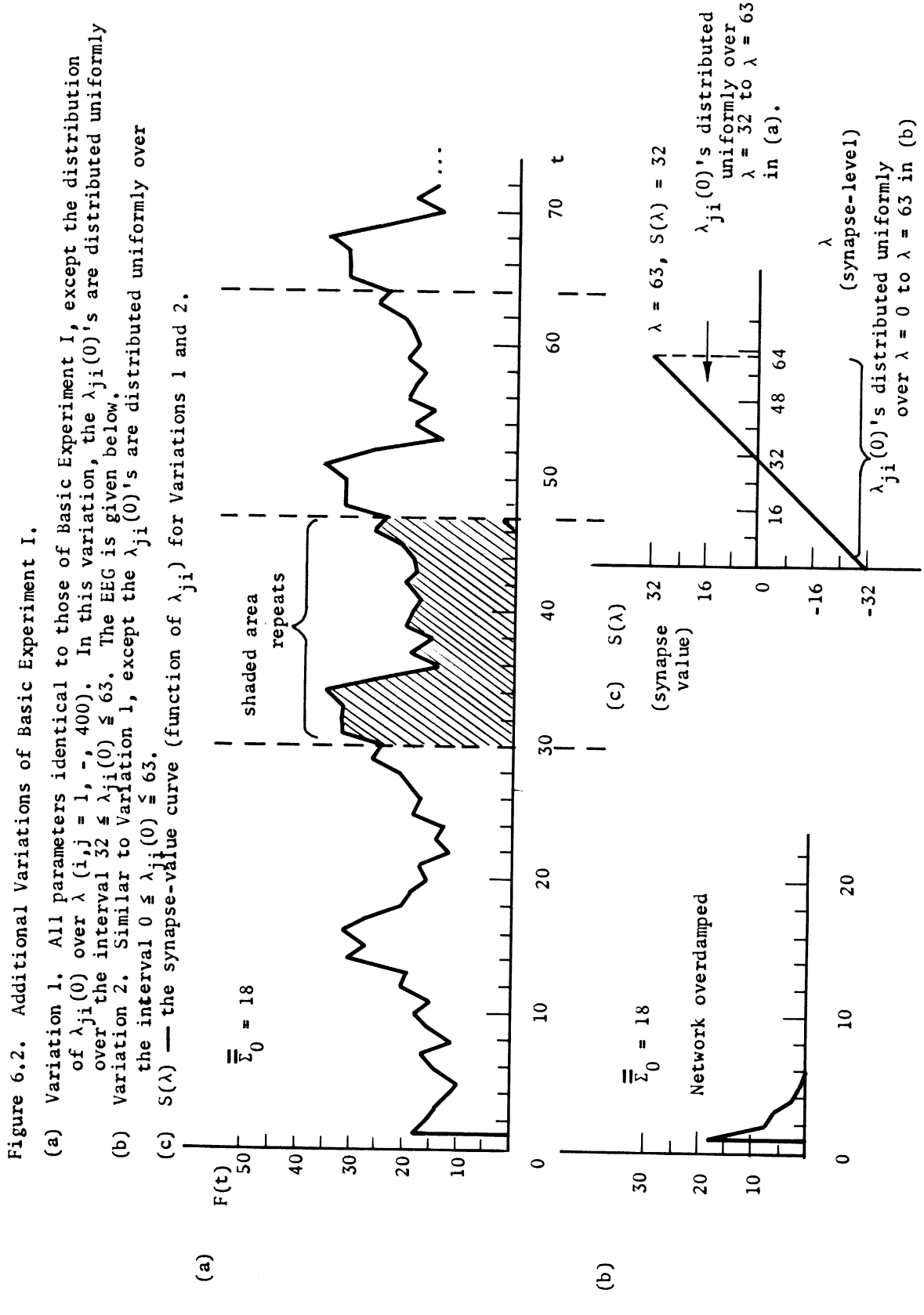

Figure 6.2. Additional Variations of Basic Experiment I.

(a) Variation 1. All parameters identical to those of Basic Experiment I, except the distribution of $\lambda_{ji}(0)$ over λ (i,j = 1, ..., 400). In this variation, the $\lambda_{ji}(0)$'s are distributed uniformly over the interval $32 \leq \lambda_{ji}(0) \leq 63$. The EEG is given below.

(b) Variation 2. Similar to Variation 1, except the $\lambda_{ji}(0)$'s are distributed uniformly over the interval $0 \leq \lambda_{ji}(0) \leq 63$.

(c) S(λ) — the synapse-value curve (function of λ_{ji}) for Variations 1 and 2.

Basic Experiments II

The preceding experiment and its variations demonstrated the validity of the claim of Chapter 4: the neurons of $\mathcal{N}$ can be forced to "cycle" with an expected period $\hat{r}_q \cong \frac{N}{F_b}$ by setting V(r) so large for $0 \leq r \leq r_q$ that no neurons in the corresponding $R_r(t)$ may fire, yet V(r) is such that for $r_q \leq r \leq r_m$, F_b neurons are expected to fire at any time step. It is now necessary to see how well the claim holds up when V(r) is chosen so that some neurons in the $R_r(t)$ may fire. This would appear to be the more realistic situation.

Tentative calculations showed that for N = 400, ρ = 6, etc. as above, threshold curves of the general form of Figure 6.3 should yield stable, steady-state behavior. More detailed calculations, such as those of Table 4.1 of Chapter 4, show that stability may occur, but — in the absence of appropriate negative feedback — fatal oscillations may build up.

Consequently a sequence of V(r)'s were tested for stability, the network otherwise precisely as it was in Basic Experiment I. These curves together with the corresponding $\overline{\overline{\Sigma}}_0$'s and EEG's are given in Figure 6.4. The results may be summarized briefly by noting that the "steeper" curves produced stability, the "shallower" ones instability. In the former case, the sets $M_k(t)$ for k = 2, 3, 4, ... are smaller in cardinality than in the latter case. For example, in curve 2 which produced stability, $E(\overline{\overline{M_2}}(t)) = 40 = E(\overline{\overline{M_3}}(t)) = E(\overline{\overline{M_4}}(t))$, etc., while in curve 3 which produced instability, $E(\overline{\overline{M_2}}(t)) = 200$. In all cases, $E(\overline{\overline{M_1}}(t)) = 80$. Since ρ is relatively small in these experiments, the $\pi_k(\lambda(t))$'s become negligible quite rapidly as k increases beyond k = 2 or

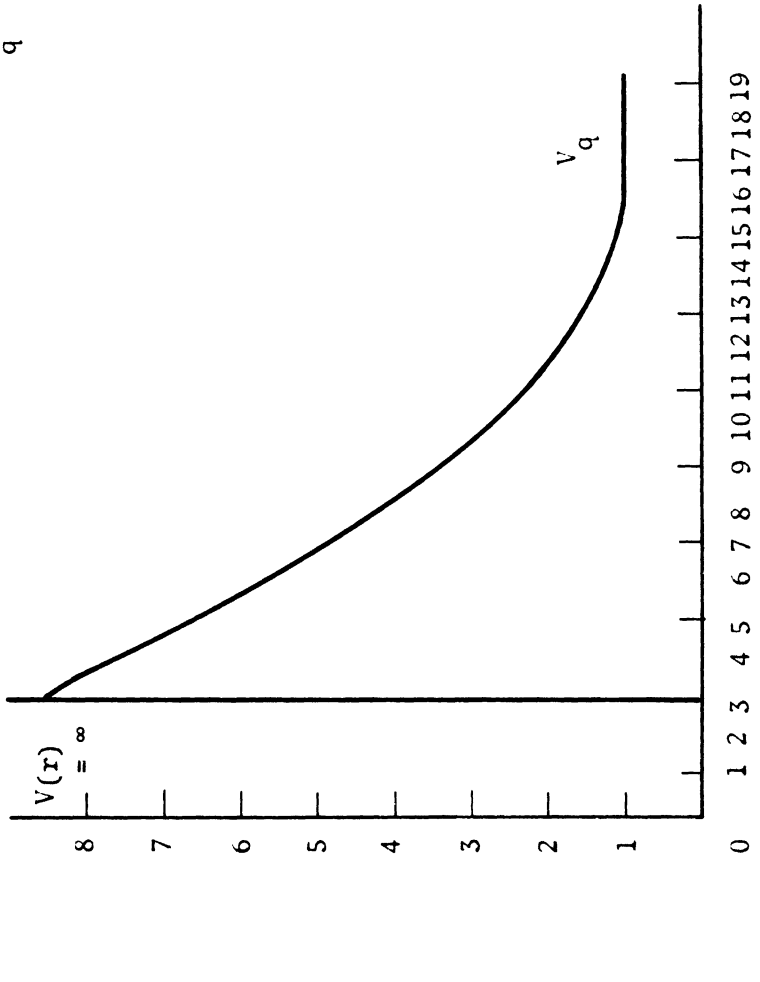

Figure 6.3. General Form of the Threshold Curve V(r).

The general form of V(r) to be used in subsequent experiments is a monotone decreasing function of r. $V(0) = V(1) = V(2) = \infty$, $V(3) = V_m$, ..., $V_{r_q} = V_{16} = 1$.

Figure 6.4. Summary of Results for Basic Experiments II.

(a) Threshold Curves (1)-(6). (b) EEG's and $\bar{\bar{\Sigma}}_0$'s for Variations (1)-(6). Curve (4) is used for Variation (7).

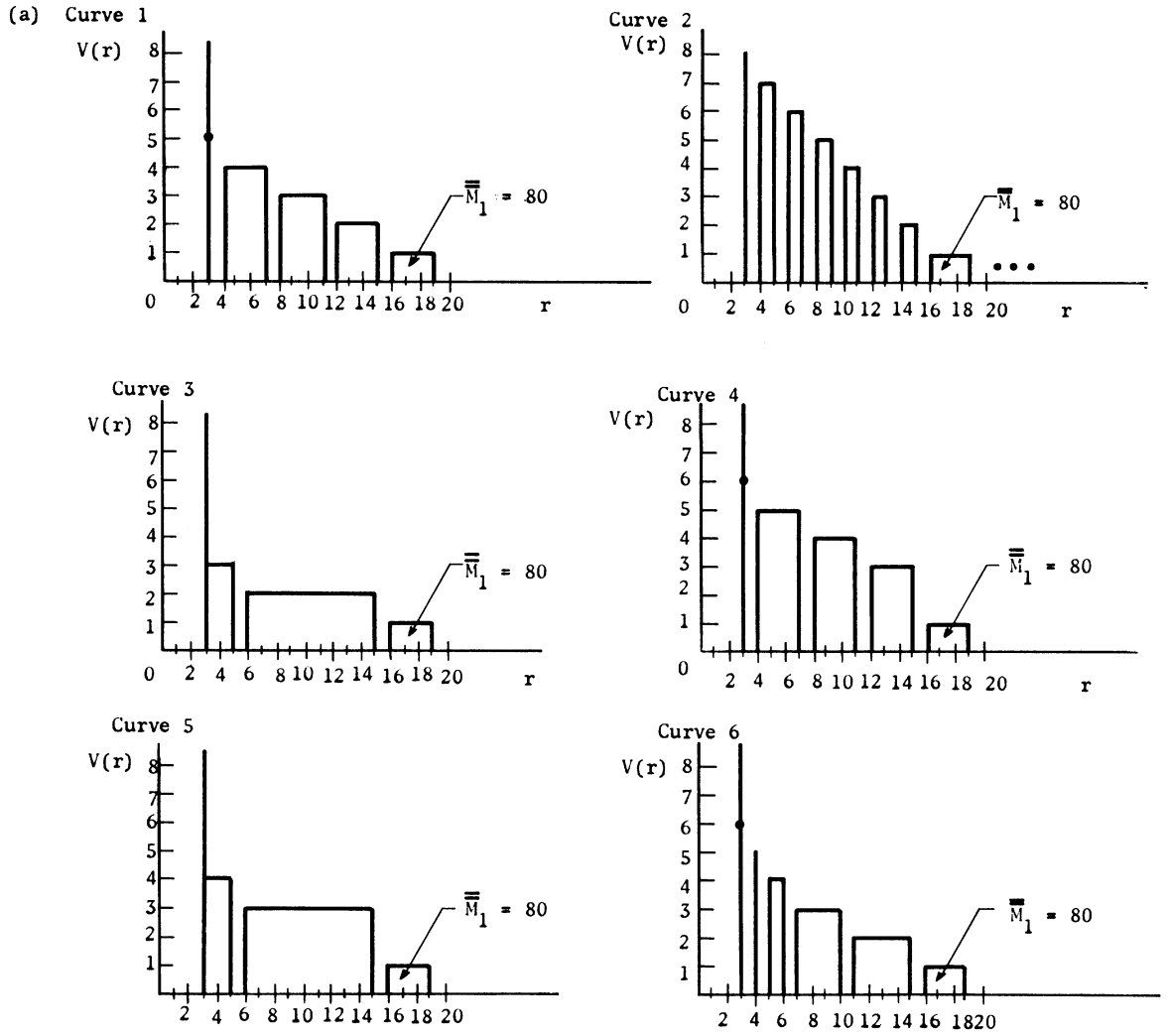

Figure 6.4. (continued). (b) EEG's for Variations (1) - (7) of Basic Experiments II.

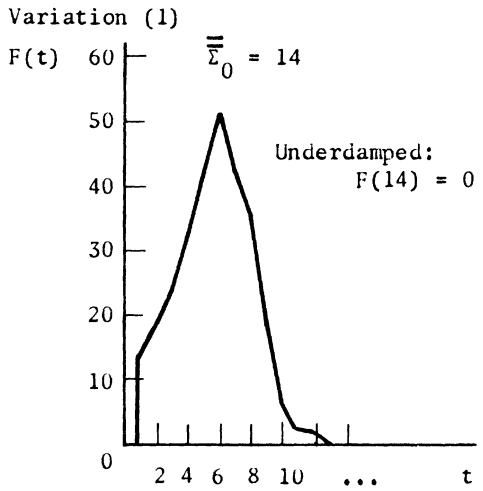

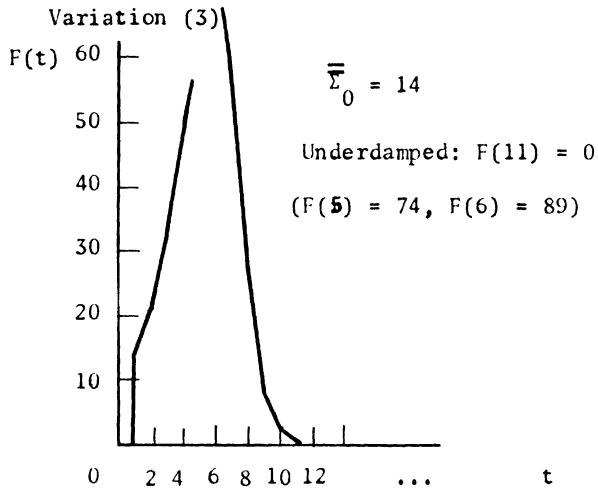

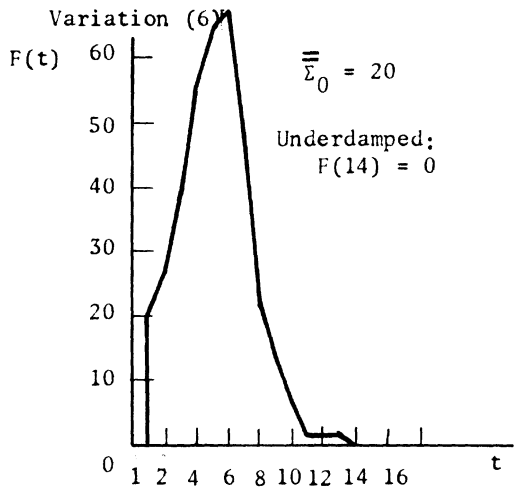

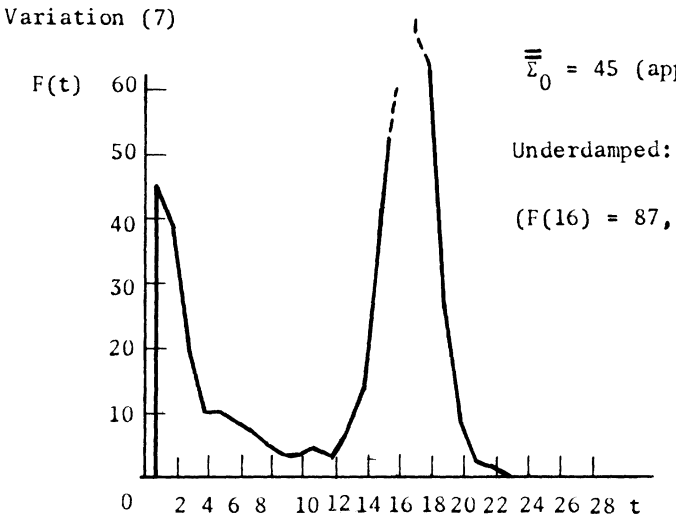

$\bar{\bar{\Sigma}}_0 = 45$ (approximately 100% increase over previous $\bar{\bar{\Sigma}}_0$'s)

Underdamped: F(23) = 0

(F(16) = 87, F(17) = 101)

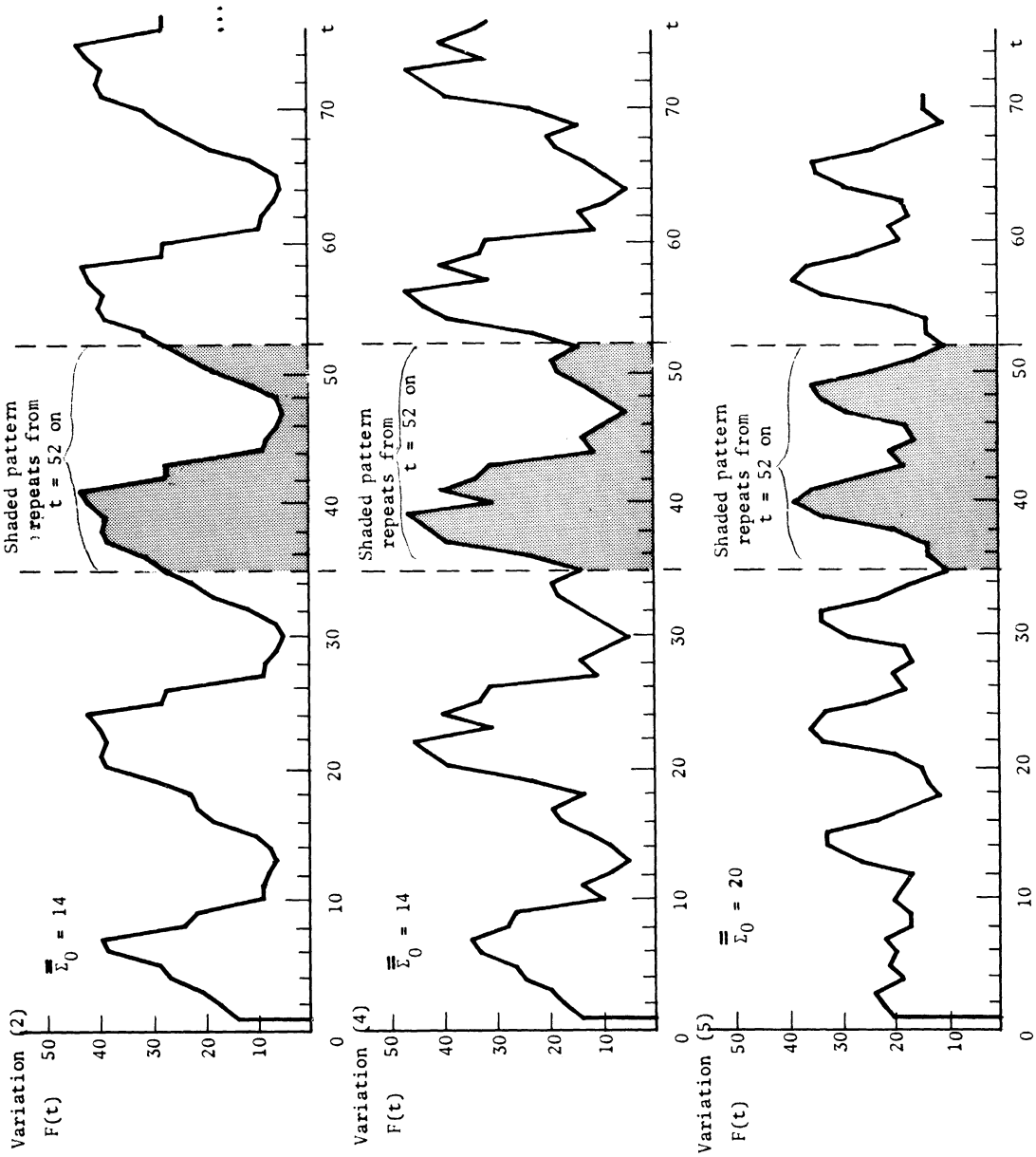

Figure 6.4 (continued). (b) EEG's for variations (1) - (7) of Basic Experiments II

k = 3. Therefore, "steepness" may be judged primarily in terms of the cardinalities $\overline{\overline{M}}_2(t)$ or $\overline{\overline{M}}_3(t)$.

Once more, the positive results of these experiments were marred by the periodicity occurring in Basic Experiment I. At this point, various mechanisms for eliminating this were studied, culminating eventually in the introduction of negative feedback and distance-bias as described in section 6.3.2 below.

Variations of Basic Experiments II

Experiments 2 and 4 of Figure 6.4 were repeated for the case that the $\lambda_{ji}(0)$'s were uniformly distributed over the range $0 \leq \lambda \leq \lambda_{max} = 63$, all other network parameters remaining the same as in Basic Experiment I. The EEG's, etc., are given in Figure 6.5, experiments 2' and 5' respectively. In 2', F(t) went to zero at t = 57. In 4', the run was terminated prematurely by a programmed "clock" error at t = 43. Inferring from the general pattern of the behavior F(t), it appeared that the network might be stable (Phase II). Notice that the behavior F(t) in 5' is not periodic and well modulated — i.e., F(t) does not fluctuate violently as in 2'. The results of experiment 5' gave considerable impetus to detailed consideration of the effects of negative feedback.

A third variation of Experiments 1 - 7 above entailed changing only the U(λ) and D(λ) tables and resuming Experiment 3. The new tables, EEG, etc., are given in Figure 6.6. For each λ, the relationship

$$\frac{D(\lambda)}{U(\lambda) + D(\lambda)} = \frac{1}{17}$$

holds (assuming $\hat{r}_q \cong 17$), however for increasing λ, U(λ) and D(λ) increase. The motivation for this will be discussed in Chapter 7, Section 7.2. Essentially, it was to encourage path closing to form cycles

Figure 6.5. Variations of Basic Experiment II, Variants (2) and (4).

Experiments (2') and (4') below are identical to Variants (2) and (4) of Figure 6.4 except that the $\lambda_{ji}(0)$'s were distributed uniformly over the range $0 \leq \lambda \leq \lambda_{max} = 63$. This means that the initial synapse-values, $S(\lambda)$, are distributed uniformly over $-32 \leq S(\lambda) \leq 32$.

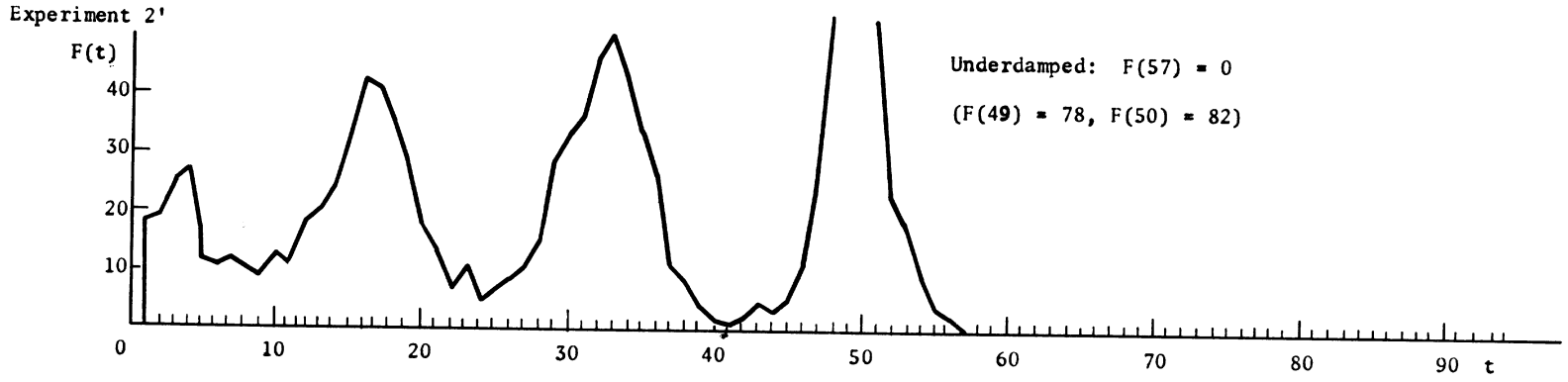

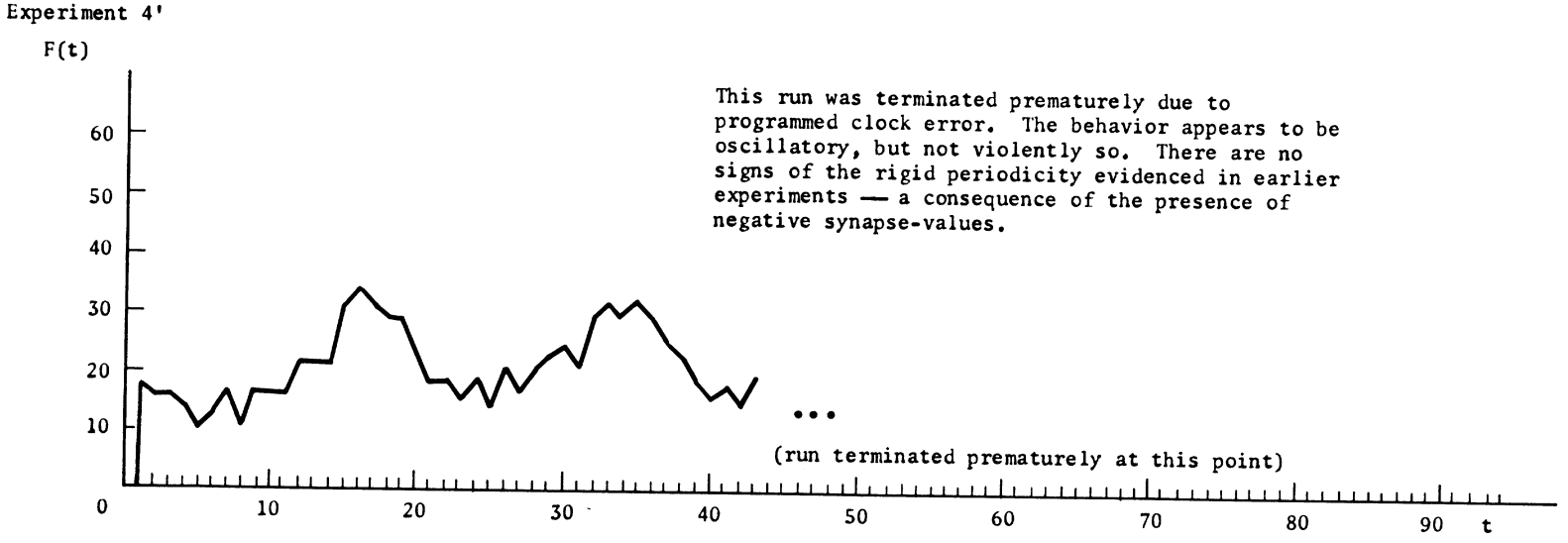

λ	U(λ)	D(λ)	λ	U(λ)	D(λ)
0	.100	.00625	33	.20	.01250
1	.103	.00645	34	.21	.01310
2	.106	.00663	35	.22	.01375
3	.109	.00670	36	.23	.01440
4	.112	.0070	37	.24	.01500
5	.115	.0072	38	.25	.01560
6	.118	.00738	39	.26	.01625
7	.121	.00756	40	.27	.01690
8	.124	.00775	41	.28	.01750
9	.127	.00794	42	.29	.01810
10	.130	.00813	43	.30	.01870
11	.133	.00830	44	.31	.01940
12	.136	.00850	45	.32	.02000
13	.139	.00870	46	.33	.02060
14	.142	.00889	47	.34	.02120
15	.145	.00908	48	.35	.02190
16	.148	.00927	49	.36	.02250
17	.151	.00945	50	.37	.02310
18	.154	.00964	51	.38	.02380
19	.157	.00982	52	.39	.02440
20	.160	.01000	53	.40	.02500
21	.163	.01020	54	.42	.02620
22	.166	.01040	55	.44	.02750
23	.169	.01055	56	.46	.02880
24	.172	.01075	57	.48	.03000
25	.175	.01094	58	.50	.03120
26	.178	.01110	59	.52	.03250
27	.181	.01130	60	.54	.03380
28	.184	.01150	61	.56	.03500
29	.187	.01170	62	.58	.03620
30	.190	.01188	63	.60	.03750
31	.193	.01205			
32	.196	.01225			

Figure 6.6 Variation of Basic Experiment II, Variant (5).

This experiment is a repetition of Variant 5, Figure 6.4, in which the U(λ) and D(λ) tables were replaced by the tables shown above. For each λ in this table, $D(\lambda)/(U(\lambda)+D(\lambda)) = 1/\hat{r}_q = 1/17$.

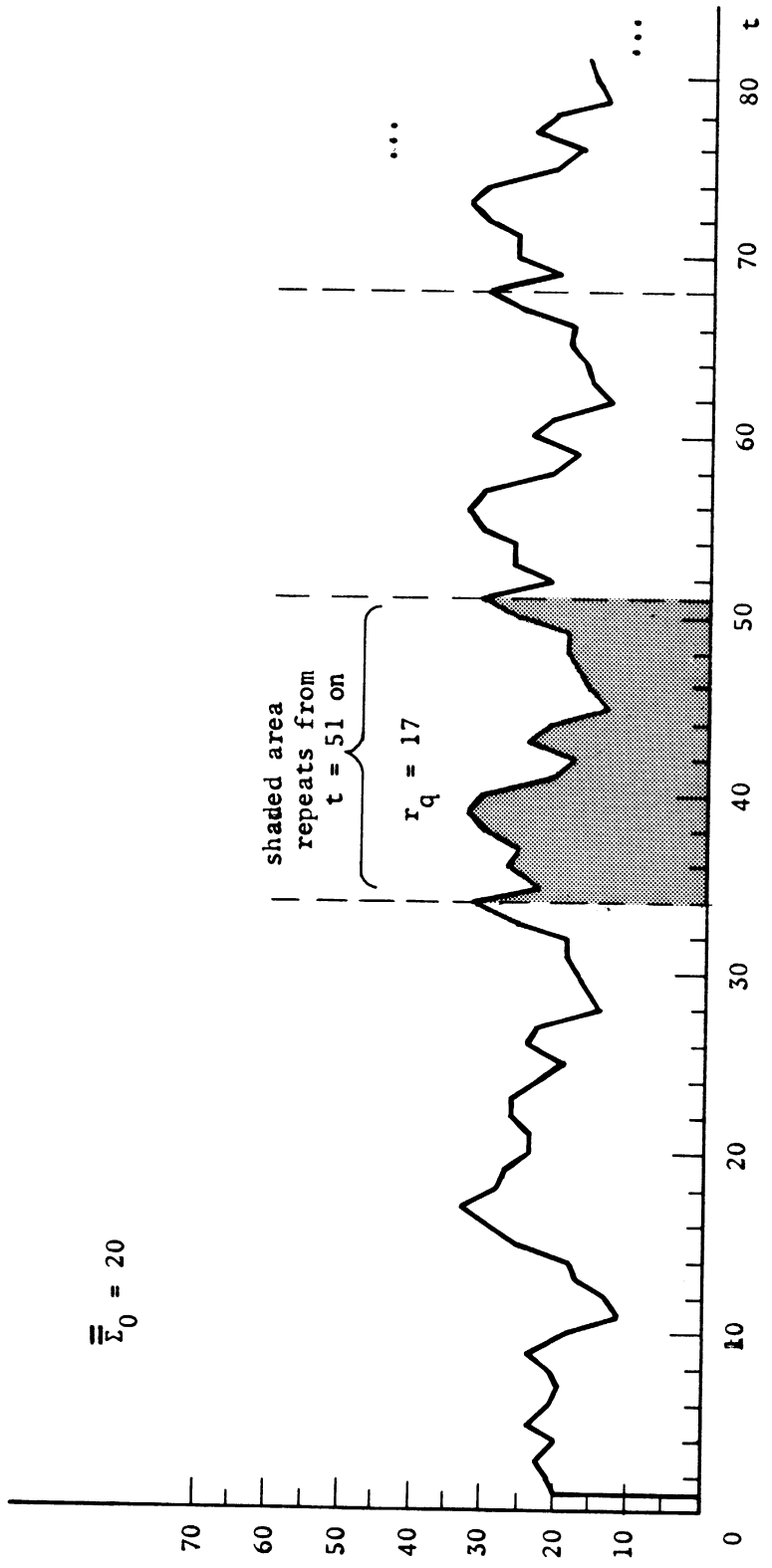

Figure 6.6. (continued). EEG.

$C(\Sigma_0)$ in the periodic stimulus experiments. Again, F(t) cycled precisely on $\hat{r}_q = 17$.

The new tables $U(\lambda)$ and $D(\lambda)$ will be assumed in subsequent experiments until further notice. Thus far a detailed study of synapse-level drift had not yet been carried out.

Threshold Curves with Dips

To anticipate somewhat the results of Chapter 7, Section 7.2.1, the stable networks exhibited so far failed to yield cycles $C(\Sigma_0)$ under periodic stimulation of a subset $\Sigma_0 \subset \mathcal{N}$ (this Σ_0 is to be distinguished from the Σ_0 used to start a network at t = 0). The following ad hoc mechanism was introduced in an attempt to encourage formation of paths $P_E(\Sigma_0 \to \Sigma_\tau)$ and closing of these paths into cycles $C(\Sigma_0)$: V(r) is no longer a monotone decreasing function of r, but decreases rather rapidly to low threshold values, increasing to a maximum, then eventually decreasing to the quiescent value V_q (=1). The general form of this type of threshold curve is shown in Figure 6.7(a). The principle was to provide sufficiently low threshold values for neurons with recovery states near $r = r_0$ that recruitment into paths $P_E(\Sigma_0 \to \Sigma_\tau)$ and eventually closing of $P_E(\Sigma_0 \to \Sigma_\tau)$ into a $C(\Sigma_0)$ would be encouraged. It is interesting to note that apparently some observed recordings of neuron membrane potentials show recovery characteristics similar to those of Figure 6.7(b), where the dip occurs around $r = r_m$ or even for $r >> r_{max}$, followed by a hyper-refractory swell. These curves were eventually completely rejected for reasons to be discussed in Chapter 7, Section 7.3.1. However, their study did provide some interesting sidelights on the behavior of networks with cycles. Therefore, it is included here.

Figure 6.7. Threshold Curves with Dips.

(a) General Form of a Threshold Curve with Dips Used in the Sequel.

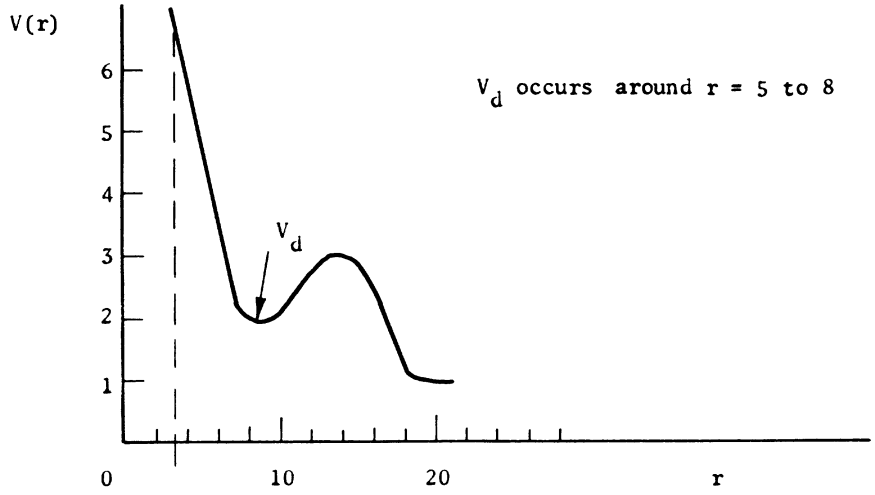

(b) Observed Resting and Action Potential of Squid Axon. (Adapted from Eccles [ ] page 51).

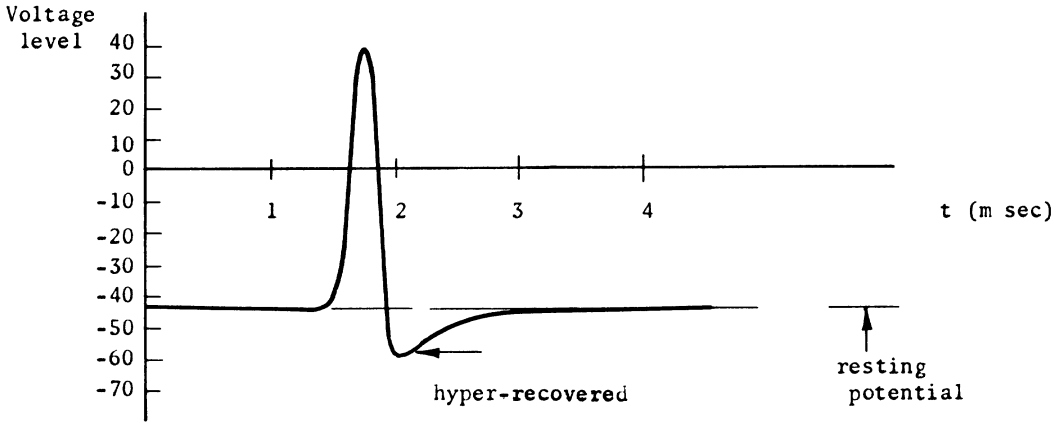

From (b) we might conclude that the threshold curve is at least bounded below by the curve for the action potential — allowing thus approximately .5 m sec of hyper-recovery for the squid axon.

Figure 6.8. λ-distribution for Experiments of Figure 6.9.

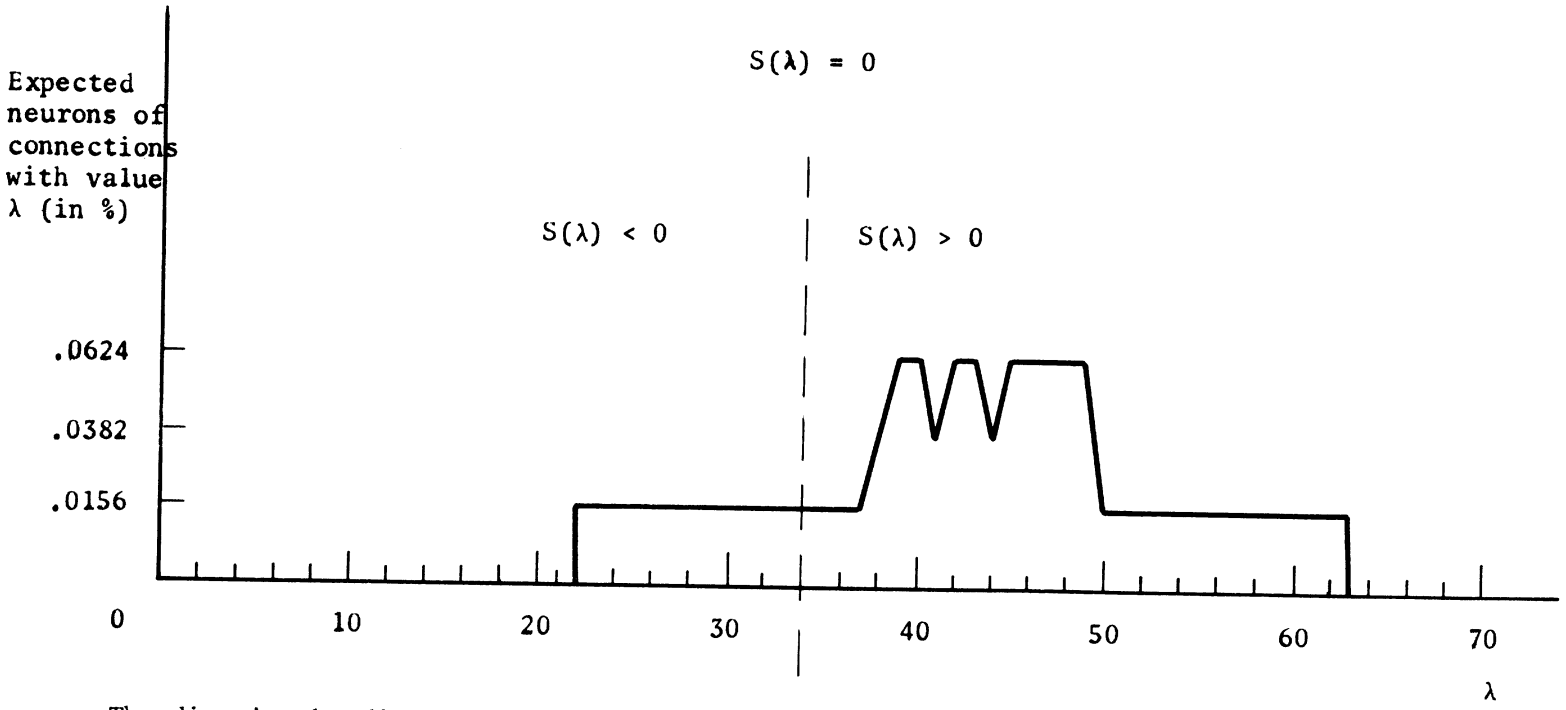

The dips in the distributions at λ = 41 and λ = 44 arose from a minor programming error and were not intentional. This distribution was selected strictly ad hoc before the theory of Chapter 4 was developed.

Figure 6.9. Threshold Curves with Dips Experiments, First Series.
Except for V(r) and the initial -distribution (see Fig. 6.8), the networks used are identical to those of Variant 3, Figure 6.4.

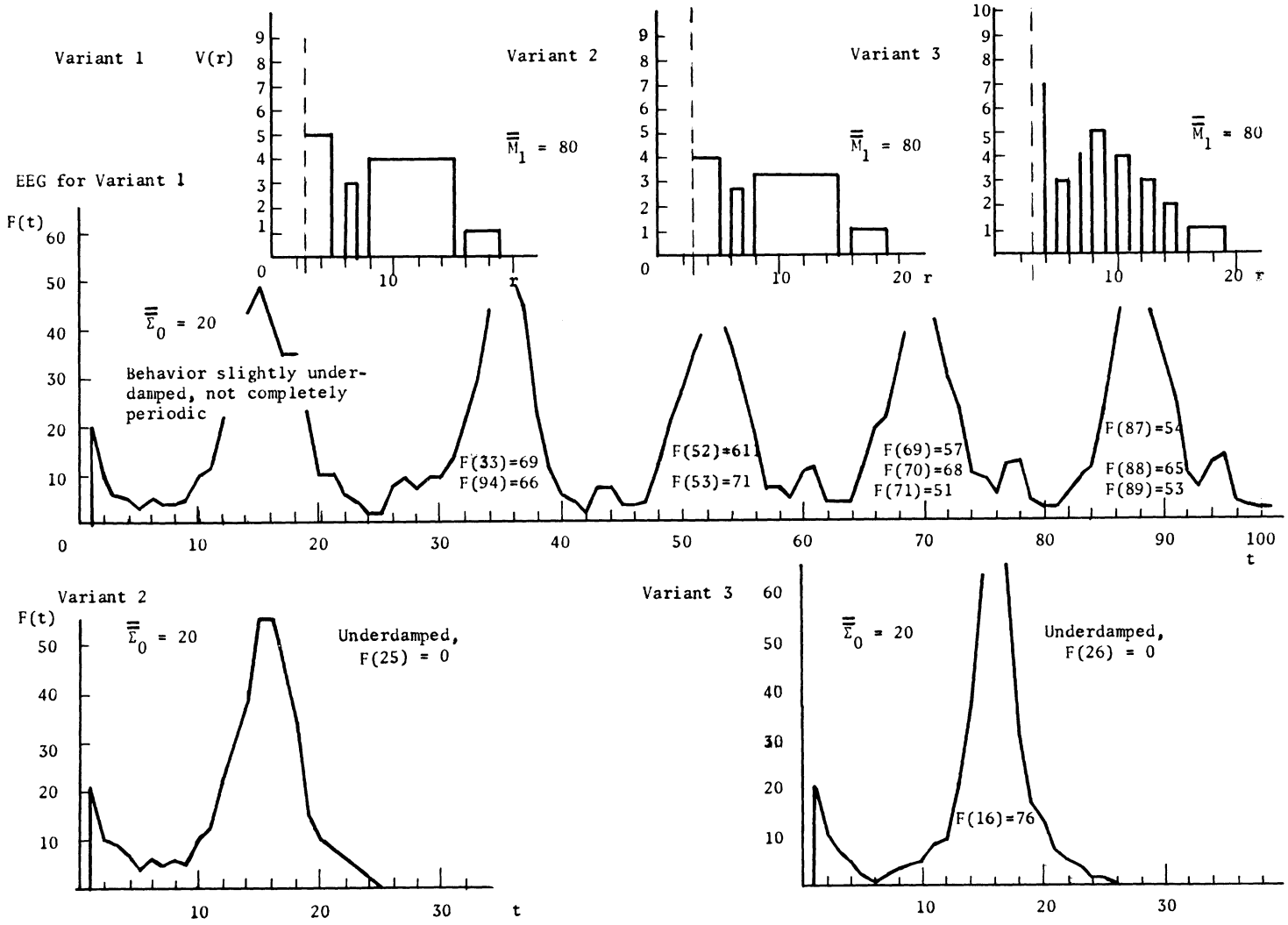

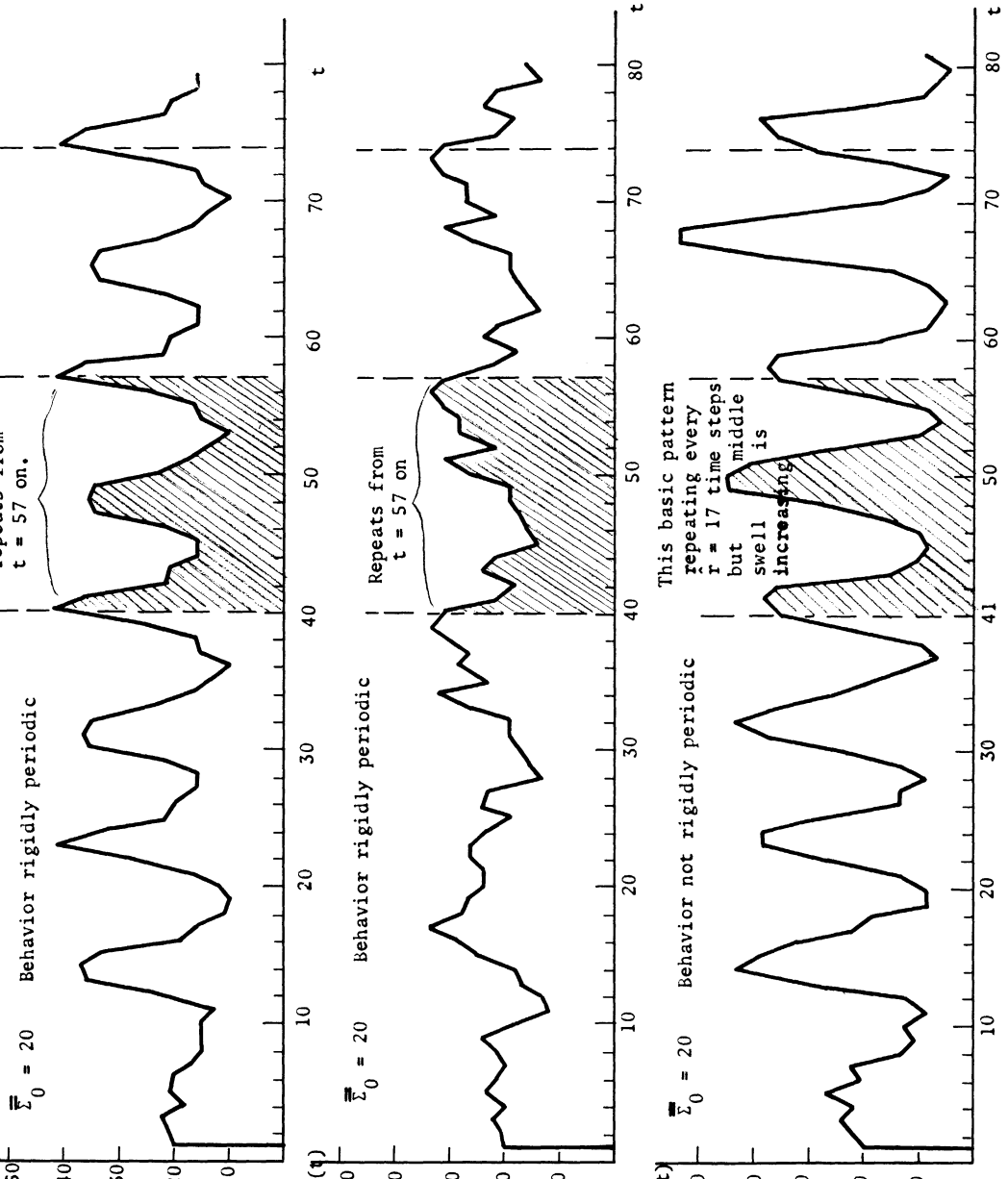

Figure 6.10. Threshold Curves with Dips Experiments, Second Series.
Repeat of Variants of Figure 6.9, all parameters identical except all $\lambda_{ji}(0)$'s set to λ_0 as in Experiment I.

Two basic series of experiments were performed using threshold curves with dips. The first entailed precisely the same network parameters as Experiments 3 above, except for V(r) and the initial λ-distribution. For the latter, the $\lambda_{ji}(0)$'s were distributed according to Figure 6.8. Some of the results of this series are given in Figure 6.9 (V(r)'s, $\bar{\bar{\Sigma}}_0$'s, EEG's). It is interesting to note that Experiment 1 of Figure 6.9 did not yield exact periodicity, although F(t) appeared to be "homing" in on an exact period of $\hat{r}_q = 17$.

The second series was a repeat of the first, with the $\lambda_{ji}(0)$'s all equal to λ_0 so that $S(\lambda_0) = 1$, just as in Basic Experiment I. The results of this series are summarized in Figure 6.10. Two interesting items emerge from these: (a) Curves 2 and 3 resulted in stability, whereas in the first series they produced instability. (b) Once again, exact periodicity reappears. This certainly strengthens the growing feeling that lack of complexity in the underlying $\hat{\lambda}$-distribution is the main determinant of this undesirable phenomena.

6.2.2 Series II - Networks with Negative Feedback

The experiments of the preceding section were devoted in the main to networks with initial positive, equal synapse-values. Growing discontent with the rigid periodicity obtained for stable networks led to a few experiments with negative feedback present. It was realized that a systematic study of the role of negative feedback was essential to the dual goals of obtaining "very stable" behavior and "adequate" networks for the periodic stimulation experiments. At this point, the basic theory of Chapter 4, Section 4.3.3, was worked out. This produced an invaluable aid to the intuition. However, the complexity of the steady-

state calculations for connection distibutions of the form

$$\rho = \sum_{s=-s_0}^{s_1} \rho_s,$$

in particular, for the cases $s_0 = s_1 \geq 2$, was sufficiently great that often crude estimates only were obtained, then refuge taken in the simulation. Of course, such calculations could be programmed for a computer. This, from the point-of-view of long-range studies of networks with cycles, eventually must be done. It was not done in the current work simply because there was a sufficient amount of programming effort involved in the simulation per se that precious little time was left for anything else. As will be seen in this and the next few sections (6.3.2), the crude approximations used to determine V(r) given $\rho = \sum_{s=-s_0}^{s} \rho_s$ were surprisingly accurate.

Three series of experiments were performed. These are described in turn below. To summarize briefly the results, stability was obtained for several V(r)'s and rigid periodicity was virtually eliminated. Unfortunately, the "best" results involved threshold curves with dips. It was to eliminate this ad hoc mechanism that gave the initial impetus to consideration of networks with distance-bias.

Negative Feedback Experiments 1, $\rho = \rho_1 + \rho_{-1} = 12$, $\rho_1 = 9$, $\rho_{-1} = 3$

The experiments of Figure 6.10 were repeated for basically the same network of that example except that the network density ρ was raised to $\rho = 12$ and the initial λ-distribution such that the initial distribution of +1 valued connections had density $\rho_1 = 9$, that of the -1 valued connections had density $\rho_{-1} = 3$. The results (V(r)'s, EEG's, $\bar{\bar{\Sigma}}_0$'s) are summarized in Figure 6.11. All networks displayed underdamped behavior,

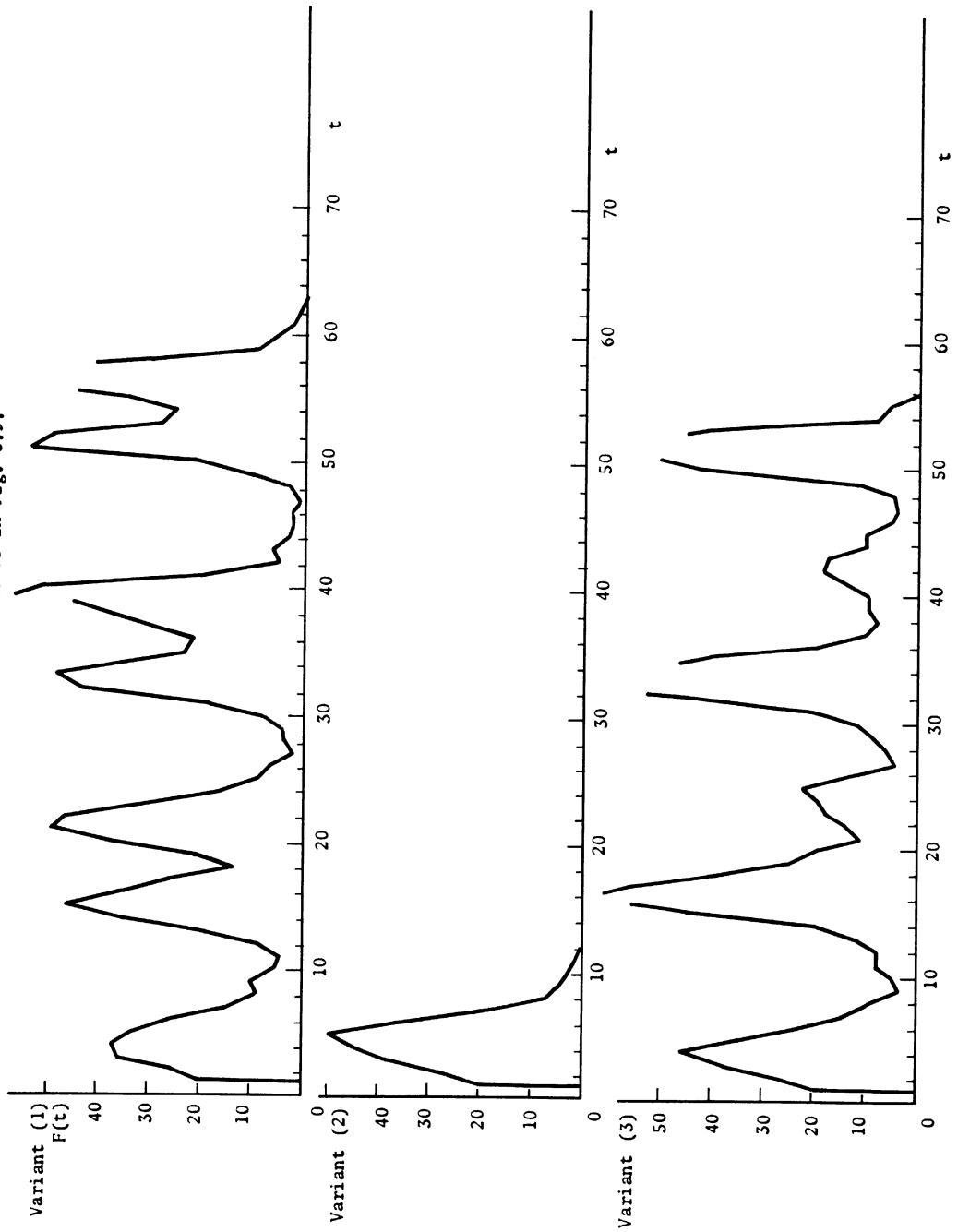

Figure 6.11. Negative Feedback Experiments 1.

Repitition of the experiments of Figure 6.9, all parameters unchanged except that the initial λ-distribution was made according to $\rho = \rho_1 + \rho_{-1}$, where $\rho_1 = 9$, $\rho_{-1} = 3$, $\rho = 12$. V(r)'s for Variants (1)-(3) below are the same as in Fig. 6.9.

with the third surviving the longest (F(89) = 0). The underdamping appears clearly to be a result of the proportionately larger number of positive than negative connections present in the network. This suggested the second series of experiements in which $\rho = 6$, $\rho_1 = 3$, $\rho_{-1} = 3$.

Negative Feedback Experiements 2: $\rho = \rho_1 + \rho_{-1} = 6$, $\rho_1 = 3$, $\rho_{-1} = 3$.

Excess of positive valued connections seemed to produce instability in the preceding experiments. Therefore, the density of +1-valued connections was reduced to 3, that of the -1 valued connections remaining 3. The network parameters (except V(r)) remain as before. The results of some of these experiments are summarized in Figure 6.12. The first two involved "normal" threshold curves (no dips). The second yielded rigid periodicity on $\hat{r}_q = 16$ (notice that $M_1(0) = 100$ in these experiments to compensate for the presence of negative connections). In the first, F(t) was homing in on a rigid period $\hat{r}_q = 16$ by the termination of the run. The second two involved threshold curves with dips. Again, in one of these the behavior was rigidly periodic, in the other no definite periodicity was present, although the average firing rate (intervals between firings) of neurons of the network was $\hat{r}_q + 16$.

Negative Feedback Experiments 3

Case 1: $\rho = \rho_{-2} + \rho_{-1} + \rho_1 + \rho_2 = 6$, $\rho_s = 1.5$, $s = -2, -1, 1, 2$.

The experiments of Figure 6.10 were repeated for this more complex synapse-value distribution. The results are summarized in Figure 6.13. One additional experiment using threshold curve 2 of Figure 5.4 was performed. It is also included in Figure 6.13, Experiment 4. The first two threshold curves produced instability. The last two, the last of which is a "normal" threshold curve, were stable for $t \in [0,99]$, but

Figure 6.12. Negative Feedback Experiments 2.

The same basic network of the preceding runs was used as basis for the experiments here except that $\rho = 6 = \rho_1 + \rho_{-1}$, $\rho_1 = \rho_{-1} = 3$. The respective threshold curves for Variants (1) - (4) are given in (a), the EEG's in (b).

(a) Threshold Curves for Variants (1) - (4).

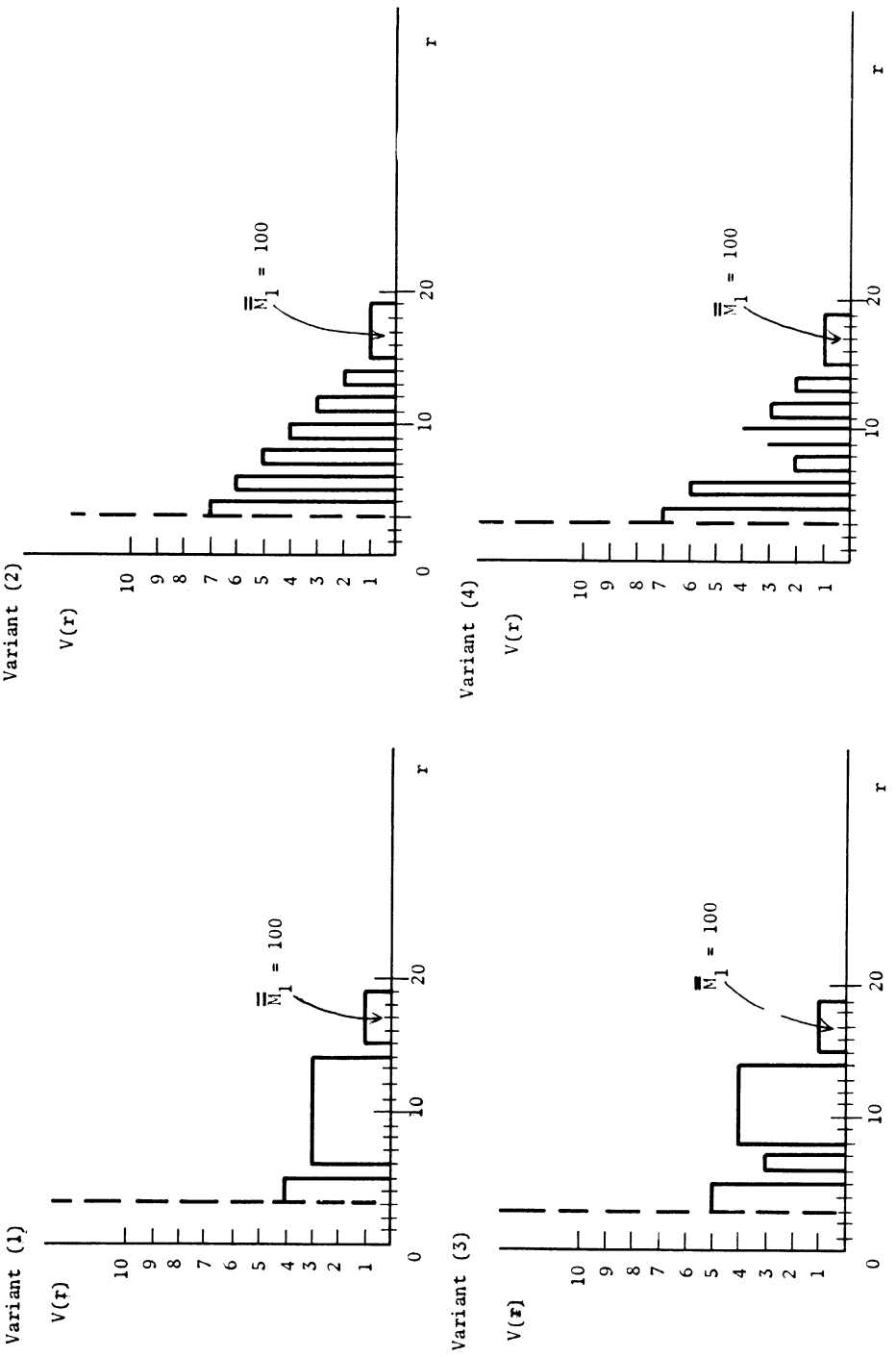

Figure 6.12 (continued). (b) EEG's for Variants (1) - (4) of Negative Feedback Experiments 2.

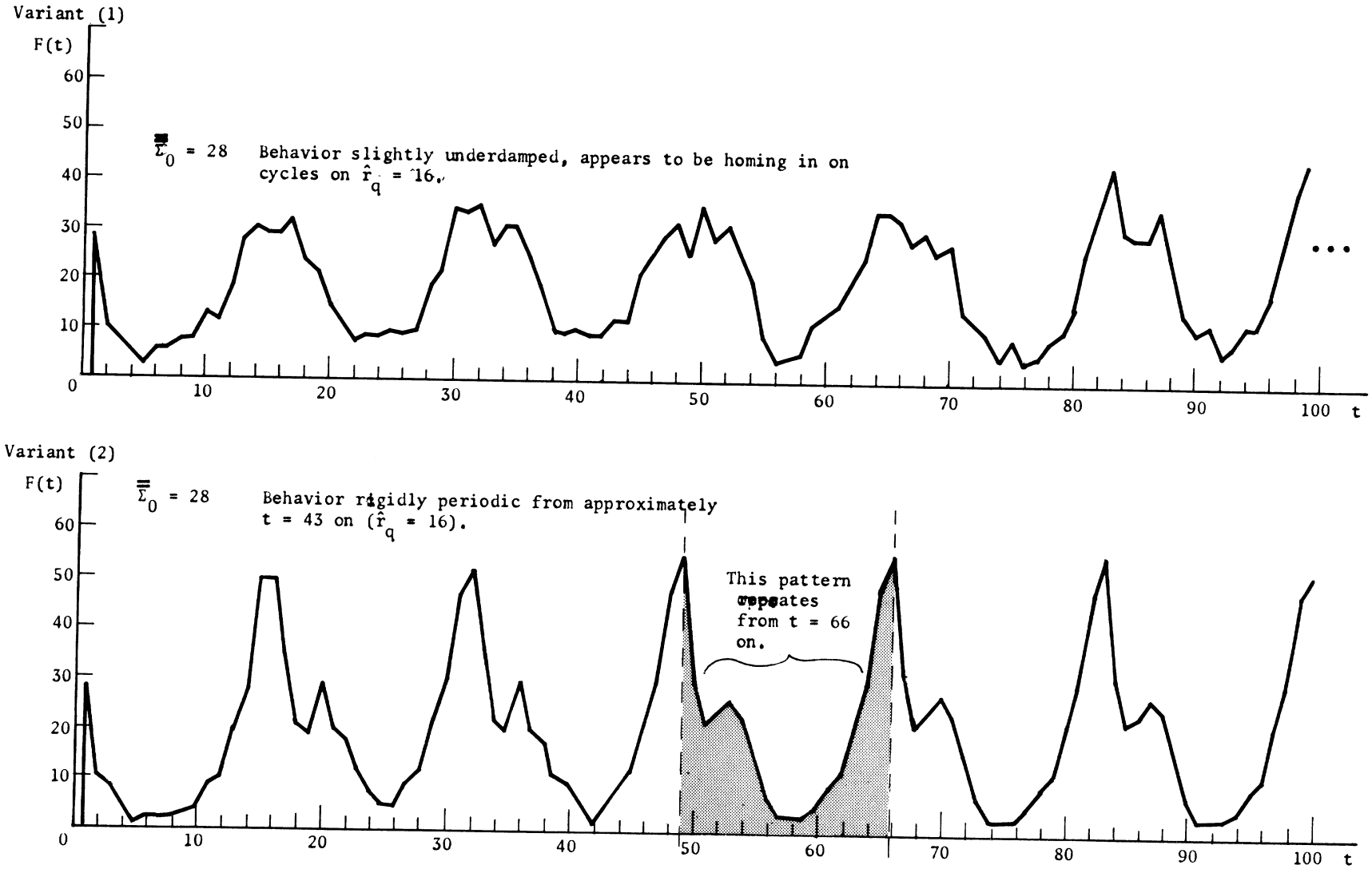

Figure 6.12 (continued).

(b) (continued) EEG's for Variants (1)-(4) of Negative Feedback Experiment 2.

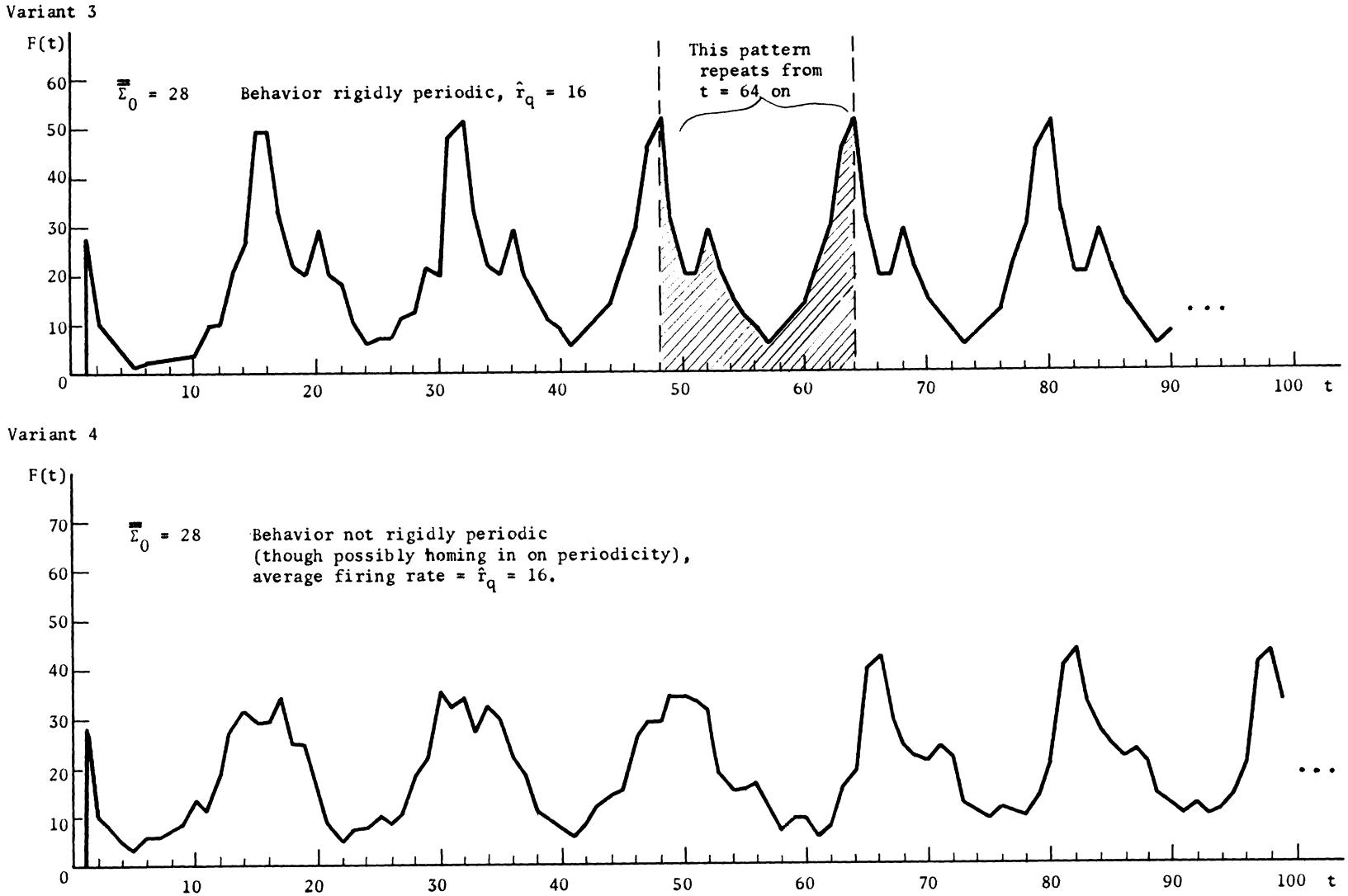

apparently underdamped. Rigid periodicity was not present in either of the last two cases.

Case 2: $\rho = \rho_{-2} + \rho_{-1} + \rho_0 + \rho_1 + \rho_2 = 24,\ \rho_0 = 12,\ \rho_s = 3,\ s = -2, -1, 1, 2$

The total network density was raised to $\rho = 24$ with a 0-valued sub-distribution with density 12. The intent was to provide connections whose effect would not be noticeable initially, but which might provide additional positive or negative connections if needed by the network later (through synapse-level drift). This would be particularly relevant to the formation of paths in the periodic stimulation experiments. The last two experiments of Figure 6.9 were repeated using this distribution. The results are summarized in Figure 6.13, Case 2. The EEG's display violent oscillations, but rigid periodicity is lacking.

6.2.3 Conclusions

Stability may be produced in networks with uniform random distributions of connections, just as predicted by the theory of Chapter 4 for this case. However, it was produced, with several exceptions, at a cost: (a) unnatural ad hoc threshold curves had to be used, or (b) rigid periodicity in F(t) occurred ($F(t) = F(t+\hat{r}_q)$ and $\Sigma_t \equiv \Sigma_{t+\hat{r}_q}$).

A detailed study of these experiments suggested that the introduction of distance-bias into the networks would eliminate both these difficulties, especially if negative feedback were present. Therefore, further work with these networks was abandoned and attention turned toward networks with distance-bias.

Periodicity

The difficulty of (b) perhaps deserves further mention. It is

Figure 6.13. Negative Feedback Experiments 3.

Case 1: $\rho = \rho_{-2} + \rho_{-1} + \rho_1 + \rho_2 = 6$, $\rho_s = 1.5$, $s = -2, -1, 1, 2$.

Case 2: $\rho = \rho_{-2} + \rho_{-1} + \rho_0 + \rho_1 + \rho_2 = 24$, $\rho_0 = 12$, $\rho_s = 3$, $s = -2, -1, 1, 2$.

For Case 1, Variants (1) - (4), threshold curves (1) - (3) of Figure 6.9 and (2) of Figure 6.4 respectively were used.

For Case 2, threshold curves (3) and (2) respectively (Fig. 6.9) were used for Variants (5) and (6).

Case 1

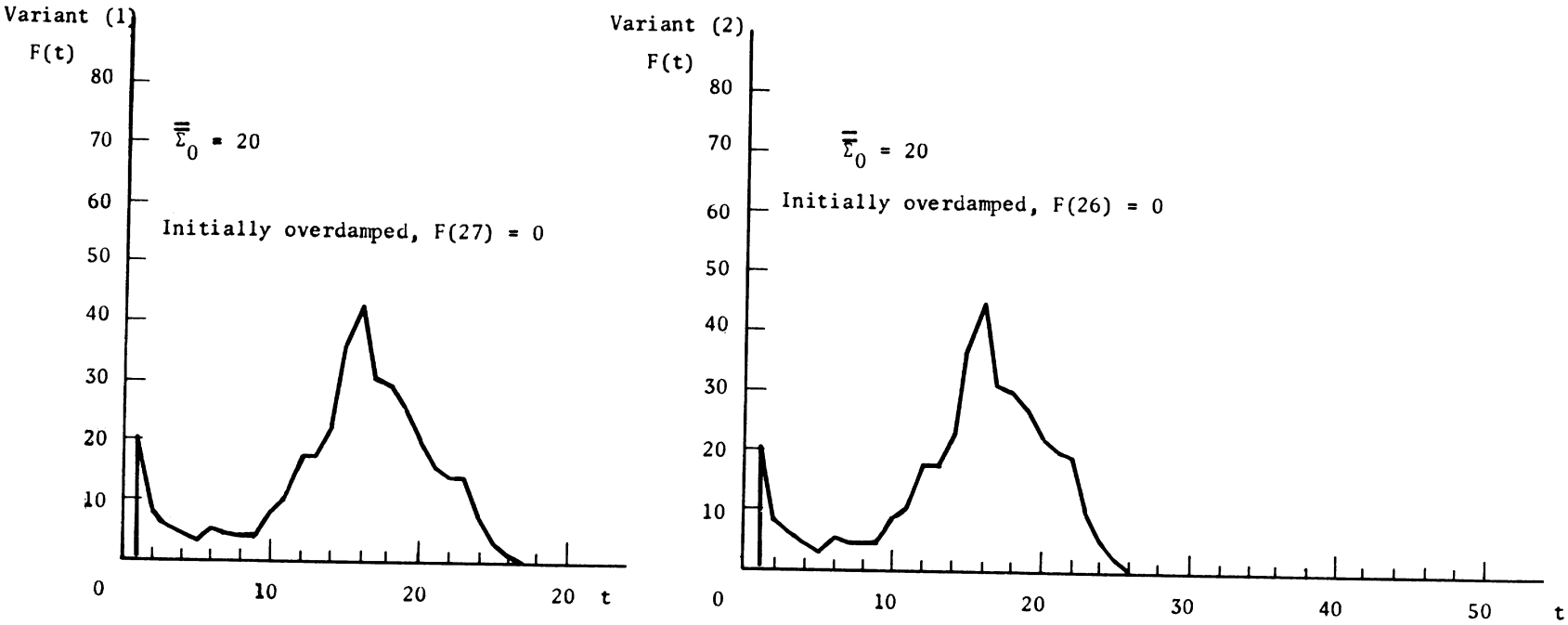

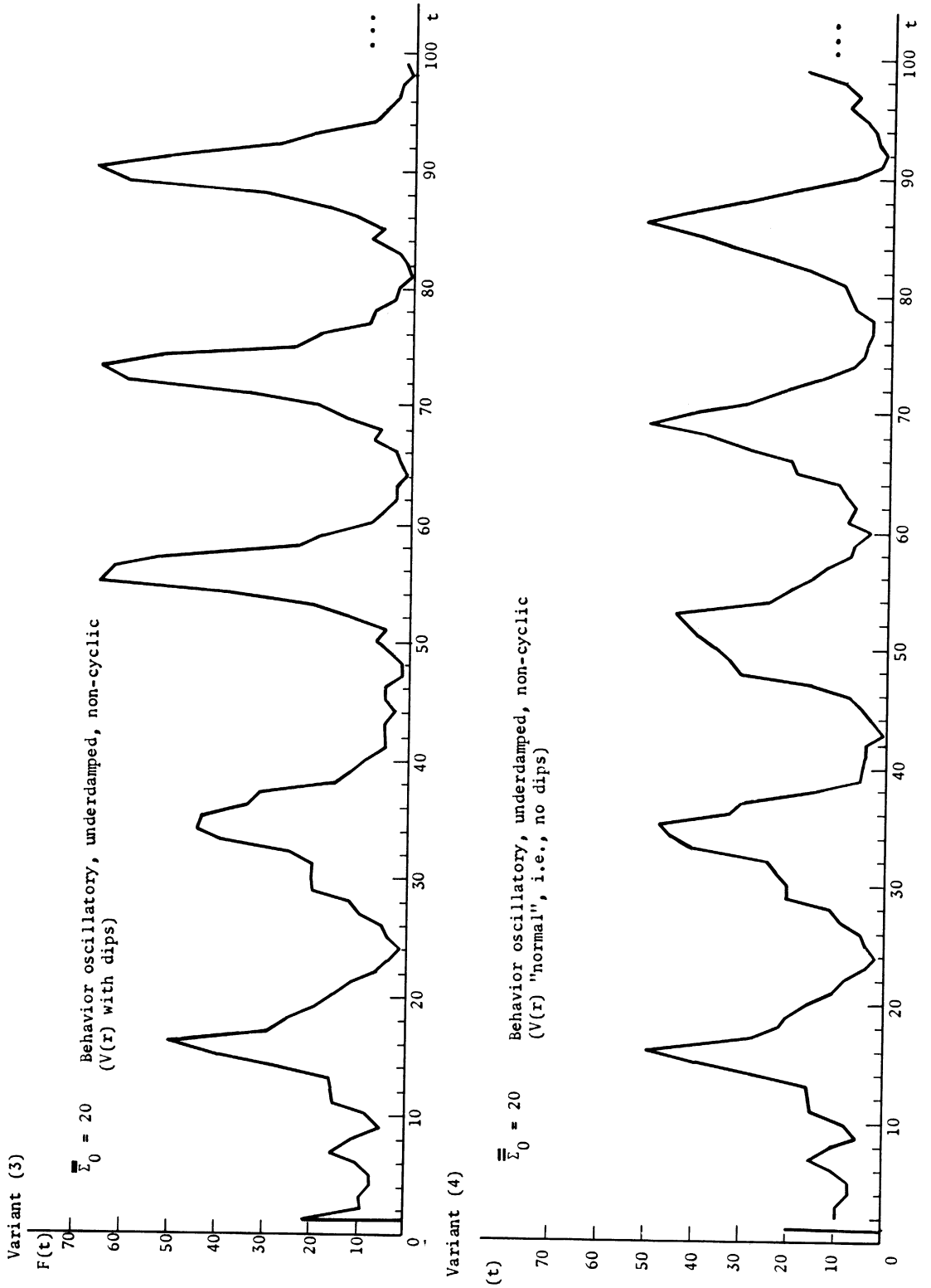

Figure 6.13. Case 1 (continued).

Figure 6.13. (continued) Case 2.

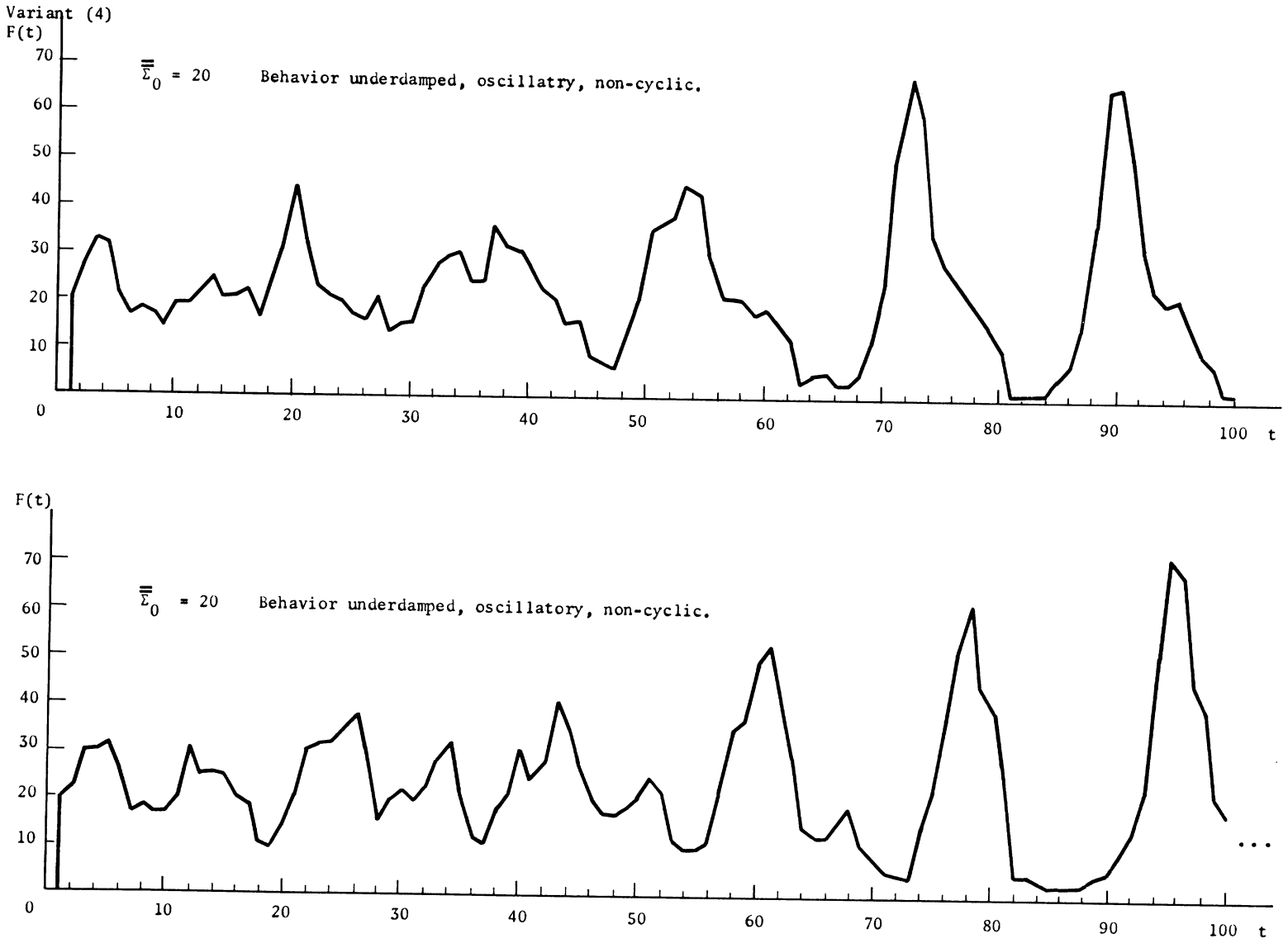

a theorem of the Theory of Finite Automata that the behavior of a finite automaton without inputs will cycle on a definite period τ, say. The period τ is, roughly, an increasing function of the number of states of the automaton. The networks of this section may be regarded as finite (probabilistic) automata. Therefore, one intuitively expects the behavior of these networks to eventually repeat itself; i.e., $F(t+\tau) = F(t)$, $\Sigma_t \equiv \Sigma_{t+\tau}$. One would like τ to be very large, essentially infinite.

If the threshold curve V(r) is very steep, with $\rho = 6$ (relatively small), $N = 400$, and positive, equal connections only present in $\mathcal{N}$, it is clear that in some sense the number of states of $\mathcal{N}$ (or state-transitions) is more restricted than if V(r) is shallower, the synapse-values are distributed over positive and negative connections, etc. Therefore, in the former case, less information is present than in the latter. The introduction of distance-bias adds another order of magnitude to τ and one would expect far richer behavioral patterns from networks with this feature.

6.3 NETWORKS WITH DISTANCE-BIAS

6.3.1 Introduction

The conclusions of the preceding section pointed to the necessity of introducing a distance-bias mechanism. The mechanism adopted was that described in Chapter 4. It has the advantage that for $r > R$, a neuron receives no connections from other neurons at distance r from itself, yet within the disk $r \leq R$, it receives connections uniformly and equiprobably from neurons at distance r. The expected number of

connections it receives from C_R is ρ. This means that within a disk C_R, a receiving neuron behaves as though it were in a network with uniform random distributions of connections, $\bar{\bar{C}}_R = N$, ρ the ρ of the disk, etc.

With this mechanism present, "very stable" and "adequate" networks were very rapidly obtained — a surprising fact in view of the analytic intractability of such networks.

To study these networks, it was necessary to start out again with the simplest cases (in particular with $\phi(\ell) \equiv 0$ and $\lambda_{ji}(0)$'s = λ_0), develop an experimental intuition for the behavior of these networks, then gradually introduce greater complexity into them. In the experiments of Section 6.2, the fatigue function was taken to be identically 0, $\phi(\ell) \equiv 0$ for $\ell = 0, 1, \ldots, \ell_{max}$. Since fatigue is a slow, cumulative function, over relatively short time intervals (t = 0 to 200, say), this should do little harm. However, for longer time intervals such as are necessary to determine "very stable" and "adequate" networks, a more realistic $\phi(\ell)$ must be used. For example, even with negative feedback present in a network $\mathfrak{N}$, there might by chance be a set of neurons that could fire at a rate much greater than $1/\hat{r}_q$ for relatively longer periods of time. These neurons then might eventually influence the behavior of $\mathfrak{N}$, either producing instability or unwanted cycles. In fact, the entire heuristic argument of Chapter 4, Sections 4.4, hinges on cycles not coming into existence spontaneously. One method of guaranteeing that this will be the case is use of the damping effect of the fatigue mechanism.

Figure 6.14. Spread-of-Excitation Experiment (Summary).

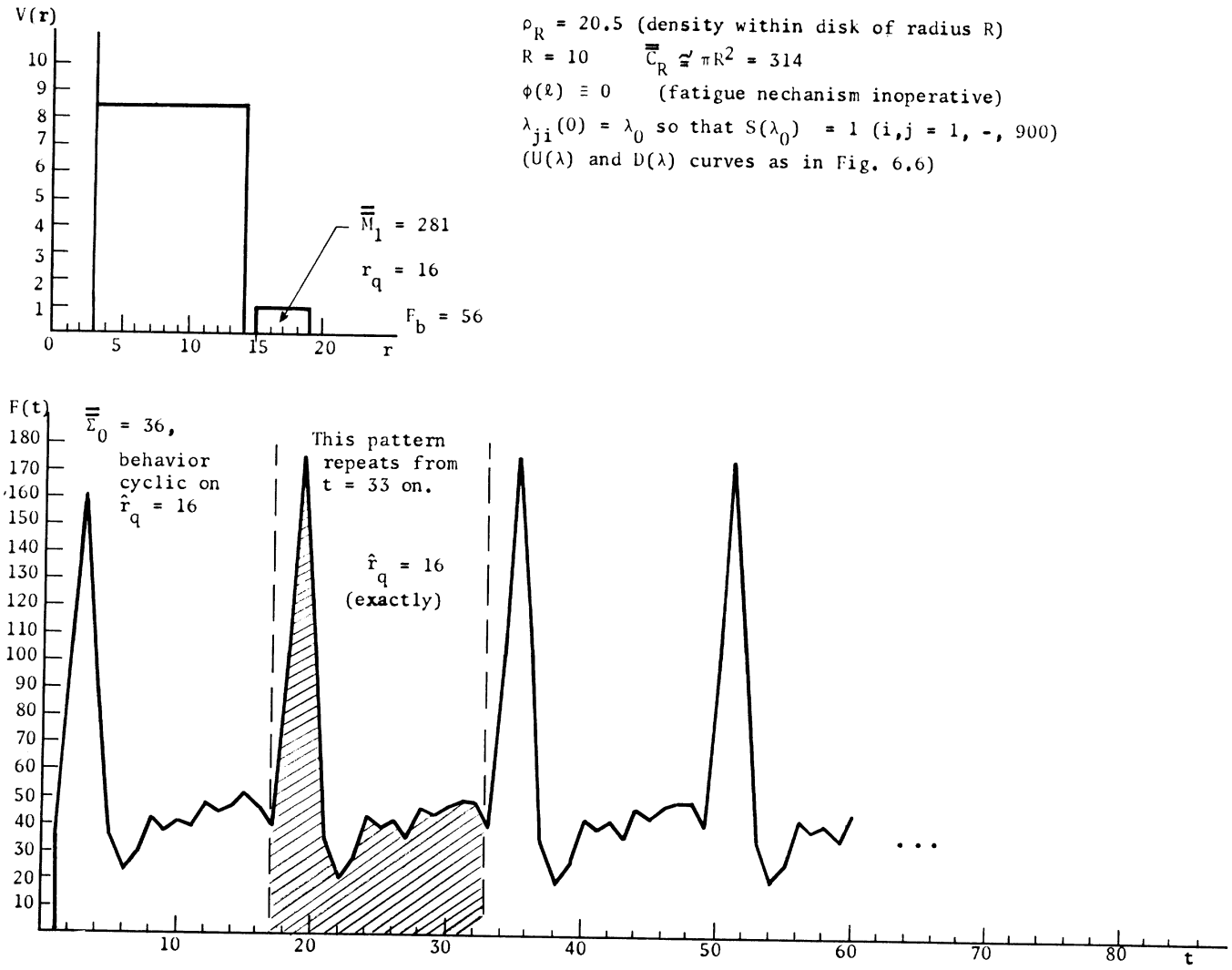

Figure 6.15. Spread of Excitation (Illustration).

(a) Firing patterns for the spread-of-excitation experiment of Figure 6.14.

(b) An hypothetical illustration of the build-up of hyper-recovered neurons in $\mathfrak{N}$ when R is too small.

(a) Firing Patterns at t = 1, 2, 3, 4 for Experiment of Figure 6.14.

Interpretation: Recall that the network is represented by a 30x30 grid of neurons. Assume that the neurons of $\mathfrak{N}$ are numbered from 1 to 900 row-wise, from right-to-left, bottom-to-top as follows:

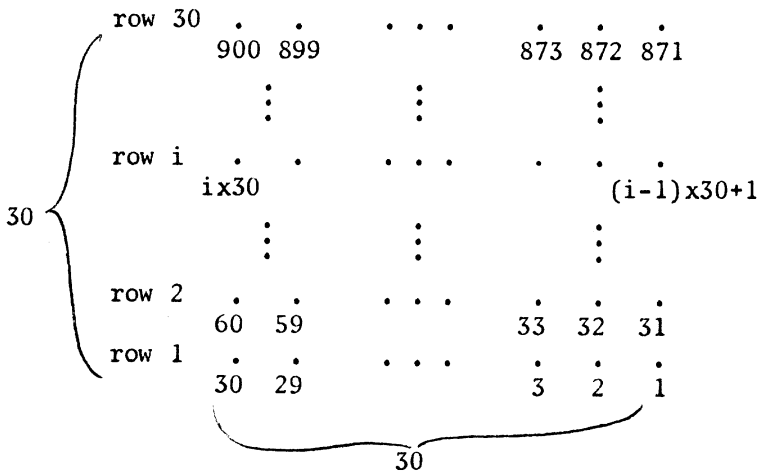

At time t, the firing of neuron K of $\mathfrak{N}$ will be indicated by a 1 in the position of the grid corresponding to neuron K; the non-firing by a 0 in the same position. The actual computer output shown below groups the neurons by fives — if all five of a group did not fire at t, the word ZERO is inserted into the appropriate position for the group. A limitation imposed by the computer restricted the number of groups per line to nineteen. Consequently, the firing pattern output is somewhat awkward to interpret. In the output given in the sequel, the boundaries of the rows (1-30) are indicated by a vertical bar. The reason for such condensed output is rather interesting. Namely, the time per time step required to produce more legible output (i.e., the 30x30 grid), or equivalently to post-edit condensed output into legible output, would simply have been far too great to be economically feasible. In fact, even the condensed output obtained was a bit of a luxury.

Figure 6.15 (a) (continued).

To illustrate the interpretation of the computer output, row 1 at time t = 1 is

```
30 29 28 27 26  25 24 23 22 21  20 19 18 17 16  15 14 13 12 11  10 9 8 7 6  5 4 3 2 1   (neuron number)
   1  0  0  0     1  0  0  0   1  1  1  0  0   1  0  1  1  0        1 1 0    1 0 0 0   (fired-not fired bit)
```

The right-hand position of each group marks the beginning of that group (e.g. 1, 6, 11, 16, 21, and 26 above). 0's to the left of the last non-zero are "suppressed" (an unfortunate property of the output routine in this case) and left blank. Thus, at t = 1 in row 1 (neurons 1-30), neurons 1, 4, 7, 8, 12, 13, 15, 18, 19, 20, 24, and 29 fired. Row 2 at t = 1 is

```
60 59 58 57 56  55 54 53 52 51  50 49 48 47 46  45 44 43 42 41  40 39 38 37 36  35 34 33 32 31
      1  0  0     Z  E  R  O        1  0  0  1                 1     1  1  0  0           1  0  0
```

On next-to-bottom line of block of ten lines for this time step, right-most three groups.

On botton line of block of ten lines for this time step, left-most three groups.

Notice that a t = 1, the neurons fired (i.e., Σ_0) are clustered in rows 1-3 of $\mathcal{N}$. At t = 2, the neurons fired "wrap around" to rows 26-30, few in rows 1-3 firing. At t = 3, the firing has moved into the center of $\mathcal{N}$ (rows 11-22), with slightly sparser firings in the top rows (26-30) and even sparser in the botton edge (rows 1-3). At t = 4, the firing has spread out fairly uniformly over $\mathcal{N}$ (still sparse at botton edge, however).

```
STIMULATED NEURONS     1  THROUGH     125
TIME       1 OUTPUT IS      36 FIRING DISPLAY
 ZERO  ZERO  ZERO  ZERO  ZERO  ZERO  ZERO  ZERO  ZERO  ZERO  ZERO  ZERO  ZERO  ZERO  ZERO  ZERO  ZERO  ZERO  ZERO
 ZERO  ZERO  ZERO  ZERO  ZERO  ZERO  ZERO  ZERO  ZERO  ZERO  ZERO  ZERO  ZERO  ZERO  ZERO  ZERO  ZERO  ZERO  ZERO
 ZERO  ZERO  ZERO  ZERO  ZERO  ZERO  ZERO  ZERO  ZERO  ZERO  ZERO  ZERO  ZERO  ZERO  ZERO  ZERO  ZERO  ZERO  ZERO
 ZERO  ZERO  ZERO  ZERO  ZERO  ZERO  ZERO  ZERO  ZERO  ZERO  ZERO  ZERO  ZERO  ZERO  ZERO  ZERO  ZERO  ZERO  ZERO
 ZERO  ZERO  ZERO  ZERO  ZERO  ZERO  ZERO  ZERO  ZERO  ZERO  ZERO  ZERO  ZERO  ZERO  ZERO  ZERO  ZERO  ZERO  ZERO
 ZERO  ZERO  ZERO  ZERO  ZERO  ZERO  ZERO  ZERO  ZERO  ZERO  ZERO  ZERO  ZERO  ZERO  ZERO  ZERO  ZERO  ZERO  ZERO
 ZERO  ZERO  ZERO  ZERO  ZERO  ZERO  ZERO  ZERO  ZERO  ZERO  ZERO  ZERO  ZERO  ZERO  ZERO  ZERO  ZERO  ZERO  ZERO
 ZERO  ZERO  ZERO  ZERO  ZERO  ZERO  ZERO  ZERO  ZERO  ZERO  ZERO  ZERO  ZERO  ZERO  ZERO  ZERO  ZERO  ZERO  ZERO
 ZERO  ZERO  ZERO   100    11 10100  ZERO   100    10 10101  1000 11001  ZERO 10100  ZERO 10100  1100  ZERO  1001
    1  1100   100  1000  1000 11100 10110   110  1000
TIME       2 OUTPUT IS     106 FIRING DISPLAY
 1000   101    10 10010 11000  1010  ZERO    10  ZERO     1     1 10000  1101   100  ZERO    10 10000   101 10110
  100 10100  ZERO  ZERO  1000  ZERO  1100     1  1000  1010  ZERO  ZERO    10   100   101  ZERO  ZERO  ZERO    10
 ZERO     1  ZERO  ZERO  ZERO  ZERO    11 10000  1001  1010  ZERO  ZERO    10     1  ZERO  1000  ZERO  ZERO  ZERO
 ZERO  ZERO  ZERO  ZERO  ZERO  ZERO  ZERO  ZERO  ZERO  ZERO  ZERO  ZERO  ZERO  ZERO  ZERO  ZERO  ZERO  ZERO  ZERO
 ZERO  ZERO  ZERO  ZERO  ZERO  ZERO  ZERO  ZERO  ZERO  ZERO  ZERO  ZERO  ZERO  ZERO  ZERO  ZERO  ZERO  ZERO  ZERO
 ZERO  ZERO  ZERO  ZERO  ZERO  ZERO  ZERO  ZERO  ZERO  ZERO  ZERO  ZERO 10000    11 10100  ZERO  ZERO  ZERO     1
   10  ZERO  ZERO     1   101  ZERO  ZERO  1001 10000 11000  ZERO    10   100   101 10001 10010  ZERO 11010   100
11000 10110    11   100  ZERO   110  ZERO  ZERO  1100 10000   100  ZERO  ZERO 11000  ZERO 11001 10000  1000   100
10000  ZERO  ZERO     1  1000  ZERO  ZERO  1010  ZERO  ZERO  ZERO  ZERO  ZERO  ZERO  ZERO  ZERO  ZERO  ZERO  ZERO
 ZERO    10  ZERO  ZERO  ZERO  ZERO  ZERO  ZERO  ZERO
TIME       3 OUTPUT IS     161 FIRING DISPLAY
 ZERO  ZERO  ZERO  1000    10 10000  ZERO  ZERO  1000 10000   100  ZERO  ZERO  ZERO  ZERO  1001  1000 10000  1000
    1     1  ZERO 11100  ZERO    10  ZERO  ZERO  ZERO  ZERO     1     1     1  ZERO  ZERO 10001    10     1  1000
10110  ZERO    11  ZERO     1 10110  ZERO  1010   100  ZERO  ZERO    10 11000   100  ZERO   110  1111 11100   100
    1 10011 11101 10101  ZERO   100 11000   100   111 10000  ZERO  ZERO   101    11 10000  1110    10 10100 11100
 ZERO  ZERO   111 10110 10000    10  1000    10  1000 10101  ZERO 10100  1000   101  1010  ZERO 11001 10000  ZERO
    1    11  ZERO  ZERO  1011 11100   110   100    10 11000  ZERO    10    10  ZERO     1   101 10001  ZERO  1000
 ZERO  ZERO   100  ZERO  ZERO 11010  ZERO  ZERO  ZERO  ZERO  ZERO     1  ZERO  ZERO    10   100  1000     1  ZERO
 ZERO  ZERO  ZERO  ZERO 10011     1 10010 11000     1  ZERO  ZERO    10  ZERO  ZERO  ZERO  ZERO    10  ZERO  ZERO
    1  ZERO  1001  ZERO  ZERO  ZERO  ZERO  ZERO  ZERO  ZERO     1  ZERO   100  1000  ZERO    10  ZERO  ZERO  ZERO
 ZERO  ZERO  ZERO  ZERO  ZERO  ZERO  ZERO  1000     1
TIME       4 OUTPUT IS      86 FIRING DISPLAY
 ZERO  ZERO  1000  ZERO   100   100  ZERO   100   100  ZERO    10     1  ZERO  ZERO  ZERO   100  ZERO  ZERO  ZERO
 ZERO  ZERO  ZERO     1    10  ZERO  ZERO 10000     1   100  ZERO 10100  ZERO  ZERO 10000  ZERO  ZERO  ZERO     1
 ZERO  ZERO 10000 10101   100  ZERO   100  ZERO  ZERO  ZERO   100  ZERO  ZERO  ZERO    10  ZERO  ZERO    11 10001
  100  ZERO  ZERO  ZERO  1001  ZERO  ZERO 10000 10000   110  ZERO  ZERO  ZERO  1100  1101 10000     1  ZERO  ZERO
  101  1000  ZERO  ZERO  ZERO 10000  ZERO  ZERO   100  1000  ZERO  ZERO     1    10 10001  ZERO   100   110   100
 1000  ZERO  1001 10010  ZERO  ZERO  ZERO    10  1000     1  1000  ZERO  ZERO 10000  ZERO  ZERO   100   100  ZERO
 1000 10001  ZERO  ZERO  ZERO  ZERO  ZERO  ZERO     1  ZERO  ZERO   100  ZERO  ZERO  ZERO  ZERO  ZERO  ZERO 10000
 ZERO  1001   100  1010  ZERO  ZERO  ZERO  ZERO    10  ZERO 10000  ZERO  ZERO  ZERO  ZERO  ZERO  ZERO  ZERO  ZERO
   10  ZERO  ZERO    10   100  ZERO  ZERO  ZERO  ZERO  ZERO  ZERO  ZERO  ZERO  ZERO  ZERO  ZERO  ZERO  ZERO  ZERO
 1000  ZERO  ZERO  ZERO  ZERO  ZERO  ZERO  ZERO  ZERO
```

Figure 6.15 (continued). (b) Illustration of Build-up of Hyper-recovered Pockets in $\mathcal{N}$ when N is Large, R Small.

Suppose $\mathcal{N}$ is represented by a square, a neighborhood C_R being shown to illustrate the magnitude of R. Assume Σ_0 "clusters" at the bottom of $\mathcal{N}$ as in (a). As the excitation moves out from Σ_0 (wrapping around as in (a)), it gradually returns to Σ_0 after roughly $N^{1/2}/R$ time steps. If R is sufficiently small, N sufficiently large so that this is r_q or greater, the neurons in the region of Σ_0 and of Σ_0 itself will be highly recovered. This raises the possibility of massive firings leading to fatal oscillations.

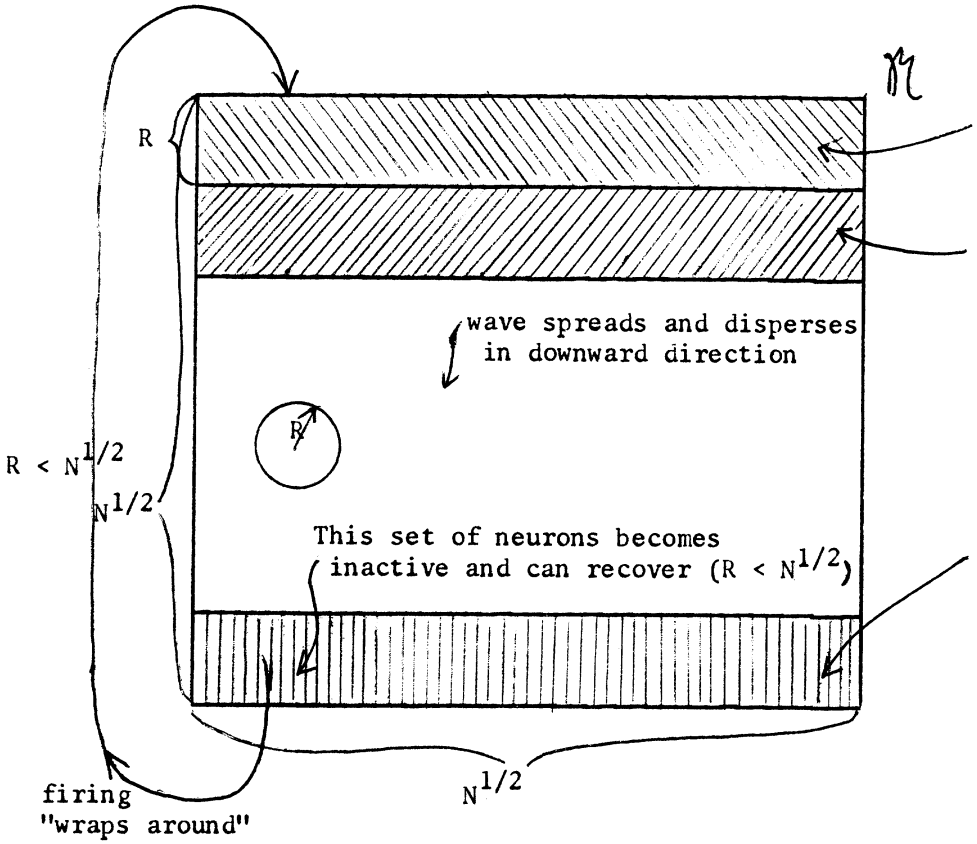

6.3.2 Series I — Familiarization

Spread of Excitation Experiment

The first experiment involving distance-bias paralleled Basic Experiment I of Section 6.2. The following network parameters were chosen: $N = 900$, $R = 10$, $\rho = 20.5$, $\lambda_{ji}(0)$'s $= \lambda_0$ so that $S(\lambda_0) = 1$, $\phi(\ell) \equiv 0$, and $D(\lambda)$, $U(\lambda)$ as in Figure 6.6. The $V(r)$ used is somewhat similar to that of Basic Experiment I, being large for $r_a \leq r \leq r_q = 14$ and equal to 1 for $r_q < r \leq r_m$. Figure 6.14 gives a summary of the parameters of this experiment, together with $\underline{\underline{\Sigma}}_0$ and the EEG. The behavior was rigidly periodic (as would be expected) with period $\hat{r}_q = 16$ after $t = 17$, i.e., for $t \geq 17$, $F(t+16) = F(t)$, $\Sigma_{t+16} = \Sigma_t$.

There is an interesting sidelight to this experiment. The starting subset Σ_0 was chosen to lie along an edge of the grid of $\mathcal{N}$. This was done deliberately to study the spread of excitation from Σ_0 over the entire network. It brings out clearly the effects of the distance-bias. This is illustrated in Figure 6.15(a) for time steps 1 through 4. Notice that the excitation spreads in both directions from Σ_0, "wrapping around" to the top of the grid since the lower and upper edges are in reality adjacent (quasi-toroidal geometry). After time step 4, a sufficient number of neurons are firing over the entire network that no clear pattern of spread of excitation exists. Since $\underline{\underline{C}}_R = \pi R^2 = 314$ neurons, the network may be covered by approximately three neighborhoods. This means that one would expect the excitation to spread over the entire network in three to four time steps, as actually occurred.

If the neighborhood radius had been very small, the excitation spread would have taken proportionately longer to cover the network. For large

N, this could lead to violent-possibly fatal-oscillations since the spreading excitation would encounter progressively more recovered neurons. Therefore, two important principles emerged from this experiment: (1) Σ_0 must be chosen so that the spread of excitation from Σ_0 will not encounter areas of recovered neurons. (2) R must be chosen so that certain neurons would not be isolated from the excitation spread too long (thus developing a pocket of recovered neurons). These ideas are illustrated in Figure 6.15(b).

Basic Experiment III

As in the case of Basic Experiment I, the preceding experiment shows that with distance-bias present a network can still be "forced" into stable (albeit periodic) behavior by a sufficiently steep threshold curve. It is now of interest to test more realistic threshold curves. For this purpose, curve 2 of Figure 6.4 was chosen. The remaining parameters were: $N = 400$, $R = 3$, $\rho = 6.78$, $\lambda_{ji}(0)$'s $= \lambda_0$ with $S(\lambda_0) = 1$, $\phi(\ell) \equiv 1$, $D(\lambda)$ and $U(\lambda)$ as above. The parameters, EEG, $\bar{\bar{\Sigma}}_0$, etc., for this experiment are given in Figure 6.16. The behavior was unstable, underdamped, F(t) going to zero at $t = 41$.

The small neighborhood radius illustrates the principles of the preceding paragraphs: during the dip in F(t) from $t = 8$ to $t = 12$, the non-firing neurons of the network recover four time steps thus contributing to the swell that starts at $t = 13$. Had R been larger, more neurons could have fired for $t = 8, \ldots, 12$, possibly avoiding the build-up of fatal oscillations.

The subset Σ_0 was taken from the set of neurons $i \in \mathcal{N}$ such that $r_i \geq 16$. These neurons are randomly distributed over $\mathcal{N}$. As Figure 6.17

Figure 6.16. Basic Experiment III.

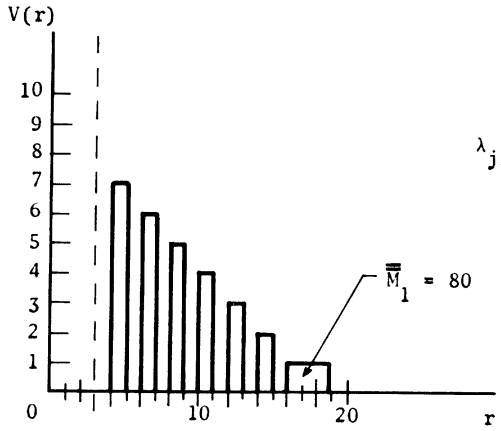

N = 400

R = 3

ρ_R = 6.78

$\lambda_{ji}(0) = \lambda_0$ so that $S(\lambda_0) = 1$ (i,j = 1, -, 400)

$U(\lambda)$ and $D(\lambda)$ as in Fig. 6.6.

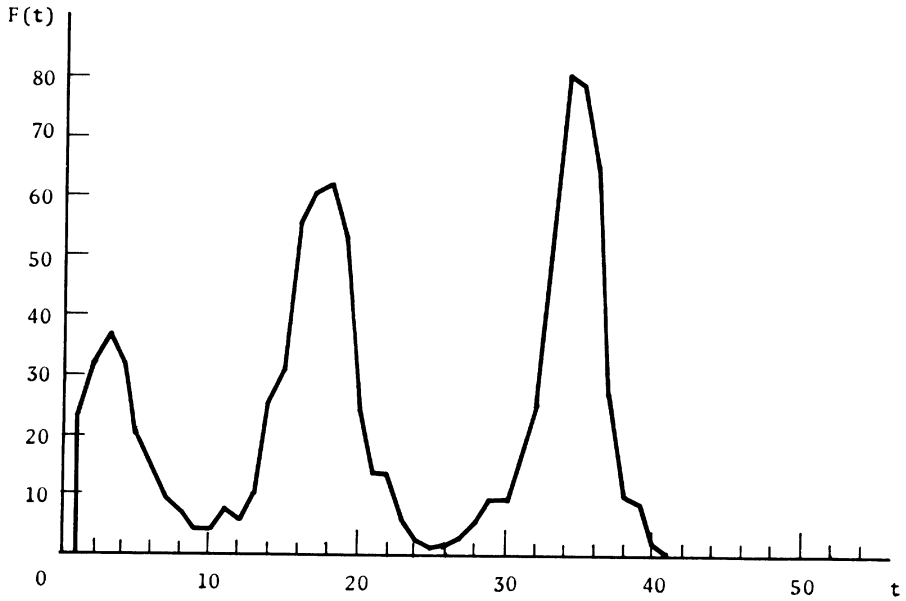

Figure 6.17. Firing Patterns for t = 1, 2, 3 of Basic Experiment III.

The same basic convention of Fig. 6.15(a) is used to interpret the computer output at time t. The main difference is that $\mathcal{N}$ is now a 20x20 grid, twenty rows of twenty neurons each, numbered as shown below:

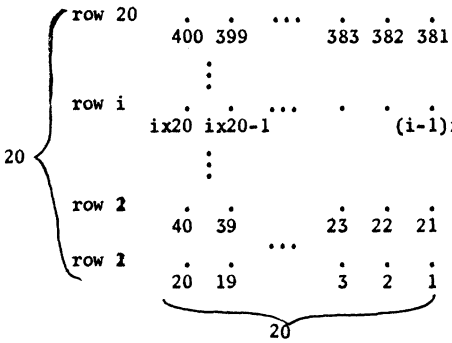

In the computer output, the neurons are again grouped by fives — if none of a group fired, the word ZERO is inserted into the position for that group. Vertical bars indicate the boundaries between rows. For example at time t = 1, rows 1 and 2 are:

row 2: 1 0 0 0 | Z E R O | 40 39 38 37 36 | 35 34 33 32 31 | 30 29 28 27 26 | 25 24 23 22 21 (right-hand four groups of line three of output)

row 1: 1 0 0 0 | Z E R O | 20 19 18 17 16 | 15 14 13 12 11 | 10 9 8 7 6 | 5 4 3 2 1 (line fine of output block)

Thus, neurons 19 and 39 (in rows 1 and 2) fired at t = 1. Notice that the neurons of Σ_0 are uniformly distributed over $\mathcal{N}$.

```
TIME      1 OUTPUT IS      23 FIRING DISPLAY
 ZERO  ZERO  ZERO  ZERO | ZERO  ZERO  ZERO  ZERO | ZERO  ZERO  1010  ZERO | ZERO   100  ZERO  ZERO | ZERO     1     1
 ZERO  ZERO  ZERO  ZERO |    1   100  ZERO  ZERO | ZERO  ZERO  ZERO  ZERO |    1  ZERO  ZERO  ZERO |  100  1000  ZERO
 ZERO   100  ZERO   100 | 1000  ZERO  ZERO 10000 | 1000  10000    1  ZERO | ZERO  ZERO  10000  ZERO | ZERO  ZERO  ZERO
 ZERO  ZERO  ZERO  ZERO |   10  ZERO    10 | 1000  ZERO     1  ZERO | ZERO  ZERO  ZERO  ZERO | 21000  ZERO  ZERO  ZERO
 1000  ZERO  ZERO  ZERO |
TIME      2 OUTPUT IS      32 FIRING DISPLAY
 ZERO  ZERO  1110  ZERO | ZERO  ZERO  ZERO  ZERO | ZERO  ZERO  ZERO     1 | ZERO  ZERO  ZERO  ZERO |  100  1000    10
11000 10000  ZERO 10000 | ZERO  ZERO  ZERO  ZERO |   10   100  ZERO  ZERO | 10000  ZERO  ZERO  1100 | ZERO    10
 ZERO  ZERO  1000  ZERO | ZERO  ZERO  ZERO    10 | ZERO  ZERO   100  ZERO |  100  ZERO     1  ZERO | 1000
  100  1000  ZERO 11000 | ZERO  ZERO  ZERO  ZERO | ZERO   100  ZERO 11000 | ZERO  ZERO  ZERO |  100  ZERO  ZERO  ZERO
 ZERO  ZERO     1  ZERO |
TIME      3 OUTPUT IS      37 FIRING DISPLAY
 ZERO  ZERO  ZERO  ZERO | ZERO  ZERO    10  ZERO | ZERO  ZERO     1  ZERO |  100     1   100  1000 | ZERO    10  ZERO
   10  ZERO  ZERO    10 | ZERO  ZERO  ZERO 10000 | ZERO   100  1000  ZERO | ZERO  ZERO 10010  ZERO | ZERO  ZERO
 ZERO  ZERO   100     1 | ZERO 10000  ZERO  ZERO |    1   100  ZERO  ZERO | 1001 10000  ZERO  ZERO |  100  ZERO   100
 ZERO 10110     1  ZERO | ZERO  ZERO  ZERO 10000 | ZERO  ZERO  ZERO   110 | ZERO     1    10  ZERO | ZERO  ZERO   100     1
 ZERO  ZERO  1010  ZERO |
```

shows, however, the small R caused the spreading excitation to cluster around Σ_0 at t = 1, 2, 3. This, of course, reinforces the arguments given above.

6.3.3 Networks with Negative Feedback, No Fatigue

In an attempt to understand better the behavior of distance-bias networks, a series of experiments was conducted for networks with various initial λ-distributions and threshold curves, ignoring the fatigue mechanism, i.e., $\phi(\ell) \equiv 0$ as in the previous experiments. These experiments, then, were intended as run-in experiments, the best of which would be isolated for further tests, using the fatigue mechanism. They allowed a precise study of (a) the effects of varying the ρ_K's, V(r), and R, (b) the synapse-level drift over the time intervals in which the experiments were run, (c) the firing histories of individual neurons, etc.

Five of these experiments are described here. As is expected, none of these experiments yielded rigid periodic behavior, the combined effects of distance-bias, negative feedback, and reasonably shallow threshold curves providing a sufficiently large number of states that the period of the networks was essentially infinite.

Experiment 1 N = 400, R = 4, $\rho = 24.4 = \sum_{K=-2}^{2} \rho_K$ where $\rho_2 = \rho_1 = \rho_{-1} = \rho_{-2} = \frac{\rho}{8}$, $\rho_0 = \frac{\rho}{2}$, V(r), U(λ), D(λ), Σ_0 as in Basic Experiment III.

This experiment was run from t = 0 through t = 276. It was "stable" in the sense that F(t) did not become zero, yet F(t) oscillated within the bounds of 1 to 50, which seems too extreme. An analysis of the synapse-levels $\lambda_{ji}(t)$'s at t = 100 revealed a net positive drift, indicating that the network was, in fact, basically underdamped — i.e., a majority of neurons were firing at rates greater than $1/\hat{r}_q$. The results

Figure 6.18. Experiment 1 (Section 6.3).

Negative feedback is present: N = 400, R = 4, $\rho = 24.4 = \rho_{-2} + \rho_{-1} + \rho_0 + \rho_1 + \rho_2$, where $\rho_s = \frac{\rho}{8}$ (s = 2, -1, 1, 2) and $\rho_0 = \frac{\rho}{2}$. V(r), Σ_0, $\phi(\ell)$, U(λ) and D(λ) as in Basic Experiment III. $\bar{C}_R = \pi R^2 = 50$.

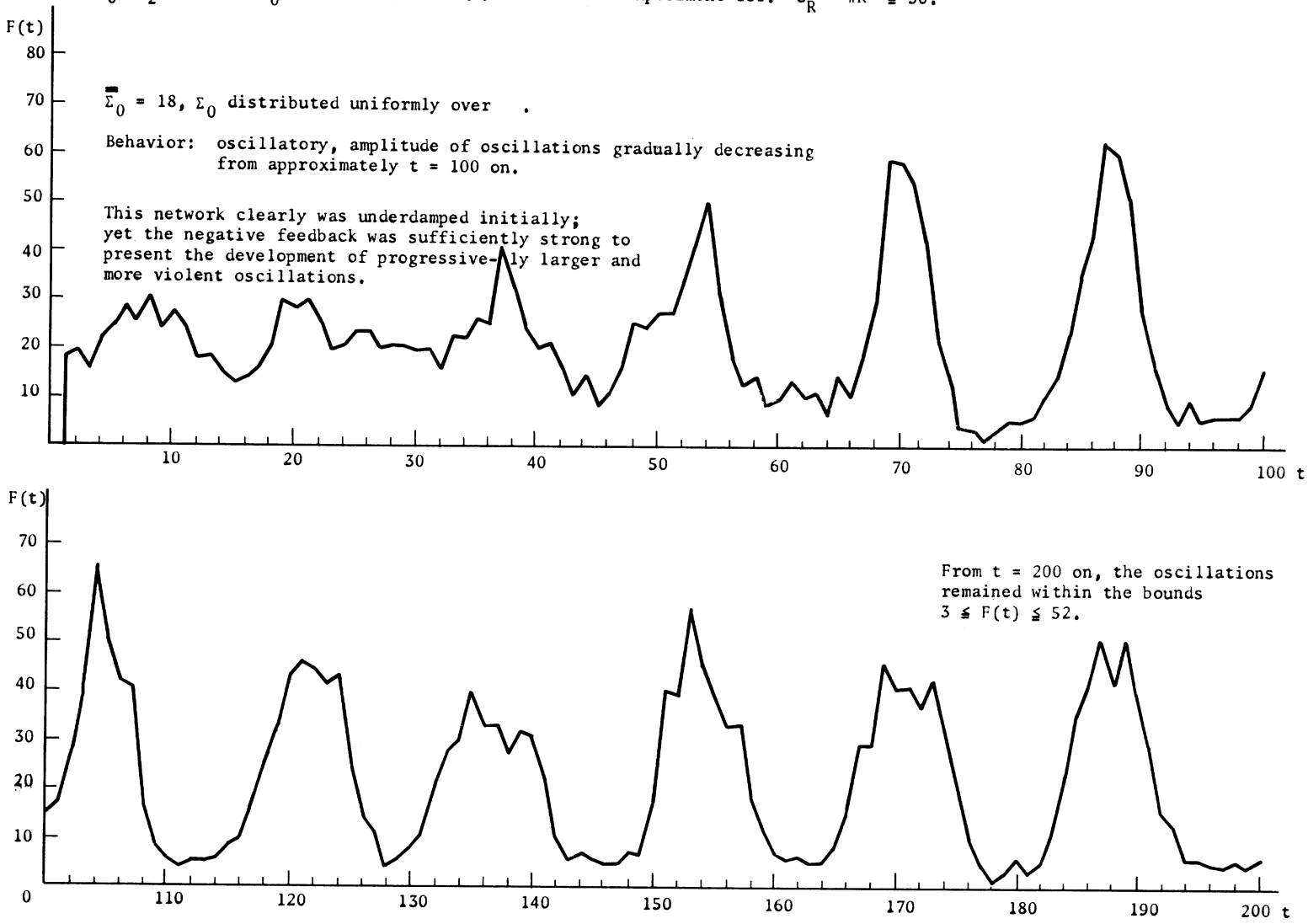

of this experiment are summarized in Figure 6.18.

While the neighborhood size might be partially a factor here, it appeared more reasonable to assume that the proportion of positive synapse-values was too great, leading to undamped behavior. Experiment 2 was devised to test this hypothesis.

Experiment 2 $N = 400$, $R = 4$, $\rho = 24.4 = \sum_{k=-2}^{2} \rho_k$ where $\rho_0 = \rho_{-1} = \rho_{-2} = \rho/4$, $\rho_1 = \rho_2 = \rho/8$, otherwise identical to Experiment 1.

This network was run from t = 0 through t = 262. The oscillations remained bounded between the limits 8 and 32 except at t = 180 when F(t) = 4. This would appear to confirm the hypothesis that more negative connections were needed, but the low value of F(t) at t = 180 suggests a slight overdamping.

The results of this experiment are summarized in Figure 6.19.

Experiment 3: $N = 400$, $R = 8$, $\rho = 25.1 = \sum_{k=-2}^{2} \rho_k$, $\rho_0 = \rho_{-1} = \rho_{-2} = \rho/4$, $\rho_1 = \rho_2 = \rho/8$; all other parameters as in Experiment 2. The results are summarized in Figure 6.20. Note that the limits on the oscillations are F(t) = 6 to F(t) = 48.

Experiment 4: Same network as in Experiment 2, but with a different curve V(r). The curve V(r) and the results are given in Figure 6.21. The bounds on F(t) were approximately 15 to 44. The behavior appeared to be somewhat underdamped.

Experiment 5: $N = 400$, $R = 6$, $\rho = 54.9 = \sum_{k=-2}^{2} \rho_k$ where $\rho_0 = \rho_{-2} = \rho_{-1} = \rho/4$, $\rho_2 = \rho_1 = \rho/8$. V(r) and all other parameters as in Experiment 4. The results are shown in Figure 6.22. The bounds on F(t) were 19 to 43. Again, F(t) appeared somewhat overdamped.

Figure 6.19. Experiment 2 (Section 6.3).

This network is identical in all respects to that of Experiment 1 (Fig. 6.18) except that the proportion of negative synapse-values has been increased: $\rho = 24.4 = \rho_{-2} + \rho_{-1} + \rho_0 + \rho_1 + \rho_2$ where $\rho_0 = \rho_{-1} = \rho_{-2} = \rho/4$, $\rho_1 = \rho_2 = \rho/8$. The run was made from t = 1 to t = 262, minimum value of F(t) was F(t) = 4 at t = 181; maximum was F(t) = 32 for several values of t. The entire EEG is shown. Notice that F(t) is better modulated in the last 70 time steps than earlier in the run. $F_{min} = 11$, $F_{max} = 30$.

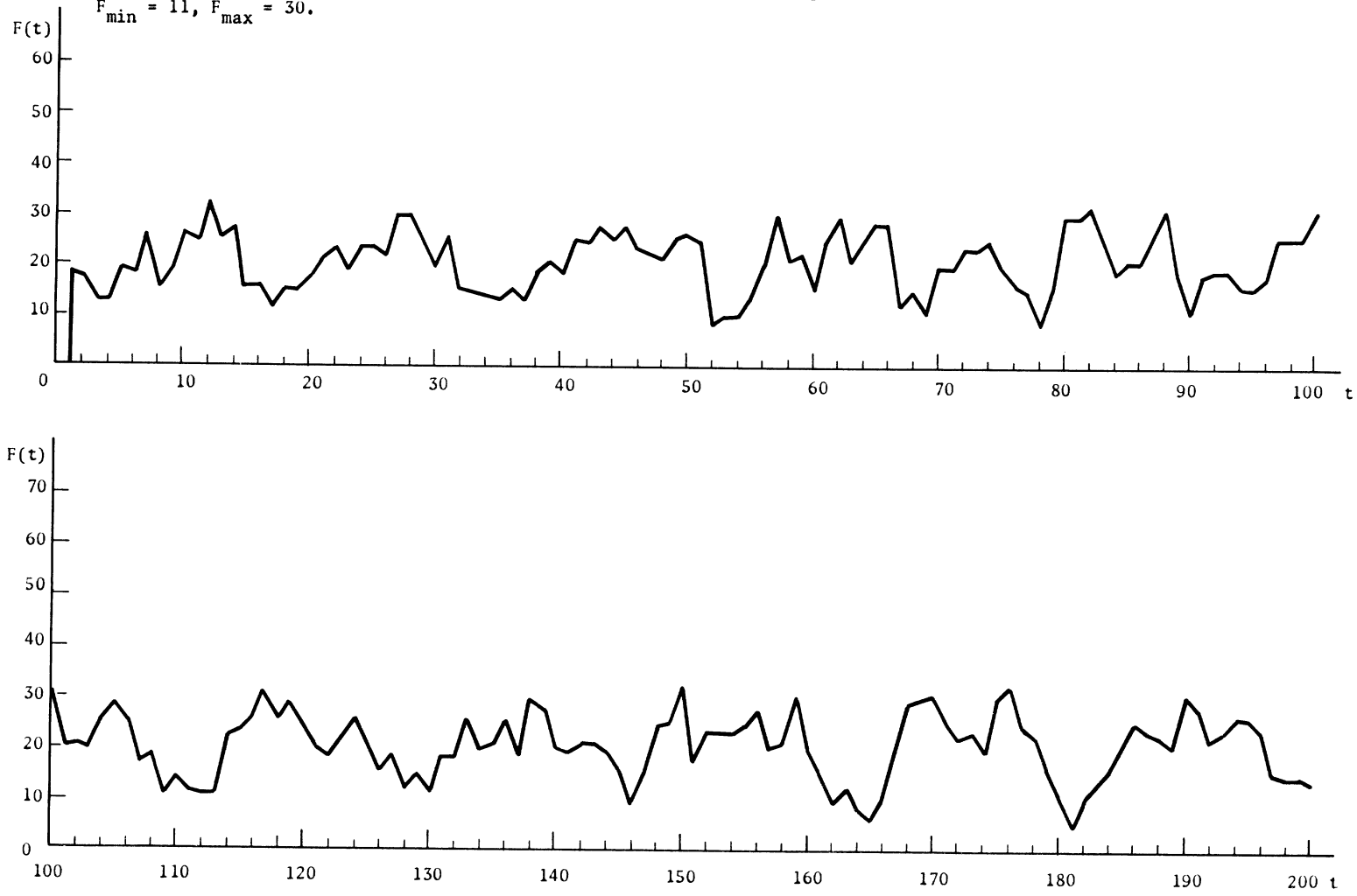

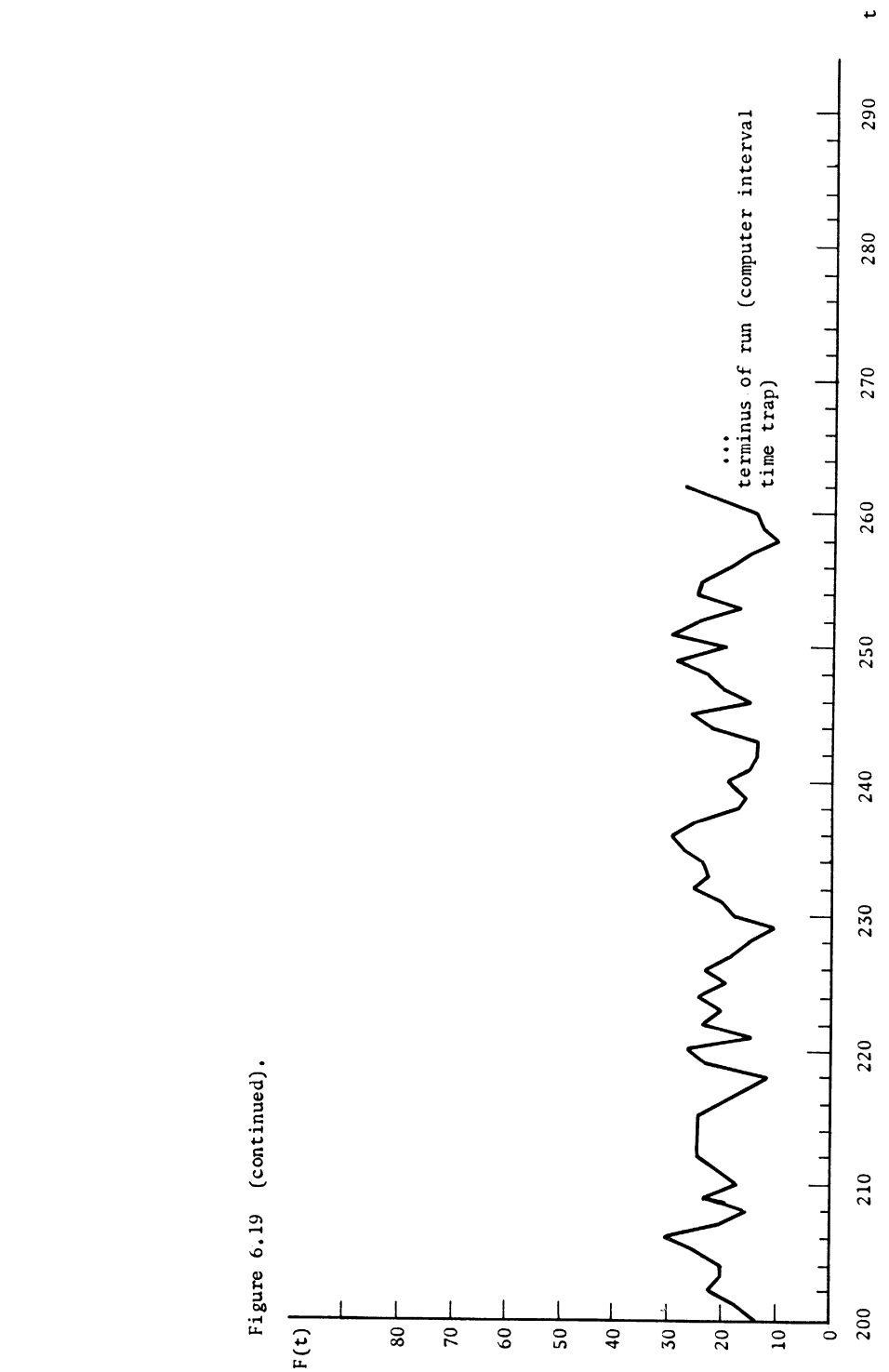

Figure 6.19 (continued).

Figure 6.20. Experiment 3 (Section 6.3)

This experiment is identical to Experiment 2 (Fig. 6.10) except that R has been doubled, R = 8 and ρ = 25.1 with ρ_s (s = -2, 1, 0, 1, 2) as in Fig. 6.19. The EEG is given only for the first and last one hundred time-steps.

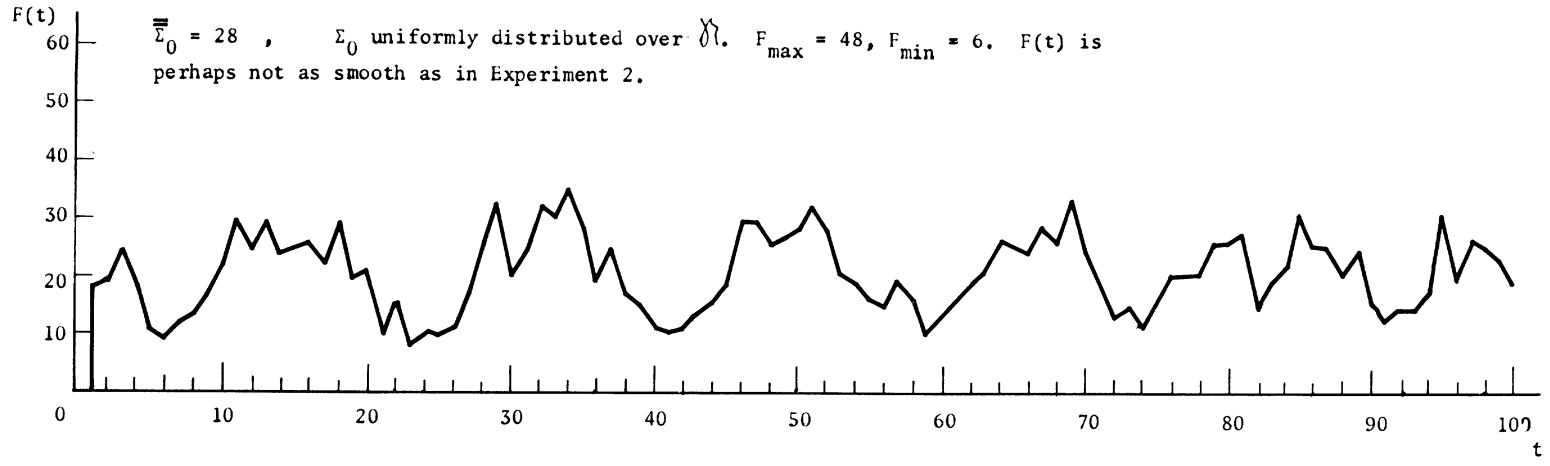

$\bar{\Sigma}_0 = 28$, Σ_0 uniformly distributed over $\mathcal{N}$. $F_{max} = 48$, $F_{min} = 6$. F(t) is perhaps not as smooth as in Experiment 2.

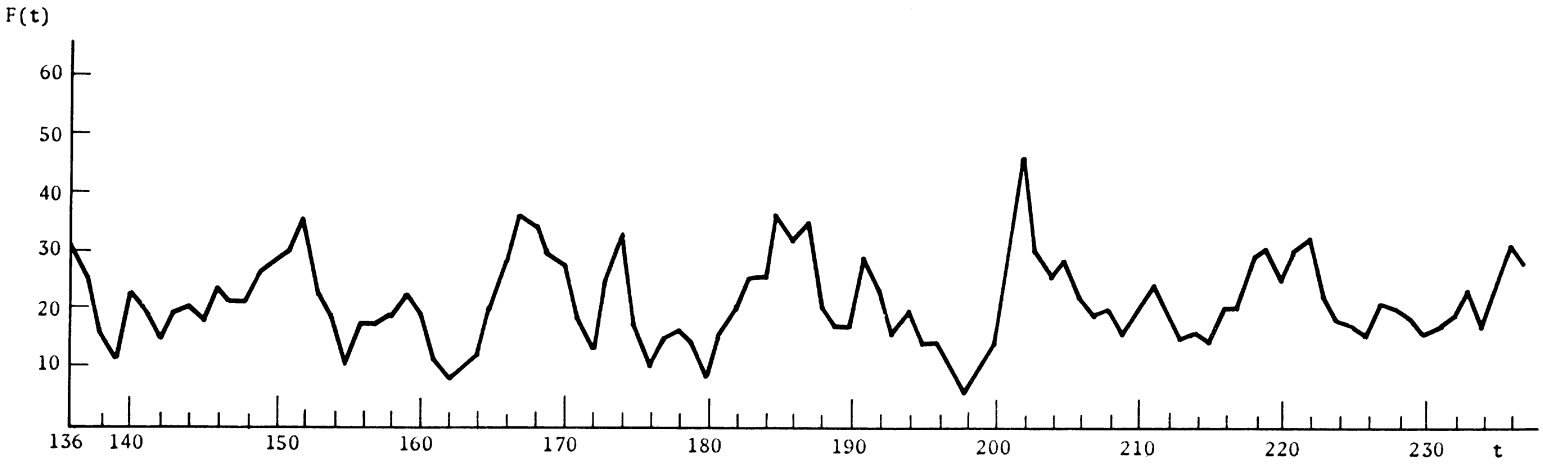

Figure 6.21. Experiment 4 (Section 6.3).

This is identically the same experiment as Experiment 2 (Fig. 6.19), except that V(r) has been replaced by the curve below. The first seventy and last one hundred time steps of the EEG are given below.

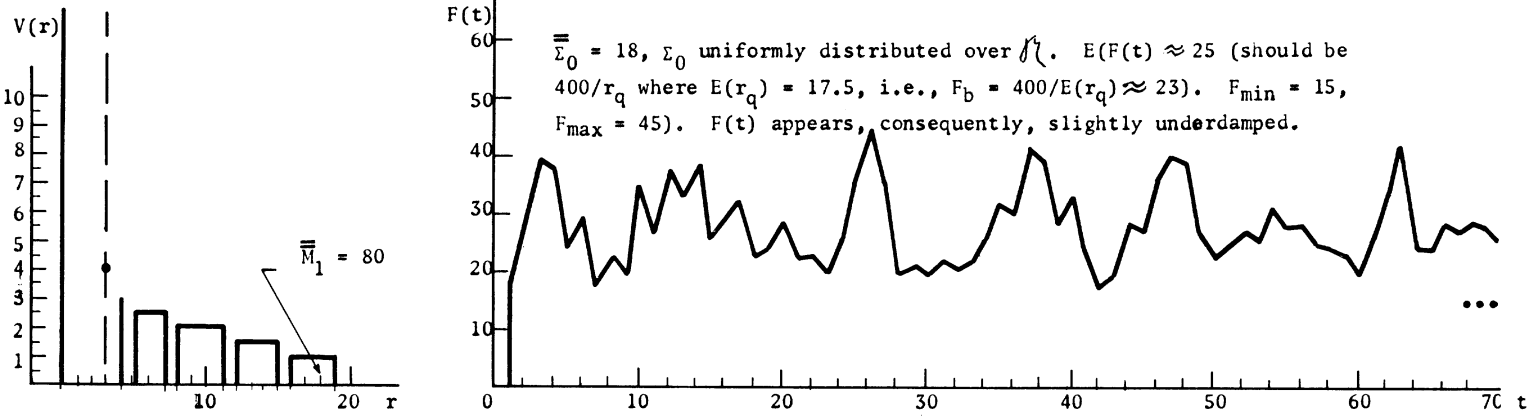

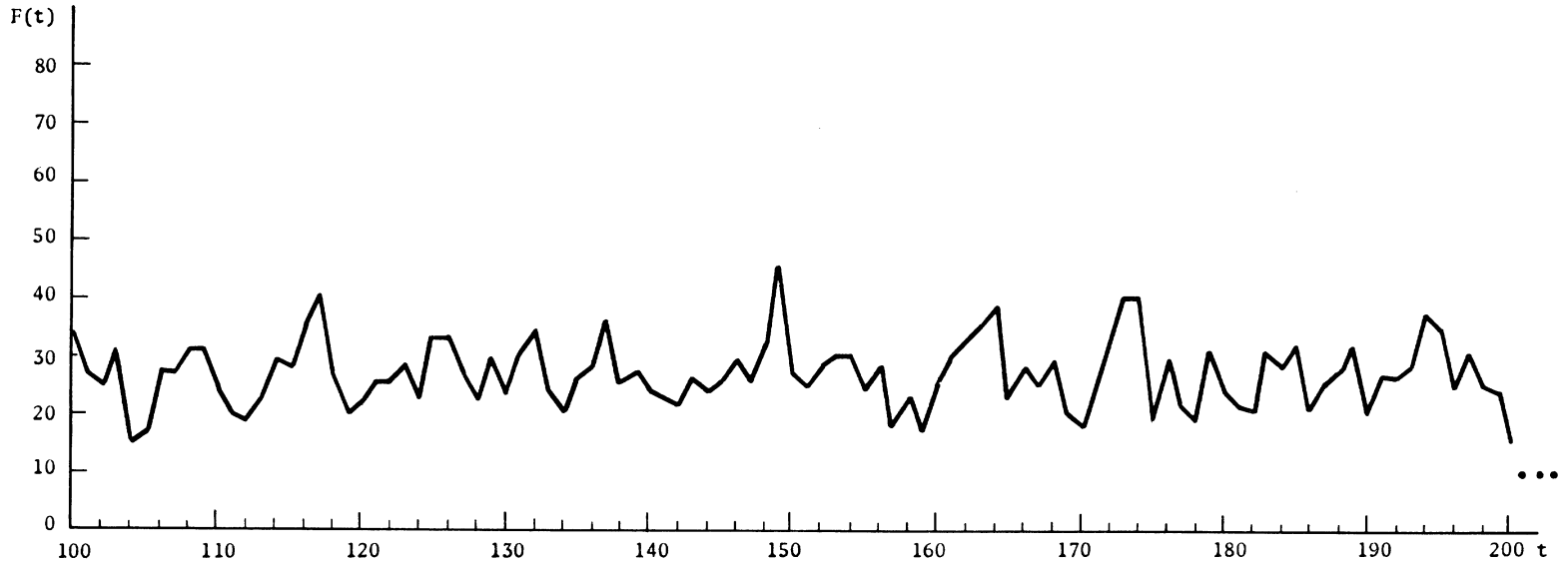

Figure 6.22. Experiment 5 (Section 6.3).

All parameters are as in Experiment 4 (Fig. 6.21) except that R has been raised from 4 to 6, $\rho = 54.9 = \rho_{-2} + \rho_{-1} + \rho_0 + \rho_1 + \rho_2$ where $\rho_0 = \rho_{-2} = \rho_{-1} = \rho/4$; $\rho_2 = \rho_1 = \rho/8$.

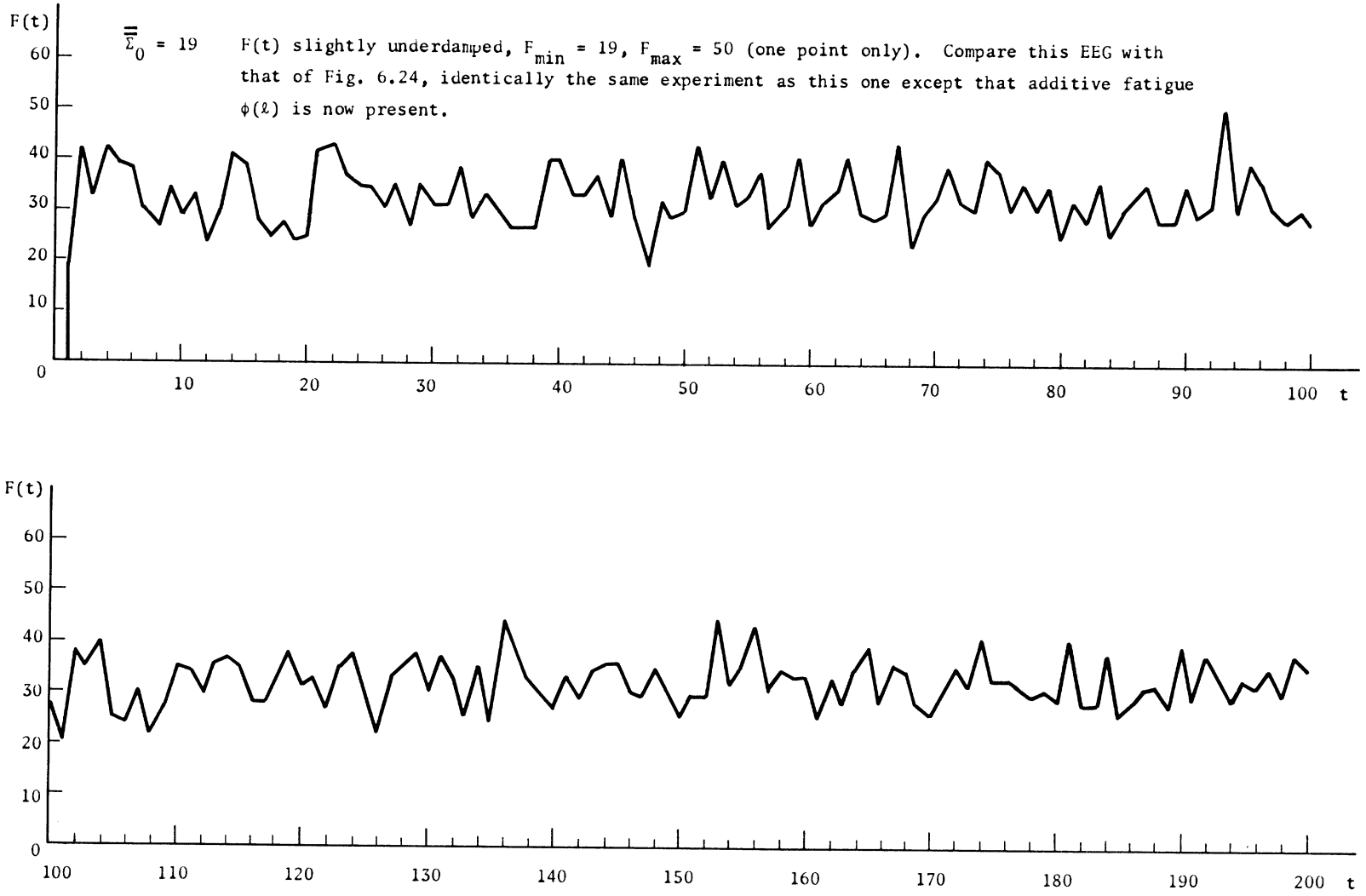

Resume of Experiments 1 - 5

By gradual "tuning" of the parameters R, ρ, ρ_k for k = -2, -1, 0, 1, 2, and V(r), assuming the fatigue mechanism to be inoperative — $\phi(\ell) \equiv 0$ — it was possible to produce nearly stable behavior. "Nearly stable" means that while F(t) lies between certain bounds, e.g., $\frac{F_b}{2} \leq F(t) \leq 2F_b$ (approximately) where $F_b \cong \frac{N}{r_q} = \frac{400}{17} = 23.5$, yet a tendency toward underdamped behavior persists. In particular, a symptom of the latter was the fact that a relatively large number of neurons of the network were firing at rates greater than the expected rate $1/\hat{r}_q$.

This suggests that it is essential to include the fatigue mechanism to obtain very stable behavior in these networks. The next section is devoted to this theme.

6.3.4 Networks with Negative Feedback, Fatigue Present

The fatigue mechanism used in the subsequent experiments differs from the one used in Chapter 3 in that $\phi(\ell)$ is, added to V(r) to determine the effective threshold. The advantage of this additive fatigue mechanism is that it does not affect the slope of V(r), whereas, of course, the multiplicative fatigue mechanism of Chapter 3 does vary the slope of the effective threshold function as $\phi(\ell)$ increases from +1. Preserving the slope of V(r) means essentially that the relationships between the sets $M_k(t)$ are preserved and the basic analysis of Chapter 4 still applies (after translation of V(r) by $\phi(\ell)$).

Four experiments (numbered in sequence with the experiments of Section 6.3.3) are described below. They form candidates for very stable and adequate networks, the last one being used as the basis for the final, long-run cell-assembly experiments of Chapter 7.

Figure 6.23. Fatigue Curve $\phi(\ell)$, Tables $\Delta_1(\ell)$, $\Delta_2(\ell)$ for Experiments 6 and 7 (Section 6.3).
The curves below were used for the experiments of Figures 6.24 and 6.25 to follow.

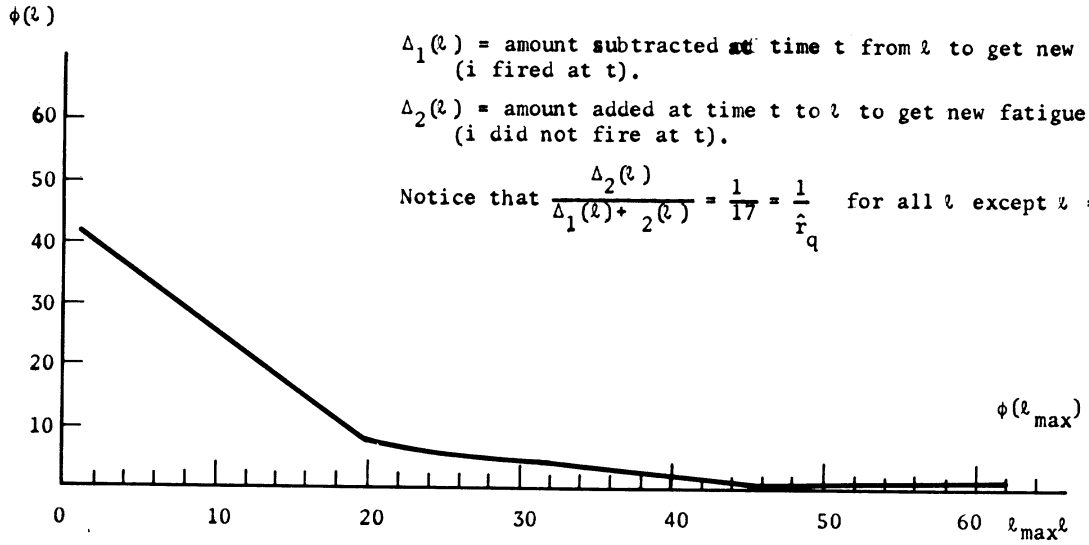

$\Delta_1(\ell)$ = amount subtracted at time t from ℓ to get new fatigue state for neuron i (i fired at t).

$\Delta_2(\ell)$ = amount added at time t to ℓ to get new fatigue state for neuron i (i did not fire at t).

Notice that $\frac{\Delta_2(\ell)}{\Delta_1(\ell) + \Delta_2(\ell)} = \frac{1}{17} = \frac{1}{\hat{r}_q}$ for all ℓ except ℓ = 0, 1, 62, and 63.

ℓ	$\Delta_1(\ell)$	$\Delta_2(\ell)$	ℓ	$\Delta_1(\ell)$	$\Delta_2(\ell)$	ℓ	$\Delta_1(\ell)$	$\Delta_2(\ell)$	ℓ	$\Delta_1(\ell)$	$\Delta_2(\ell)$
0	0	1/16	17	2	2/16	34	2	2/16	51	1	1/16
1	0	1/16	18	2	⎫	35	2	⎫	52	1	⎫
2	1	1/16	19	2	2/16	36	2	⎪	53	1	⎪
3	1	1/16	20	4	4/16	37	2	⎪	54	1	⎪
4	1	⎫	21	4	⎪	38	2	⎭	55	1	⎪
5	1	⎪	22	4	⎪	39	2	2/16	56	1	⎪
6	1	⎪	23	4	⎪	40	1	1/16	57	1	⎪
7	1	⎪	24	4	⎪	41	1	⎫	58	1	⎪
8	1	⎭	25	4	⎪	42	1	⎪	59	1	⎪
9	1	1/16	26	4	⎪	43	1	⎪	60	1	⎭
10	2	2/16	27	4	⎪	44	1	⎪	61	1	1/16
11	2	⎫	28	4	⎪	45	1	⎪	62	1	0
12	2	⎪	29	4	⎪	46	1	⎪	63	1	0
13	2	⎪	30	4	4/16	47	1	⎪			
14	2	⎪	31	4	2/16	48	1	⎪			
15	2	⎭	32	4	⎭	49	1	⎪			
16	2	2/16	33	4	2/16	50	1	1/16			

Experiment 6: $N = 400$, $R = 6$, $\rho = 54.9 = \sum_{k=-2}^{2} \rho_k$, $\rho_0 = \rho_{-1} = \rho_{-2} = \rho/4$, $\rho_1 = \rho_2 = \rho/8$. Same network and parameters as in Experiment 5. Additive fatigue function and tables of Figure 6.23.

Except for the fatigue function, this is precisely the same network as in Experiment 5. The results are summarized in Figure 6.24. Notice that F(t) is bounded, $17 \leq F(t) \leq 40$, obeying approximately the desired limits. The fatigue function definitely appears to have modulated F(t) somewhat, as is seen by comparing the EEG's of Figures 6.22 and 6.24.

Experiment 7: The exact network of Experiment 6 was used except that the synapse-values were re-scaled as follows: In all previous experiments, one unit of synapse-value was equivalent to 12 subunits. The threshold curve and the fatigue curve basically are represented in terms of these subunits. If, for example, a threshold value of 12 subunits is added to a fatigue value of 3, the effective threshold is 1.25 (= 12+3/12) synapse-values. The relationship between synapse-values and subunits was rescaled to 1:4 — one synapse-value is equivalent to four subunits. If a threshold value of 4 subunits is added to a fatigue value of 3, the effective threshold is now 1.75 (= 4+3/4) synapse-values. Given precisely the same network as in Experiment 6, this rescaling should make the effects of fatigue more pronounced, and it did, as seen in Figure 6.25. The oscillations remained, after an initial transient, in the bounds $16 \leq F(t) \leq 38$.

Experiment 8: This is a repeat of Experiment 7 with different $\Delta_1(\ell)$ and $\Delta_2(\ell)$ tables (see Figure 6.26). After an initial transient, $14 \leq F(t) \leq 49$. Some neurons, however, were firing at rates $> 1/\hat{r}_q = 1/17$. See Figure 6.27 for summary of results of this run.

Experiment 9: The exact network of Experiment 8 was used with a new threshold V(r). The new curve and results of the run are given in

Figure 6.24. Experiment 6 (Section 6.3).

This experiment is identical to Experiment 5 (Fig. 6.22) except that additive fatigue is present and $\phi(\ell)$, $\Delta_1(\ell)$, and $\Delta_2(\ell)$ are as given in Fig. 6.23.

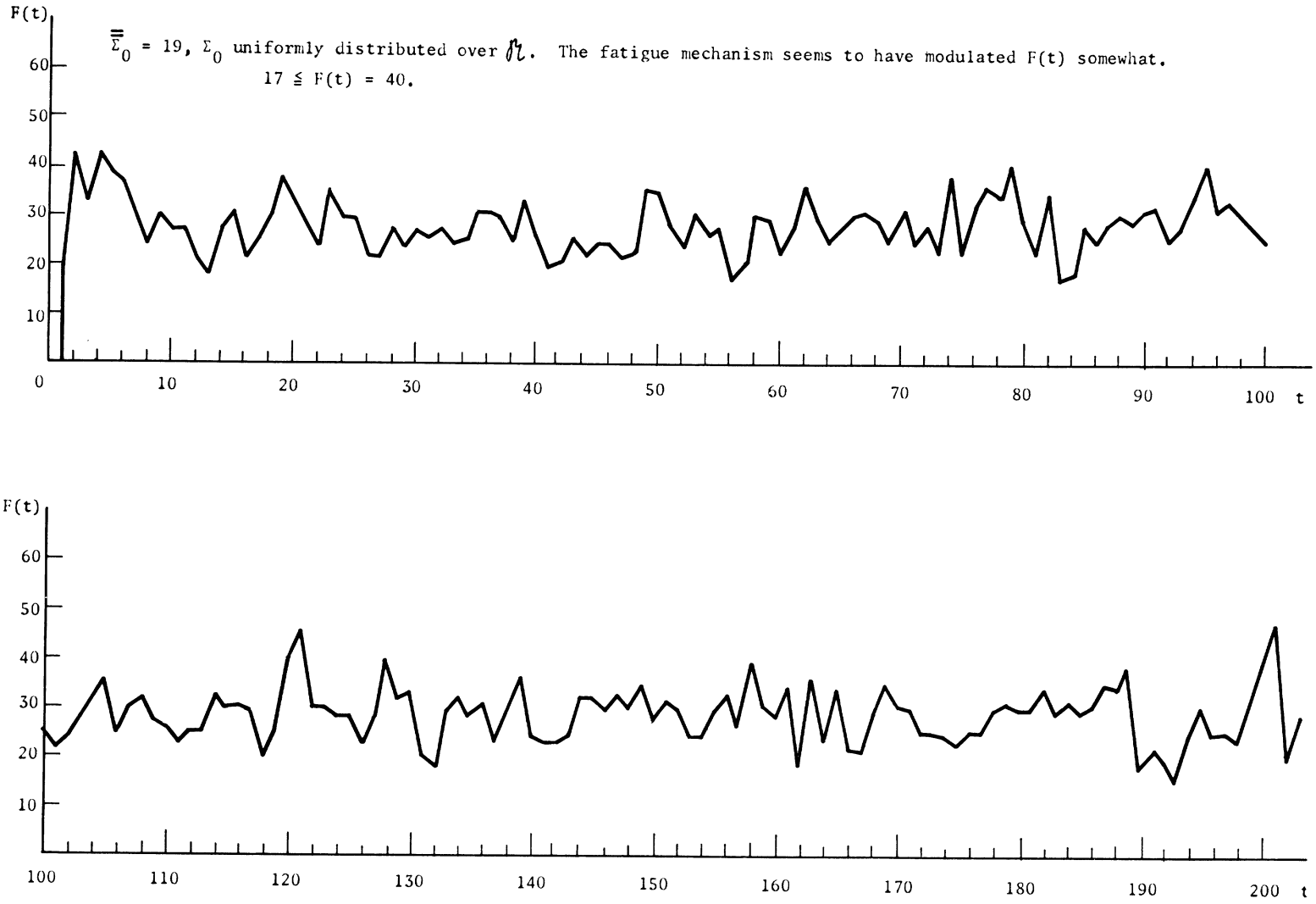

Figure 6.25. Experiment 7 (Section 6.3).

Precisely, the same network as Experiment 6 (Fig. 6.24), except that V(r) is expressed in terms of re-scaled (compressed) synapse-value subunits (see text).

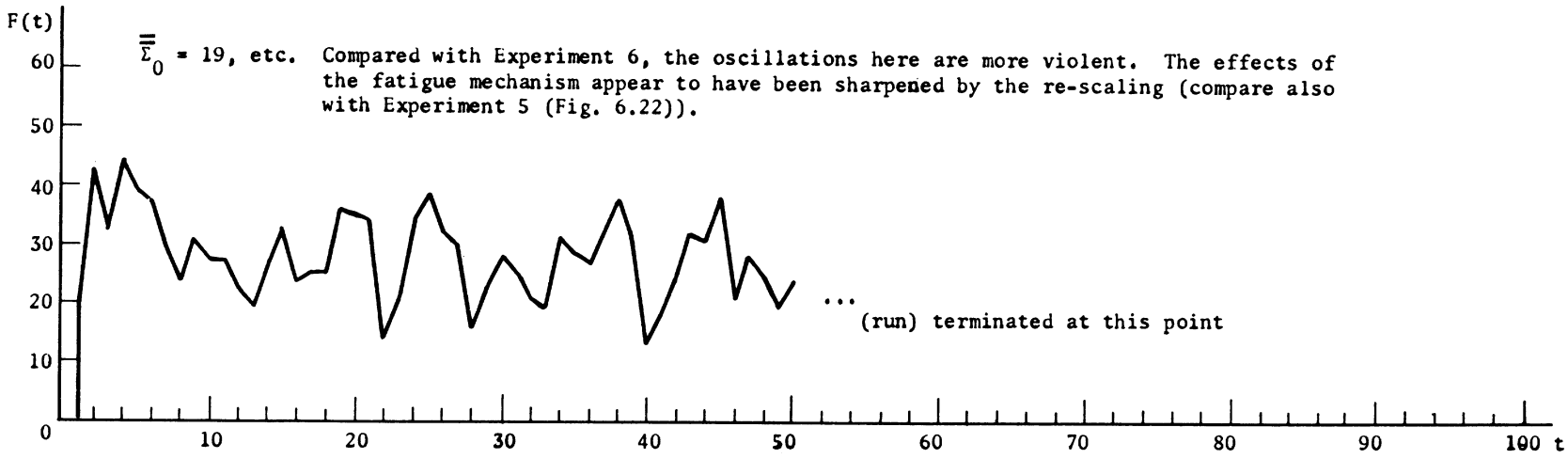

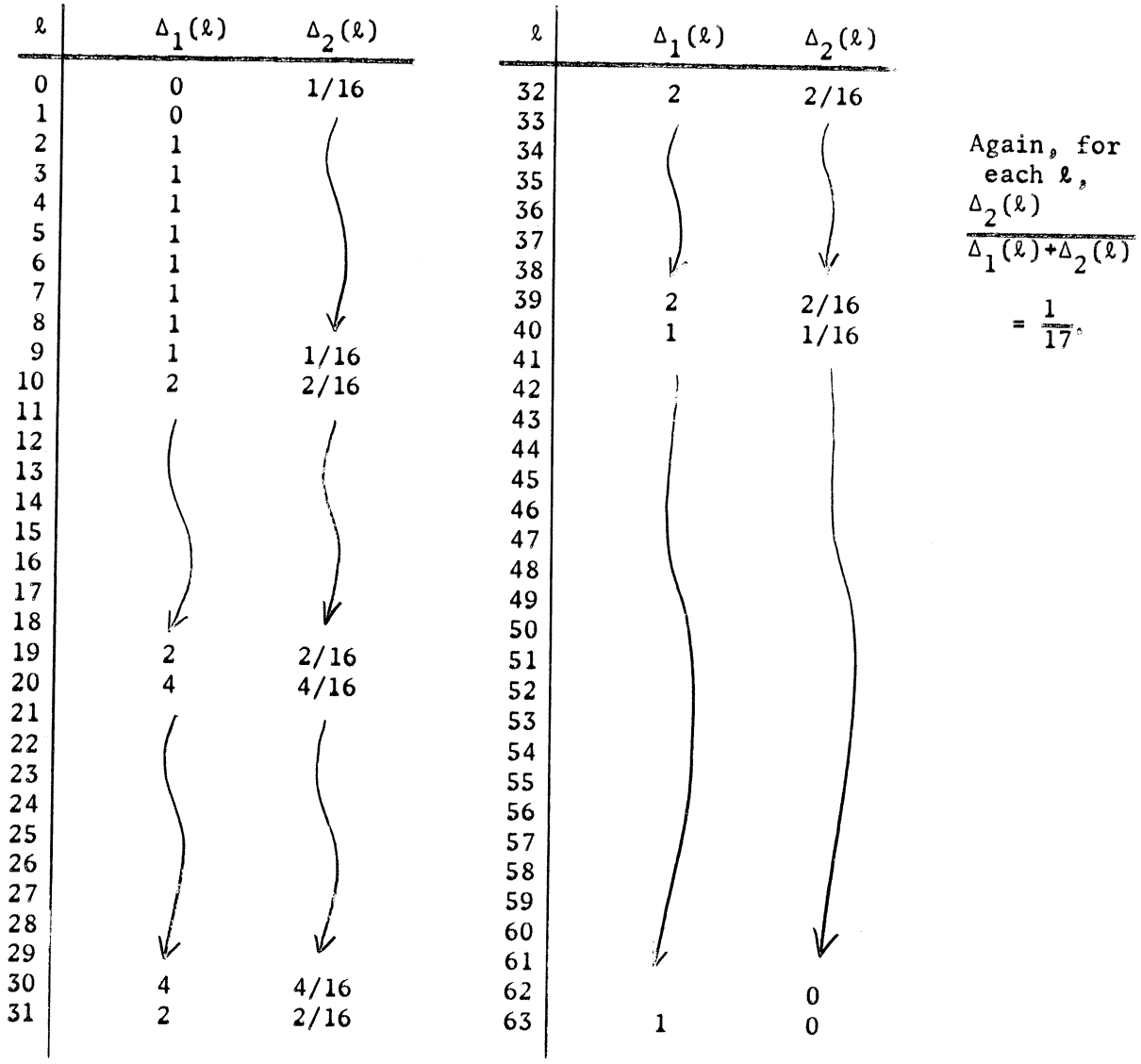

Figure 6.26. $\Delta_1(\ell)$ and $\Delta_2(\ell)$ Tables for Experiments 8 and 9 (Section 6.3).

The above $\Delta_1(\ell)$ and $\Delta_2(\ell)$ tables were used for the experiments of Figs. 6.27 and 6.28.

Figure 6.28. The experiment was run from t = 0 to t = 399; apart from an initial transient, $8 \leq F(t) \leq 36$.

Resume of Experiments 6 - 9

Introduction of the fatigue mechanism into the networks of Experiments 1-5, where for each ,

$$\frac{\Delta_1(\ell)}{\Delta_1(\ell) + \Delta_2(\ell)} = \frac{1}{\hat{r}_q} = \frac{1}{17}$$

and $\phi(\ell)$ is an additive function; did indeed appear to smooth out the behavior of the networks. Rescaling of underlying synapse-value unit sharpened the effects of the mechanism.

6.4 SUMMARY OF EXPERIMENTAL RESULTS

Stable behavior was readily produced both in networks with uniform random distributions of connections and networks with distance-bias when negative feedback was present. In the former case, however, an ad hoc design of V(r) had to be introduced to eliminate the rigidly periodic type of stable behavior frequently obtained there. If positive connections only were present, such rigidly periodic behavior, $F(t+\hat{r}_q) = F(t)$, $\Sigma_{t+\hat{r}_q} \equiv \Sigma_t$, appeared to be the order of the day.

In the distance-bias case, quasi-stable behavior was obtained, that is, behavior with underdamped tendencies, until the additive fatigue mechanism was introduced. This appeared to yield several "very stable" networks.

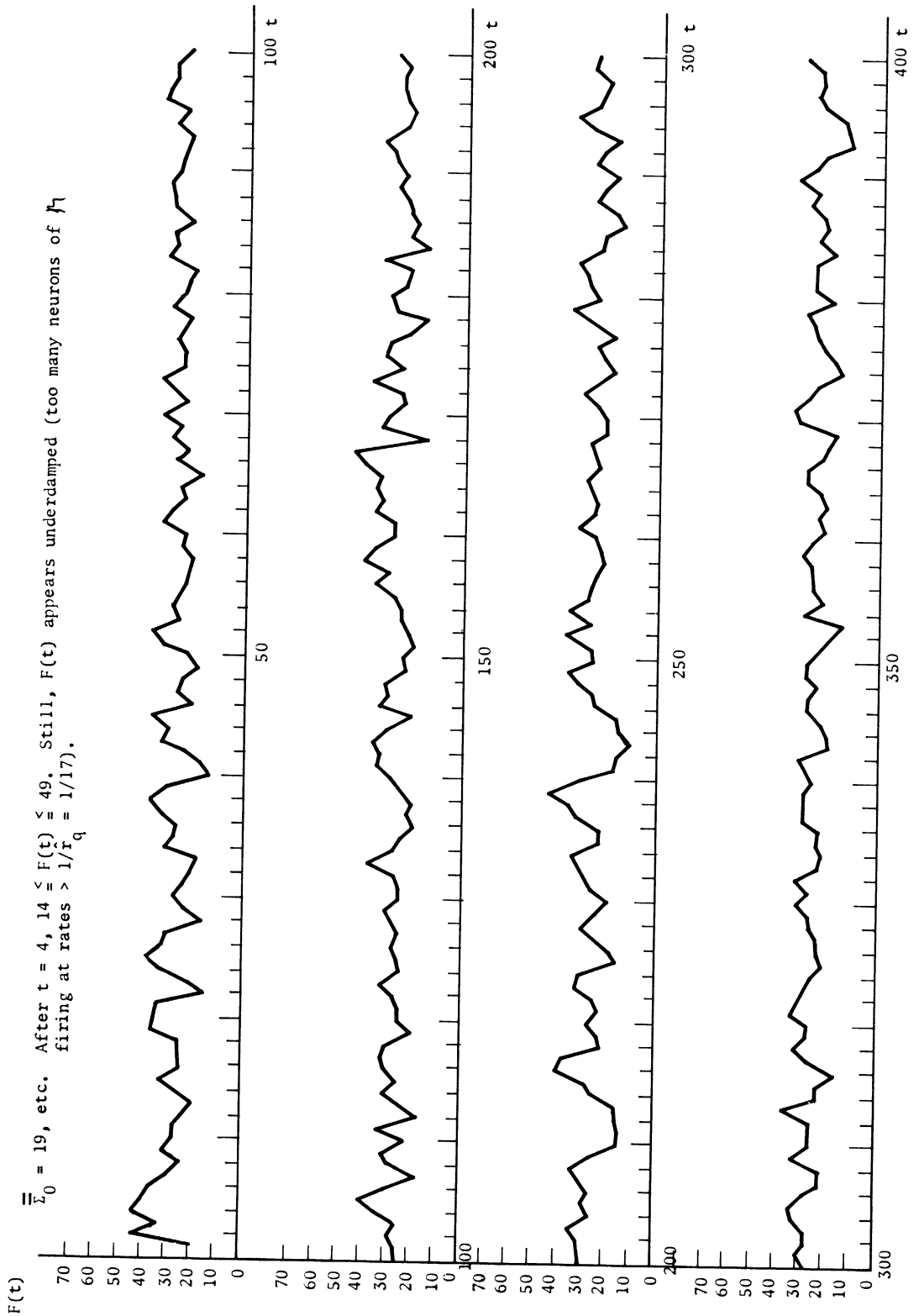

Figure 6.27. Experiment 8 (Section 6.3).

This is identically the same experiment as Experiment 7 of Fig. 6.25 with the $\Delta_1(\ell)$ and $\Delta_2(\ell)$ tables of Fig. 6.26.

$\Sigma_0 = 19$, etc. After t = 4, $14 \leq F(t) \leq 49$. Still, F(t) appears underdamped (too many neurons of $\mathcal{H}$ firing at rates $> 1/\hat{r}_q = 1/17$).

Figure 6.28. Experiment 9 (Section 6.3).

This is a repeat of Experiment 8 (Fig. 6.27) with the V(r) curve given below.
Experiment 9 forms the basis for the Cell-Assembly experiments of Chapter 7, Section 7.5.

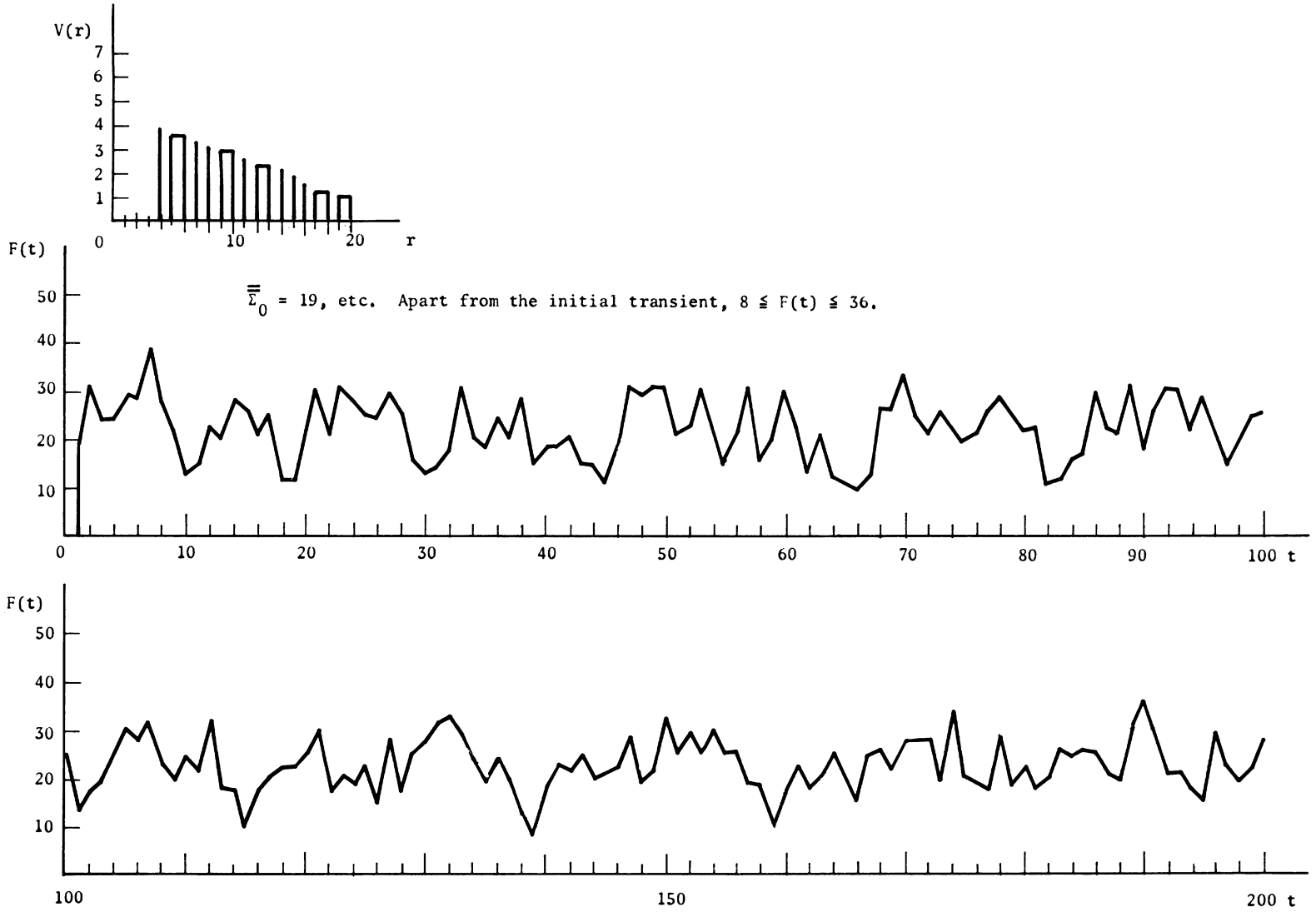

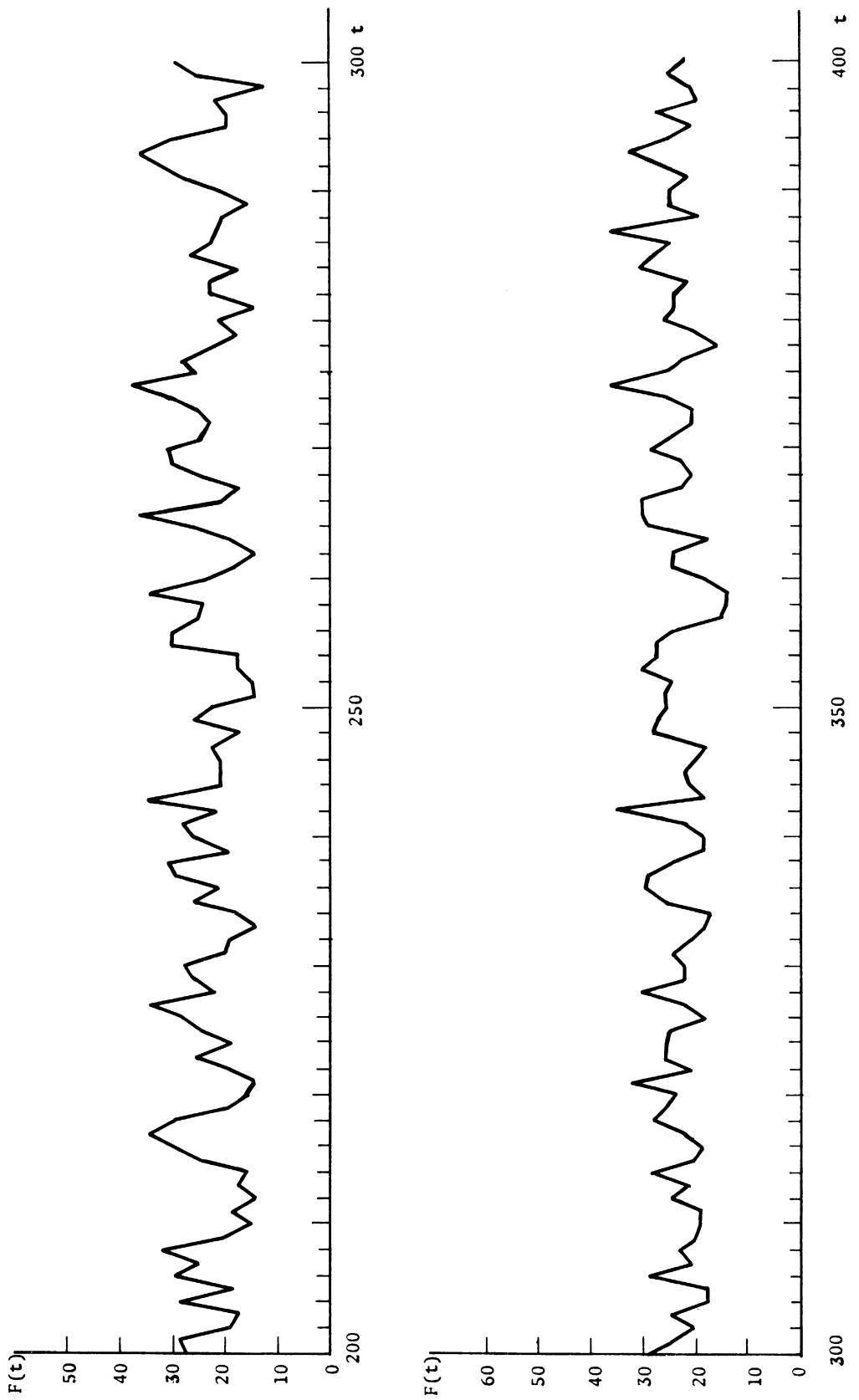

Figure 6.28 (continued).

7. NETWORKS UNDER PERIODIC STIMULI

7.1 INTRODUCTION AND SURVEY OF RESULTS

The substance of this chapter is to verify claims (2) and (3) of Chapter 5, Section 5.1. In summary form, these are

(2) It is possible to produce in some networks with cycles closed cycles (cell-assemblies) $C(\Sigma_0)$ as a result of periodic stimulation of an input set Σ_0 within an "on-off" stimulus envelope.

(3) It is possible to produce in some networks with cycles, mutually inhibiting self re-exciting cycles $C(\Sigma_0)$ and $C(\Sigma_0^*)$ as a consequence of applying periodic stimuli to Σ_0 and Σ_0^*, the stimulus to the one alternating with the stimulus to the other in "on-off" envelopes (stimulus to Σ_0 "on" over an interval I_0, stimulus to Σ_0^* off, $t \in I_0$; conversely, stimulus to Σ_0 "off" over I_0^*, stimulus to Σ_0^* "on" $t \in I_0^*$).

The development of the material of this chapter parallels that of Chapter 4, Sections 4.4 and 4.5. First the two basic classes of networks, those with uniform random distributions of connections and those with distance-bias, are considered under the effects of single periodic stimuli (claim (2)). Secondly, a specific distance-bias network in which a cycle $C(\Sigma_0)$ has already been formed is considered under the effects of alternating perodic stimuli.

In general, networks (with or without distance-bias) with negative feedback only are considered. In the first case above, however, several networks with uniform random distributions of connections and positive connections only are considered under periodic stimulation. This is done merely to complete the argument of the preceding chapter, Section 6.2.3, on periodicity. There the claim was made that periodicity implied lack

of information, specifically, the lack of a reservoir of recruitable neurons. It will be seen that this is, in fact, the case. Hence, the greater is the necessity for introducing mechanisms such as negative feedback and distance-bias in order to increase the amount of information present in the networks at hand.

Even with the negative feedback mechanism present, the results using networks with uniform random distributions of connections were disappointing. Therefore, these networks were abandoned for the more complex distance-bias networks, for which some very stable examples had been obtained (Chapter 6, Section 6.3.4, Experiments 6-9). Just as these had been readily obtained, once distance-bias was introduced, so were "adequate" networks (allowing path and cycle-formation) equally readily produced when distance-bias was present.

Next (Section 7.5), an "adequate" network was subjected to long-term training. Unfortunately, this uncovered an imbalance in the fatigue mechanism. The latter necessitated a series of control runs to isolate the exact nature of the imbalance. This being done, the experiment was continued using alternating periodic stimuli. The latter was prematurely terminated because of lack of funds and time — not, however, until a partial second cycle $C(\Sigma_0^*)$ and the development of cross-inhibition were observed.

Once again, lack of time and money forbad continuation of the training period to the point that self-reexcitation could be positively demonstrated. With the knowledge gained from these experiments, however, and by taking advantage of the larger computers emerging today, this most likely can be done using larger, richer, and more complex networks without undue difficulty.

7.2 EXPERIMENTAL OBJECTIVES AND PROCEDURES

7.2.1 Objectives

Claims (2) and (3) of Section 7.1 imply several subgoals. (1) The network must remain stable under stimulation ("adequacy") — i.e., F(t) must not become zero and it must not oscillate violently (epilepsy). Once stability is obtained, this implies that the formation of one cycle $C(\Sigma_0)$ must not "rob" the network of so many neurons that $C(\Sigma_0^*)$ can never be formed, etc.

(2) All the characteristics of cell-assemblies enumerated in Chapter 4, Sections 4.4 and 4.5, must be exhibited. In brief, these are;

(a) the presence of strong positive connections in the cycle $C(\Sigma_0)$ from the successor-set $\Sigma_{\tau-1}$ to Σ_τ ($\tau = 0, 1, \ldots, \tau_0 \equiv 0$).

(b) the similar condition for the alternating cycles $C(\Sigma_0)$ and $C(\Sigma_0^*)$, including the presence of cross inhibitory connections between subsets of each cycle.

(c) the "learning" or response to the particular stimulus at $\Sigma_0(\Sigma_0$ and $\Sigma_0^*)$, leading to input-independent self-reexcitation for an interval of time (alternation of activity, input-independent for a brief period of time).

(d) path and cycle formation are assisted by the recruitment of available neurons.

(e) cycle formation may be followed by fractionation, i.e., the dropping out of the cycle of relatively inactive (or ineffectual) neurons. This is especially important since it returns certain neurons to the reservoir of recruitable neurons.

Figure 7.1. (a) Typical stimulus envelope for single periodic stimulus experiments.

(b) Firing patterns for six consecutive time steps for Experiment 9. (Section 6.3) of Figure 6.28.

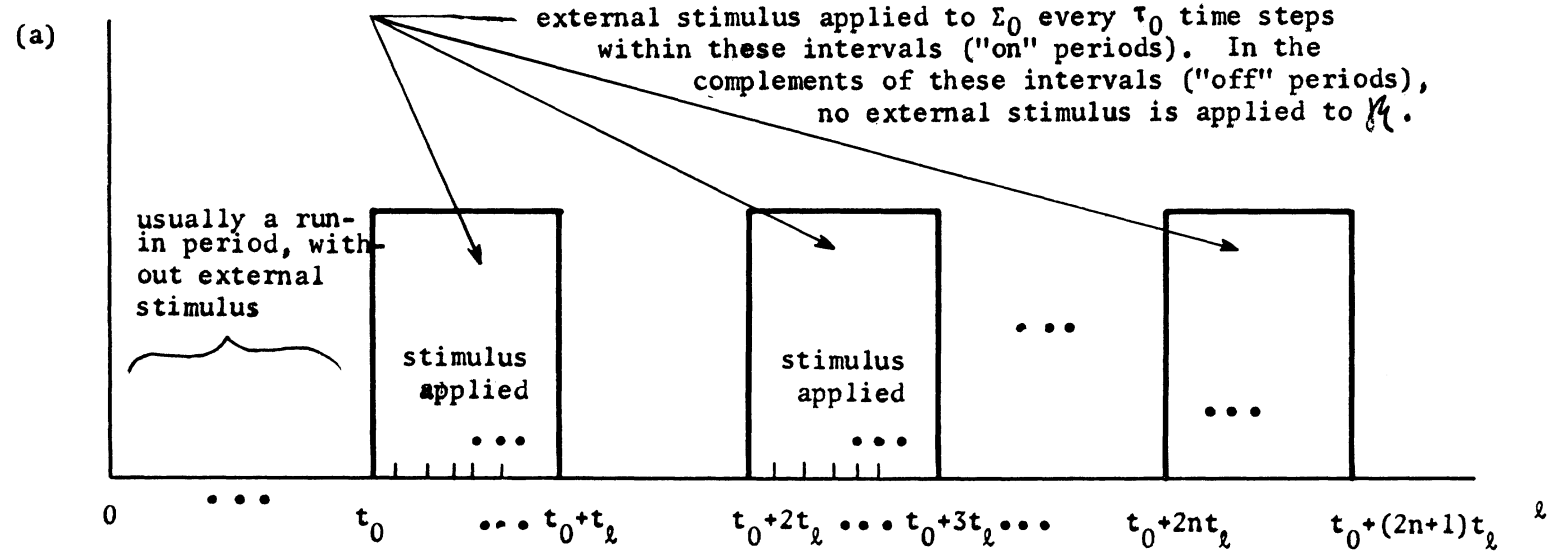

Note: The symbol Σ_0 has been used both to indicate the set that is used to "start" or "prime" a network $\mathcal{N}$ to run at $t = 0$, no other external stimulus being applied (as in Chapter 6) and the subset of $\mathcal{N}$ that is subjected to periodic external stimulus (as in Chapter 4, Section 4.4 and the current chapter). No confusion should arise out of this, since in Chapter 7, Σ_0 will always refer exclusively to the input subset (receiving the external stimulus every τ_0 times in the "on" periods) of $\mathcal{N}$.

Figure 7.1 (continued)

(b) For an interpretation of these firing patterns, see Chapter 6, Figs. 6.15(a) and 6.17.

```
TIME    367 OUTPUT IS      23 FIRING DISPLAY
 ZERO  ZERO  ZERO  ZERO 10000  ZERO  ZERO  ZERO    1  ZERO  ZERO  ZERO  1001     1  ZERO  1000  1000  ZERO  ZERO
 ZERO  ZERO  ZERO 10000  ZERO  ZERO 10000  ZERO  ZERO  ZERO  ZERO 10000  ZERO    10   100  ZERO  1000  ZERO  1000
  100  ZERO  ZERO 10000  ZERO  ZERO  ZERO  ZERO  ZERO  ZERO  ZERO  ZERO  ZERO  ZERO  ZERO  ZERO  ZERO  ZERO
 ZERO     1  ZERO  ZERO  ZERO  1000  ZERO  1000  ZERO  ZERO  ZERO  ZERO   100  ZERO  ZERO  ZERO  ZERO  ZERO  1000
 ZERO  ZERO     1     1
TIME    368 OUTPUT IS      21 FIRING DISPLAY
 10000  ZERO  ZERO  ZERO  1000  ZERO  ZERO  ZERO  ZERO  ZERO  ZERO  ZERO  ZERO  ZERO  ZERO  ZERO 10000  ZERO 11000
 10000  ZERO  ZERO  ZERO  1010  ZERO  ZERO  ZERO 10000  ZERO  ZERO  ZERO 10000  ZERO  ZERO  ZERO  ZERO    10  ZERO
 ZERO  ZERO 10000  ZERO  ZERO  ZERO  ZERO  ZERO  ZERO  ZERO  ZERO  ZERO  ZERO 10000  ZERO  ZERO  ZERO  ZERO  ZERO
    11  ZERO  1100  ZERO  ZERO  ZERO  ZERO   100  ZERO  ZERO  ZERO  ZERO  1001  ZERO  ZERO   100  ZERO  ZERO  ZERO
 ZERO  ZERO  ZERO  ZERO
TIME    369 OUTPUT IS      23 FIRING DISPLAY
 1000  ZERO  ZERO  ZERO  ZERO  ZERO  ZERO 10000  ZERO  ZERO 10000  ZERO  ZERO  ZERO  1000 10010  ZERO  ZERO  ZERO
 ZERO  ZERO  ZERO  ZERO  ZERO  ZERO  1000  ZERO  ZERO   101  ZERO  ZERO  ZERO  ZERO  ZERO  ZERO  ZERO    11
 ZERO  ZERO  ZERO  ZERO  ZERO  1000  ZERO  ZERO  ZERO  ZERO 10000  ZERO  ZERO  ZERO  ZERO 10001  ZERO  ZERO  ZERO
 ZERO  ZERO    10  1000  ZERO 10000  ZERO  ZERO    10     1  ZERO  ZERO  ZERO     1 10000  ZERO  ZERO  ZERO   100
 ZERO  ZERO  ZERO  ZERO
TIME    370 OUTPUT IS      28 FIRING DISPLAY
  100 10010  ZERO  ZERO  ZERO 10000  1000    10  ZERO  ZERO     1  ZERO  ZERO  1000     1  ZERO  ZERO     1  ZERO
 ZERO 10000  ZERO     1  ZERO  ZERO  ZERO  ZERO  ZERO    10  ZERO  ZERO  ZERO    10  ZERO    10 10000  ZERO
 ZERO   100  ZERO    10  ZERO 10001  ZERO  ZERO  ZERO  ZERO  ZERO  ZERO  ZERO  ZERO  ZERO  1000  ZERO  ZERO
 ZERO  ZERO  ZERO    11  ZERO  ZERO  ZERO  ZERO  ZERO  ZERO  1100    10  ZERO  ZERO  ZERO    10 10000  ZERO  ZERO
 ZERO  ZERO  ZERO  ZERO
TIME    371 OUTPUT IS      24 FIRING DISPLAY
 ZERO  ZERO   100  ZERO   100  ZERO    10  ZERO    10   100  ZERO 10000    10  ZERO  ZERO  ZERO  ZERO  ZERO  ZERO
 ZERO  ZERO     1  ZERO  ZERO 10000  ZERO  ZERO    10  ZERO  ZERO 10011  1000  1000  ZERO  ZERO  ZERO  ZERO  ZERO
 ZERO  ZERO    10  ZERO    10  ZERO  ZERO  ZERO  ZERO  ZERO  1000    11  ZERO  ZERO    10  ZERO  ZERO  ZERO  ZERO
 ZERO 10000  ZERO  ZERO  ZERO  ZERO  ZERO  ZERO  ZERO  ZERO  ZERO  ZERO 10000  ZERO  ZERO  ZERO  ZERO 10000  ZERO
 ZERO  ZERO  ZERO  ZERO
TIME    372 OUTPUT IS      21 FIRING DISPLAY
    10  ZERO  ZERO  ZERO  ZERO  ZERO  ZERO  ZERO  ZERO  ZERO  ZERO     1  1000  ZERO    10  ZERO  ZERO  1000    10
    10  ZERO  ZERO   100  ZERO  ZERO  ZERO  ZERO  ZERO  ZERO  ZERO  ZERO   100  ZERO 10000  ZERO  ZERO  ZERO  ZERO
  1000  ZERO  ZERO     1  ZERO  ZERO  ZERO  ZERO  ZERO  ZERO  ZERO  ZERO    10  ZERO 10000  ZERO  ZERO  ZERO  ZERO
 ZERO  ZERO  ZERO 10000  ZERO  ZERO  ZERO  ZERO  ZERO  ZERO     1   100    10  ZERO  ZERO  ZERO  ZERO  ZERO    10
 ZERO  ZERO    10  1000
```

7.2.2 Experimental Procedure

The experimental procedure of this chapter begins with successful completion of Phase III (Chapter 6) for a particular network. There are four over-all phases to this procedure:

Phase IV Single Periodic Stimulus — Path Formation Tests

Given a network $\mathcal{N}$ that has passed Phase III of Chapter 6, first a selection of the following is made:

1. The input set $\Sigma_0 \subset \mathcal{N}$;
2. The stimulus period τ_0 ; $r_a < \tau_0 < r_q$.
3. The external stimulus value S_0 (added to the incoming stimulus for each neuron of Σ_0, see Chapter 4, Section 4.4.1);
4. The length of the "on" and "off" intervals, t_ℓ.

Next, the network is subjected to the stimulus for a number t_0 of time steps — See Figure 7.1(a). Typically t_0 ranged from 200 to several thousand time steps. At each time step, the firing pattern of the network was obtained. The firing pattern at time t shows precisely, in coded form, which neurons of $\mathcal{N}$ fired at time t, forming thus a display of $\mathcal{N}$'s activity at each time step. The firing patterns for Experiment 9, Chapter 6, Section 6.3 for a few consecutive time steps are shown in Figure 7.1(b).

From a close study of the firing patterns within the "on" interval of stimulation, it can be determined whether or not overlapping paths $P(\Sigma_0 \rightarrow \Sigma_\tau)$, $\tau < \tau_0$ are being formed. This is accomplished by scanning for overlaps of the subsets Σ_τ and $\Sigma_{\tau+\tau_0}$ for successive values of τ throughout the "on" interval.[1] One would not expect to find paths

[1] Recalling the notation of 4.4.2, the set Σ'_τ firing τ time steps after stimulation, may be decomposed into a steady-state component Σ''_τ and a component Σ_τ arising directly from stimulation: $\Sigma'_\tau = \Sigma_\tau \cup \Sigma''_\tau$, this decomposition holding true only for a few time steps after stimulation. It is the latter component that is meant here.

$P(\Sigma_0 \rightarrow \Sigma_\tau)$ closing back on themselves after a relatively short training period, although this might occur.

If overlapping paths $P(\Sigma_0 \rightarrow \Sigma_\tau)$, $\tau < \tau_0$, are detected, the network is cleared for Phase V. If overlapping paths are not detected, then two possibilities arise: (a) Further analysis indicates that the network is not adequate: such paths will never form. (b) Analysis suggests that a variation of one or several of the parameters Σ_0, τ_0, S_0 or t_ℓ might produce overlapping paths.

In case (a), the network is abandoned, and return is made to Phases I - III in an attempt to produce an adequate network. In case (b), the appropriate changes are made and the whole experiment is repeated.

Phase V Single Periodic Stimulus — Cycles Formation Tests

Given a network $\mathcal{N}$ that has passed Phase IV, i.e., exhibits overlapping paths, the experiment is continued for a large number of time steps ($\geq$ 1000). Periodically the firing patterns are examined for closure of the paths $P(\Sigma_0 \rightarrow \Sigma_\tau)$ into a cycle $C(\Sigma_0)$. If closure occurred, the network is passed on the Phases VI and, possibly, VII. If closure did not occur, again several possibilities arise: (a) Analysis suggests that closure may never occur. (b) Analysis suggests that closure may occur by variation of one of the parameters 1-4 of Phase IV. In case (a), the network is abandoned. In (b), Phase IV is repeated using the modified parameter values, etc.

Phase VI Control Experiments

This is really an intermediate phase that may be performed during or after Phases IV and V. The object is to determine whether or not prolonged stimulation of the network produced anomalies that would destroy the basic stability of the network. For example — extreme to be sure,

but nontheless possible — cycle formation might recruit all neurons of $\mathcal{N}$: Once the stimulus were turned off, F(t) would tend to zero since the fund of steady-state neurons would be exhausted and the fatigue mechanism would damp out circulating pulses in $C(\Sigma_0)$. Another type of anomaly that actually occurred, resulting in a prolonged series of control experiments, will be discussed in Section 7.5.3 below.

The basic procedure in the control experiments was to turn off stimulation at a certain point and allow the network to operate without inputs for an interval of time (100 to several thousand time steps). If it did not return to stable, steady state behavior, an analysis was undertaken to determine the cause. The one example in which this occurred involved modification of the fatigue mechanism, $\phi(\ell)$, $\Delta_1(\ell)$, and $\Delta_2(\ell)$ (Section 7.5.3).

Phase VII Alternating Periodic Stimuli — Alternating Cycles Test

Once a network $\mathcal{N}$ displayed a single cycle $C(\Sigma_0)$, another input subset Σ_0^*, stimulus period τ_0^*, stimulus S_0^* and intervals t_ℓ, t_ℓ^* were selected. Stimulation proceded as indicated in Figure 7.2. Tests for overlapping paths, then overlapping cycles were conduced. Appropriate control experiments were performed.

As mentioned earlier, this work was terminated before a cycle $C(\Sigma_0^*)$ had definitely been formed. However, excellent overlapping paths were obtained with the desired relationships between subsets of $C(\Sigma_0)$ and those of the evolving $C(\Sigma_0^*)$.

7.2.3 Hypothesis

The specific hypotheses being tested in this chapter are:

(Closed-Cycle Formation Hypothesis) Given a network $\mathcal{N}$ obtained from

Figure 7.2. Typical Stimulus Envelope for Alternating Periodic Stimulus Experiments.

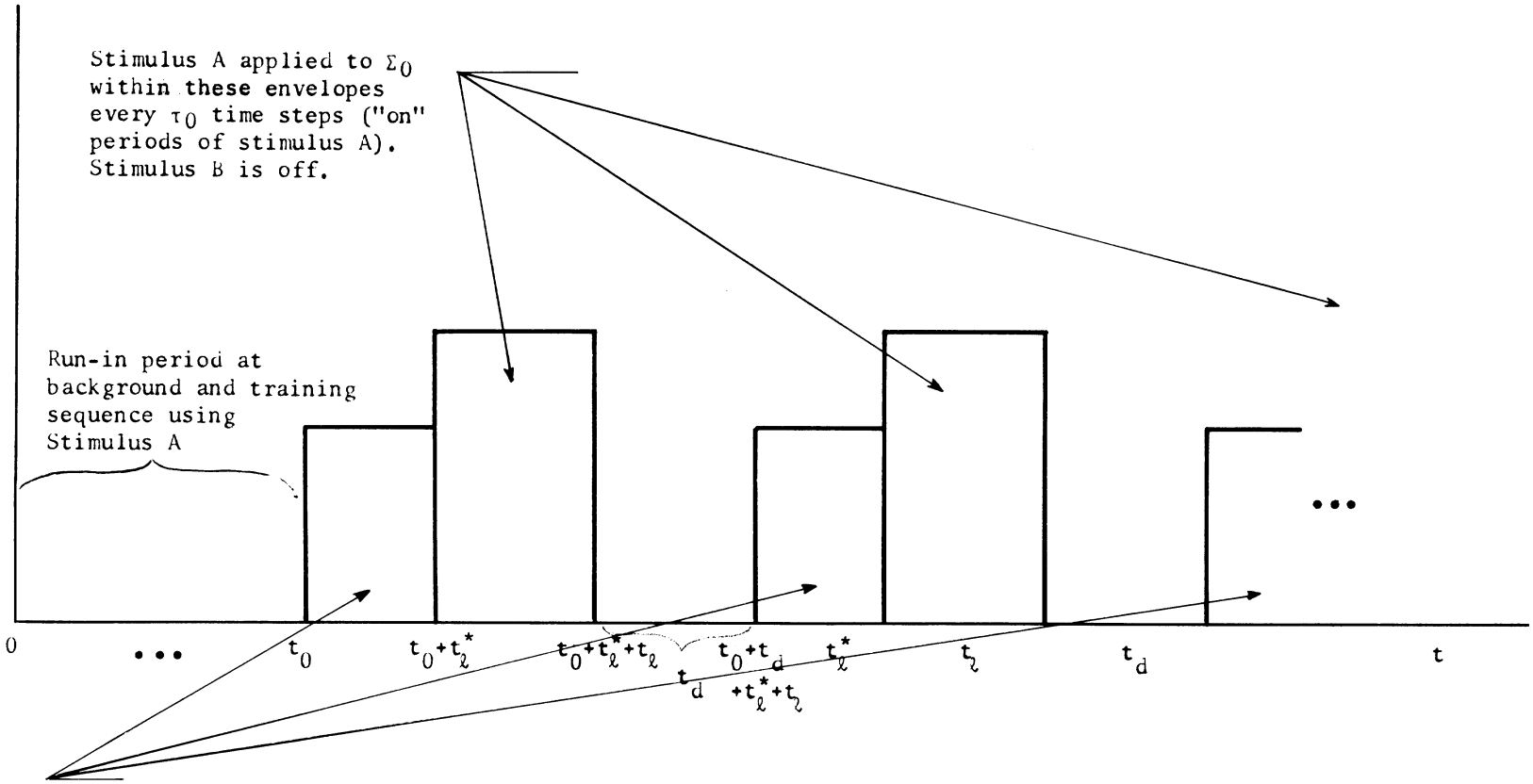

Note: Here it is assumed that a $C(\Sigma_0)$ has already been formed in an earlier training sequence ($t = 0 - t_0 - 1$).

Phase III displaying very stable behavior, then for appropriate choices of Σ_0, τ_0, S_0, and t_ℓ, it is possible to produce a cycle $C(\Sigma_0)$ in $\mathfrak{N}$ as a result of periodic stimulation of Σ_0 in a sequence of "on-off" intervals. (Alternating Closed Cycles Formation Hypothesis) Given a network $\mathfrak{N}$ in which a closed cycle $C(\Sigma_0)$ has been obtained (from Phase V), then for appropriate Σ_0^*, τ_0^*, t^* a new cycle $C(\Sigma_0^*)$ will emerge after prolonged alternating periodic stimulation of $C(\Sigma_0)$ and $C(\Sigma_0^*)$. $C(\Sigma_0^*)$ will send inhibitory connections to $C(\Sigma_0)$ and conversely.

7.3 NETWORKS WITH UNIFORM RANDOM DISTRIBUTIONS OF CONNECTIONS

As mentioned in the Introduction, the results obtained using networks with uniform random distributions of connections were disappointing. Consequently, in the sequel, experiments representing typical results only are displayed. The many varied attempts to produce success (overlapping paths and cycles) are omitted from description since they were all futile — a "barking up the wrong tree" situation.

7.3.1 Series I — Networks with Positive Connections Only

Experiment 1 — Fatigue Inoperative

The network of Figure 6.4, 2, of Basic Experiments II (Chapter 6, Section 6.2.1) was taken as the basis for this experiment. The behavior of that network was "stable", albeit rigidly periodic. $\Sigma_0 = 10$, $\tau_0 = 6$, $S_0 = 7$ (synapse-values), and $t_\ell = \infty$("on" envelope only present). The stimulus was started at $t = 0$ with $F(0) = 25$. The network was run for 602 time steps. As in the Basic Experiment, $\phi(\ell) \equiv 0$ (additive fatigue inoperative).

The results of this experiment are summarized in Figure 7.3. The behavior remained stable, although the oscillations are a more pronounced than in the steady-state experiment. The EEG's for both these experiments

Figure 7.3. Experiment 1 (Section 7.3) — Fatigue Inoperative.

(a) EEG for time steps 1-204. Notice that behavior is rigidly periodic on period $\tau_0 \times \hat{r}_q = 6 \times 17 = 102$ time steps. The network is that of Fig. 6.4, Variant 2, of Chapter 6.

(b) The EEG for the same time interval for experiment of Fig. 6.4, Variant 2, is given immediately below.

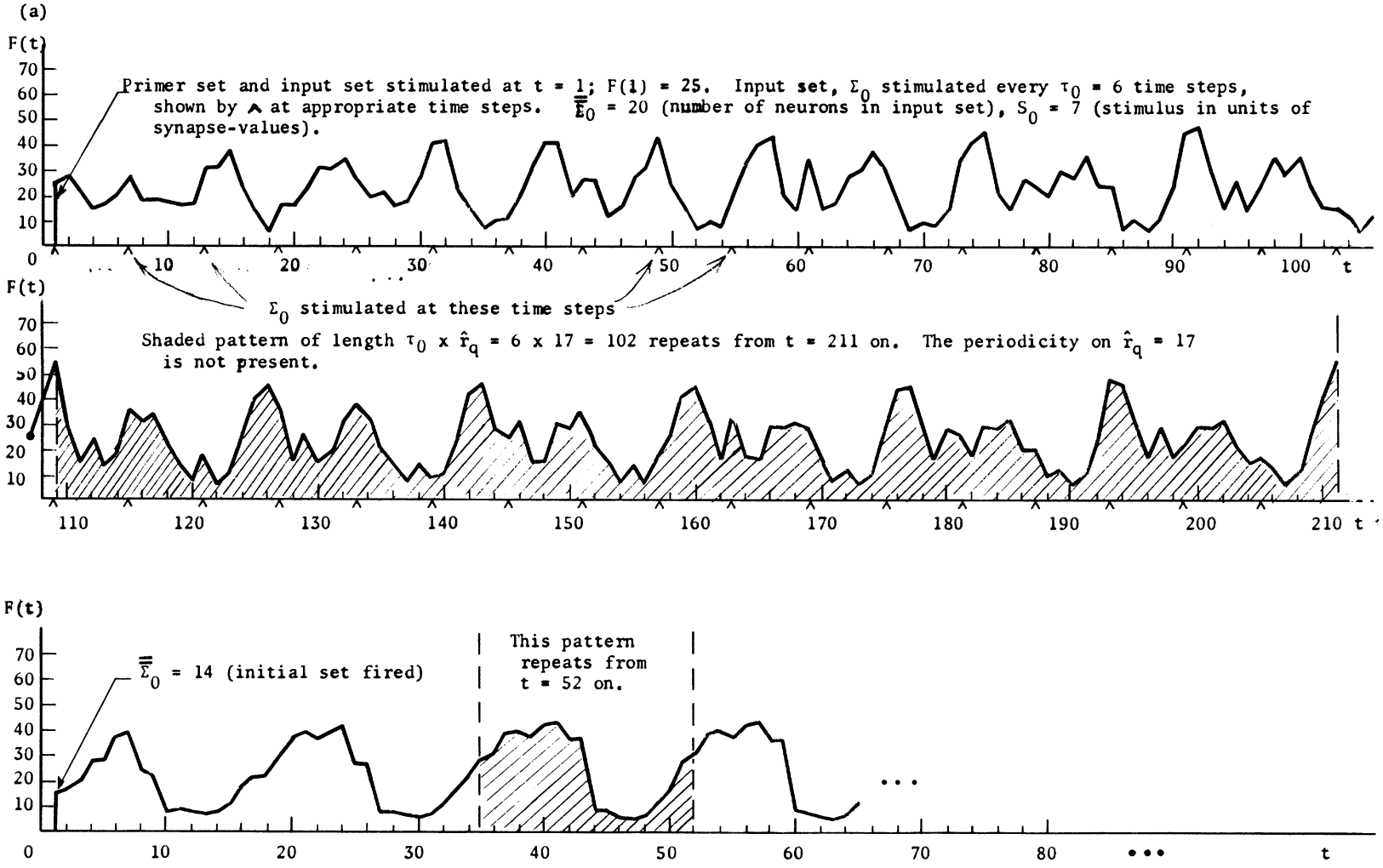

Figure 7.4. Firing Patterns for Experiment 1 (Section 7.3), t = 451 - 462.

The firing patterns for two consecutive stimulus periods are given below. Except for some neurons of Σ_0 (Σ_0 = neurons 381 - 400), there is no overlap whatsoever between the set of neurons firing at **t** and those firing at $t+\tau_0 = t+6$.

```
STIMULATED NEURONS  391  THROUGH      400
TIME    451 OUTPUT IS      30 FIRING DISPLAY
 111 11110  ZERO     1  ZERO  ZERO    10  ZERO  ZERO  ZERO  ZERO  ZERO    10  ZERO  ZERO    10  100  ZERO  ZERO
 ZERO  ZERO  ZERO  ZERO 11001  ZERO  ZERO  ZERO  ZERO  ZERO    10  ZERO  ZERO  ZERO    10  ZERO    10     1 10000
 ZERO  ZERO  ZERO     1  1000  ZERO  ZERO  ZERO  ZERO  ZERO  1000  ZERO  ZERO  ZERO  ZERO   100  ZERO  ZERO  ZERO
 ZERO   100  ZERO  ZERO  1000  ZERO  ZERO     1  ZERO  ZERO 11000  ZERO  ZERO  ZERO  ZERO  ZERO  ZERO  ZERO  ZERO
 ZERO  ZERO  ZERO    10
TIME    452 OUTPUT IS      31 FIRING DISPLAY
 ZERO  ZERO  ZERO  ZERO  ZERO 10000  ZERO  ZERO   100  ZERO    10   100  ZERO  ZERO     1  ZERO    10  ZERO  ZERO
 1000  ZERO  ZERO   100  ZERO     1  ZERO  ZERO  ZERO    10  ZERO  ZERO  ZERO  ZERO  ZERO    10  ZERO 10000   100
   10   100  1000    10  ZERO 10000  1000  1000    10 10001  ZERO 10000  ZERO  ZERO  ZERO  1000   100    10  ZERO
 ZERO  ZERO  ZERO  ZERO 10000  ZERO  ZERO  ZERO  ZERO  ZERO  ZERO  ZERO  ZERO  ZERO  ZERO  ZERO  ZERO  ZERO     1
    10  ZERO    10  ZERO
TIME    453 OUTPUT IS      15 FIRING DISPLAY
 ZERO  ZERO  ZERO  ZERO  ZERO  ZERO  ZERO  ZERO     1     1 10000  ZERO  ZERO  ZERO   100  ZERO  ZERO  ZERO  ZERO
     1 10100  ZERO  ZERO  ZERO  ZERO  ZERO  ZERO  ZERO     1  ZERO  ZERO     1  ZERO  ZERO  ZERO  ZERO    10  ZERO
 ZERO  ZERO  ZERO  ZERO  ZERO  ZERO  ZERO  ZERO  ZERO  ZERO  ZERO  ZERO  ZERO  ZERO  ZERO  ZERO    10  ZERO  ZERO
 ZERO  ZERO   100  ZERO  ZERO  ZERO 10000  ZERO  ZERO    10  ZERO  ZERO  ZERO  ZERO  ZERO  ZERO   100  ZERO  ZERO
 ZERO  ZERO  ZERO  ZERO
TIME    454 OUTPUT IS      14 FIRING DISPLAY
 ZERO  ZERO   100  ZERO  ZERO  ZERO  ZERO  ZERO  ZERO  ZERO  ZERO  ZERO  ZERO  ZERO  ZERO  1000  ZERO  ZERO  ZERO
 ZERO  ZERO  ZERO  ZERO  ZERO  ZERO  ZERO  ZERO  ZERO  ZERO  ZERO  ZERO  ZERO  ZERO  ZERO  ZERO  ZERO  ZERO  ZERO
 ZERO  ZERO  ZERO  ZERO  ZERO  ZERO  ZERO  ZERO 10000  ZERO   100  1100  1001  ZERO   110  ZERO  ZERO  ZERO  ZERO
 1000  ZERO  ZERO  ZERO  ZERO  1000  ZERO    10  ZERO  ZERO  ZERO  ZERO  ZERO  ZERO  ZERO    10  ZERO  ZERO  ZERO
 ZERO  ZERO  ZERO  ZERO
TIME    455 OUTPUT IS      14 FIRING DISPLAY
 ZERO  ZERO  ZERO  ZERO  ZERO  ZERO  ZERO    10  ZERO  ZERO  ZERO  ZERO   100  ZERO 10000  ZERO  ZERO  ZERO
 ZERO  ZERO  ZERO  ZERO  ZERO  ZERO  ZERO  ZERO 10000  ZERO  ZERO  ZERO     1  ZERO  ZERO     1  ZERO  ZERO
 ZERO  ZERO  ZERO  ZERO  ZERO  ZERO  ZERO  ZERO    10  ZERO  ZERO  ZERO  ZERO  ZERO  ZERO  ZERO  ZERO  ZERO
 ZERO  1000  ZERO  ZERO  ZERO  ZERO  ZERO  ZERO  ZERO   100  ZERO     1  ZERO  1000   100  ZERO 10000  ZERO
 ZERO  ZERO  ZERO     1
TIME    456 OUTPUT IS      20 FIRING DISPLAY
 ZERO  ZERO  ZERO   100  ZERO  ZERO     1  ZERO 10000  ZERO  ZERO     1  ZERO     1  ZERO   100  ZERO  ZERO    10
 ZERO  ZERO  ZERO  1000  ZERO  ZERO  ZERO     1    10  ZERO  ZERO     1  ZERO  ZERO 10000  ZERO  ZERO  ZERO  ZERO
 ZERO  ZERO  ZERO  ZERO  ZERO  ZERO  ZERO  ZERO  ZERO  ZERO  ZERO  ZERO  ZERO  ZERO     1     1  ZERO  ZERO     1
 ZERO 10000  ZERO  ZERO  ZERO  ZERO   110  ZERO  ZERO  ZERO  ZERO  1000  ZERO  ZERO  ZERO  ZERO  ZERO  ZERO  ZERO
 ZERO  1000  ZERO  ZERO
STIMULATED NEURONS  391  THROUGH      400
TIME    457 OUTPUT IS      34 FIRING DISPLAY
 11100    11     1  ZERO  ZERO  ZERO  ZERO  ZERO  ZERO  ZERO 10000  ZERO  ZERO  ZERO  ZERO     1     1  ZERO
 10010  ZERO   100  ZERO  ZERO  ZERO  ZERO  ZERO  1000  ZERO  ZERO  1000  ZERO  1000  ZERO  ZERO 10000  ZERO  ZERO
 ZERO  ZERO    10  ZERO  ZERO  ZERO    11 10000  ZERO  ZERO  ZERO  ZERO  ZERO  ZERO  ZERO 10010  ZERO 10000   100
 ZERO  ZERO  1000 11000  ZERO  ZERO  ZERO  ZERO     1 10000  ZERO    10  ZERO  ZERO 10000  ZERO  ZERO   110  ZERO
 10000  ZERO  ZERO  ZERO
TIME    458 OUTPUT IS      29 FIRING DISPLAY
 ZERO  ZERO  ZERO  ZERO  ZERO    10  ZERO  ZERO  ZERO  ZERO  ZERO  ZERO  1000  ZERO  ZERO  ZERO  ZERO     1
 ZERO    10 10000    10  ZERO  1100  ZERO 10000     1   100  1000  ZERO  ZERO   100  ZERO  1001  ZERO  ZERO  ZERO
 ZERO 10000 10000  ZERO  ZERO  1010   100    10   100   100  ZERO    11  ZERO  ZERO  ZERO  ZERO  ZERO  1000  ZERO
   100  ZERO  ZERO  ZERO  ZERO  ZERO  ZERO  ZERO  ZERO  ZERO    10  ZERO  ZERO  ZERO  ZERO  ZERO  ZERO  ZERO
 ZERO  ZERO  ZERO   100
TIME    459 OUTPUT IS      23 FIRING DISPLAY
 ZERO  ZERO  ZERO  ZERO    10     1 10000   100  ZERO   100  ZERO  ZERO  ZERO 10000  ZERO  ZERO  ZERO  ZERO   100
 ZERO  ZERO  ZERO 10000    10    10  1000  ZERO   100  ZERO  ZERO 10000  ZERO  ZERO  ZERO  ZERO  ZERO     1
 ZERO  ZERO  ZERO  ZERO  ZERO  ZERO  ZERO  ZERO     1  1000 10010  ZERO  ZERO  ZERO  ZERO  ZERO  ZERO  ZERO
 ZERO    10  ZERO  ZERO  ZERO  ZERO  ZERO   100  ZERO  ZERO  ZERO  ZERO   100  ZERO    10  ZERO  ZERO  ZERO    10
 ZERO  ZERO  ZERO  ZERO
TIME    460 OUTPUT IS      16 FIRING DISPLAY
 ZERO  ZERO  ZERO 10000  ZERO  ZERO  1000 10000  ZERO  ZERO  ZERO  ZERO  ZERO    10  ZERO  ZERO  ZERO  1000  ZERO
 ZERO  1000  ZERO  ZERO   100  ZERO  ZERO  ZERO  ZERO  ZERO  ZERO  ZERO  1000  ZERO  ZERO  ZERO  1000  ZERO  ZERO
 ZERO  ZERO  ZERO  1000 10000  ZERO  ZERO  ZERO  ZERO  ZERO  ZERO   100  ZERO  ZERO  ZERO  ZERO  ZERO  ZERO
 ZERO  ZERO    10  ZERO  ZERO   100  ZERO  ZERO  1000  ZERO     1  ZERO  ZERO  ZERO  ZERO  ZERO  ZERO  ZERO
 ZERO  ZERO  ZERO  ZERO
TIME    461 OUTPUT IS      13 FIRING DISPLAY
 ZERO  ZERO  ZERO  ZERO  ZERO  ZERO  ZERO  ZERO  ZERO  1010  ZERO  ZERO  ZERO  ZERO  ZERO  ZERO  ZERO  ZERO  ZERO
 ZERO  ZERO  ZERO  ZERO  ZERO  ZERO  ZERO  ZERO  ZERO  ZERO  ZERO  ZERO  ZERO  ZERO  ZERO 10100  ZERO  ZERO  ZERO
 ZERO  ZERO  ZERO  ZERO  ZERO     1  ZERO  ZERO  ZERO  ZERO     1  ZERO  ZERO    10  ZERO  ZERO  ZERO  ZERO 10000
 ZERO  ZERO  ZERO  ZERO  ZERO  ZERO  ZERO  ZERO   100     1  ZERO  ZERO  ZERO    11  ZERO 10000  ZERO  ZERO  ZERO
 ZERO  ZERO  ZERO  ZERO
TIME    462 OUTPUT IS       8 FIRING DISPLAY
 ZERO  ZERO  ZERO  ZERO  ZERO  ZERO  ZERO     1  ZERO  ZERO  ZERO  ZERO  ZERO  ZERO  ZERO  ZERO  ZERO    10  ZERO
 ZERO  ZERO  ZERO  ZERO  ZERO  ZERO  ZERO  ZERO  ZERO  ZERO  ZERO  ZERO  ZERO  ZERO  ZERO  ZERO  ZERO  ZERO  ZERO
 ZERO  ZERO  ZERO  ZERO    10  ZERO  ZERO  ZERO  ZERO  ZERO  ZERO  ZERO  ZERO  ZERO  ZERO  ZERO  ZERO  ZERO     1
 ZERO  ZERO  ZERO  ZERO  ZERO 10000  ZERO  ZERO  ZERO  ZERO  ZERO  ZERO  ZERO  1000  ZERO  ZERO  1000  ZERO  ZERO
 ZERO 10000  ZERO  ZERO
```

are given for comparison in Figure 7.3. No overlapping paths developed as may be seen in Figure 7.4 where the firing patterns for twelve consecutive time steps starting at t = 451 are shown.

Although the experiment was not successful, there are several interesting sidelights worthy of mention. First, the effect of the stimulus seems to have been much like that of an AM radio signal upon the carrier wave: The steady-state pattern still predominates but it has been "modulated" by the signal (periodic stimulus). Notice, however, that the rigid periodicity of the steady-state behavior has been destroyed. This leads to the second observation: the behavior repeats itself after $\tau_0 \times \hat{r}_q = 6 \times 17 = 102$ time steps, $F(t+102) \equiv F(t)$, $\Sigma_{t+102} \equiv \Sigma_t$. This, no doubt, is a combinatoric consequence of the informal argument given in Chapter 6 explaining the origin of the periodicity occurring there. It is as though there were six additional ways each sequence $F(t), \ldots, F(t+16)$ might occur, giving 6 x 17 total combinations before repetitions of a given sequence $F(t), \ldots, F(t+16)$ may occur. Whatever the cause, this result once again implies zero information; recruitment is not possible.

Experiment 2 — Fatigue Present

This experiment is basically a repetition of the preceding one, except that the fatigue mechanism is now operation. The function $\phi(\ell)$ and tables $\Delta_1(\ell)$, $\Delta_2(\ell)$ used are given in Figure 7.5, together with the EEG. The run was terminated at t = 598. At t = 0, neurons were distributed randomly and uniformly over fatigue states (as well as over recovery states). S_0 was increased to 10 synapse-values to compensate for this.

Figure 7.5. Experiment 2 (Section 7.3) — Fatigue Present.

This is essentially a repetition of Experiment 1 (Fig. 7.4) with the additive fatigue machanism present. The curve $\phi(\ell)$ and tables $\Delta_1(\ell)$, $\Delta_2(\ell)$ used are given below together, with a segment of the EEG. Again, F(t) became periodic with period $\tau_0 \times \hat{r}_q = 6 \times 17 = 102$ (after an initial transient period of several hundred time steps). Overlapping paths were not present.

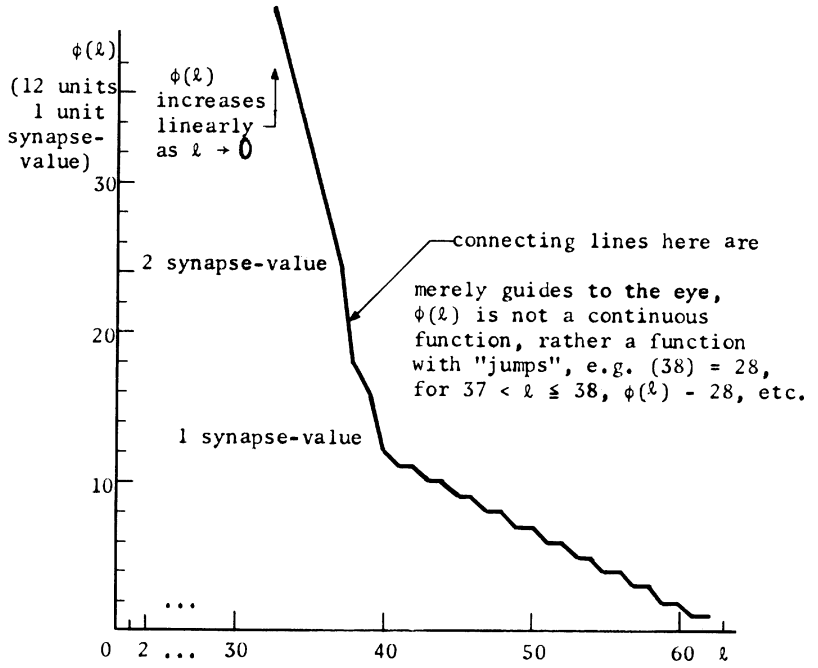

ℓ	$\Delta_1(\ell)$	$\Delta_2(\ell)$	ℓ	$\Delta_1(\ell)$	$\Delta_2(\ell)$
0	0	1/16	32	2	1/16
1	0	1/16	33		
2			34		
3			35		
4			36		
5			37		
6			38		
7			39	2	
8			40	1	
9	1		41		
10	2		42		
11			43		
12			44		
13			45		
14			46		
15			47		
15			48		
16			49		
17			50		
18			51		
19	2		52		
20	4		53		
21			54		
22			55		
23			56		
24			57		
25			58		
26			59		
27			60		
28			61		
29			62		
30	1		63	1	0
31	4	1/16			

Figure 7.5 (continued).

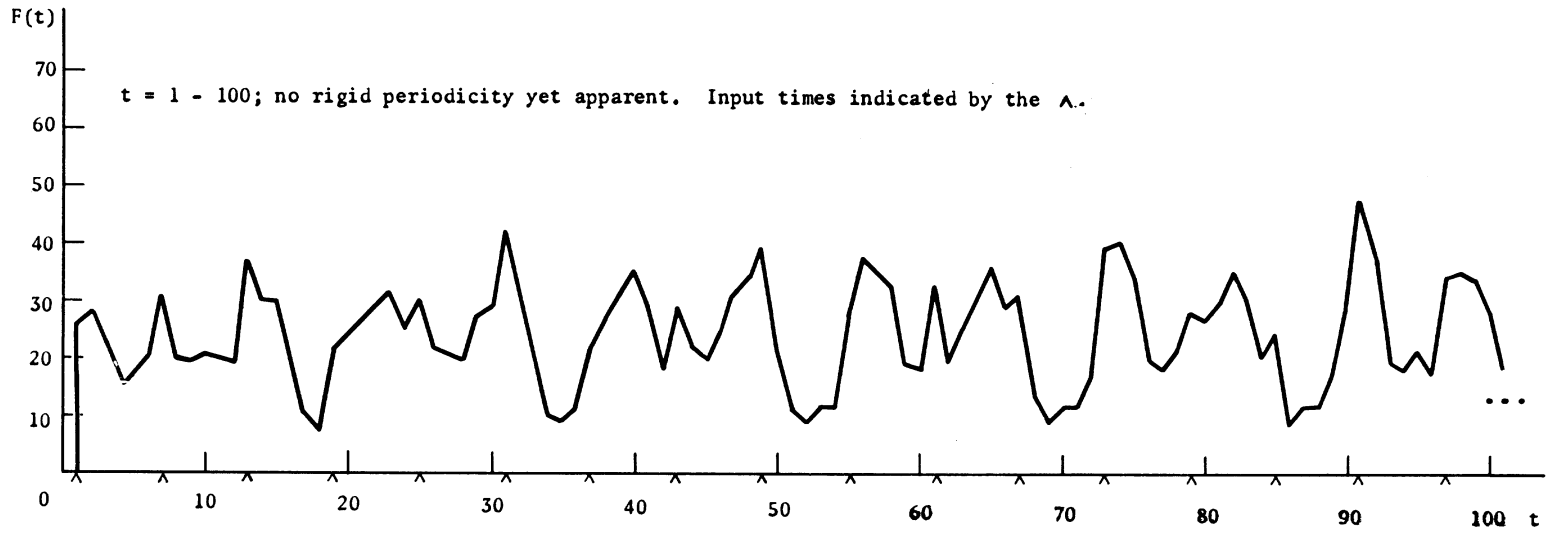

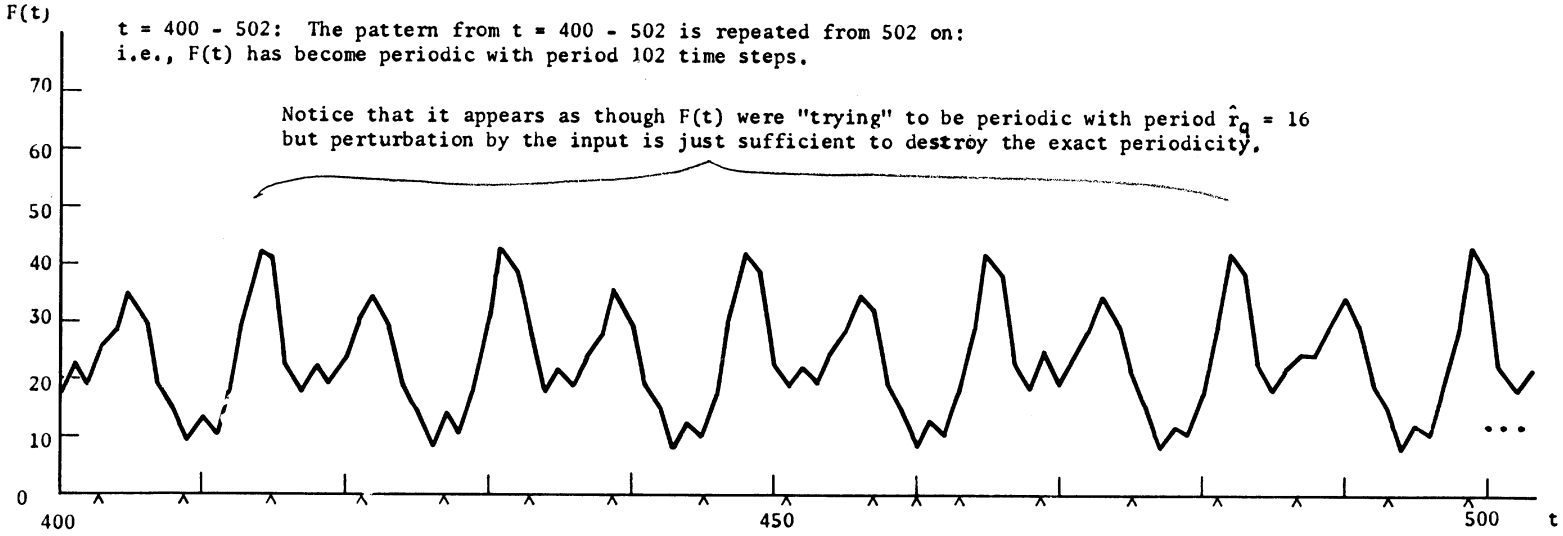

No overlapping paths were present. As before, F(t) repeated itself after $\tau_0 \times \hat{r}_q = 6 \times 17 = 102$ time steps. It took several hundred time steps before this occurred, however.

A number of variations (with and without fatigue) of the above experiments were carried out — varying $\bar{\bar{\Sigma}}_0$, S_0, and τ_0. In no case did overlapping paths occur. Therefore, negative feedback was introduced into the networks, Phases I - III conducted for the new networks, and the experiments of the next section carried out.

7.3.2 Series II — Networks with Negative Feedback

Experiment 3 — Fatigue Inoperative

The basic network used was that of Figure 6.9 with the threshold curve of Figure 7.6. Notice that this curve has a dip at r = 5, 6, and 7. $N = 400$, $\rho = 12 = \sum_{k=-2}^{2} \rho_k$ where $\rho_0 = 0$, $\rho_{-2} = \rho_{-1} = \rho_1 = \rho_2 = \rho/4$. $\phi(\ell) \equiv 0$. $\bar{\bar{\Sigma}}_0 = 20$, $F(0) = 37$. $\tau_0 = 6$, $S_0 = 10$, $t_\ell = 100$. The first "on" period started at t = 0. The results are summarized in Figure 7.6. Figure 7.7 displays firing patterns from t = 419 through t = 431. It can be seen that some overlapping paths appear to be present.

Several experiments similar to Experiment 3 were conducted. All involved threshold curves with dips. All yielded some overlapping paths, but no cycles. These experiments likewise were abandoned in favor of networks with distance-bias.

7.3.3 Conclusions

In general, the experiments of this section resulted in failure — no overlapping paths or cycles. An interesting periodicity of length $\hat{r}_q \times \tau_0$ was observed in the positive connections only case. Success of

Figure 7.6. Experiment 3 (Section 7.3) — Fatigue Inoperative.

This is the same network as that of Fig. 6.9, Variant 3. The "primer" subset consisted of thirty-seven neurons of $\mathcal{N}$, $\bar{\Sigma}_0 = 20$ (size of input subset). The first "on" period commenced at $t = 1$. $\tau_0 = 6$, $t_\ell = 100$, $s_0 = 10$ (synapse-value units).

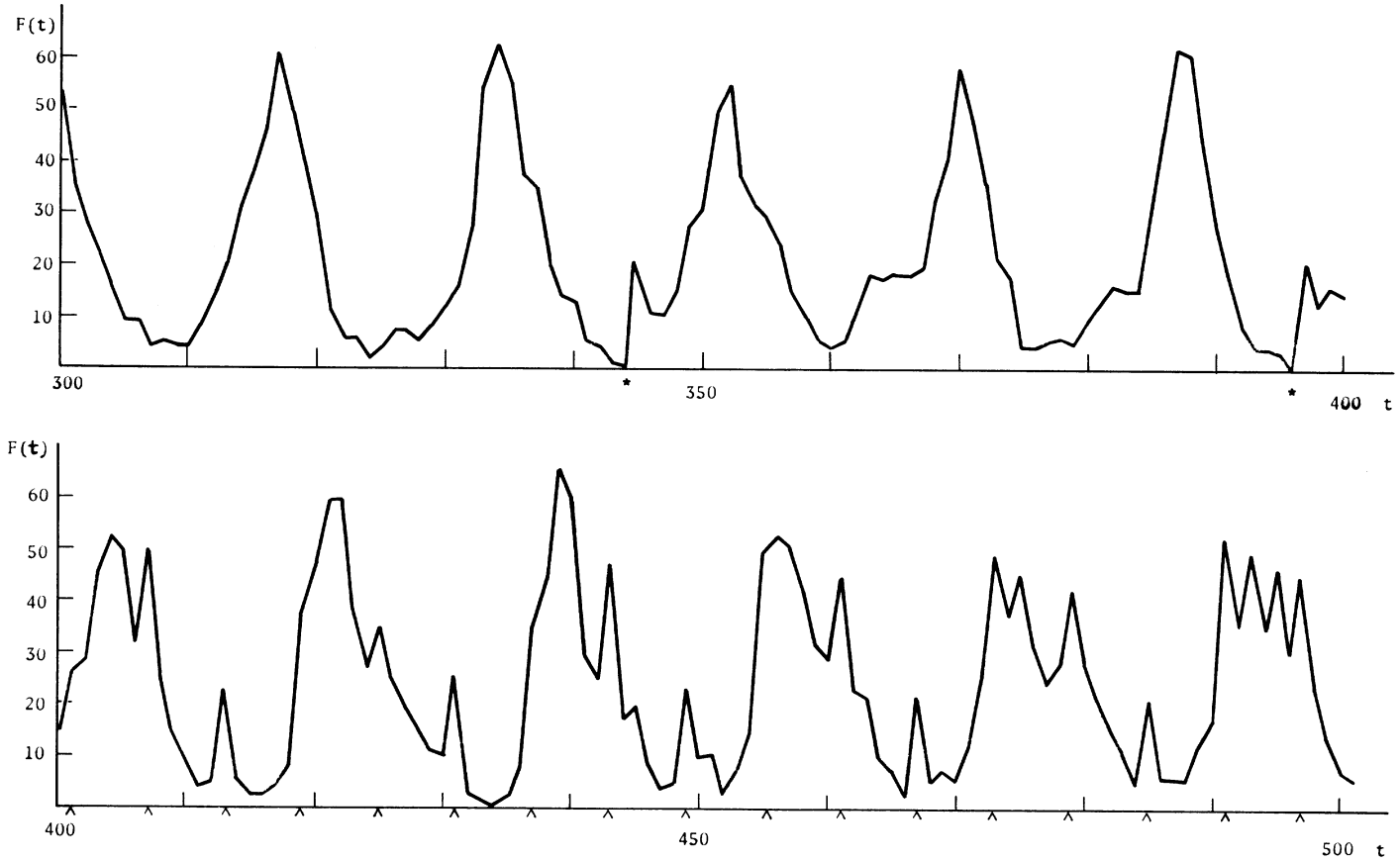

Note on this EEG: The interval t = 300 - 400 is an "off"-period for the stimulus, t = 400 - 500 an "on" period. Clearly, F(t) is underdamped, going to zero at t = 344 and t = 396 (marked by an asterisk) in the "off"-period. At these two time steps, the network was revived by stimulating the "primer" set ($\neq \Sigma_0$). This is the only time in this work that a "revival" artifact was used, since (according to the theory of Chapter 4), such behavior indicates a serious imbalance in the network parameters.

Figure 7.7. Overlapping Paths in Experiment 3 (Section 7.3).

Interpretation: The firing patterns for t = 419 - 431 are given below. The neurons of Σ_0 are enclosed within square brackets (neurons 1-20 of $\mathcal{N}$). Σ_0 was stimulated at t = 419 and t = 425. Neurons that fired at t then again at $t+\tau_0 = t+6$ are shown encircled (excluding Σ_0). These neurons are candidates for a path (in the sense of Chapter 4) from Σ_0. They will be in such a path, if the connections from Σ_0 to Σ_1, Σ_1 to Σ_2, etc. exist, since it is just possible that these connections do not exist and their firing at $t+\tau_0$ is a coincidence. Since the results of Experiment 3 in general are so poor, the matter was not pursued further, and attention was directed towards networks with distance-bias. In the future, however, when overlapping paths are displayed as below, it may be assumed that the connection-matrix of the network was examined and the appropriate connections from a subset Σ_τ to its successor-set $\Sigma_{\tau+1}$ actually exist.

```
STIMULATED NEURONS     1  THROUGH       20
TIME    419 OUTPUT IS      37 FIRING DISPLAY
 ZERO  ZERO  ZERO  ZERO  ZERO  ZERO  ZERO  ZERO  ZERO  ZERO  ZERO  1000 10000  ZERO     1  ZERO  ZERO  ZERO
 ZERO  ZERO   100  ZERO   100  ZERO  ZERO  ZERO    10  ZERO   100  ZERO  ZERO  ZERO   100  ZERO  ZERO  ZERO
 ZERO  ZERO  ZERO  ZERO  ZERO  ZERO     1  ZERO   100  ZERO  1100  1000  ZERO  ZERO  ZERO  1000  ZERO  ZERO  ZERO
 ZERO  ZERO  ZERO  ZERO  ZERO 10000  ZERO  ZERO     1  ZERO  ZERO  ZERO  ZERO  ZERO  ZERO  1000  ZERO  ZERO  ZERO
[11111 11111 11111 11111]
TIME    420 OUTPUT IS      47 FIRING DISPLAY
 ZERO  1001    10  ZERO    10   100     1 10000  1010    10     1  ZERO     1  1000 10000   100  ZERO    10  ZERO
 1100     1  1001  ZERO  ZERO  ZERO  ZERO 10000  ZERO  ZERO  ZERO  ZERO  ZERO  1000 (1) 10000  ZERO  ZERO  ZERO
 1000  1000  ZERO   100  1011     1  ZERO   110  ZERO  ZERO 10001  ZERO  ZERO 10000  ZERO  ZERO  ZERO  ZERO
   10  ZERO  ZERO     1 10100     1  ZERO (1)000  ZERO     1 (1)0  ZERO  ZERO  ZERO  ZERO   100   100  ZERO  ZERO
 ZERO  ZERO  ZERO  ZERO
TIME    421 OUTPUT IS      59 FIRING DISPLAY
 1100   100     1  1010  1000  ZERO   100     1  ZERO  ZERO 10100  ZERO   100  ZERO  1000  ZERO 10000   100  ZERO
   10 10010  ZERO  ZERO  1000  ZERO  ZERO  ZERO  ZERO  ZERO  ZERO  1000 10000   100  ZERO  ZERO  ZERO   101
  100    10    10 10001  ZERO (1)00  ZERO  ZERO 10(1)0  ZERO  ZERO    10 10010  ZERO  1000  ZERO  1000  1100    10
10000   110  ZERO  ZERO  ZERO  1000  ZERO  ZERO   110 10000  ZERO  1110 11000    10 10101    10  ZERO    10     1
 ZERO  ZERO  ZERO  ZERO
TIME    422 OUTPUT IS      59 FIRING DISPLAY
   10 10000 10000 10100 10000  ZERO  1000  ZERO   100  ZERO  ZERO  ZERO    10    10  ZERO  ZERO  ZERO 10001  ZERO
 ZERO  ZERO 10010  1000 10001    10  ZERO (1)000  ZERO  ZERO    10 10000   110  1000  ZERO   110  1000  1010    10
   10 10000 11000    10 10100 10000   110 11000  ZERO  1001  ZERO   101  ZERO  ZERO  ZERO   100     1  ZERO  ZERO
 ZERO  1000  ZERO  ZERO  1001  ZERO 10000  ZERO 10000  1000  1001     1     1  ZERO  ZERO     1  ZERO  ZERO  ZERO
 ZERO  ZERO  ZERO  ZERO
TIME    423 OUTPUT IS      38 FIRING DISPLAY
 ZERO    10  ZERO  ZERO  ZERO  ZERO   100  ZERO  ZERO  1010  1010  ZERO  ZERO     1  ZERO    10  ZERO  ZERO
 ZERO   100  ZERO   101  ZERO 10001  ZERO    10  ZERO 11000  1000  ZERO  ZERO     1  ZERO  ZERO  ZERO 10000
 ZERO  ZERO  ZERO  ZERO  ZERO  ZERO  1000  ZERO  1000   100  ZERO  ZERO  ZERO     1   110  ZERO    10  ZERO  1000
    1 10001 10000   100  ZERO  ZERO    10  ZERO  ZERO   100 10000  ZERO  ZERO   100  ZERO 10000  ZERO  1000  ZERO
 ZERO  ZERO  ZERO  ZERO
TIME    424 OUTPUT IS      27 FIRING DISPLAY
 ZERO  ZERO  ZERO  ZERO  ZERO 10000 10000  ZERO     1 10001  ZERO   100  ZERO  ZERO  ZERO  1000  ZERO  ZERO  ZERO
 ZERO  1000  ZERO  ZERO  ZERO  ZERO 11000   100  ZERO    10     1  ZERO  1000    10  ZERO  ZERO  ZERO     1  ZERO
 ZERO   100  ZERO  ZERO  ZERO  1000 10000  ZERO  ZERO  ZERO  ZERO  ZERO  ZERO  ZERO  ZERO  ZERO   100  ZERO  ZERO
  100  ZERO     1    10  ZERO    10  ZERO   100  ZERO  ZERO  ZERO  ZERO  ZERO  ZERO  ZERO  ZERO     1  ZERO   100
 ZERO  ZERO  ZERO  ZERO
STIMULATED NEURONS     1  THROUGH       20
TIME    425 OUTPUT IS      34 FIRING DISPLAY
 ZERO  ZERO  ZERO  ZERO     1  ZERO  ZERO  ZERO  ZERO  ZERO  ZERO  ZERO  ZERO  ZERO  ZERO  ZERO  ZERO  ZERO
 ZERO  ZERO  ZERO  ZERO  ZERO  1000     1  ZERO     1  ZERO 10000  ZERO  ZERO  ZERO  ZERO  1000    10  ZERO  1000
 ZERO  ZERO  ZERO  ZERO  ZERO  ZERO  ZERO  ZERO  ZERO  ZERO  ZERO  ZERO  ZERO  ZERO     1  ZERO     1 10100
 ZERO  ZERO   100  ZERO  ZERO  ZERO  ZERO    10  ZERO  ZERO  ZERO  ZERO  ZERO  ZERO  ZERO  ZERO  ZERO  ZERO
[11111 11111 11111 11111]
TIME    426 OUTPUT IS      25 FIRING DISPLAY
 ZERO  ZERO  1000  ZERO  ZERO  ZERO  ZERO    10  ZERO  1000  ZERO  ZERO  ZERO  1001    10  ZERO  ZERO  ZERO 10000
 ZERO  ZERO  ZERO  ZERO   100   100  ZERO  ZERO  ZERO  ZERO  ZERO   100  ZERO  ZERO     1  ZERO  ZERO  ZERO  ZERO
 ZERO  ZERO  ZERO  ZERO  ZERO  ZERO  ZERO  ZERO  ZERO    10  ZERO  ZERO     1 10100  ZERO 10000  ZERO    10  ZERO
 ZERO  ZERO  ZERO  ZERO  ZERO  ZERO  ZERO (1)0000  ZERO  ZERO (1)0  ZERO    10  ZERO  ZERO   100  ZERO   100  1000
 ZERO  ZERO  ZERO  ZERO
TIME    427 OUTPUT IS      19 FIRING DISPLAY
 ZERO  ZERO  ZERO  ZERO  ZERO    10  ZERO  ZERO  ZERO  ZERO  ZERO  ZERO  ZERO  ZERO  ZERO  ZERO    10  ZERO  ZERO  ZERO
10000  ZERO   100  ZERO  ZERO  ZERO  ZERO     1  ZERO  ZERO  ZERO     1  ZERO  ZERO  ZERO  ZERO 10001  ZERO  ZERO
    1  ZERO   100 10000  ZERO  ZERO  ZERO  ZERO (1)0  ZERO    10  ZERO  ZERO  ZERO 10001  ZERO  ZERO  ZERO  ZERO
 ZERO  ZERO  1010  ZERO  ZERO  ZERO   100  ZERO  ZERO  ZERO  ZERO  ZERO  ZERO  ZERO  ZERO  ZERO  ZERO  ZERO  ZERO
 ZERO  ZERO  ZERO  ZERO
TIME    428 OUTPUT IS      15 FIRING DISPLAY
 ZERO  ZERO  ZERO  ZERO  ZERO  ZERO  ZERO  1000  ZERO  ZERO  ZERO  ZERO 10000  ZERO  ZERO  ZERO  ZERO  ZERO  1000
    1  ZERO  ZERO  ZERO  ZERO  ZERO  ZERO  ZERO  ZERO   101  ZERO    10  ZERO  ZERO  ZERO  ZERO  ZERO  ZERO  ZERO
 ZERO  ZERO  ZERO  ZERO (1)00  ZERO  ZERO  ZERO  ZERO  1000  ZERO  ZERO   100  ZERO  ZERO  ZERO 10000  ZERO     1
 ZERO  ZERO  ZERO  ZERO  ZERO  ZERO  ZERO  ZERO  1000    10  ZERO  ZERO  ZERO  ZERO  ZERO  ZERO  ZERO  ZERO 10000
 ZERO  ZERO  ZERO  ZERO
TIME    429 OUTPUT IS      11 FIRING DISPLAY
    1  ZERO  ZERO  ZERO  ZERO  ZERO  ZERO  ZERO   100  ZERO  ZERO  ZERO  ZERO  ZERO  ZERO  ZERO  ZERO   100
 ZERO  ZERO  ZERO  ZERO  ZERO  ZERO   100  ZERO  ZERO  ZERO  ZERO  ZERO  ZERO  ZERO  ZERO  ZERO 10000  ZERO
10000  ZERO  ZERO  ZERO  ZERO  ZERO  1000     1  ZERO  ZERO  ZERO  ZERO  ZERO  ZERO  ZERO  ZERO  ZERO  ZERO
 ZERO  ZERO  ZERO  ZERO  ZERO  ZERO  1000  ZERO  ZERO  ZERO  ZERO 10000  ZERO  ZERO  ZERO  ZERO  ZERO  ZERO    10
 ZERO  ZERO  ZERO  ZERO
TIME    430 OUTPUT IS      10 FIRING DISPLAY
 ZERO  ZERO  ZERO  ZERO  ZERO  ZERO  ZERO  ZERO  ZERO  ZERO  ZERO  ZERO  ZERO  ZERO   100  ZERO     1  ZERO  ZERO
 ZERO  ZERO  ZERO  ZERO  ZERO  ZERO  ZERO  ZERO  ZERO  ZERO  ZERO  ZERO     1  ZERO  ZERO     1  ZERO  ZERO  ZERO
 ZERO  ZERO  ZERO  ZERO  ZERO  ZERO  ZERO  ZERO  ZERO  ZERO  ZERO  ZERO  ZERO    10  ZERO  ZERO  ZERO  ZERO  ZERO
 ZERO  ZERO  ZERO  1000    10  ZERO     1  ZERO  ZERO  ZERO  ZERO  ZERO  ZERO  1000    10  ZERO  ZERO  ZERO  ZERO
 ZERO  ZERO  ZERO  ZERO
STIMULATED NEURONS     1  THROUGH       20
TIME    431 OUTPUT IS      25 FIRING DISPLAY
 ZERO  ZERO  ZERO  ZERO   100  ZERO  ZERO  ZERO  ZERO  ZERO  ZERO  ZERO  ZERO  ZERO  ZERO  ZERO  ZERO  1000  ZERO
 ZERO  ZERO  ZERO 10000  ZERO  ZERO  ZERO  ZERO  ZERO  ZERO  ZERO  ZERO  1000  ZERO  ZERO  ZERO  ZERO  ZERO  ZERO
 ZERO  ZERO  ZERO  ZERO  ZERO  ZERO  ZERO  ZERO  ZERO  ZERO  ZERO  ZERO  ZERO  ZERO  ZERO  ZERO  ZERO  ZERO  ZERO
 1000  ZERO  ZERO  ZERO  ZERO  ZERO  ZERO  ZERO  ZERO  ZERO  ZERO  ZERO  ZERO  ZERO  ZERO  ZERO  ZERO  ZERO  ZERO
11111 11111 11111 11111
```

a sort was obtained using simultaneously threshold curves with dips and negative feedback. However, the threshold curves so used appear to be too ad hoc for general use: while a given curve V(r) might work for $\tau_0 = 6$, say, the same curve probably would fail for $\tau_0 = 10$. This certainly is an undesirable facet of V(r)'s with dips. Unless some mechanism be introduced to "scale" the V(r) for use with any τ_0, $r_a \leq \tau_0 \leq r_q$ — and such a mechanism is difficult to envisage — the use of these curves is to be discouraged.

Further effort might have been expended on networks with uniform random distributions of connections. Admittedly, the experiments of this section were in reality familiarization runs — the experimenter was learning about stimulating networks. Consequently the experiments were crude and often unrealistic. Possibly raising the network density ρ and carefully selecting the λ-distribution $\rho = \sum_{k=-k_0}^{k_1} \rho_k$, the set Σ_0, etc. would have yielded the desired results without the ad hoc threshold curve with dips mechanism. However, it appeared that networks with distance-bias (and negative feedback) offerred the same results far more readily. This is due to the "localization" effect found in such networks which prevents the effects of an external stimulus from dispersing itself too rapidly over the entire network. This idea seemed so attractive that the current networks were abandoned altogether and networks with distance-bias alone considered from this point on.

7.4 NETWORKS WITH DISTANCE-BIAS

In the sequel only networks with negative feedback are considered. All stimulation experiments begin after completion of Phase III, usually at t = 200 or t = 400. First, experiments were conducted with fatigue

Figure 7.8. Experiment 1 (Section 7.4) — Fatigue Inoperative.

The network of Fig. 6.18 was used for this experiment. Σ_0 consisted of neurons 1-20, i.e., the bottom row of $\mathcal{N}$ (considered as a 20x20 grid). Through an oversight, simulation began at t = 0, instead of after a run-in period of several hundred time steps. The resulting EEG is shown below for selected time intervals.

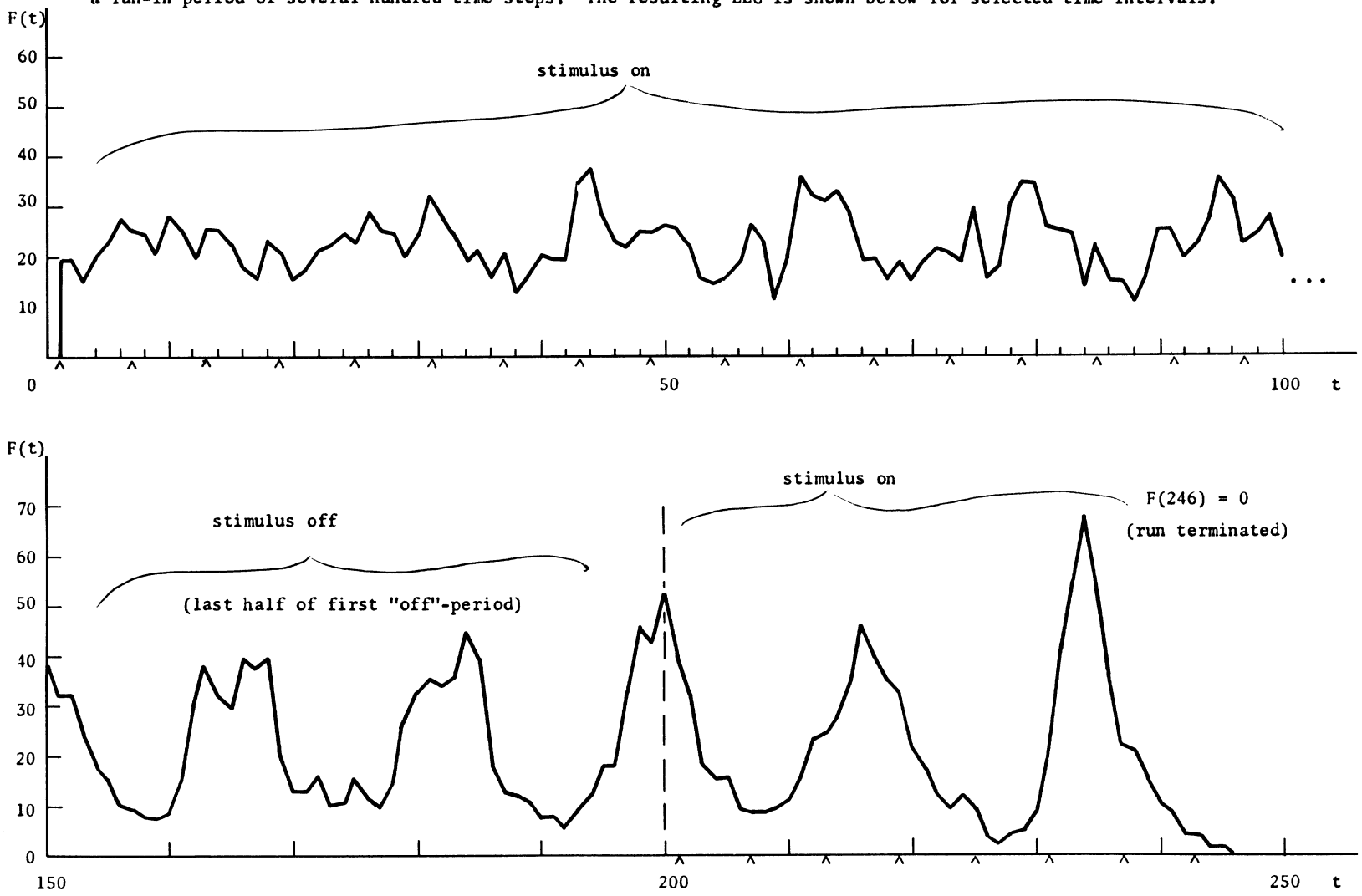

Figure 7.9. Experiment 2 (Section 7.4) — Fatigue Inoperative.

This experiment continues Experiment 1, Section 6.3 (see Fig. 6.18) from t = 201 to t = 482. t = 100, $\tau_0 = 6$, $S_0 = 8.3$ (units of synapse-values). The "on" and "off" periods were 200 - 300, 400 - 500, ... and 300 - 400, 500 - 600, ... respectively. Σ_0 is shown disgramatically below. Since Σ_0 forms a rather compact set, stimulation probably produced a refractory zone around and including Σ_0.

N = 400

R = 4 (neighborhood radius), $\overline{\overline{C}}_R \cong 50$

$\rho = 24.4 = \rho_{-2} + \rho_{-1} + \rho_0 + \rho_2$, $\rho_s = \frac{\rho}{8}$, $s \neq 0$; $\rho_0 = \frac{\rho}{2}$

V(r), $\phi(\ell)$, U(λ), D(λ) as in Basic Experiment III

Σ_0 = {168 - 172, 188 - 192, 208 - 212, 228 - 232} (shaded on diagram)

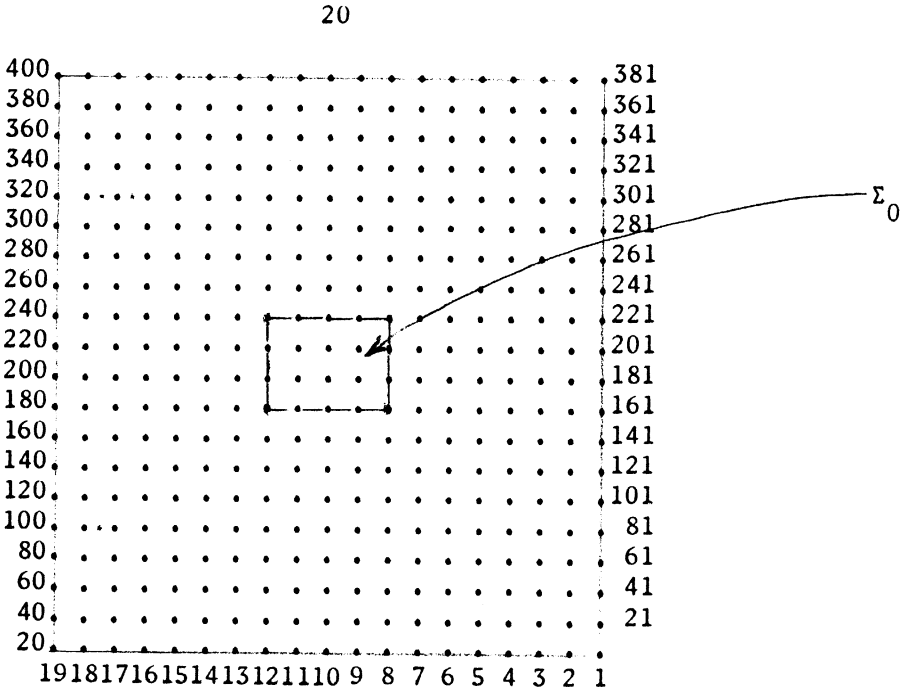

Figure 7.9 (continued).

EEG for t = 201 - 400.

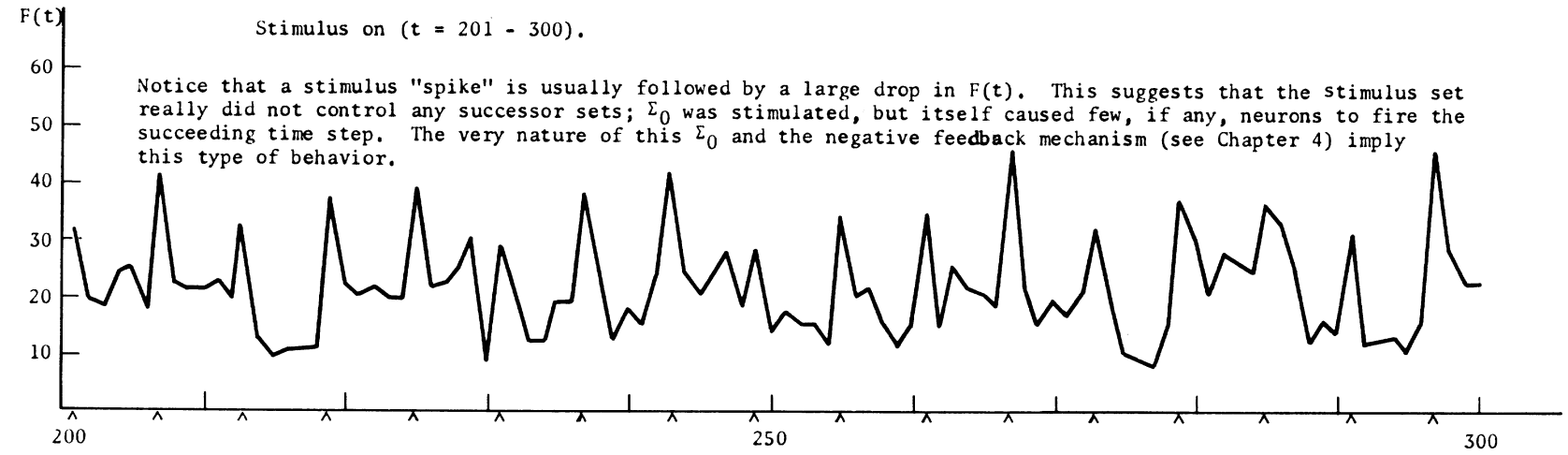

Stimulus on (t = 201 - 300).

Notice that a stimulus "spike" is usually followed by a large drop in F(t). This suggests that the stimulus set really did not control any successor sets; Σ_0 was stimulated, but itself caused few, if any, neurons to fire the succeeding time step. The very nature of this Σ_0 and the negative feedback mechanism (see Chapter 4) imply this type of behavior.

Firing patterns given for these time steps.

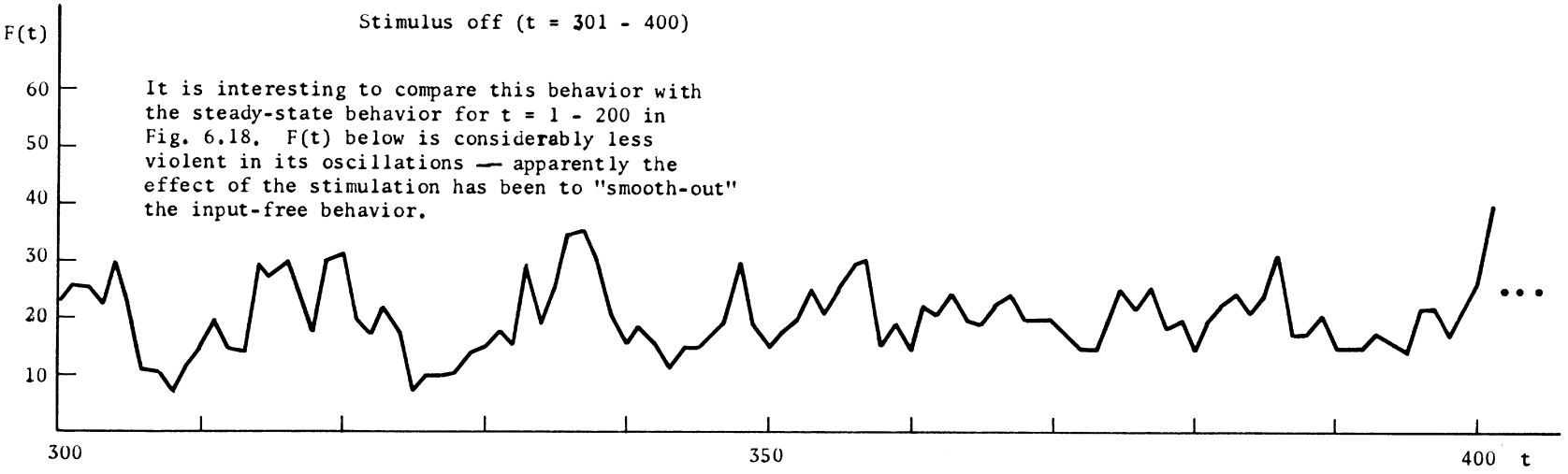

Stimulus off (t = 301 - 400)

It is interesting to compare this behavior with the steady-state behavior for t = 1 - 200 in Fig. 6.18. F(t) below is considerably less violent in its oscillations — apparently the effect of the stimulation has been to "smooth-out" the input-free behavior.

Figure 7.9 (continued).

Firing Patterns for t = 279 - 286. Neurons of Σ_0 are enclosed within brackets. Notice there is no overlap whatsoever between the sets of neurons firing at t = 280 and t = 286: Σ_0 controls no neurons directly.

```
STIMULATED NEURONS  168  THROUGH      172
STIMULATED NEURONS  188  THROUGH      192
STIMULATED NEURONS  208  THROUGH      212
STIMULATED NEURONS  228  THROUGH      232
TIME    279 OUTPUT IS     37 FIRING DISPLAY
   10  ZERO   110  ZERO  ZERO  ZERO  ZERO  ZERO  ZERO  ZERO  ZERO  ZERO  ZERO  1000 10000     1     1
 1001  ZERO  ZERO  ZERO  ZERO  ZERO  ZERO  ZERO   100  ZERO  ZERO  ZERO   101  ZERO    11 11100     1  ZERO     1
11100  ZERO  ZERO    11 11000  ZERO  ZERO    11  1100  ZERO  ZERO  ZERO  ZERO  ZERO  ZERO  ZERO  ZERO     1
 ZERO  ZERO  ZERO  ZERO  ZERO  ZERO  ZERO  ZERO 10000  ZERO  ZERO  ZERO   100  ZERO  ZERO  ZERO  1000  ZERO  1000
 1000  ZERO  ZERO    10
TIME    280 OUTPUT IS     31 FIRING DISPLAY
10000  ZERO  ZERO  ZERO  ZERO  ZERO  ZERO  ZERO  ZERO  ZERO    10  ZERO  ZERO  ZERO 10000    11  ZERO  ZERO 10100
 ZERO 10000  ZERO  ZERO  ZERO   100  ZERO     1  ZERO  1000  ZERO 10000    10  1001  1000  ZERO    10   100  1000
 ZERO 10111  ZERO  ZERO  ZERO   100  ZERO  ZERO  ZERO  ZERO  ZERO  ZERO  ZERO  ZERO  ZERO     1  ZERO  ZERO  ZERO
 ZERO   110  ZERO   100  ZERO  ZERO  ZERO  ZERO  ZERO  ZERO  ZERO   110  ZERO  ZERO  ZERO  ZERO 10000  ZERO  ZERO
 ZERO  ZERO  ZERO  ZERO
TIME    281 OUTPUT IS     21 FIRING DISPLAY
 ZERO  ZERO  ZERO  ZERO  ZERO  ZERO  ZERO  ZERO  ZERO   100  ZERO  ZERO  ZERO  ZERO  ZERO  ZERO  ZERO  ZERO  ZERO
10000     1   100  ZERO  ZERO  1001  ZERO  ZERO 10010  ZERO   100  1000  1000 10000  ZERO  ZERO  ZERO  ZERO 10000
 ZERO  ZERO  ZERO  ZERO  ZERO  ZERO  ZERO  ZERO  ZERO  ZERO 10000     1  ZERO   110  1000  ZERO  ZERO  ZERO  ZERO
 ZERO  ZERO  1000  ZERO  ZERO  ZERO  ZERO  ZERO   100  ZERO  ZERO  ZERO  ZERO  ZERO  ZERO  ZERO  ZERO  ZERO  ZERO
 ZERO  ZERO  ZERO     1
TIME    282 OUTPUT IS     27 FIRING DISPLAY
 ZERO     1  ZERO  ZERO  ZERO  ZERO    10  ZERO  1100 10000  ZERO  ZERO  ZERO 10000  ZERO  ZERO  1000    10  ZERO
 ZERO    10  ZERO    10 10000  ZERO  ZERO   100  ZERO    11  ZERO    10  ZERO  ZERO  ZERO  ZERO  ZERO 10000  ZERO
 ZERO  ZERO  ZERO  ZERO  ZERO 11001    10  ZERO  ZERO  ZERO  ZERO  ZERO  ZERO  ZERO  ZERO  ZERO   100  ZERO  ZERO
 ZERO     1     1 10000  ZERO  ZERO  ZERO    10  ZERO  ZERO  ZERO  1000  ZERO  ZERO  ZERO  ZERO  ZERO  ZERO  ZERO
   10  ZERO  ZERO  ZERO
TIME    283 OUTPUT IS     26 FIRING DISPLAY
  100 10000  ZERO  1000  ZERO  ZERO  1000 10000  ZERO  ZERO  ZERO  ZERO  ZERO    10   100  ZERO     1  ZERO    10
   10  ZERO  ZERO  ZERO  ZERO  ZERO     1    10  ZERO  ZERO  ZERO  ZERO  ZERO  ZERO  ZERO  ZERO  ZERO  1000  ZERO
 ZERO  1000   100  ZERO  ZERO  ZERO  ZERO  ZERO  ZERO  1000  ZERO  ZERO  ZERO 11000 10000  ZERO  ZERO  ZERO   100
 ZERO 10000    10  ZERO  ZERO  ZERO  ZERO  ZERO  ZERO  ZERO   110  ZERO  ZERO  ZERO  ZERO     1  ZERO  ZERO 10000
 ZERO  ZERO  ZERO  ZERO
TIME    284 OUTPUT IS     24 FIRING DISPLAY
 1001  1000  ZERO     1  ZERO  ZERO   101  ZERO  ZERO  ZERO 10000  1000  ZERO  ZERO  ZERO  ZERO  ZERO  ZERO  ZERO
 ZERO   100  ZERO  1000  ZERO  ZERO  1000  ZERO  ZERO 10000  1000  ZERO  ZERO  ZERO  ZERO    11  ZERO  ZERO  ZERO
 ZERO  ZERO  1000  ZERO  ZERO  ZERO  ZERO  ZERO  ZERO   101  ZERO  ZERO  ZERO  ZERO  ZERO  ZERO  1000  ZERO
 ZERO  ZERO  ZERO  ZERO  ZERO    10  ZERO  ZERO  ZERO  ZERO 10000  ZERO  ZERO  ZERO  1000  ZERO  ZERO  ZERO  ZERO
 ZERO 10100  ZERO  ZERO
STIMULATED NEURONS  168  THROUGH      172
STIMULATED NEURONS  188  THROUGH      192
STIMULATED NEURONS  208  THROUGH      212
STIMULATED NEURONS  228  THROUGH      232
TIME    285 OUTPUT IS     37 FIRING DISPLAY
 ZERO  ZERO  ZERO   100    10 11000  ZERO  ZERO  ZERO  1000  ZERO     1     1     1  1000  ZERO    10  ZERO  ZERO
 ZERO  ZERO  1000     1    10  ZERO  ZERO  ZERO  1000  ZERO 10000  ZERO  ZERO  ZERO     1 11000  ZERO  ZERO    11
10100  ZERO     1    11 10100  ZERO   100    11 11100  ZERO  ZERO  ZERO  ZERO  ZERO  ZERO  ZERO  ZERO  ZERO
 ZERO  ZERO  ZERO  ZERO  ZERO  ZERO  ZERO     1  ZERO  ZERO  1000  ZERO  ZERO  ZERO 10000  ZERO  ZERO 10000  ZERO
 ZERO  ZERO  ZERO  ZERO
TIME    286 OUTPUT IS     33 FIRING DISPLAY
 ZERO  ZERO 10000  ZERO 10000    10 10000   100    10  ZERO  ZERO  ZERO 10010  ZERO  ZERO  ZERO  ZERO  ZERO  ZERO
 ZERO  ZERO  ZERO  ZERO  1000 10000  ZERO  ZERO  ZERO  ZERO    10     1 10000    10  ZERO  ZERO   100  ZERO  ZERO
 ZERO  ZERO  ZERO  ZERO  ZERO  ZERO  ZERO   100  ZERO  ZERO  ZERO   100  ZERO     1   100   100 10000  ZERO    10
 ZERO  ZERO  ZERO  ZERO  ZERO  ZERO    11  1000  ZERO  ZERO  ZERO  ZERO  ZERO  1000    10  1110  ZERO   100     1
 ZERO  ZERO  ZERO  1000
```

inoperative. Next, some of these experiments were repeated and some new experiments performed with fatigue present.

The input area Σ_0 plays a crucial role in these experiments. The selection of Σ_0 is almost as important here as was the selection of V(r) in Sections 6.2 and 6.3 of Chapter 6.

Overlapping paths were readily obtained, using "normal" (monotone decreasing) threshold curves. In one case, overlapping cycles were formed. On this basis, a "very" stable network was selected for a thorough test of cycle and alternating cycles formation. This experiment is de scribed in Section 7.5.

7.4.1 Networks with Fatigue Inoperative

Experiment 1: The network of Experiment 1, Section 6.3.3 of Chapter 6, was used. Through an oversight, stimulation began at t = 0 (before the run-in of Phase III). Σ_0 was taken as an edge of the iterated square (Figure 7.8). $\bar{\Sigma}_0 = 6$, $t_\ell = 200$, $S_0 = 1.7$, $\phi(\ell) \equiv 0$.

The results are summarized in Figure 7.8. F(245) became zero in the second "on" period with large swells developing around t = 200. It was not possible to revive the network with further application of the stimulus. Recall that Experiment 1 (Section 6.3.3) appeared to be under-damped.

This run is of interest since it shows the need for selecting Σ_0 and S_0 carefully.

Experiment 2: The network of Experiment 1, Section 5.5.3, at t = 200 (i.e., after running input-free from t = 0 to t = 199) was used. Σ_0 was chosen as a 4 x 4 subgrid of $\mathcal{M}$ (see Figure 7.9). $\bar{\Sigma}_0 = 6$, $t_\ell = 100$, $S_0 = 8.3$ synapse-values. The stimulus was turned on at t = 200 (first

Figure 7.10. Experiment 3 (Section 7.4) — Fatigue Inoperative.

This experiment is a continuation of Experiment 4 (Section 6.3.3) of Fig. 6.21 from t = 200 on. Σ_0 consisted of an 8x8 grid (shown diagrammatically below). Consequently, as is evident from the sampled EEG below, many of the comments on Experiment 3 of Fig. 7.9 apply here as well: in a word, Σ_0 is too compact.

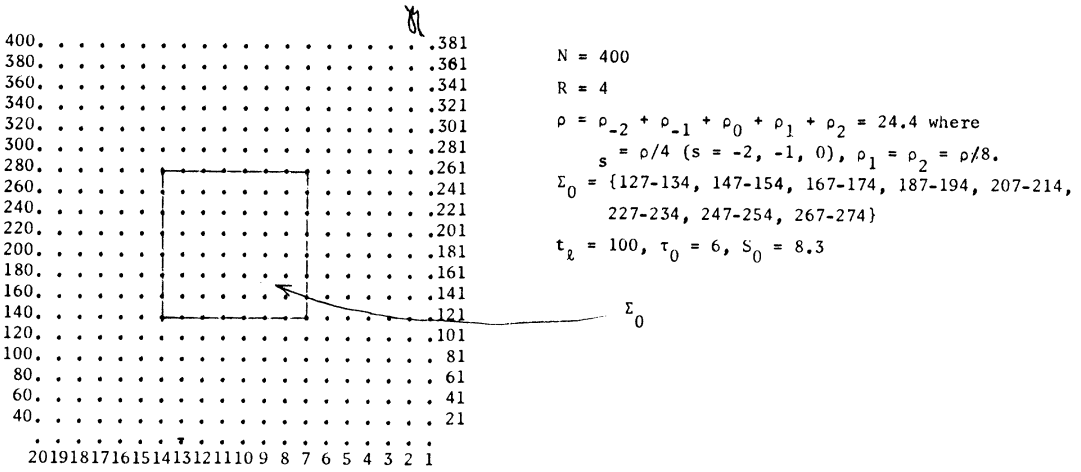

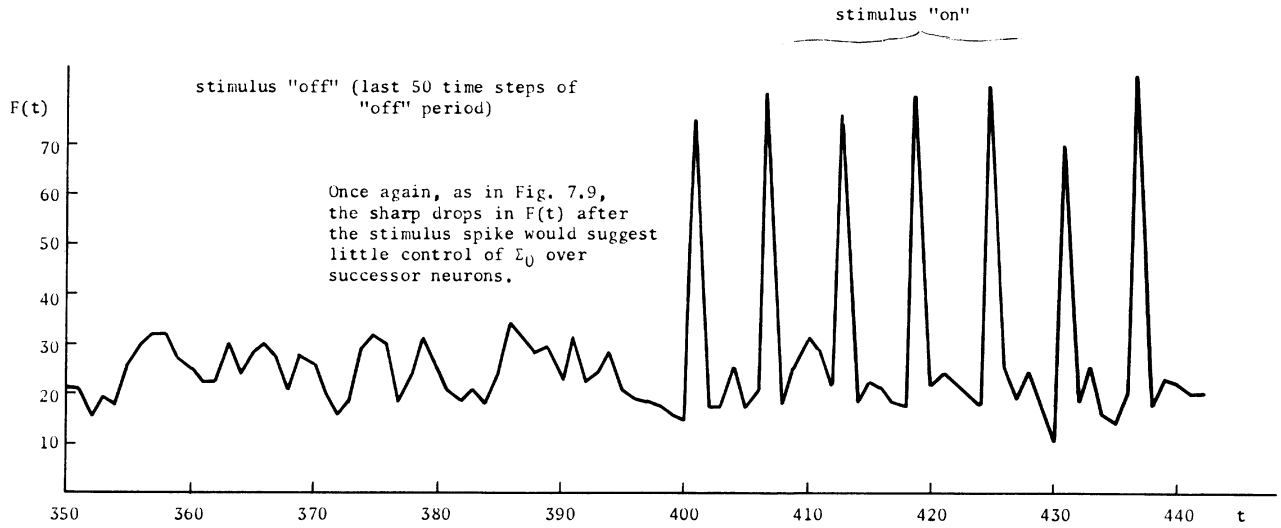

Figure 7.10 (continued).

Although overlapping paths were not expected in this experiment, there were some isolated examples as the following sample of the firing patterns shows. The sample is from time-steps t = 425 - 434 (see EEG). Neurons overlapping at t and $t+\tau_0$ are encircled. Neurons of Σ_0 are bracketed.

```
STIMULATED NEURONS  127  THROUGH      134
STIMULATED NEURONS  147  THROUGH      154
STIMULATED NEURONS  167  THROUGH      174
STIMULATED NEURONS  18   THROUGH      194
STIMULATED NEURONS  207  THROUGH      214
STIMULATED NEURONS  227  THROUGH      234
STIMULATED NEURONS  247  THROUGH      254
STIMULATED NEURONS  267  THROUGH      274
TIME    425 OUTPUT IS     83 FIRING DISPLAY
 ZERO    10  ZERO  100    10  1000  ZERO  ZERO  ZERO  ZERO  ZERO   10  ZERO  ZERO  ZERO   10 11000  ZERO
 ZERO  ZERO    1     1 ZERO 10000 [1111 11110) ZERO  ZERO [1111 11110) 1100  ZERO [1111 11110] ZERO  ZERO [1111
11110) ZERO  ZERO [1111 11110) ZERO  ZERO [1111 11110) ZERO  ZERO [1111 11110 ) ZERO  ZERO [1111 11110) ZERO 10000
 ZERO  ZERO  ZERO  ZERO  100  ZERO  ZERO  ZERO  ZERO  ZERO   10    1  ZERO  100  ZERO    1  ZERO  ZERO  ZERO
 ZERO  ZERO  ZERO  ZERO
TIME    426 OUTPUT IS     26 FIRING DISPLAY
 1000   100  ZERO  ZERO    1  ZERO  ZERO  ZERO  ZERO   100  ZERO  ZERO 10000   (1) ZERO    1  ZERO  ZERO  ZERO
 ZERO     1  ZERO    10 ZERO  1000  ZERO  ZERO  ZERO  ZERO  ZERO  ZERO 10000 10000  ZERO  ZERO  ZERO  ZERO  ZERO
 ZERO  ZERO  ZERO  ZERO ZERO 10000  1001  ZERO  ZERO   100  ZERO  ZERO   100   (1) ZERO  ZERO  ZERO  ZERO  ZERO
 ZERO  ZERO  ZERO  ZERO ZERO  ZERO  ZERO  ZERO  ZERO  ZERO     1  ZERO  ZERO  ZERO  1001    10    10  ZERO  ZERO
    1   100  ZERO     1
TIME    427 OUTPUT IS     19 FIRING DISPLAY
 ZERO  ZERO  ZERO  ZERO ZERO 10000  ZERO    10 ZERO 10000  ZERO  ZERO  ZERO   100  1101  ZERO  ZERO  ZERO     1
 ZERO  ZERO  ZERO  ZERO ZERO  ZERO  ZERO  ZERO  ZERO  ZERO  ZERO  ZERO  ZERO  ZERO  ZERO  ZERO   (1)  ZERO  ZERO
 ZERO     1  ZERO  ZERO ZERO  ZERO  ZERO (1)0000 ZERO     1  ZERO  ZERO  ZERO    10  ZERO  ZERO  ZERO  ZERO  ZERO
 1000  ZERO  ZERO  ZERO   1  ZERO 10000     1  ZERO  ZERO  1000  ZERO  ZERO  ZERO  ZERO  ZERO  ZERO  ZERO  ZERO
   10  ZERO  ZERO  ZERO
TIME    428 OUTPUT IS     24 FIRING DISPLAY
  100  ZERO  ZERO  ZERO ZERO     1   100  ZERO  ZERO  ZERO  ZERO  ZERO  ZERO 10000  ZERO  ZERO  ZERO   100
10100  ZERO  ZERO  ZERO ZERO  ZERO 10000  ZERO  ZERO   100  ZERO  ZERO  ZERO  ZERO  ZERO  ZERO     1  ZERO  ZERO
 ZERO  ZERO     1  ZERO ZERO    11  ZERO  ZERO  ZERO  ZERO  ZERO  ZERO 10001  ZERO  ZERO  ZERO  ZERO  ZERO
 ZERO   100   (1) ZERO ZERO   100  ZERO  ZERO  ZERO  1000   100  ZERO 10010 10000  ZERO  ZERO  ZERO  ZERO  ZERO
 ZERO  ZERO  ZERO  ZERO
TIME    429 OUTPUT IS     17 FIRING DISPLAY
 ZERO  ZERO  ZERO  ZERO ZERO  ZERO    10  ZERO  ZERO  ZERO  ZERO  ZERO  ZERO  ZERO  ZERO   110  ZERO  ZERO  ZERO
 ZERO  ZERO 10000 10000 ZERO  ZERO  ZERO  ZERO  ZERO  ZERO  ZERO  ZERO  ZERO  ZERO  ZERO  ZERO  101 10000
 ZERO  ZERO  ZERO  ZERO ZERO  ZERO  ZERO  ZERO  ZERO  ZERO  ZERO  ZERO  ZERO  1000  ZERO  ZERO 10000  ZERO     1
   10  ZERO  ZERO  ZERO 1000  ZERO  ZERO  ZERO  1000  ZERO  ZERO  ZERO  ZERO  ZERO  ZERO  ZERO  ZERO  ZERO  ZERO
  100     1  1000  ZERO
TIME    430 OUTPUT IS     11 FIRING DISPLAY
    1  ZERO  ZERO     1 ZERO  ZERO 10000  ZERO  ZERO  ZERO  ZERO  ZERO  ZERO  ZERO  ZERO  ZERO  ZERO  ZERO  ZERO
 ZERO  ZERO  ZERO  ZERO ZERO  ZERO  ZERO  ZERO  ZERO  ZERO  ZERO  ZERO  ZERO  ZERO  ZERO  ZERO  ZERO  ZERO  ZERO
 ZERO  ZERO  ZERO  ZERO ZERO  ZERO    10  ZERO  ZERO  ZERO  ZERO  ZERO  ZERO  ZERO    10  ZERO  ZERO  ZERO
 ZERO    10  1000  ZERO ZERO  1000  ZERO  ZERO  ZERO  ZERO  ZERO   100  ZERO  7ERO  ZERO  ZERO   100  ZERO  ZERO
 ZERO 10000  ZERO  ZERO
STIMULATED NEURONS  127  THROUGH      134
STIMULATED NEURONS  147  THROUGH      154
STIMULATED NEURONS  167  THROUGH      174
STIMULATED NEURONS  187  THROUGH      194
STIMULATED NEURONS  207  THROUGH      214
STIMULATED NEURONS  227  THROUGH      234
STIMULATED NEURONS  247  THROUGH      254
STIMULATED NEURONS  267  THROUGH      274
TIME    431 OUTPUT IS     70 FIRING DISPLAY
 ZERO  ZERO  ZERO  ZERO ZERO  ZERO  ZERO   100  ZERO  ZERO  ZERO  ZERO     1  ZERO  ZERO  ZERO  ZERO  ZERO  ZERO
 ZERO  ZERO  ZERO  ZERO ZERO  ZERO [1111 11110] ZERO  ZERO [1111 11110] ZERO  ZERO [1111 11110] ZERO  ZERO [1111
11110) ZERO  ZERO [1111 11110) ZERO  ZERO [1111 11110) ZERO  ZERO [1111 11110] ZERO  ZERO [1101  1110) ZERO  ZERO
 ZERO  ZERO  ZERO  1010 ZERO  ZERO  ZERO  ZERO    10  ZERO  ZERO  ZERO     1     1    10  ZERO  ZERO  ZERO  ZERO
 ZERO  ZERO  ZERO  ZERO
TIME    432 OUTPUT IS     18 FIRING DISPLAY
 ZERO  ZERO  ZERO  ZERO ZERO  ZERO  ZERO  ZERO 10000  ZERO  ZERO    10  ZERO   (1) ZERO  ZERO     1  ZERO  ZERO
    1  ZERO  ZERO  ZERO ZERO  ZERO  ZERO  ZERO  ZERO  ZERO  ZERO  ZERO  ZERO    10  ZERO  ZERO  ZERO  ZERO  ZERO
 ZERO  ZERO  ZERO  ZERO ZERO  ZERO     1  ZERO  ZERO  ZERO 10000  ZERO  ZERO  ZERO   (1) ZERO     1 10000    10
 ZERO  ZERO  ZERO  ZERO ZERO 10000  ZERO  ZERO  ZERO  ZERO  ZERO  ZERO  1000  ZERO  ZERO  ZERO  ZERO   100   100
 ZERO    10  ZERO  ZERO
TIME    433 OUTPUT IS     25 FIRING DISPLAY
 ZERO  ZERO  ZERO    10 ZERO  ZERO  ZERO     1   100  ZERO  1101  ZERO  ZERO  ZERO  ZERO 10000  ZERO  ZERO  ZERO
 ZERO  ZERO  ZERO  ZERO ZERO  ZERO  ZERO  ZERO  ZERO  ZERO  ZERO  ZERO  ZERO 10000  ZERO  ZERO  ZERO    10  ZERO
 ZERO  ZERO 10000  ZERO ZERO  ZERO  ZERO (1)0000     1 10000     1  ZERO  ZERO  ZERO 10000  ZERO  ZERO   100  ZERO
 ZERO  1000  ZERO  ZERO ZERO    11  ZERO  ZERO 10000  ZERO  ZERO  ZERO   100  ZERO  ZERO  ZERO  ZERO  ZERO 10000
    1  ZERO   101  ZERO
TIME    434 OUTPUT IS     16 FIRING DISPLAY
 ZERO 10000  ZERO  ZERO ZERO  ZERO  ZERO  1010  ZERO  ZERO  ZERO  ZERO  ZERO  ZERO  ZERO  1000  ZERO  ZERO     1
 1000 10010  ZERO   100 ZERO  ZERO  ZERO  ZERO  ZERO  ZERO  ZERO  ZERO  ZERO  ZERO  ZERO  ZERO  ZERO  ZERO  ZERO
 ZERO    10   (1) ZERO ZERO  ZERO  ZERO  ZERO  ZERO  ZERO  ZERO  ZERO  ZERO  ZERO  ZERO  ZERO  ZERO  ZERO  ZERO
 ZERO    10 10000     1 ZERO  ZERO  ZERO  ZERO  ZERO  ZERO  ZERO  ZERO  ZERO  ZERO 10000  ZERO  ZERO  ZERO  1000
```

Figure 7.11. Experiment 4 (Section 7.4) — Fatigue Inoperative.

(a) Identical to Experiment 3 (Fig. 7.10), except Σ_0 is spartially distributed as shown below.
(b) Identical to (a), except $\tau_0 = 7$.

(a)

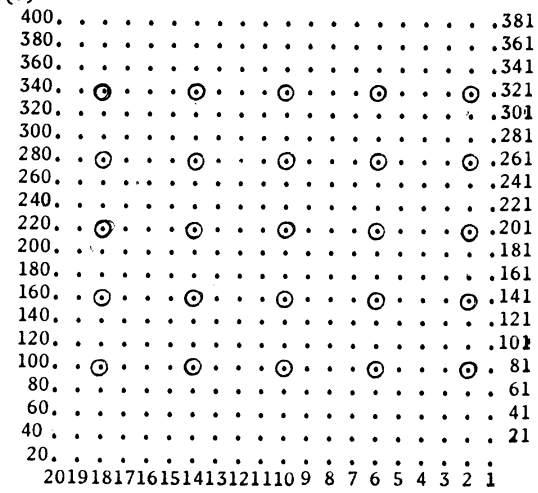

N = 400, R = 4, etc.

Overlapping paths were present, albeit very scantily so. The input set is too diffuse over $\mathcal{R}$ to consistently recruit neurons for successive successor sets Σ_1, Σ_2, etc. (i.e., build a path from $\Sigma_0 \to \Sigma_1 \to \Sigma_2 \to \ldots$). This case, therefore, represents an opposite extreme to that of the preceding two experiments in which Σ_0 was too compact.

Neurons of Σ_0 lie on the rows consisting of neurons 81 - 100, 141 - 160, 201 - 200, 261 - 280, and 321 - 340 respectively of $\mathcal{R}$. These neurons are encircled.

EEG for last half of an "on" period and first half of an "off" period.

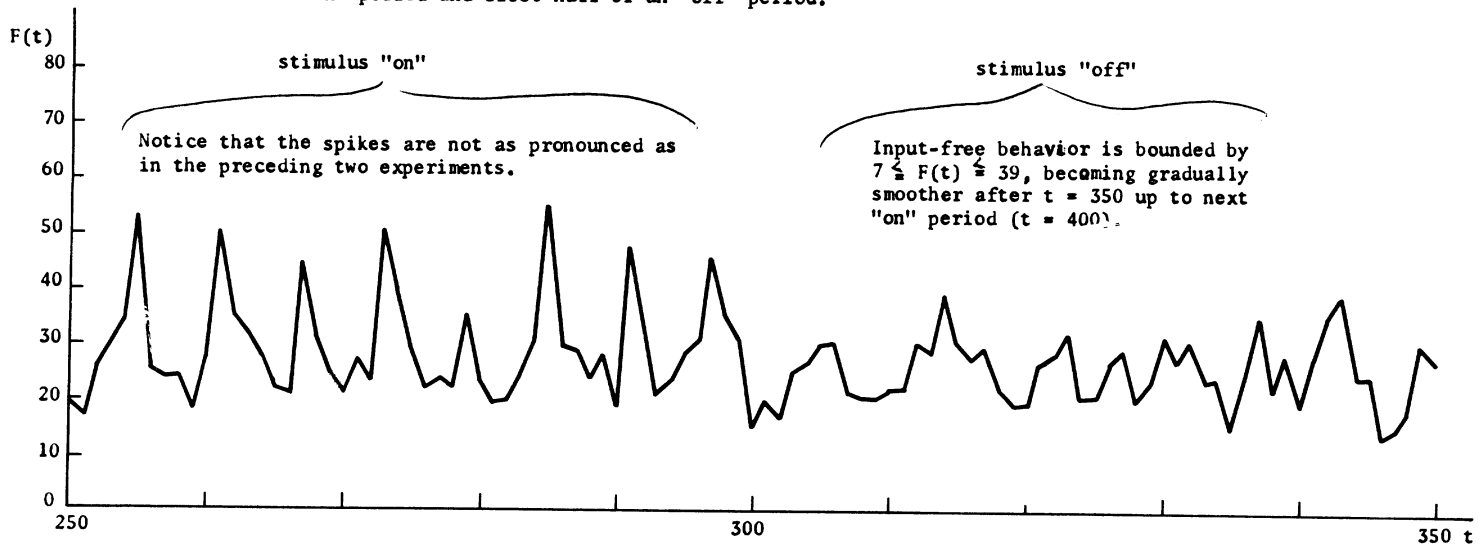

Figure 7.11. (continued).

(b) EEG for the same period as in (a), but with τ_0 = 7. The results were similar to those of (a).

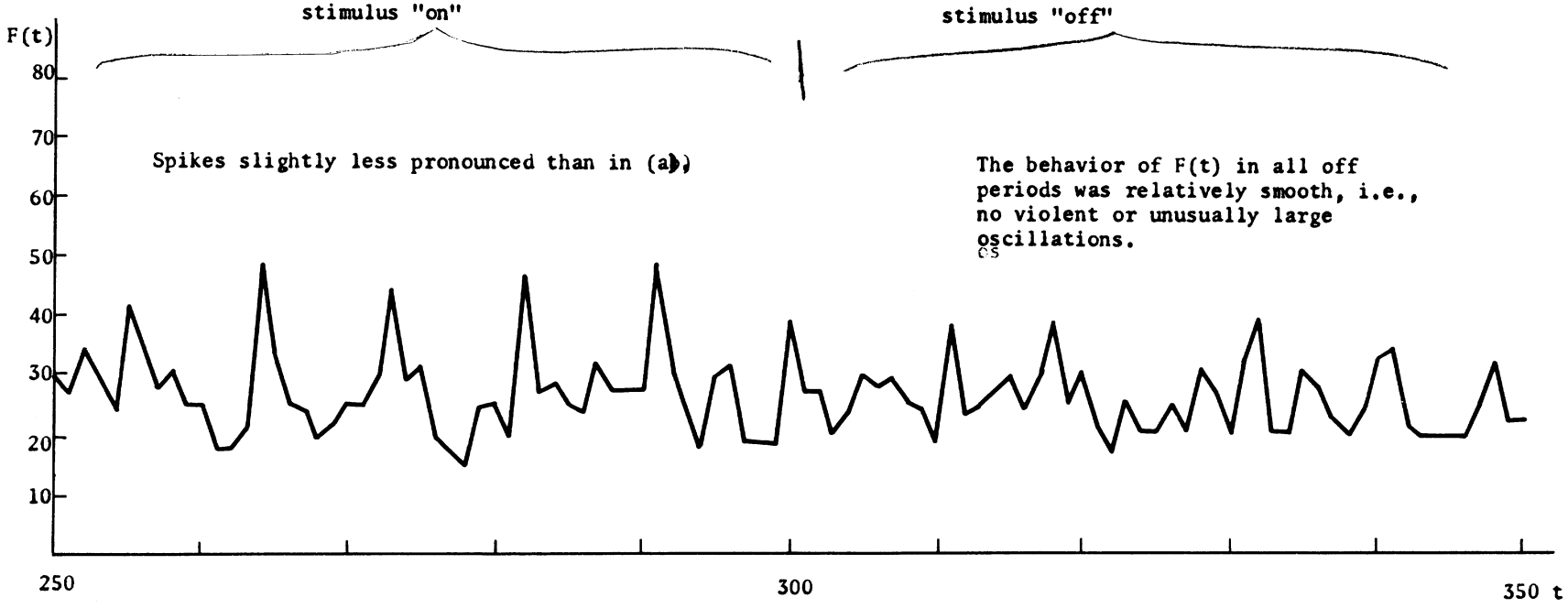

"on" period), off at 300, etc. The run was terminated at t = 482. Samples from the EEG and firing patterns are given in Figure 7.9.

No overlapping paths were detected in this experiment. It appeared that the input area created a refractory zone which did not allow direct successor neurons of Σ_0 to fire after stimulation (the danger of this occurring was noted in Chapter 4). The input area was therefore enlarged for the next experiment.

Experiment 3: The network of Experiment 4, Section 6.6.3, at t = 200 was used. Σ_0 was taken as an 8 x 8 subgrid of $\mathcal{M}$, $\tau_0 = 6$, $S_0 = 8.3$, t = 100. The run was terminated at t = 442. The results are summarized in Figure 7.10. As is drawn in the firing pattern samples, some overlapping paths were present. Nonetheless, the input area seems too large and too dense for effective path formation. This led to the spatially distributed input set of the next experiment.

Experiment 4: Again the network of Experiment 4, Section 6.3.3, at t = 200 was taken as the starting point of this experiment. Everything is as in Experiment 3, except that Σ_0 is "spatially distributed", i.e., fixed neurons are chosen for Σ_0, but they are not clustered tightly about each other as in the preceding experiments (see Figure 7.11(a)). The experiment was terminated at t = 444 in the second off period. Overlapping paths were detected. The results are summarized in Figure 7.11(a).

Experiment 5: This was a repetition of Experiment 4 above with $\tau_0 = 7$. The results are summarized in Figure 7.11(b). Again, overlapping paths were present.

Resume of Experiments 1 - 5 (7.4.1.)

The above experiments clearly show that, using "normal" (monotone decreasing from V_{max} to V_q) threshold curves V(r), overlapping paths may

Figure 7.12. Experiment 6 (Section 7.4) — Fatigue Operative.

The network of Fig. 6.27, Experiment 8 (Section 6.3), at t = 400 was used. V(r) is that of Fig. 6.21, $\phi(\ell)$ — Fig. 6.23, $\Delta_1(\ell)$ and $\Delta_2(\ell)$ — Fig. 6.26. N = 400, R = 6, $\rho = 54.9 = \sum_{s=-2}^{2} \rho_s$, with $\rho_0 = \rho_{-1} = \rho_{-2} = \rho/4$, $\rho_2 = \rho_1 = \rho/8$. Σ_0 as in the preceding two experiments, $\tau_0 = 7$, $S_0 = 8.3$, $t_0 = 100$. The EEG for a complete "on-off" cycle t = 1101 - 1300 is given in (a), the firing patterns for t = 1215 - 1228 displaying overlapping cycles is given in (b)

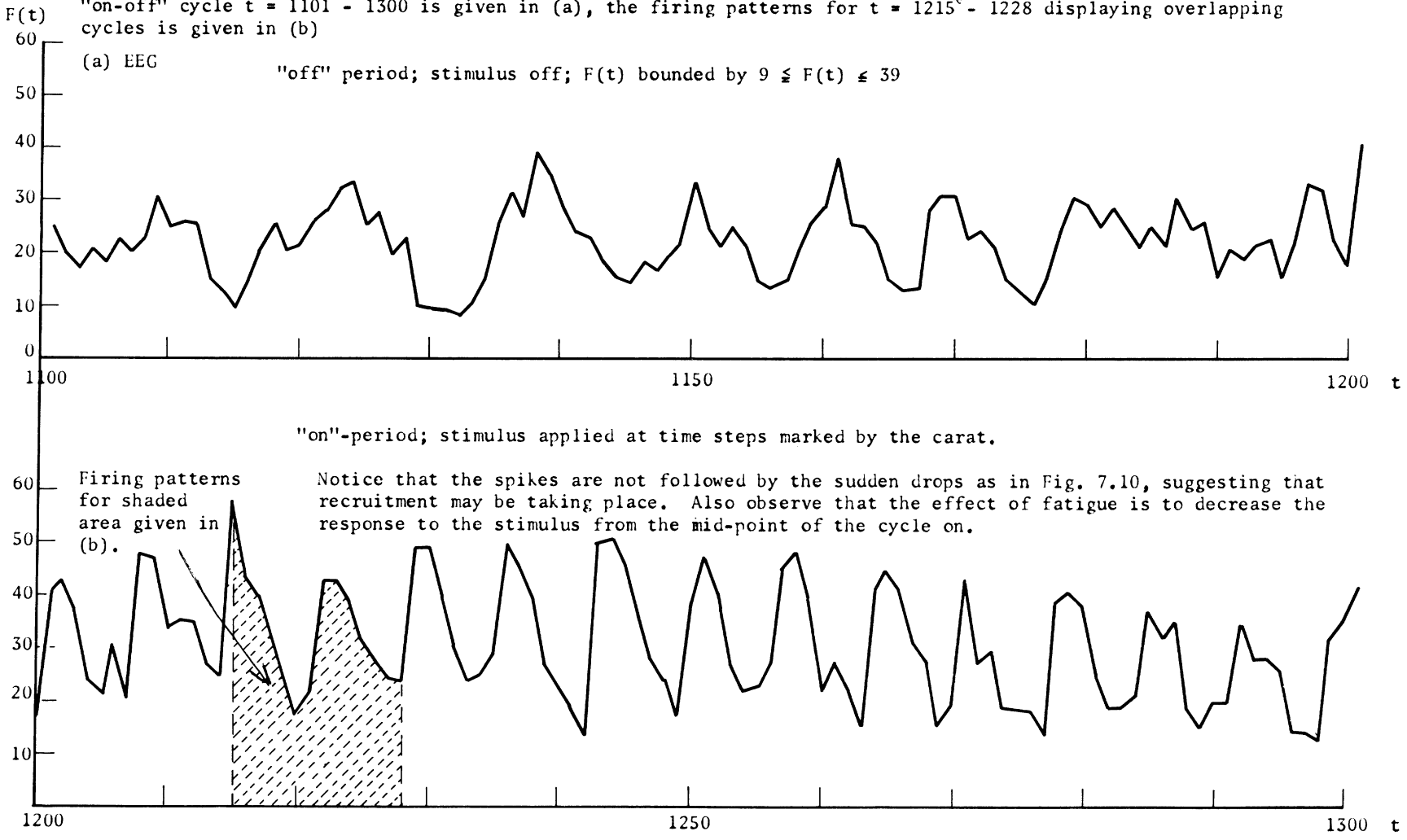

```
INPUT AREA STIMULATED
TIME    1215 OUTPUT IS      58 FIRING DISPLAY
10000  ZERO  ZERO  1010  ZERO  ZERO  ZERO 10000  ZERO     1  ZERO 10000    10  1001  1100 10010  ZERO 11000  1100
 ZERO  ZERO  ZERO    10  ZERO    10  0101   100 10000  ZERO   100  ZERO  ZERO  ZERO  ZERO  ZERO  ZERO    11  1100
  100 10000  1000  ZERO  ZERO  ZERO 10000  ZERO  ZERO  ZERO   100  1001   100 10000  ZERO  1000 10000  ZERO  1000
 1000  ZERO  ZERO   100  1001   000 10000    10    10  ZERO  ZERO  ZERO     1  ZERO  ZERO 10000  1000  ZERO
 ZERO  ZERO     1   100
TIME    1216 OUTPUT IS      44 FIRING DISPLAY
 ZERO  ZERO  ZERO  ZERO  ZERO  ZERO   100  1000 10010    10  ZERO  ZERO 10000  ZERO  ZERO  ZERO  ZERO  ZERO 10010
 ZERO  ZERO    11  1000  ZERO  1000  ZERO  ZERO  1000  ZERO    10     1     1  ZERO     1  ZERO    10  ZERO  ZERO
    10   100  ZERO   110   100  1000  ZERO   100    11 10110 10000    10 10000  ZERO  ZERO 10000  ZERO  ZERO  ZERO
     1  ZERO  ZERO     1  ZERO  ZERO    10  ZERO     1  ZERO  ZERO   100  ZERO    10 10000  ZERO  ZERO  ZERO   100
 ZERO   100  1000  ZERO
TIME    1217 OUTPUT IS      40 FIRING DISPLAY
 ZERO  1000   100  ZERO    10  ZERO  ZERO   100 10000     1  ZERO  ZERO   100 10000  ZERO  1000  ZERO  ZERO
 ZERO  ZERO  ZERO  ZERO 10001  ZERO  ZERO  1000  ZERO  ZERO  1000  ZERO  ZERO 1100  1100   100  ZERO  ZERO 10000
 ZERO  ZERO  ZERO  ZERO    10    10    10     1  1000  ZERO  ZERO  ZERO    10  ZERO  ZERO    10  100  ZERO  ZERO
 ZERO     1 10000  ZERO  ZERO 10001     1  ZERO  ZERO   110  ZERO  ZERO  1001  ZERO  ZERO  ZERO  ZERO  ZERO  ZERO
  010     1 10000  ZERO
TIME    1218 OUTPUT IS      32 FIRING DISPLAY
    1  ZERO  ZERO  ZERO  1000  ZERO  ZERO  ZERO  ZERO  ZERO   100  ZERO   100  ZERO  ZERO  ZERO  ZERO  ZERO  ZERO
 ZERO  1000   100  ZERO  1000  ZERO  ZERO  ZERO  ZERO  ZERO  1100  ZERO  ZERO  ZERO  ZERO  ZERO  ZERO  ZERO
 1000  ZERO  ZERO  1000  1000   100  ZERO 10000   100  ZERO  1000  ZERO     1   100  ZERO   101  0000  ZERO  ZERO
 ZERO  1000  ZERO  ZERO 10100  ZERO  ZERO     1  ZERO  ZERO  ZERO 10010  ZERO 10100  ZERO  ZERO   100  ZERO     1
 ZERO  1000  ZERO  ZERO
TIME    1219 OUTPUT IS      25 FIRING DISPLAY
   10    10  ZERO  ZERO  ZERO  1000  1000   100  ZERO  ZERO  ZERO  ZERO  1000  ZERO  ZERO  ZERO  ZERO  ZERO  ZERO
 ZERO  ZERO  1000  ZERO  ZERO  ZERO 10000  ZERO  ZERO    11  ZERO    10  ZERO  1000  ZERO 11001   100  ZERO  ZERO
 ZERO     1  ZERO  ZERO  ZERO  ZERO  ZERO  ZERO  ZERO  1000  ZERO  ZERO  ZERO  ZERO  ZERO  ZERO  ZERO  ZERO
 ZERO 10000  ZERO  ZERO  ZERO  ZERO  ZERO  ZERO  ZERO 10000   100  ZERO   100  ZERO  ZERO  ZERO  ZERO     1  ZERO
    1 10000  ZERO  ZERO
TIME    1220 OUTPUT IS      18 FIRING DISPLAY
 ZERO     1  ZERO  ZERO     1  ZERO    10    10  ZERO  ZERO  ZERO  ZERO  ZERO  ZERO    10  ZERO  ZERO  ZERO  ZERO
 ZERO  ZERO  ZERO  ZERO  ZERO  ZERO  ZERO  ZERO  ZERO  ZERO   100  ZERO  ZERO  ZERO  ZERO  ZERO  ZERO  1000   100
 ZERO  ZERO   101     1     1  ZERO  ZERO  ZERO 10000  ZERO  ZERO  ZERO  1000  ZERO  ZERO  ZERO  ZERO  ZERO     1
 ZERO  ZERO  1000  ZERO  ZERO  ZERO  ZERO  ZERO  ZERO  ZERO  ZERO  ZERO  ZERO    10 10000  ZERO  ZERO  ZERO
 ZERO  ZERO  ZERO  ZERO
TIME    1221 OUTPUT IS      22 FIRING DISPLAY
 ZERO  ZERO 10000  ZERO  ZERO  ZERO  ZERO  ZERO  ZERO 11000  ZERO  ZERO  ZERO  ZERO  ZERO  ZERO  ZERO  ZERO
 ZERO  ZERO  ZERO  ZERO  ZERO  ZERO  ZERO 10000  ZERO  ZERO  ZERO 10000    10  ZERO  ZERO  1000     1  ZERO
 ZERO  ZERO  ZERO  ZERO  ZERO  ZERO  ZERO  ZERO  ZERO  ZERO  ZERO   100  ZERO     1    10  ZERO    11  ZERO 10000
 ZERO  ZERO  ZERO  ZERO  ZERO  ZERO  ZERO  1000  ZERO  ZERO  ZERO   100  ZERO  ZERO     1    10  ZERO 10000  ZERO
  100  ZERO  ZERO  1001
INPUT AREA STIMULATED
TIME    1222 OUTPUT IS      43 FIRING DISPLAY
 ZERO  ZERO  ZERO  ZERO  ZERO 10000 10100  ZERO  ZERO  ZERO  ZERO  ZERO    00 10000  1000 10000    10  ZERO  ZERO
10000  ZERO  ZERO     1   100    00  0001 10000  ZERO  ZERO  ZERO 10000  ZERO  ZERO  ZERO  ZERO  1100  1001
1001 00000 10000  ZERO  ZERO  ZERO  ZERO  ZERO  ZERO  ZERO    10  1001   000 00000  ZERO  ZERO  ZERO  ZERO  ZERO
 ZERO  ZERO  ZERO     1  1000  000 10000   100   100  ZERO  ZERO  ZERO  ZERO  ZERO  1000   100  ZERO  ZERO  1000
 ZERO  ZERO  ZERO  ZERO
TIME    1223 OUTPUT IS      43 FIRING DISPLAY
 1000  ZERO  ZERO  ZERO  ZERO     1  ZERO  ZERO  ZERO    10  ZERO  ZERO  ZERO    10  ZERO  ZERO  ZERO  0000
 ZERO  ZERO    11  1000  ZERO     1   100  ZERO  ZERO  ZERO  ZERO  ZERO     1  ZERO  ZERO  ZERO 10000  ZERO 10000
    0  ZERO  1000   100  ZERO  0000  ZERO   100    11 10100 10000    00 10000  1010  1000  0000  ZERO  ZERO  ZERO
  100   100  ZERO  ZERO    10  ZERO     1  ZERO     1     1    10  ZERO  ZERO  ZERO 10000  ZERO  ZERO  ZERO 10000
 ZERO  1000    10  ZERO
TIME    1224 OUTPUT IS      39 FIRING DISPLAY
 ZERO     1   100   100  ZERO   100  ZERO  ZERO  1001  ZERO     1  ZERO  ZERO  ZERO 10000  ZERO  ZERO  1000  ZERO
 ZERO   101  ZERO  ZERO 10000  ZERO  ZERO  0000  ZERO  ZERO  ZERO  ZERO  ZERO   100  0001  0000  ZERO  ZERO  ZERO
 ZERO  ZERO  ZERO     1  1000     1  ZERO    10 10000  ZERO     1  ZERO  ZERO  ZERO  ZERO   100  1000  ZERO    10
 ZERO  ZERO 10100     1  ZERO  1001  ZERO  ZERO  ZERO   100  ZERO    10  ZERO  ZERO  ZERO  ZERO  ZERO  ZERO     1
    1     1     1  ZERO
TIME    1225 OUTPUT IS      32 FIRING DISPLAY
 ZERO  ZERO  1000  1000  ZERO  ZERO  ZERO     1  ZERO  ZERO   110   100  ZERO  ZERO  ZERO     1  1000  ZERO  1000
    1  ZERO  ZERO   100  ZERO   100  ZERO  ZERO  ZERO  ZERO    10  1000    10  ZERO  ZERO  ZERO  ZERO  ZERO  ZERO
 1000  ZERO  ZERO  1000 10000  ZERO  1000 10000  ZERO  ZERO  ZERO  ZERO  ZERO  ZERO     1  ZERO  1000  ZERO  ZERO
10000  1000    10  ZERO  100  ZERO  ZERO  ZERO  ZERO  ZERO 10000  ZERO  ZERO  1000  ZERO     1  ZERO  ZERO  ZERO
10000  ZERO  ZERO  ZERO
TIME    1226 OUTPUT IS      28 FIRING DISPLAY
 ZERO  ZERO  ZERO     1  1000  ZERO  ZERO  ZERO  1000   101  ZERO    10 10001  ZERO  ZERO   100     1   100  ZERO
  100  ZERO  ZERO 10000  ZERO  ZERO  ZERO    10  ZERO  ZERO  ZERO    00  ZERO    10  ZERO  1000  ZERO  ZERO    00
 ZERO  ZERO  ZERO 10000  ZERO  ZERO  ZERO  1000   100  ZERO  ZERO  ZERO  ZERO  ZERO  ZERO  ZERO  ZERO  ZERO  ZERO
 ZERO 10001  ZERO  ZERO  ZERO  ZERO  ZERO  ZERO  ZERO  1001  ZERO  ZERO  ZERO  ZERO  ZERO    10  ZERO
 ZERO  ZERO  ZERO 10000
TIME    1227 OUTPUT IS      25 FIRING DISPLAY
 ZERO  ZERO    10    10  ZERO  ZERO  ZERO    10  ZERO  ZERO  ZERO  1000  ZERO 10100  ZERO  ZERO    10    10  ZERO
 1000  ZERO  ZERO    10  ZERO  ZERO  ZERO  ZERO  ZERO  ZERO  ZERO   100  ZERO  ZERO  ZERO  ZERO  ZERO  ZERO  ZERO
 ZERO    10  ZERO  ZERO     1  ZERO    10  ZERO 10010  ZERO  ZERO  ZERO  0000  ZERO  ZERO  1000  ZERO 10000  ZERO
 ZERO    10  ZERO  ZERO  ZERO  ZERO  ZERO  ZERO    10  ZERO  ZERO  ZERO    10  ZERO     1  ZERO  ZERO   100  ZERO
 ZERO    10  ZERO  ZERO
TIME    1228 OUTPUT IS      24 FIRING DISPLAY
10000  ZERO     1 10000   100    10  ZERO 10000 10000  ZERO  ZERO 10000  ZERO  ZERO  1000  1000  ZERO  ZERO  ZERO
 ZERO  ZERO  ZERO  ZERO    10  1000 10000  ZERO  ZERO  ZERO  ZERO  1000  ZERO  ZERO     1  ZERO  ZERO  ZERO  ZERO
 ZERO  ZERO    10  ZERO  ZERO 10010   100  ZERO  ZERO  ZERO  ZERO  ZERO  ZERO  ZERO  ZERO  ZERO     1  ZERO  ZERO
 ZERO  ZERO  ZERO  ZERO  ZERO  ZERO  ZERO  ZERO  ZERO  ZERO  ZERO  ZERO  ZERO  ZERO  ZERO  ZERO 10000  ZERO 10000
 ZERO  ZERO   100     1
```

Figure 7.13. Input Set Σ_0 of Experiment 7.

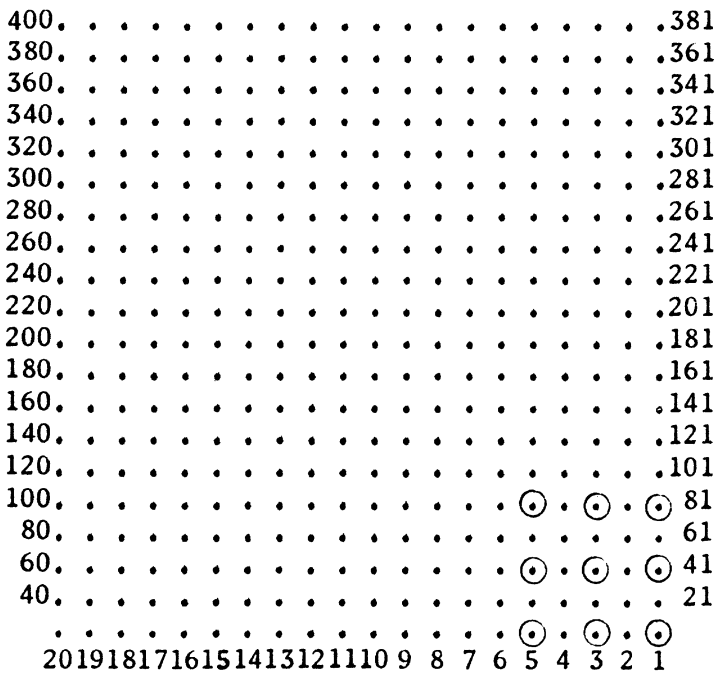

$N = 400$, $R = 6$, $\overline{\overline{C}}_R \cong 13$, $\rho = 54.9 = \sum_{s=-2}^{2} \rho_k$,

$\rho_0 = \rho_{-1} = \rho_{-2} = \rho/4$; $\rho_2 = \rho_1 = \rho/8$.

$\Sigma_0 = \{1, 3, 5, 41, 43, 81, 83, 85\}$

Σ_0 can be covered by a single neighborhood. It is more compact than the Σ_0 of the preceding experiments, but more diffuse than the earlier experiments. The neurons are spaced sufficiently far apart from one another that hyperrecovered regions should not develop, yet sufficiently close that some neurons in $\mathcal{N} - \Sigma_0$ will be directly controllable by Σ_0 (again, in such a fashion as not to create a hyperrecovered "pocket" around Σ_0).

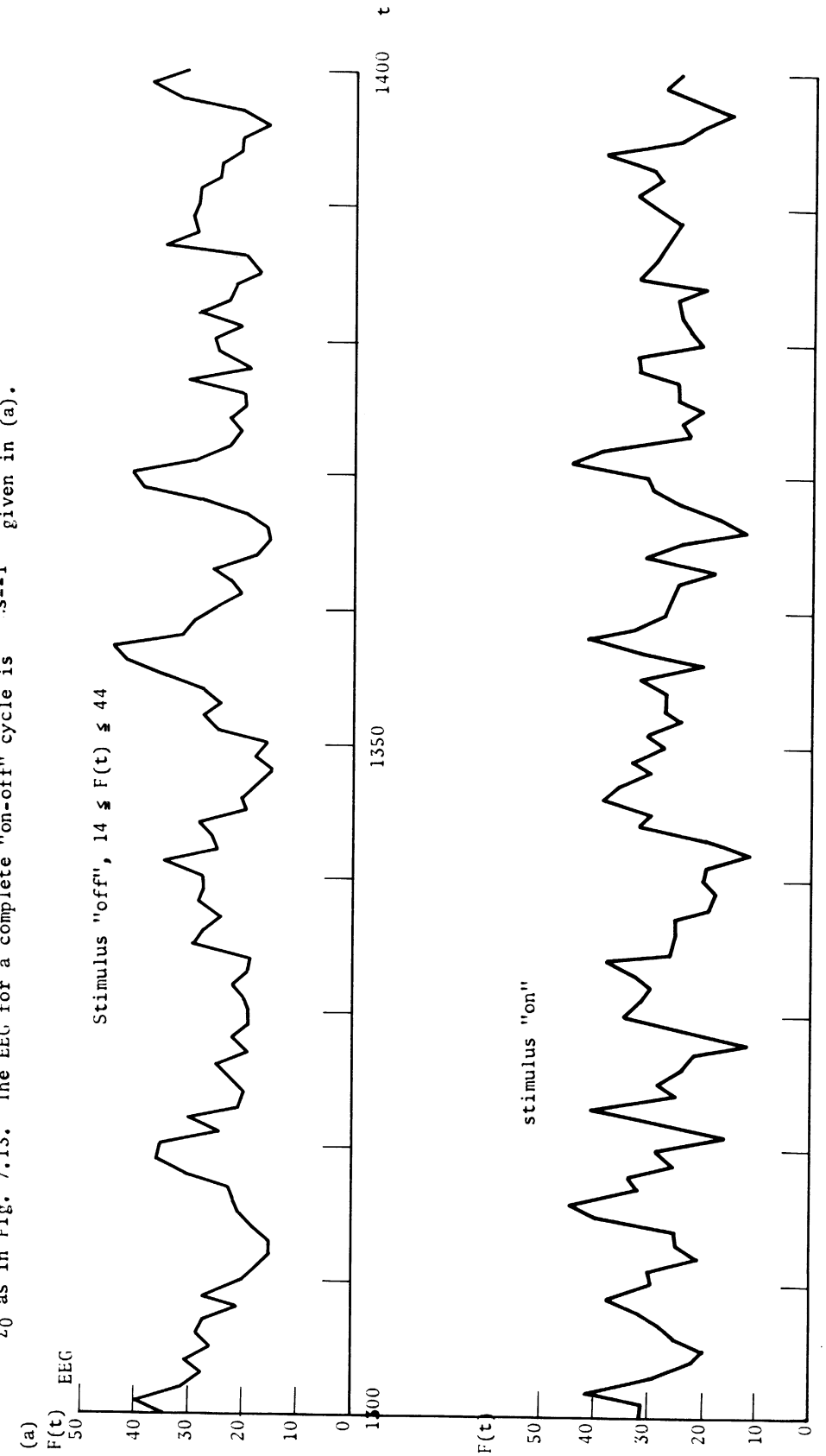

Figure 7.14. Experiment 7 (Section 7.4) — Fatigue Operative.

The network of Fig. 6.28, Experiment 9 (Section 6.3) at $t = 400_2$ was used. V(r) is that of Fig. 6.28, $\phi(\ell)$ - 6.23, $\Delta_1(\ell)$ and $\Delta_2(\ell)$ - 6.26. $N = 400$, $R = 6$, $\rho = 54.9 = \sum_{s=-1}^{L} \rho_s$ with $\rho_0 = \rho_{-1} = \rho_{-2} = \rho/4$, $\rho_2 = \rho_1 = \rho/8$, Σ_0 as in Fig. 7.13. The EEG for a complete "on-off" cycle is given in (a).

Figure 7.14 (continued).

(b) Fragment of an embryonic cycle. The neurons of Σ_0, Σ_1, Σ_2, ... are given together with the connections from a subset Σ_τ to its successor-set $\Sigma_{\tau+1}$. Notice that overlaps occur for $\tau = 0 - 6$, but the connections persist only down through $\tau = 3$. This is a typical situation. Prior to the "closing" of paths $P_\xi(\Sigma_0 \to \Sigma_\tau)$ into cycles $C(\Sigma_0)$, such overlaps occur with the connections either absent or present, but with a moderate synapse-value. Through gradual recruitment and reinforcement, the path eventually will close into a cycle. (A specimen of a cycle is given in Section 7.5).

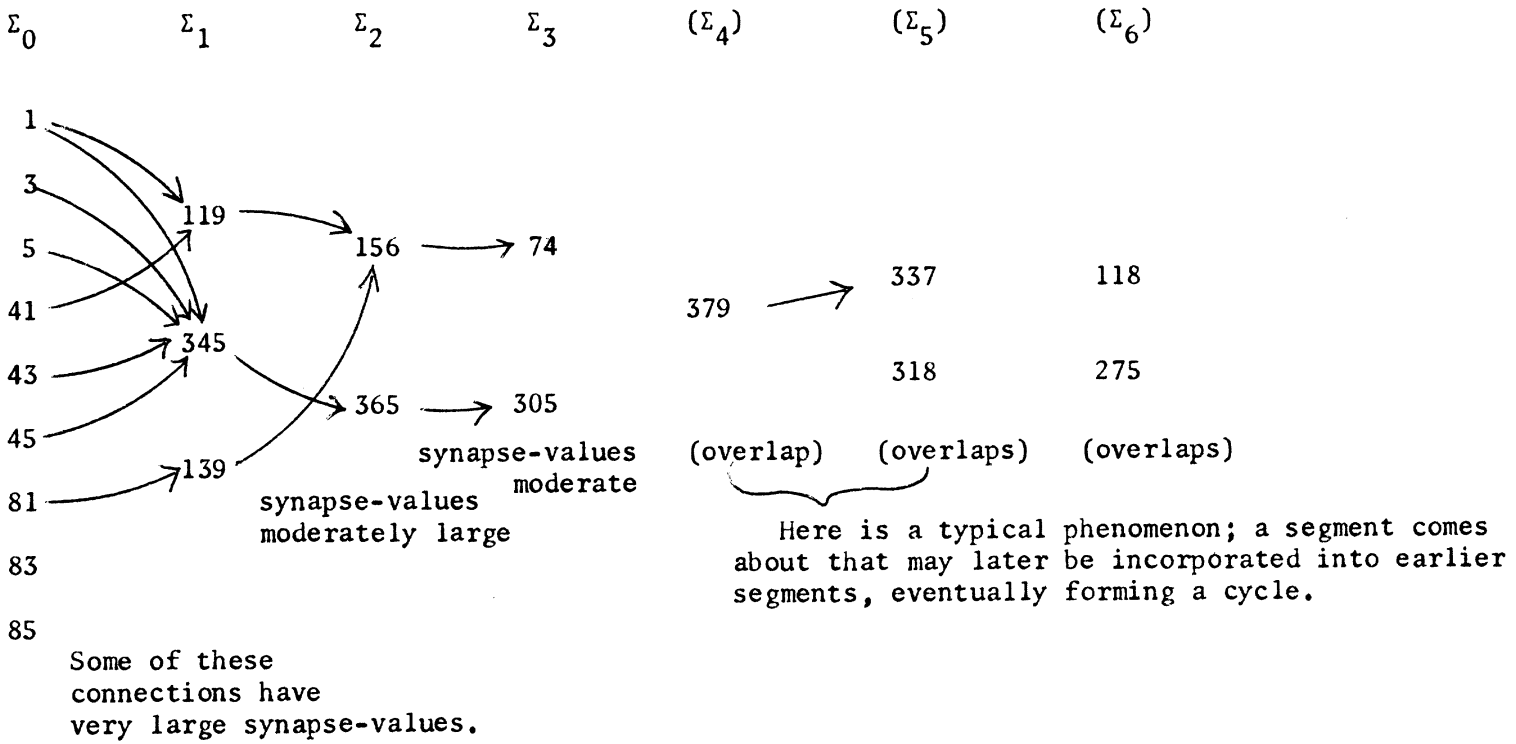

be formed for several values of τ_0 provided Σ_0 and S_0 are judiciously chosen. It now remains to introduce the fatigue mechanism as preparation for more realistic long-run experimentation.

7.4.2 Networks with Fatigue Operative

Experiment 6: The network of Experiment 8, Section 6.3.4, at t = 400 was used. Σ_0 was spatially distributed as in Experiments 4 and 5 above, $\bar{\Sigma}_0 = 7$, $S_0 = 8.3$, $t_\ell = 100$. The run was terminated at t = 1399. The results are summarized in Figure 7.12. Overlapping cycles appear to be present.

This experiment was repeated for lighter stimuli S_0, once for $S_0 = 2.75$, again for $S_0 = 6.25$. As is to be expected, the lighter stimuli did not produce as strong results as the original value $S_0 = 8.3$. However, in both cases, some overlapping paths were present.

The results of this experiment gave the first real hope that overlapping cycles $C(\Sigma_0)$ could be produced.

Experiment 7: The network of Experiment 9, Section 6.3.4, at t = 400 was used as the starting point for this experiment. Σ_0 was chosen as shown in Figure 7.13: The neurons of Σ_0 are spaced regularly over a 5 x 5 grid: $\tau_0 = 7$, $S_0 = 12.25$, $t_\ell = 100$. The network was run through t = 2799. Overlapping cycles were produced, as shown in Figure 7.14 which contains a summary of results for the run.

This run would have been used for further detailed work. However, a minor error in the $D(\lambda)$ and $U(\lambda)$ table handling was uncovered. This error only occurred when a λ_{ji} would reach λ_{max}, therefore it was not uncovered until after the lengthy run above. It did not invalidate the basic result: cycles will form in this network.

Figure 7.15. Input Set Σ_0 for Variant of Experiment 7.

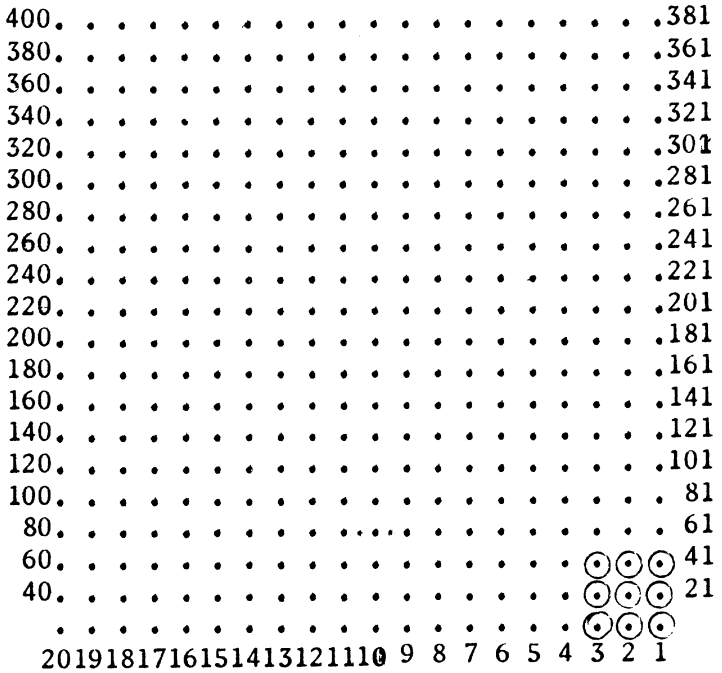

$\Sigma_0 = \{1, 2, 3, 21, 22, 23, 41, 42, 43\}$

This Σ_0 is very compact, thus giving rise to the objection that pockets of hyper-recovered neurons will develop, possibly leading eventually to undesirable (violently oscillatory) behavior. At the same time, however, Σ_0 is sufficiently small with respect to N that this effect should be negligible.

A variant of Experiment 7 was performed using the "tighter" input are Σ_0 of Figure 7.15. As is to be expected, the results were far weaker than those of the original experiment: overlapping paths formed, but not cycles. This demonstrates quite conclusively that Σ_0 must not be either too diffuse or too compact to achieve the best results.

7.4.3 Conclusions

The experiments of this section show that networks $\mathfrak{N}$ exist in which closed cycles $C(\Sigma_0)$ may be produced as a consequence of a patterned stimulation of the subset $\Sigma_0 \subset \mathfrak{N}$.

7.5 CELL ASSEMBLY EXPERIMENTS

In this section, the couse of a particular "learning" experiment is described in detail. First, the very stable network used as the basis for the experiment was selected (network of Experiment 9, Chapter 6, Section 6.3). This was followed by a "training" period of approximately three thousand time steps during which a periodic stimulus was applied in an "on-off" envelope to a subset Σ_0. During this training period overlapping cycles came into being. However, towards the end of the period, undamped oscillations arose, resulting in that scourge of neural-network simulation, namely F(t) going to zero.

Consequently, to determine and to eliminate the cause of these fatal oscillations, a detailed series of control experiments was conducted by returning to an earlier point in the experiment and proceding from that point on with new parameter settings.[1] The difficulty, essentially

[1] This represents an instance in which the "roll-back" or "back-up" feature mentioned earlier proved to be absolutely indispensable. The cost of this experiment was prohibitive to begin with. It would have been impossible to repeat the entire sequence anew — were this even desirable. Since the entire state of the experiment was recorded periodically on magnetic tape, it was possible to return to an earlier point, adjust whichever parameter seemed pertinent and continue on from there. Thus, the necessity of multiple (and exhorbitantly costly) reruns of the entire experimental sequence was sidestepped.

an imbalance in the fatigue function, was uncovered and rectified.

Following all this, the network was subjected to an alternating periodic stimulus sequence, one of the stimuli being applied to the Σ_0 of the earlier phase of the experiment at the same rate as before, the other to another disjoint subset Σ_0^* at a different rate. Unfortunately, it was not possible to carry this sequence out to its conclusion. Precious funds for computer-time were exhausted. However, it did produce (a) a closed cycle $C(\Sigma_0)$ as a consequence of the earlier training portion of the experiment; (2) the beginnings of a closed cycle $C(\Sigma_0^*)$ as a consequence of the last phase; (3) strong symptoms of the development of cross-inhibition between the cycle $C(\Sigma_0)$ and the embryonic cycle $C(\Sigma_0^*)$. It is the author's contention that the results of these experiments are sufficiently strong to warrant more extensive investigation in the future using considerably larger and more complex networks than was possible here. This could be achieved via the superior computer facilities emerging today.

7.5.1 An Adequate Network

The most impressive of the steady-state experiments (using networks with distance-bias and negative feedback) was Experiment 9 of Section 6.6.3. For the network of that experiment, some of the pertinent parameters are

$N = 400$

$R = 6$ (hence, $\overline{\overline{C}}_R \cong \pi R^2 = 113$ neurons)

$\rho = \rho_{-2} + \rho_{-1} + \rho_0 + \rho_1 + \rho_2 = 55$ where $\rho_0 = \rho_{-2} = \rho_{-1} = \rho/4$, $\rho_2 = \rho_1 = \rho/8$

(see Figure 6.28, Chapter 6). Fatigue was operative.

Figure 7.16. Example of a Closed Chain within a Cycle $C(\Sigma_0)$.

(a) Neurons of the respective successor-sets are given, together with the synapse-levels at t = 2000 (above the arrows) and t = 2900 (below the arrows). Notice that all synapse-levels have increased, that from Σ_0 to $\Sigma_\tau \equiv \Sigma_0$ the least.

$$\Sigma_0 \to \Sigma_1 \to \Sigma_2 \to \Sigma_3 \to \Sigma_4 \to \Sigma_5 \to \Sigma_6 \to \Sigma_7 \equiv \Sigma_0$$

$$5 \xrightarrow[63]{56} 30 \xrightarrow[63]{44} 395 \xrightarrow[47]{46} 393 \xrightarrow[47]{40} 31 \xrightarrow[50]{40} 151 \xrightarrow[61]{52} 50 \xrightarrow[34]{33} 5$$

Note: Scaling of the synapse-levels. A synapse-level of 32 corresponds to 0 synapse-value, 36 to +1, 40 to +2, etc.

(b) The chain given above is shown in the geometry of $\mathfrak{N}$. The neurons of Σ_0 are encircled; neurons of the chain are marked with an "X". Recalling that R = 6, one notices that several of the neurons of the chain are not directly connectable to any neuron of Σ_0.

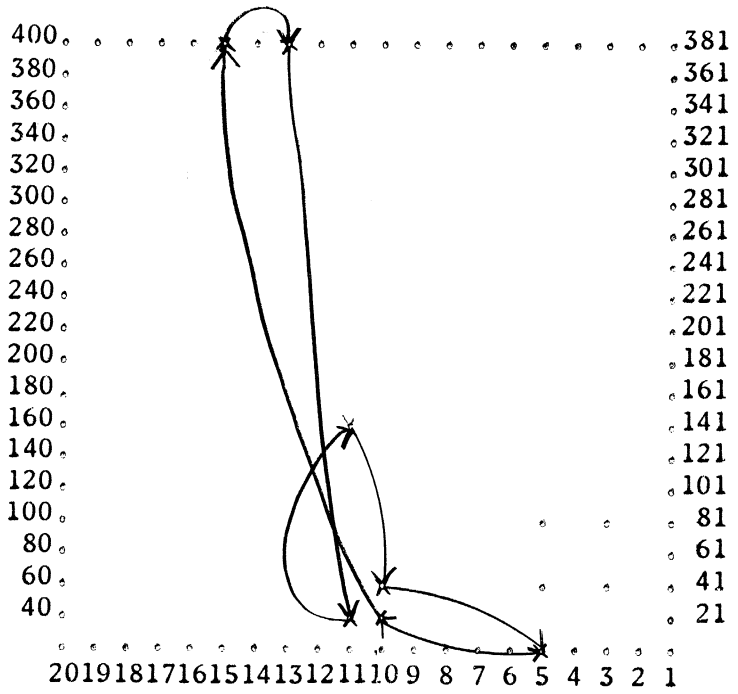

This experiment was run from t = 1 to t = 400 and appeared to be very stable. $F_{max} = 36$, $F_{min} = 8$. Synapse levels drifted of course from their initial settings, but the net drift based on a sample of synapse-levels appeared to be zero. The slight tendency towards underdamping, it was reasoned, should be suppressed by action of the fatigue mechanism, since all neurons were fully recovered with respect to fatigue initially.

7.5.2 Single Periodic Stimulus Series

This series basically is a repitition and a continuation of Experiment 7 of Section 7.4 with the relatively minor error in the $D(\lambda)$ and $U(\lambda)$ tables corrected. The network of the preceding section at t = 400 was taken as the starting point. Just as in Experiment 7, Section 7.4, Σ_0 consisted of nine neurons spaced over a 5 x 5 grid in $\mathcal{G}$ (see Figure 7.13), $\tau_0 = 7$ (the interval between successive stimuli), $S_0 = 12.5$ (constant external stimulus added every τ_0 time steps to total input stimulus for each neuron of Σ_0), and $t = 100$ (length of "on-off" envelopes). The experiment was run through t = 3721 with the stimulus "on" (being applied every τ_0 time steps) in intervals t = 401 - 500, 601 - 700, 801 - 900, ... and "off" (no external stimulus) otherwise (t = 501 - 600, 701 - 800, 901 - 1000, ...).

As in Experiment 7, the results were quite good. By t = 2900, overlapping cycles had formed. A closed chain within one of these cycles is displayed in Figure 7.16. Included in the figure are the synapse-levels from each neuron of this chain to its successor which were sampled at t = 2000 and t = 2900. Notice that they have all increased, as predicted by the theory. It is also interesting to observe that the synapse-level increasing the least is the last "link" of the chain, i.e., from Σ_{τ_0-1} to

Figure 7.17. Selected EEG's for the Cell-Assembly Experiment (Section 7.5.2).

(a) t = 2950 - 3050. The interval t = 2950 - 3000 is the last half of an "off" period; t = 3001 - 3050 the first half of an "on" period. The sequence is typical of all but the last several hundred time steps of the run. The slight underdamping referred to in the text is noticeable here. The abrupt dip at t = 3049 suggests that an excessive number of neurons have been overfatigued and are not available for recruitment.

(b) t = 3620 - 3721, F(3721) = 0. The interval t = 3620 - 3699 is the last part of the last "on" period; t = 3700 begins the last "off" period, aborting when F(t) becomes zero t = 3721. The decay in F(t) over t = 3620 to 3668 and over t = 3694 to 3721, large spikes being absent, suggests again that a fatally excessive number of neurons have been over-fatigued, not recovering sufficiently fast to sustain steady-state when the stimulus is turned off at t = 3700.

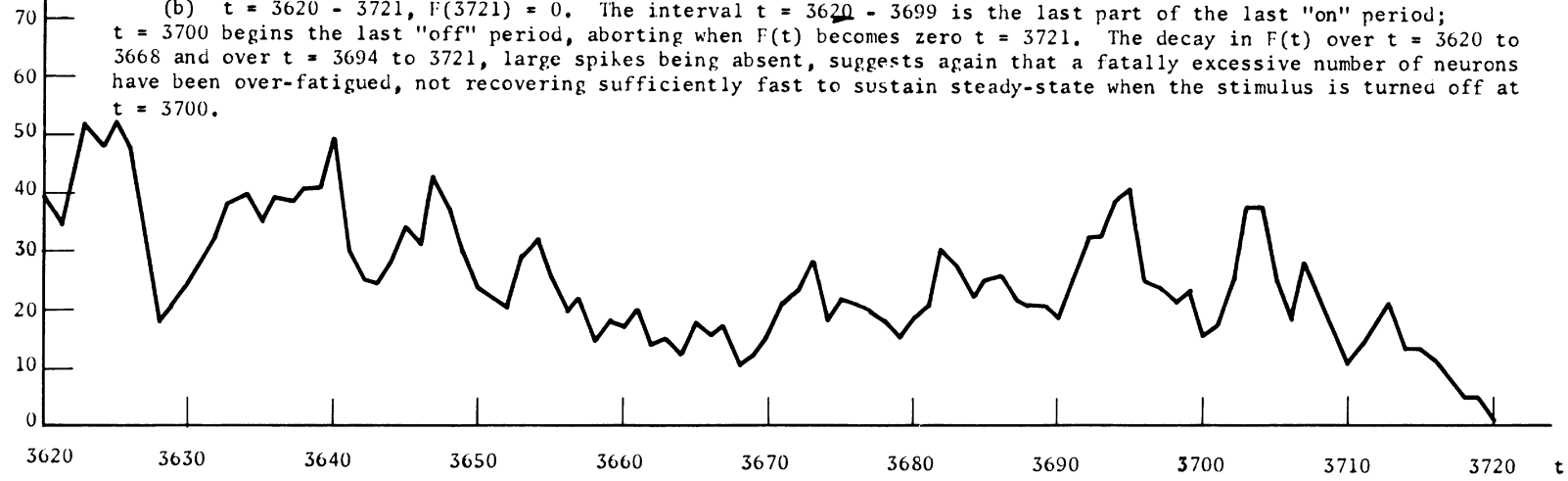

Σ_{τ_0}. Typically the strongest (greatest increase) occurs in the first half of the cycles $C(\Sigma_0)$, the weakest in the last half, especially in the link from Σ_{τ_0-1} to Σ_{τ_0}.

The behavior of the network in this experiment appeared to be quite normal up to approximately t = 3500. From then on, progressively more and more violent oscillations developed, resulting in F(t) going to zero at t = 3721 (an "off" period of the stimulus). EEG's for selected intervals of this experiment are given in Figure 7.17, contrasting the early behavior of the network with the later.

Since all network parameters had been quite carefully chosen, this was a most unexpected result. However, analysis revealed that the most probable culprit was the fatigue mechanism. It appeared that large groups of neurons were getting "trapped" in lower fatigue states, ℓ, (higher fatigue values, $\phi(\ell)$) and not recovering sufficiently fast so as to prevent pockets of hyper-refractory neurons from developing. Thus a hyper-refractory pocket develops. If F(t) does not go to zero, sooner or later the neurons of this pocket will recover. Then, the entire group could be forced to fire by a relatively small number of neurons firing the preceding time step. Once again, as suggested in Chapter 4, Section 4, violent and possibly fatal oscillations are possible.

Assuming the fatigue mechanism to be the source of the difficulty, the following questions then arise:

(1) what defect in the fatigue mechanism caused this "trapping"?

(2) how can this defect (if one is discovered) be corrected?

(3) would it be possible to back up to an earlier point in the experiment, making the necessary changes to eliminate the defect, and continue the experiment?

In the next section, the assumption above is shown to be valid, the defect is isolated and rectified. Most important of all, the answer to (3) is shown to be in the affirmative.

7.5.3 Analysis and Control Experiments

To show the assumption that the fatigue mechanism is primarily responsible for F(t) going to zero in the experiment of Section 7.5.2, it is first necessary to examine carefully all basic assumptions regarding fatigue made so far. Sufficient details of the relationship between $\phi(\ell)$ (fatigue value), ℓ(fatigue level or state), and $\Delta_1(\ell)$ and $\Delta_2(\ell)$ have been given in Chapter 2 and need not be repeated here. What is lacking so far is a calculus for the fatigue function analogous to that of Chapter 4 for the threshold function. This calculus would relate the functional forms of $\phi(\ell)$ and V(r) with the distributions $\mathcal{R}(t)$ of neurons over recovery states and $\mathcal{F}(t)$ of neurons over fatigue states which preserve a steady-state behavior F(t) $(E(F(t)) = F_b)$.

Such a calculus was not developed here. Instead the following heuristic reasoning was made (which, until the last experiment, worked quite well). Consider the distribution of intervals r_{q_i} between firings for all neurons i of $\mathcal{N}$. In steady-state, one would expect these to be distributed approximately normally about the mean $\hat{r}_q = \frac{N}{F_b}$. The variance $\sigma^2_{r_q}$ would be determined empirically by the variations in F(t) from F_b. This would seem to imply the following general characteristics of $\mathcal{F}(t)$ (distribution of neurons over fatigue levels): in steady-state, the neurons of $\mathcal{N}$ tend to cluster normally about a mean $\hat{\ell}$ with a variance σ^2_{ℓ} again determined by the variation of F(t) from F_b. Periodic stimulation of a subset $\Sigma_0 \subseteq \mathcal{N}$ would tend to make this distribution bimodal —

the neurons of Σ_0 and those affected by Σ_0 going into lower fatigue states (higher fatigue values), clustering about a level $\hat{\ell}'$ (determined by the stimulus-rate Σ_0 and period t_ℓ). After cessation of the stimulus, the distribution should gradually "drift" back to its normal unimodal state. The rate of "drift" back to $\hat{\ell}$ and the rate of increase to the second mode $\hat{\ell}'$ are determined by $\Delta_1(\ell)$ and $\Delta_2(\ell)$ respectively.[1] The choice of $\phi(\ell)$ (lacking our fatigue calculus) is still made on intuitive grounds as described below.

There are then two problems; (1) the determination of $\hat{\ell}$ and (2) determination of $\phi(\ell)$. The following procedure was used: set $\ell_i(0)$ for each neuron $i \in \mathcal{N}$ to ℓ_{max}. Set $\phi(\ell)$ so that it gradually increases from zero (as ℓ decreases from ℓ_{max}) at a constant rate (see Figure 7.5) until $\ell = \ell_1 \ (= 38) = \ell_{max}/2$, then let $\phi(\ell)$ increase at a much greater rate. The reasoning was that $\mathcal{G}(t)$ should tend from its initial distribution (all ℓ_i's equal to ℓ_{max}) to the one postulated above around some $\hat{\ell}$ with $\ell_1 < \hat{\ell} < \ell_{max}$. The sharp upward bend in $\phi(\ell)$ at ℓ_1 was to ensure that the rare neurons (lower tail of the distribution $\hat{r}_{q_i}$ about $\hat{r}_q$) firing at much greater rate than once every $\hat{r}_q$ time steps will eventually be "damped out" and forced back to the background rate.

This reasoning worked quite well in earlier experiments and possibly

---

[1] At the risk of being pedantic, an observation is in order here. If $\mathcal{N} = N$ is very large relative to $\bar{\Sigma}_0$,

$$\mathcal{N} >> \bar{\Sigma}_0,$$

there is a serious doubt in the author's mind that such a shift to bimodality would be observable, since the relative number of neurons of $\mathcal{M}$ affected would be quite small. In the present situation, with $\bar{\Sigma}_0/\mathcal{N} \cong 2\%$, the shift definitely is observable.

would have worked in the experiment of Section 7.5.2 above had the author been more careful. For, detailed study of the distributions $\mathcal{J}(t)$ for that experiment and for control experiments performed by "backing-up" to earlier points in the experiment revealed the following facts:

(1) $\mathcal{J}(t)$ did not settle down as expected to a distribution about a stationary $\hat{\ell}$, rather $\hat{\ell}$ seemed to be gradually decreasing (toward ℓ_1).

(2) The interval t_ℓ was too short to allow the neurons of Σ_0 (hence the neurons of $\mathcal{N}$ driven by Σ_0, etc.) to completely recover with respect to fatigue during the "off" period of the stimulus. Thus these neurons became progressively more and more fatigued, eventually creating a large zone of hyper-refractory neurons.

(2) is easily seen a priori from the following calculations: if a neuron of $\mathcal{N}$ fires at an average rate of $1/\tau_0$ (once every τ_0 time steps), then the net change in ℓ over τ time steps would be:

$$\Delta_\tau = (\Delta_2 \frac{1}{\tau_0} - \Delta_1 (1-\frac{1}{\tau_0}))$$

Assuming $\tau_0 = 7$, $\Delta_1 = 1/16$, $\Delta_2 = 1.0$ (assuming Δ_1 and Δ_2 constant for all ℓ for the moment), this gives

$$\Delta_\tau/\tau \cong 1/11.2$$

For $\tau = t_\ell = 100$, then,

$$\Delta_\tau = 8.92$$

Thus, in an "on" period, ℓ would go from ℓ_0 to $\ell_0 - \Delta_\tau = \ell_0 - 8.92$.

With the stimulus "off", on the other hand, ($\tau_0 = \infty$, $1/\tau_0 = 0$)

$$\Delta_\tau/\tau = \Delta_2 \cdot 0 - \frac{1}{16}(1-0) = -1/16$$

and for $\tau = t_\ell = 100$,

$$\Delta_\tau = -6.35$$

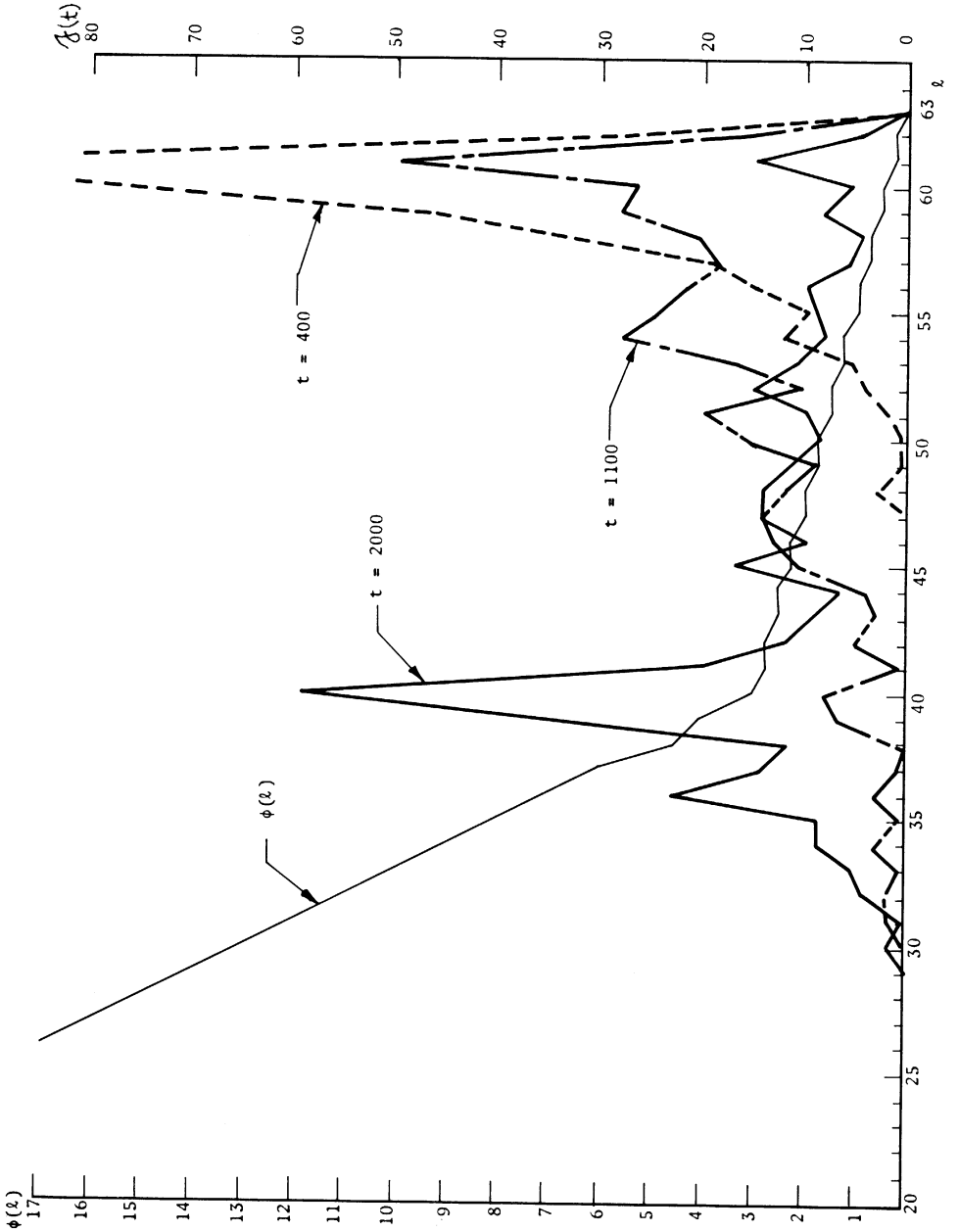

Figure 7.18. $\mathcal{F}(t)$'s for Cell-Assembly Experiment (Section 7.5.2).

The fatigue distributions $\mathcal{F}(t)$ for t = 400, 1100, and 2000 are given below. Notice the shift in the apparent ℓ from approximately ℓ = 58 at t = 400 to ℓ = 40 at t = 2000. Also, observe the secondary peak around ℓ = 36 at t = 2000. This is typical and represents the bimodality mentioned in the text arising from stimulating Σ_0. This secondary peak is most pronounced after an "on" period, less so after an "off" period (since neurons affected by Σ_0 have partially recovered with respect to fatigue). t = 2001 begins the next "on" period. Interpretation: The left-hand vertical ordinate indicates $\phi(\ell)$ in units of synapse-value; the right-hand ordinate the number of neurons of $\mathcal{H}$ with fatigue-state ℓ.

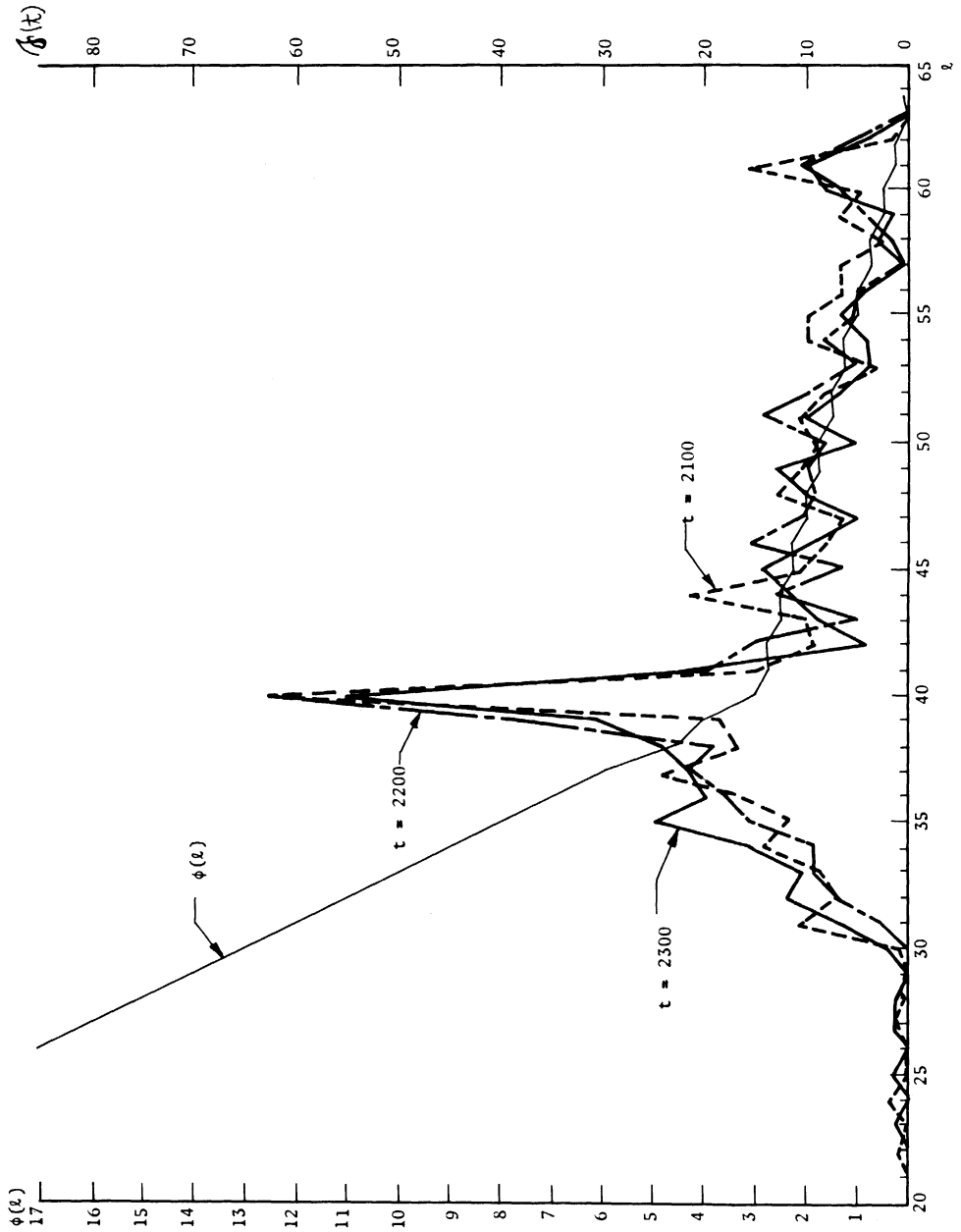

Figure 7.19. $\mathcal{F}(t)$'s for Cell-Assembly Experiment (Section 7.5.2) — Continued.

The fatigue distributions $\mathcal{F}(t)$ for t = 2100 (end of an "on" period), t = 2200 (end of an "off" period), and t = 2300 (end of an "on" period) are given below. Interpretation: same as Fig. 7.18, q.v.. Additional neurons appear to be drifting from large values of ℓ towards the apparent $\hat{\ell}$ = 40. The bimodality is perhaps most pronounced at t = 2300 at the end of the last stimulus period.

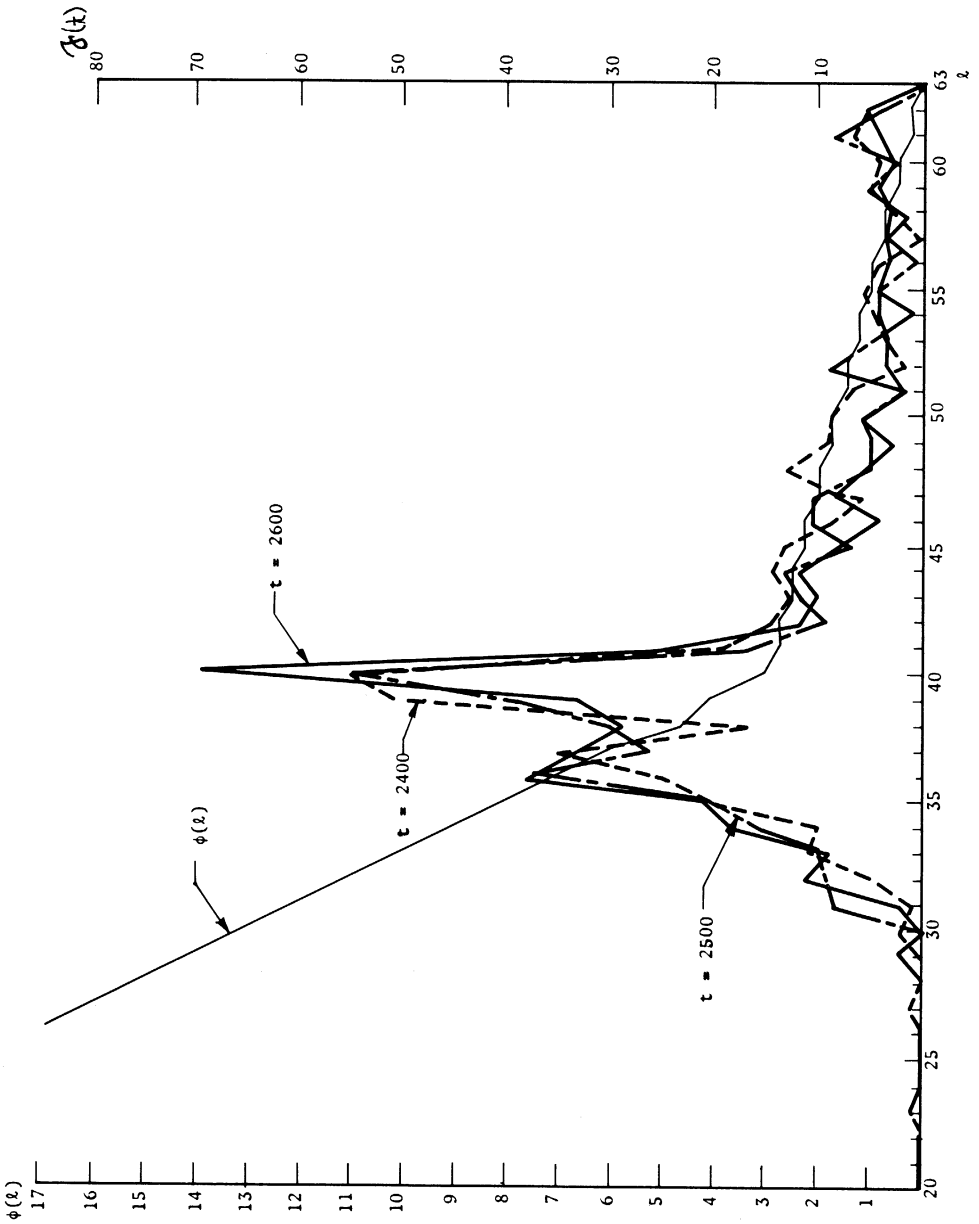

Figure 7.20. $\mathcal{J}(t)$'s for Cell-Assembly Experiment (Section 7.5.2) — Continued.

The fatigue distributions $\mathcal{J}(t)$ for t = 2400 (end of an "off" period), t = 2500 (end of an "on" period), and t = 2600 (end of an "off" period) are given below. Interpretation: same as Fig. 7.18, q.v.. Notice that additional neurons appears to be drifting towards ℓ = 40 from higher values of ℓ. Notice also that the bimodality is more striking, especially at the end of the "on" period t = 2500, the more highly fatigued neurons recovering somewhat by t = 2600.

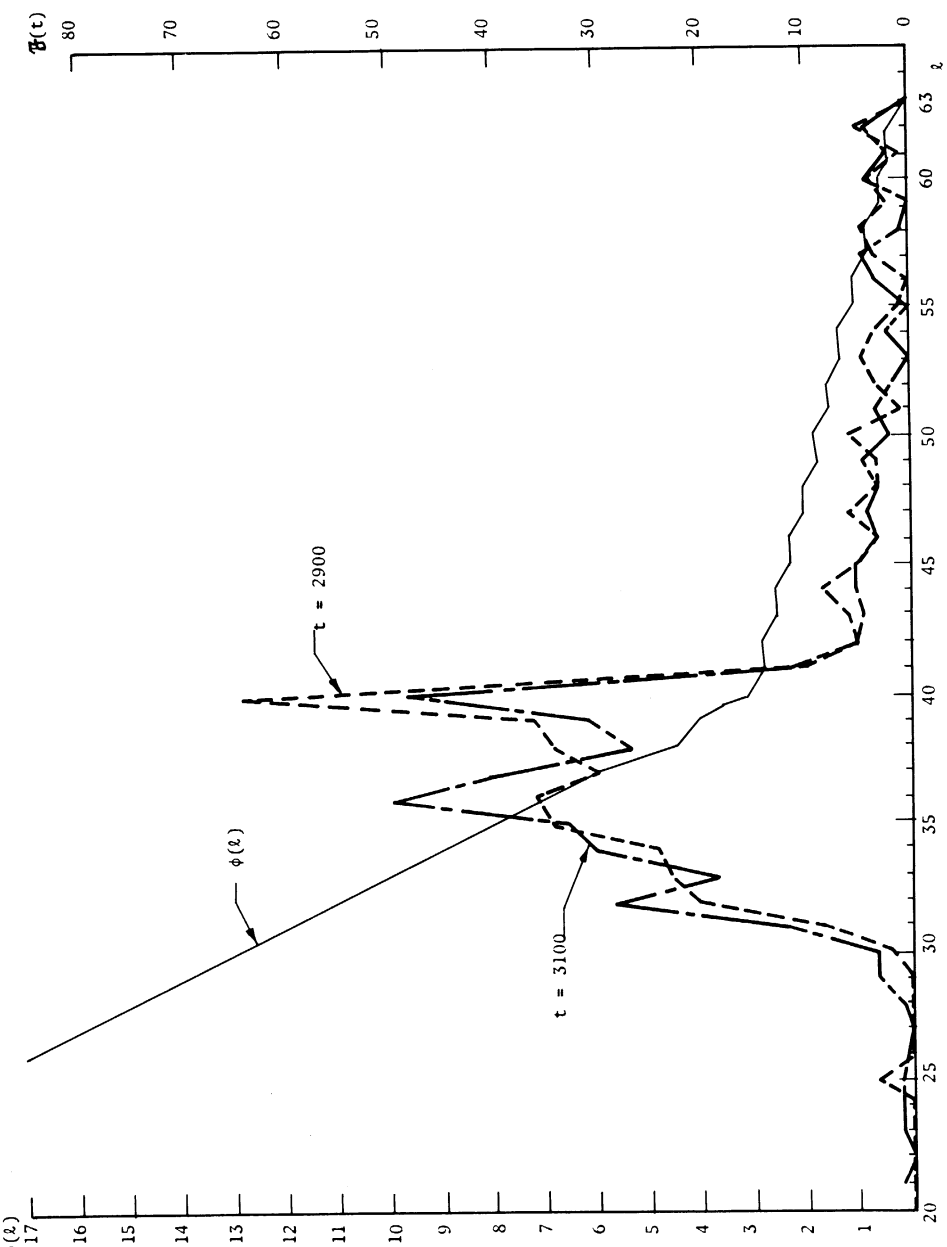

Figure 7.21. $\mathcal{F}(t)$'s for Cell-Assembly Experiment (Section 7.5.2) — Continued.

The fatigue distributions $\mathcal{F}(t)$ for t = 2900 (end of an "on" period) and t = 3100 (end of an "on" period) are given below. The bimodality in $\mathcal{F}(t)$ is even more obvious now than previously. In fact, the peak at t = 36 and the dearth of neurons at lower fatigue values (larger fatigue states ℓ) suggest that excessively many neurons have been driven above the apparent $\hat{\ell}$ of ℓ = 40 — i.e., these neurons are highly fatigued and becoming progressively less accessible to the steady-state pool of neurons needed to guarantee a stable, steady-state behavior in $\mathcal{H}$. Interpretation: same as Fig. 7.18, q.v..

Figure 7.22. Terminal $\mathcal{T}(t)$ for Cell-Assembly Experiment.

The fatigue distribution $\mathcal{F}(t)$ at t = 3720, one time step before $\mathcal{T}(t)$ went to zero, is given here. Notice that the largest peak occurs at ℓ = 37, the majority of neurons of $\mathcal{A}$ have fatigue state $\leq$ 40, hence are excessively fatigued ($\phi(\ell)$ large). This suggests the "trapping" defect of the fatigue mechanism mentioned in the text.

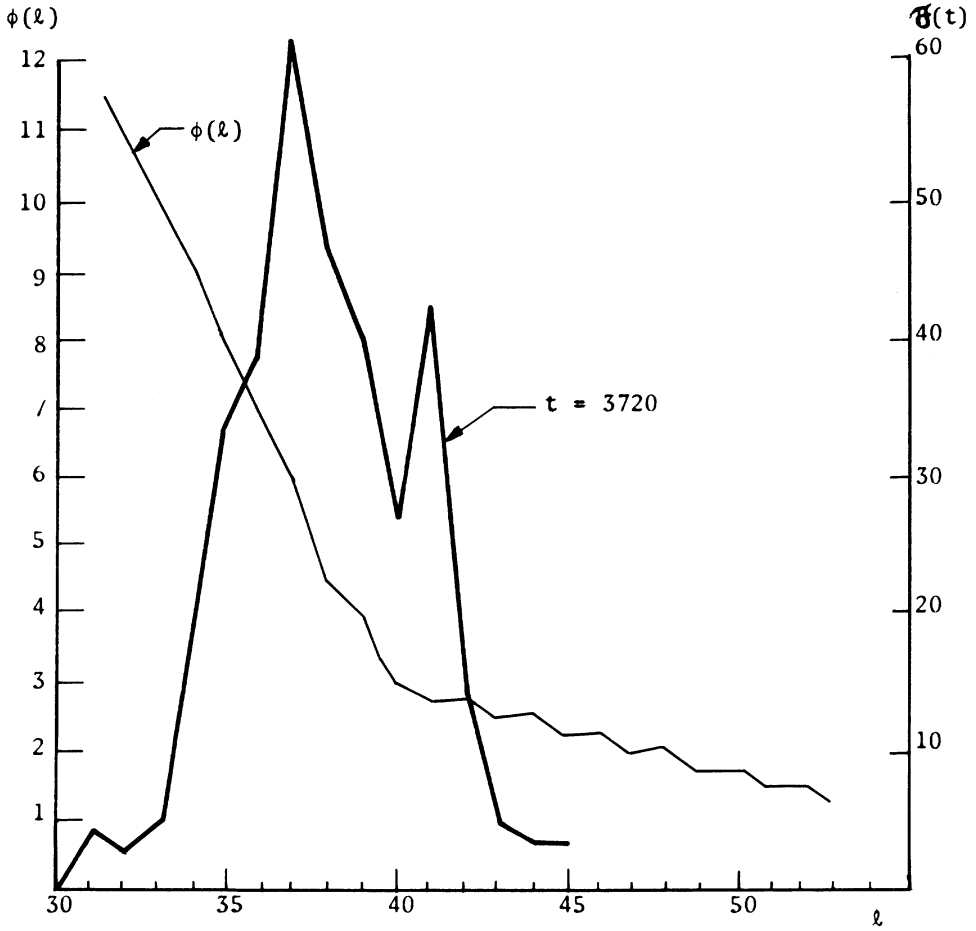

Over a complete "on-off" cycle, then, ℓ would vary from ℓ_0 to $\ell_0 - 8.92 + 6.35 = \ell_0 - 2.57$. Thus, neurons of Σ_0 (and those controlled by Σ_0) will tend to accumulate larger and large fatigue values.[1]

(1) is more subtle. However, the basic problem appeared to be $\mathcal{F}(t)$ not reaching its stationary form by the time (t = 401) the periodic stimulation was begun. Thus, the "drift" in $\hat{\ell}$ toward ℓ_1.

One final factor greatly aggravated the effects of (2). As noted previously $\Delta_1(\ell)$ and $\Delta_2(\ell)$ vary with ℓ, although $\Delta_1(\ell)/(\Delta_1(\ell) + \Delta_2(\ell)) =$ constant for all ℓ. It was hoped that by this mechanism, an hysteresis could be introduced in $\phi(\ell)$. Unfortunately (aside from making the analysis more difficult), this tended all the more to allow large groups of neurons to obtain high fatigue values ($\phi(\ell)$ large), since as ℓ decreases, $\Delta_2(\ell)$ and $\Delta_1(\ell)$ <u>increase</u>.

Figures 7.18 - 7.22 show a sample of the sequence of distributions of $\mathcal{F}(t)$ from the experiment of the preceding section. The bimodality of $\mathcal{F}(t)$ is apparent, and towards the end of the experiment (as more neurons become fatigued) becomes more pronounced. It is evident from these figures that progressively more and more neurons are being forced into higher fatigue values $\phi(\ell)$. A control experiment was performed with the stimulus suppressed from t = 2001 to t = 2800 using the network of the cell-assembly experiment at t = 2000. A sample of the fatigue distribution for this experiment is given in Figure 7.23. A study of this figure reveals that the highly fatigued neurons tended to recover to the (apparent) $\hat{\ell}$ at $\ell = 40$. The few neurons remaining in the lower fatigue states

---

[1] This is a case of experimenter error, pure and simple. Notice, however, that the $\Delta_1(\ell)$'s and $\Delta_2(\ell)$'s actually vary with ℓ, so this effect could become more or less pronounced as ℓ varies. It was hoped that in this way the Δ_τ's would tend to cancel out.

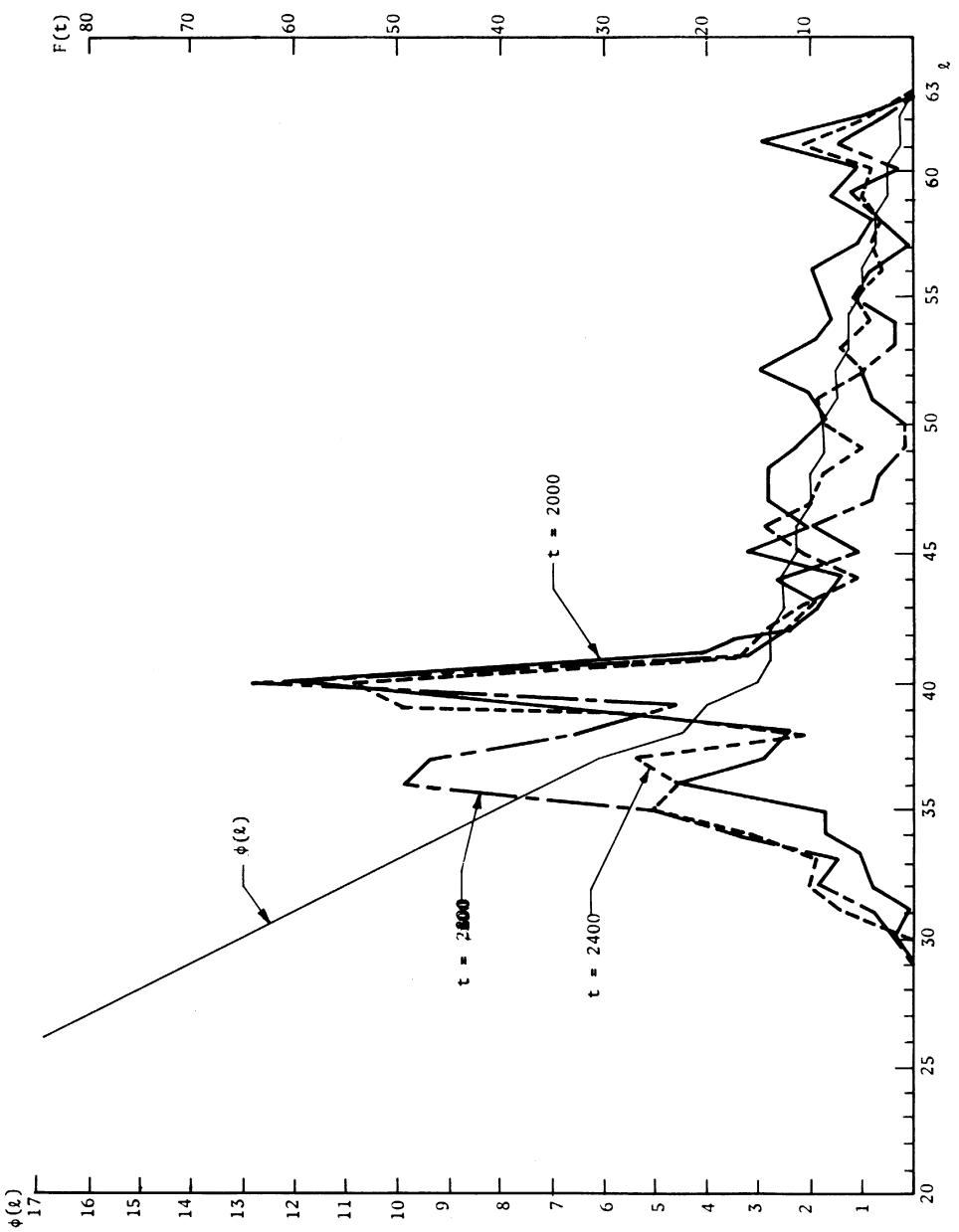

Figure 7.23. Sample of Fatigue Distributions for First Control Experiment.

The network of the cell-assembly experiment at t = 2000 was run from t = 2001 to t = 2800. The fatigue distributions $\mathcal{F}(t)$ are given for t = 2000 (from the cell-assembly experiment), t = 2400, and t = 2800. Notice that the two peaks at ℓ = 40 and ℓ = 35 seem to be closing in on an intermediate $\hat{\ell}$. Thus, while some neurons are recovering, some neurons still are seeking a lower value of $\hat{\ell}$. Recall from the discussion of the text that the network is slightly underdampled — a stable value of $\hat{\ell}$ has not yet been obtained.

($\phi(\ell)$ large) were found to correspond to neurons of Σ_0 and the successor-sets of Σ_0. The behavior F(t) for this experiment appeared stable, i.e., no violent fluctuations, although E(F(t)) exceeded the theoretical value $F_b = N/\hat{r}_q = 400/17 = 23.5$, thus revealing another contributing factor to the drift in ℓ; the behavior of the network appears to be slightly underdamped.

At this point the reader is reminded that a slight underdamping had been noticed in the initial steady-state phase of the experiment (see Section 7.5.1). However, it was reasoned there that this should only continue to the point that $\mathcal{F}(t)$ had stablized about a $\hat{\ell}$ Regrettably, the stimulus was turned on before this had occurred, superimposing an additional drift on $\hat{\ell}$ to that caused by the mismatch in the lengths of the "on" and "off" periods of the stimulus. Presumably, had the control experiment been continued, the behavior eventually would have been damped so that $E(F(t)) = F_b$ as $\hat{\ell}$ finally converged to a stable value.

At this point, it was decided to eliminate the hysteresis feature (Δ_1 and Δ_2 being functions of the fatigue state ℓ) from the fatigue mechanism. The immediate reason for this is that a detailed study of the $\mathcal{F}(t)$ from the cell-assembly experiment and various control experiments revealed that groups of neurons with the same fatigue-level would recover (from higher values of $\phi(\ell)$) abruptly to lower fatigue values $\phi(\ell)$, thus forming a hyperrecovered pool of neurons in $\mathcal{M}$ (with all the attendant dangers). This occurred around $\ell = 36$, a region of abrupt change in $\phi(\ell)$ as well as $\Delta_1(\ell)$ and $\Delta_2(\ell)$. Thus, a significant distortion was introduced into the long run behavior of $\mathcal{M}$.

To test this, the first control experiment above was repeated from

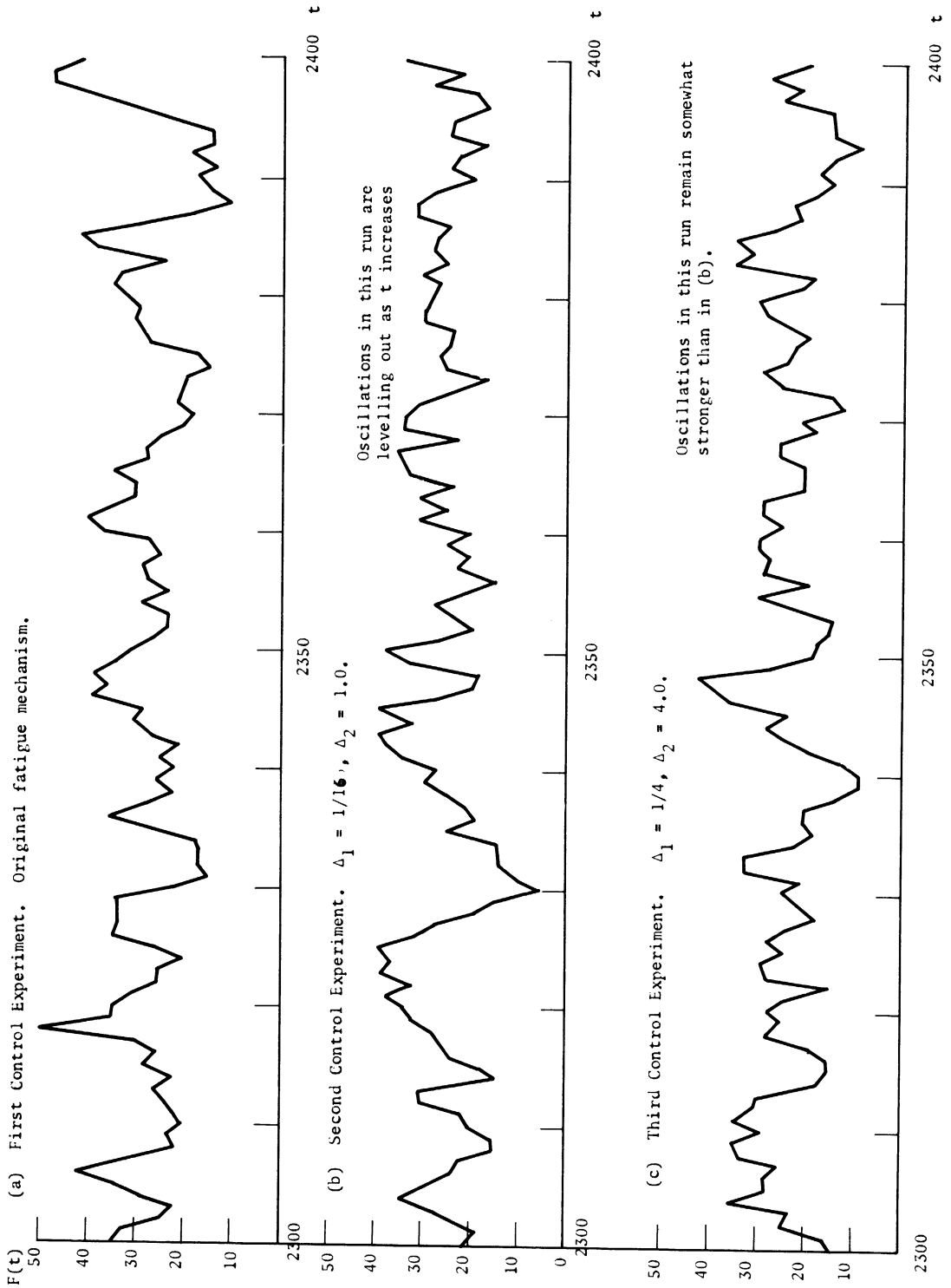

Figure 7.24. EEG's for First, Second, and Third Control Experiments.

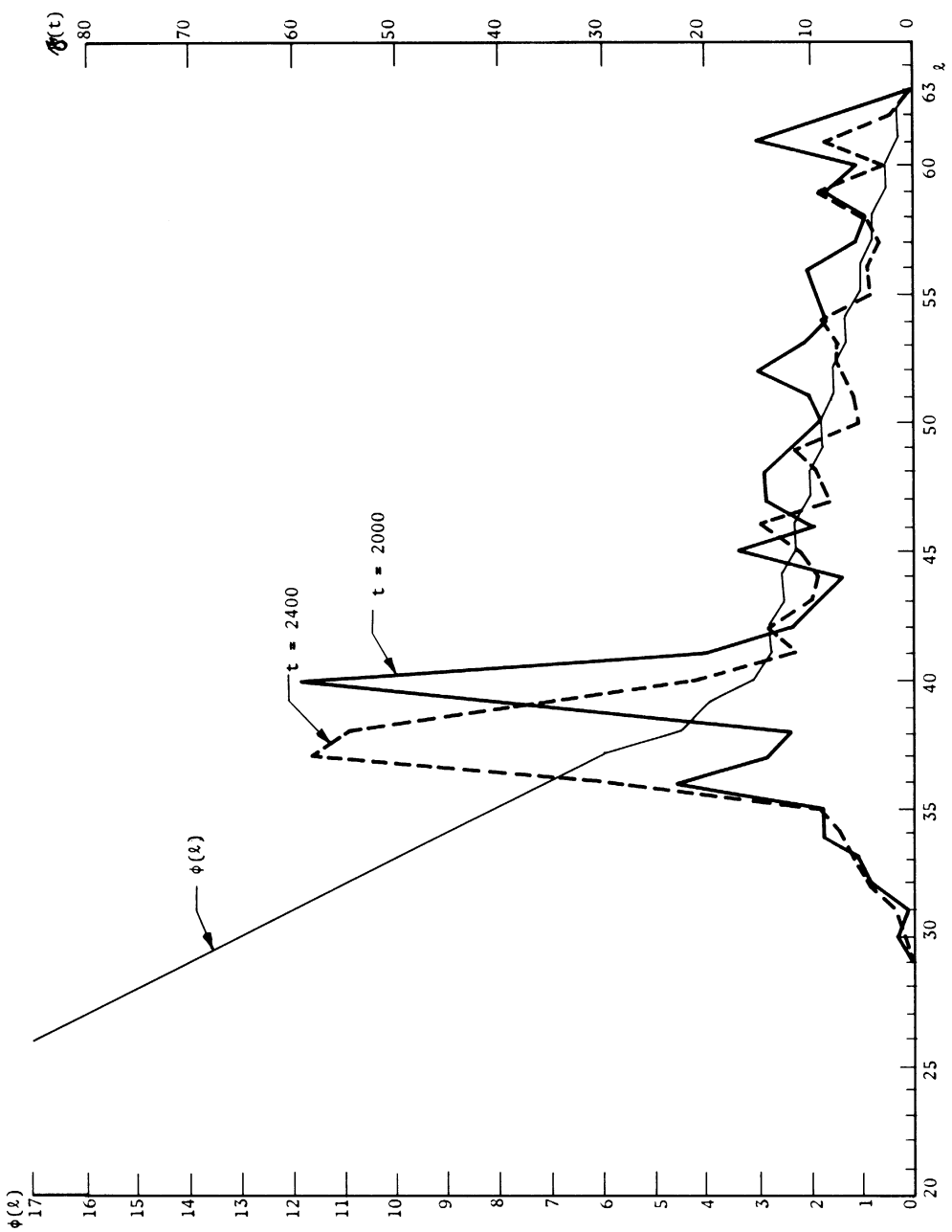

Figure 7.25. $\mathcal{F}(t)$'s for Second and Third Control Experiments (Section 7.5.3).

(a) Second Control Experiment.
This fatigue distributions $\mathcal{F}(t)$ at t = 2000 (from the cell-assembly experiment) and at t = 2400 are given below. The second control experiment was a modification of the first in which $\Delta_1 = 1/16$, $\Delta_2 = 1.0$. Interpretation: same as Fig. 7.18, q.v..

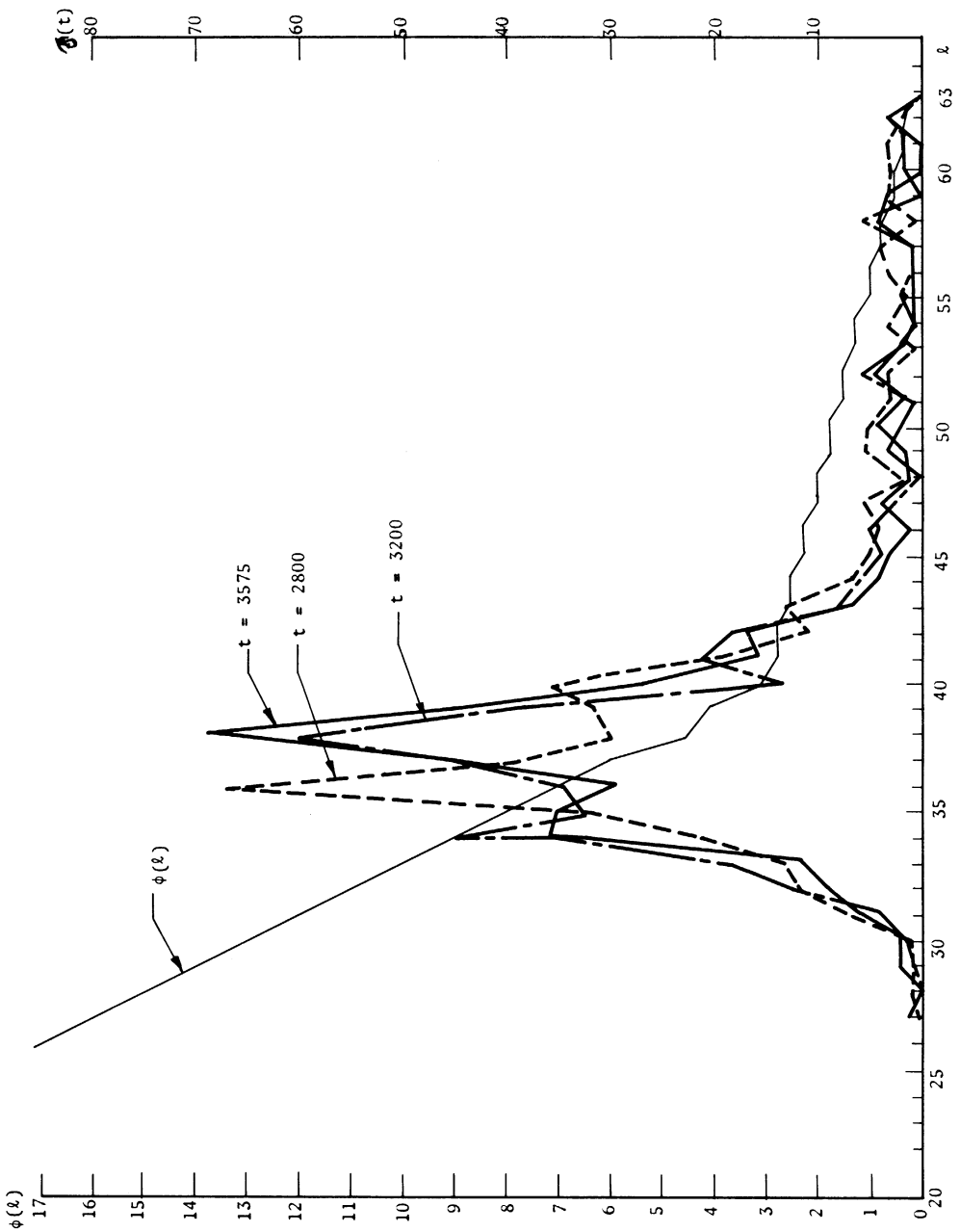

Figure 7.25 (continued).

(b) $\mathcal{F}(t)$'s for Third Control Experiment.
This experiment was identical to the second control run, except now $\Delta_1 = 1/4$, $\Delta_2 = 4$. The $\mathcal{F}(t)$'s are given for t = 2800, 3200, and 3575. $\mathcal{F}(t)$ appears to be stabilizing about $\ell = 36$.

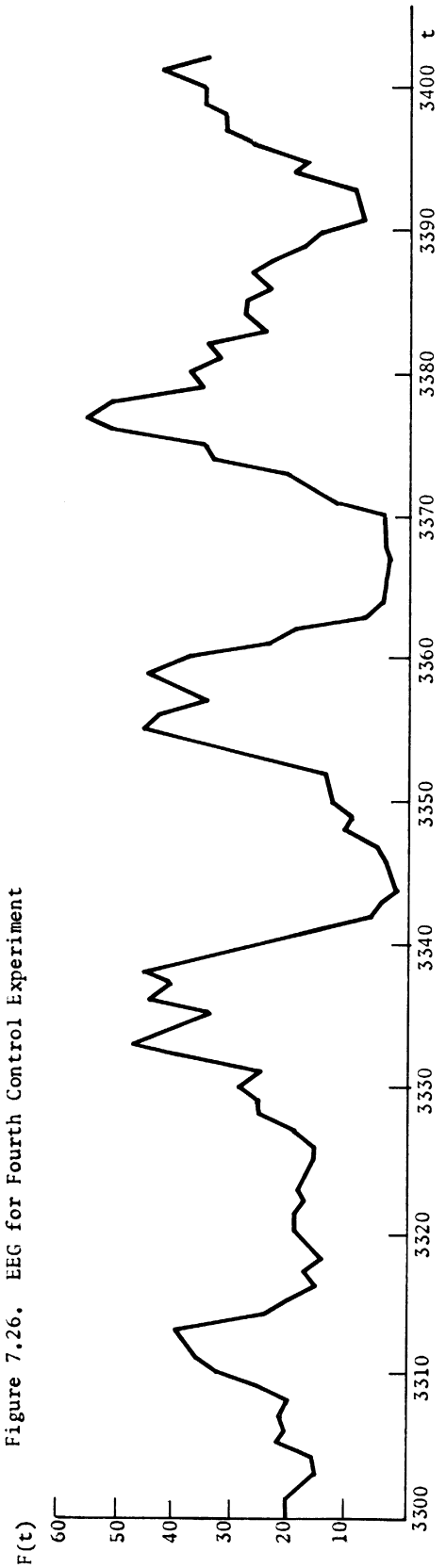

Figure 7.26. EEG for Fourth Control Experiment

t = 2001 to t = 2400 with $\Delta_1(\ell) \equiv \Delta_1 = 1/16$, $\Delta_2(\ell) \equiv \Delta_2 = 1.0$. The EEG's for the two experiments are given for t = 2301 - 2400 in Figure 7.24 (a) and (b), $\mathcal{J}(t)$ at t = 2000 and t = 2400 for the second control experiment is given in Figure 7.25 (a). The second control experiment was repeated using larger values of Δ_1 and Δ_2: $\Delta_1 = 4/16$, $\Delta_2 = 4.0$. As is to be expected, such large changes in tended to produce very uneven behavior, F(t) tended to oscillate more violently than in the second control run above. The EEG for t = 2301 - 2400 and F(t) for selected time steps for this control experiment are given in Figures 7.24 (c) and 7.25(b) respectively.

An interesting contrast to the second control experiment above was obtained by continuing the cell-assembly experiment from t = 2901 on without stimulus and with $\Delta_1 = 1.0$, $\Delta_2 = 1/16$. The behavior, up to t = 3400, as shown in Figure 7.26, was considerably less stable than in the earlier control run with F(t) going to zero at t = 3509, the stimulus being turned back on at t = 3401 until t = 3500. $\mathcal{J}(t)$'s for this run are given in Figure 7.27. Analysis of this run suggested that a sufficient number of neurons did not recover in time to sustain the steady-state behavior, bearing in mind the fact that an excessive number of neurons were highly fatigued at t = 2900 in the original experiment.

At this juncture, the harsh reality of a nearly-exhausted budget raised its ugly head. There simply were not sufficient funds to allow a complete rerun of the run-in and cell-assembly experiments of Sections 7.5.1 and 7.5.2 above. The positive reuslts of Section 7.5.2 seemed genuine, the difficulty arising from the combined effects (1) and (2) mentioned earlier and of a transient (though fatal, in this case) nature.

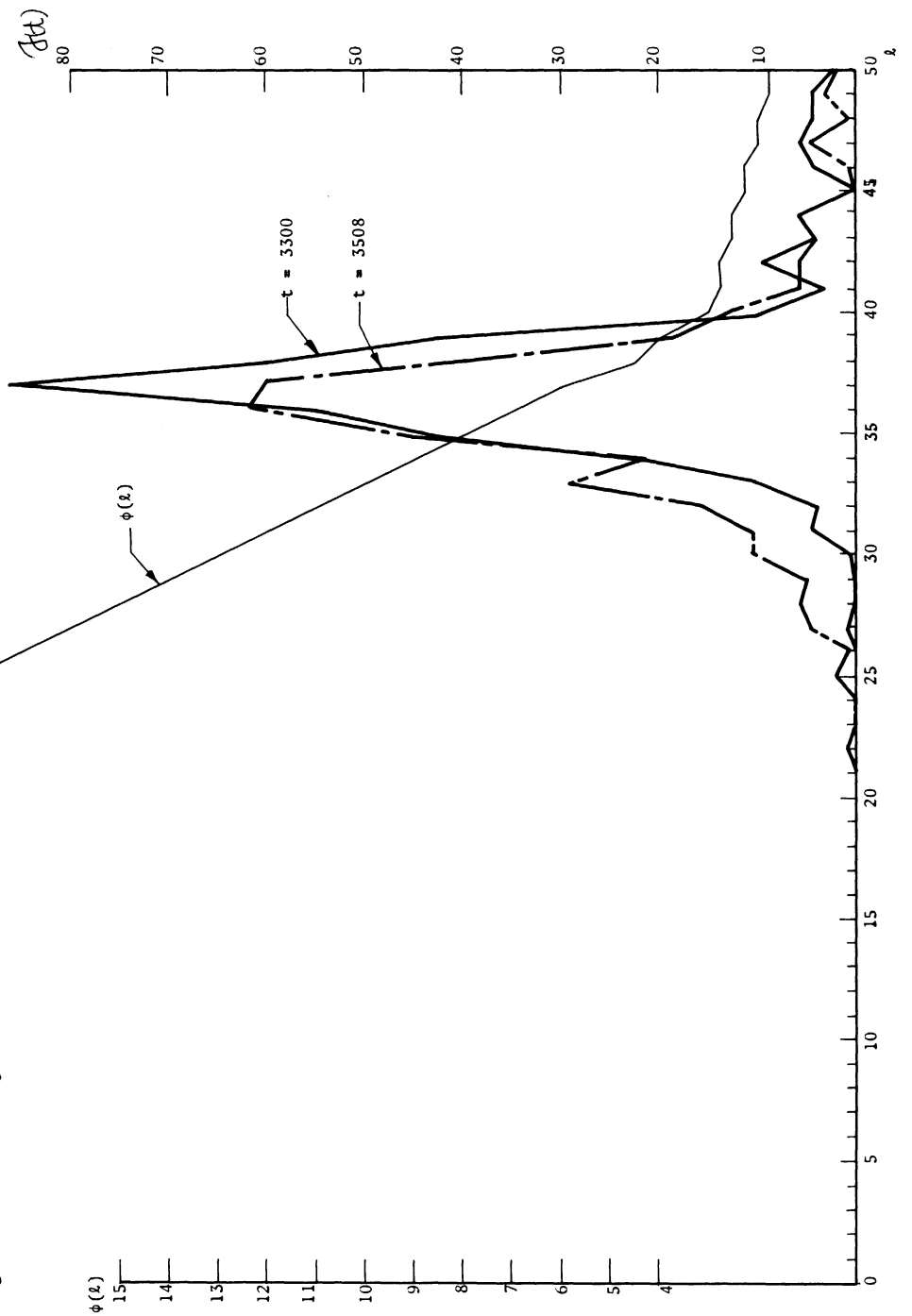

Figure 7.27. $\mathcal{F}(t)$'s for Fourth Control Experiment.

$\mathcal{F}(t)$ is given for t = 3300 and t = 3508 of this run. $\mathcal{F}(t)$ went to zero at t = 3509. Notice that the neurons of $\mathcal{M}$ appear to be clustered around ℓ = 36 at t = 3508, some neurons still at lower values of ℓ (hence higher values of $\phi(\ell)$). The effect of the stimulus (t = 3401 - 3500) was responsible for the peak at ℓ = 23. Since the $\Delta_1(\ell)$ and $\Delta_2(\ell)$ tables still contain the hysteresis of the cell-assembly experiment, there appear to be three factors operating here: (1) the trapping of too many neurons in lower fatigue states (larger $\phi(\ell)$) due to the stimulus; (2) the distortion in F(t) due to the hysteresis; and (3) the presence yet of a slight underdamping of F(t), resulting in neurons "hunting" for ℓ.

Therefore, the decision was made to attempt to salvage from the forth control experiment a network for the alternating periodic stimulus series. To this end, an artifact was introduced into V(r) in an attempt to encourage the more highly fatigued neurons of $\mathcal{N}$ to fire, without creating excessively violent fluctuations in F(t). This artifact consisted of allowing V(r) to take on negative values for $r \geq 21$. A control experiment was performed using such a V(r) (see Figure 7.28) continuing the fourth control run above from t = 3301 to t = 3400. The EEG is displayed in Figure 7.29 and $\mathcal{N}(t)$ at t = 3301 and 3400 in Figure 7.30. Notice that F(t) appears to be levelling out towards t = 3400 and that $\hat{\ell}$ seems to gradually be conveying to $\ell = 38$.

The results of the fifth control run fanned the sparks of hope that the alternating periodic stimulus experiment could be performed without further difficulties due to the fatigue mechanism. This last sequence of experiments will be described in the next section.

In conclusion, a simple cycle $C(\Sigma_0)$ formed in the cell-assembly experiment. Unfortunately, toward the end of the experiment, fatal oscillations in F(t) arose. These were correctable by adjusting an imbalance in the fatigue mechanism and the introduction of an artifact into V(r).

7.5.4 Alternating Periodic Stimuli Sequence

Σ_0^* was chosen as shown in Figure 7.31, Σ_0 as in Section 7.5.2. The network of the fifth control experiment of Section 7.5.3 at t = 3400 was used as the starting place fo this sequence. $\tau_0 = 7$ (as before), $\tau_0^* = 8$, $t_\ell = 100$ (as before), $t_\ell^* = 150$. For the first run, $\delta = 0$, giving the stimulus sequence I I^* I I^* ... , I the interval in which the stimulus to Σ_0 is "on", that to Σ_0^* "off", I^* the interval in which the stimulus to

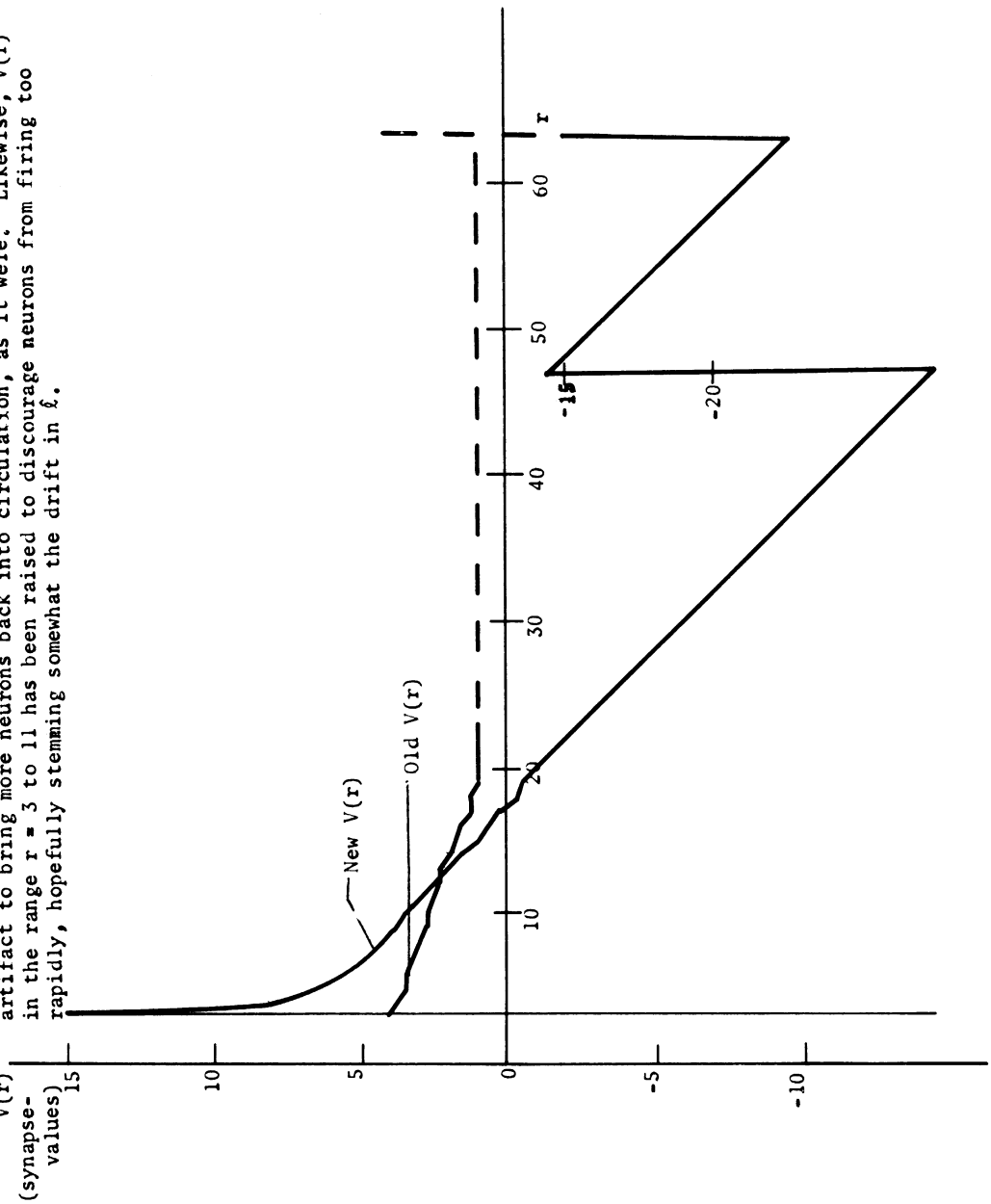

Figure 7.28. V(r) for Fifth Control Experiment.

The V(r) used in the cell-assembly experiment where it differs from the new V(r) with negative entries, is indicated by a dotted line. Notice that in the range r = 12 to 17, the new V(r) is less than the old. This was just another artifact to bring more neurons back into circulation, as it were. Likewise, V(r) in the range r = 3 to 11 has been raised to discourage neurons from firing too rapidly, hopefully stemming somewhat the drift in ℓ.

Figure 7.29. EEG for Fifth Control Experiment (V(r) with Negative Entries).

Initially, the behavior is highly oscillatory, but the negative feedback mechanism appears to level it out towards t = 3400. The large oscillations are most likely due to a slight initial excess of neurons made available by the artifact in V(r).

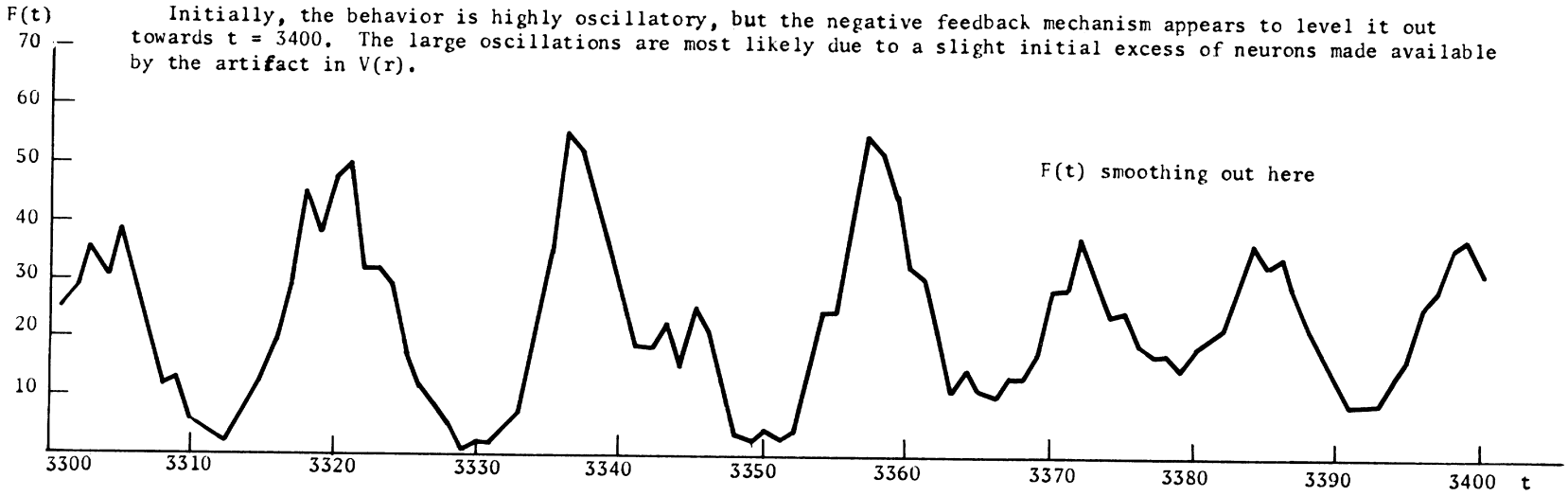

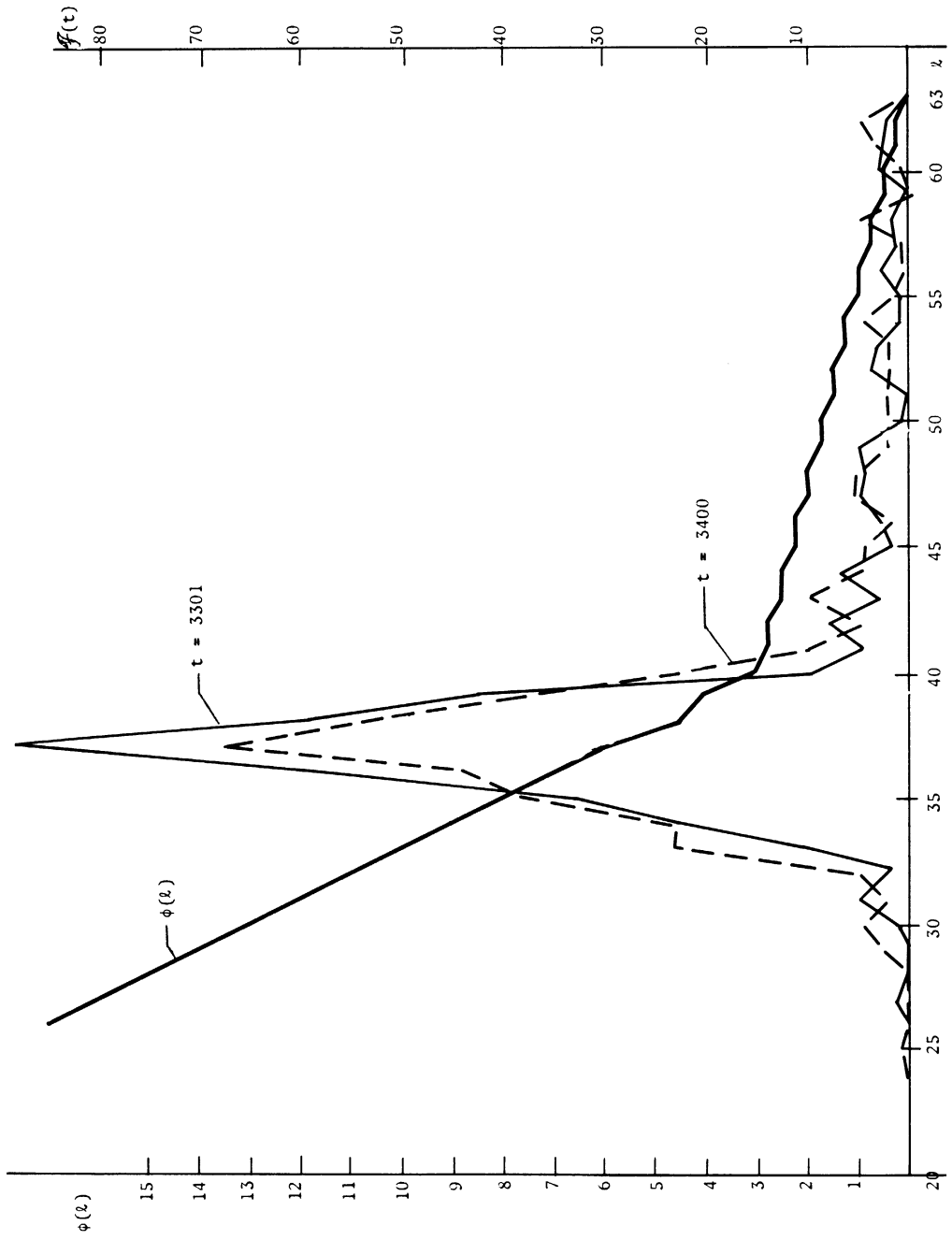

Figure 7.30. $\mathcal{F}(t)$'s for Fifth Control Experiment.
The fatigue distributions $\mathcal{F}(t)$ at t = 3301 and t = 4000 are given here. $\hat{\ell}$ seems to have settled around ℓ = 37, although $\mathcal{F}(t)$ has broadened out somewhat by t = 3400.

Σ_0^* is "on", that to Σ_0 "off". This network was run through t = 4000. The experiment was then continued from t = 4001 through t = 4350 with the sequence I^* I δ I^* I δ ... and δ = 50. δ was introduced to allow $\mathcal{M}$ to recover from the effects of stimulation of the two areas Σ_0 and Σ_0^* (see Chapter 4, Section 4.5.2).[1] The experiment was terminated at t = 4350 because funds for computer time were exhausted.

In spite of the somewhat premature termination of this run, some interesting results were observed. First of all, the cycle $C(\Sigma_0)$ seemed firmly established; the connections from $\Sigma_{\tau-1}$ to Σ_τ, τ = 1, 2, ..., $\tau_0 \equiv 0$ were all close to their maximal values, while the "back" connections, e.g. connections from Σ_0 to Σ_{τ_0-1} were moderate or inhibitory. Part of $C(\Sigma_0)$ is given in Figure 7.32 together with the synapse-values in the directions τ-1 to τ. Thus, the artifact in V(r) and the changes in $\Delta_1(\ell)$ and $\Delta_2(\ell)$ did not destroy $C(\Sigma_0)$.

Secondly, an embryonic cycle $C(\Sigma_0^*)$ appeared to be in the process of formation. Fragments of this cycle are shown in Figure 7.33.

Both of these results were expected. Given time, no doubt, $C(\Sigma_0^*)$ would have become as well formed as $C(\Sigma_0)$. The next result, however, seems to give great hope to future, deeper study of cell-assembly theory via computer simulation; (thirdly), connections between the cycle $C(\Sigma_0)$ and $C(\Sigma_0^*)$ (not yet a cycle) tended toward negative (inhibitory) values. That is, cross-inhibition — as predicted by the theory — appeared to be evolving between $C(\Sigma_0)$ and $C(\Sigma_0^*)$. This is illustrated in Figure 7.34.

---

[1] In fact, a control run, without stimulus, starting at t = 4001 was conducted. F(t) went to zero at t = 4126. A study of the $\mathcal{F}(t)$'s bore out the claims of Chapter 4, Section 4.5.2, about the necessity of the δ.

Figure 7.31. Σ_0 and Σ_0^* for Alternating Periodic Stimuli Sequence.

Notice that Σ_0 and Σ_0^* are disjoint and cannot affect each other directly (R = 6). Yet they are sufficiently close that the paths $P_E(\Sigma_0 \to \Sigma_\tau)$ and $P_E(\Sigma_0 \to \Sigma^*)$, hence eventually the cycles $C(\Sigma_0)$ and $C(\Sigma_0^*)$, should be "proximate" in the sense of Chapter 4.

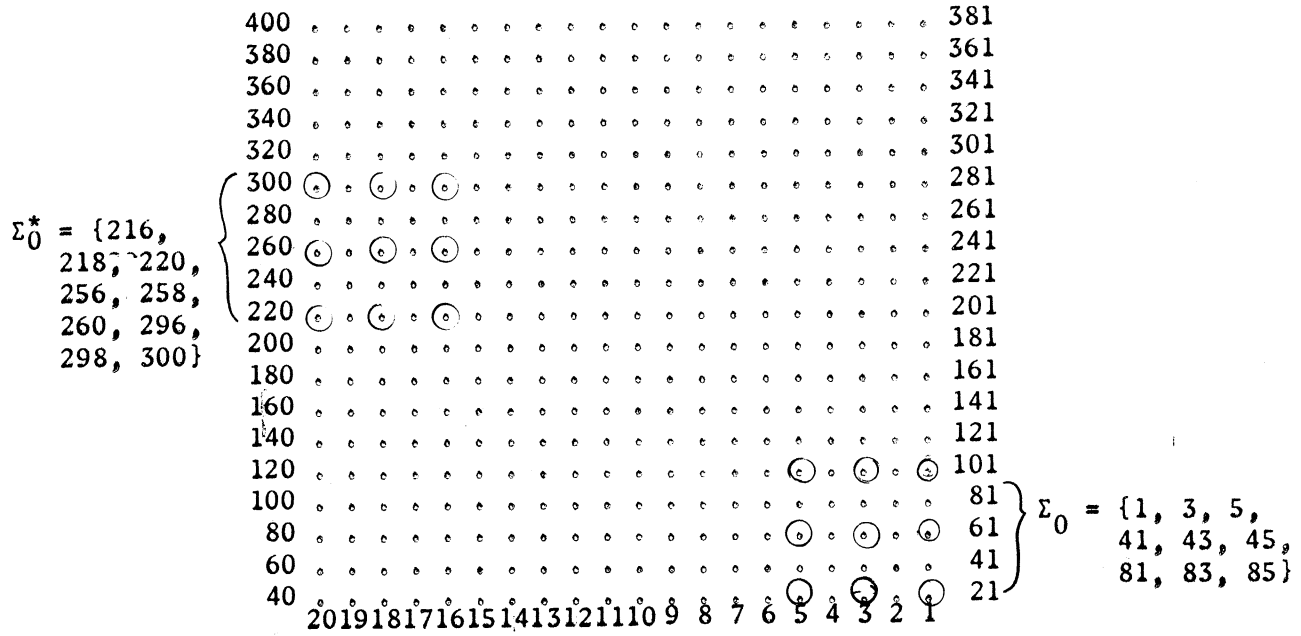

Figure 7.32. Part of $C(\Sigma_0)$ from the Alternating Periodic Stimuli Experiment.

Only two branches emanating from, and returning to, neuron $1 \in \Sigma_0$ are shown. These are respectively:

$\Sigma_0 \quad \Sigma_1 \quad \Sigma_2 \quad \Sigma_3 \quad \Sigma_4 \quad \Sigma_5 \quad \Sigma_6 \quad \Sigma_0$

$1 \to 63 \to 61 \to 56 \to 157 \to 73 \to 36 \to 1$ (light lines in diagram)

$1 \to 63 \to 62 \to 180 \to 155 \to 117 \to 36 \to 1$ (heavy lines)

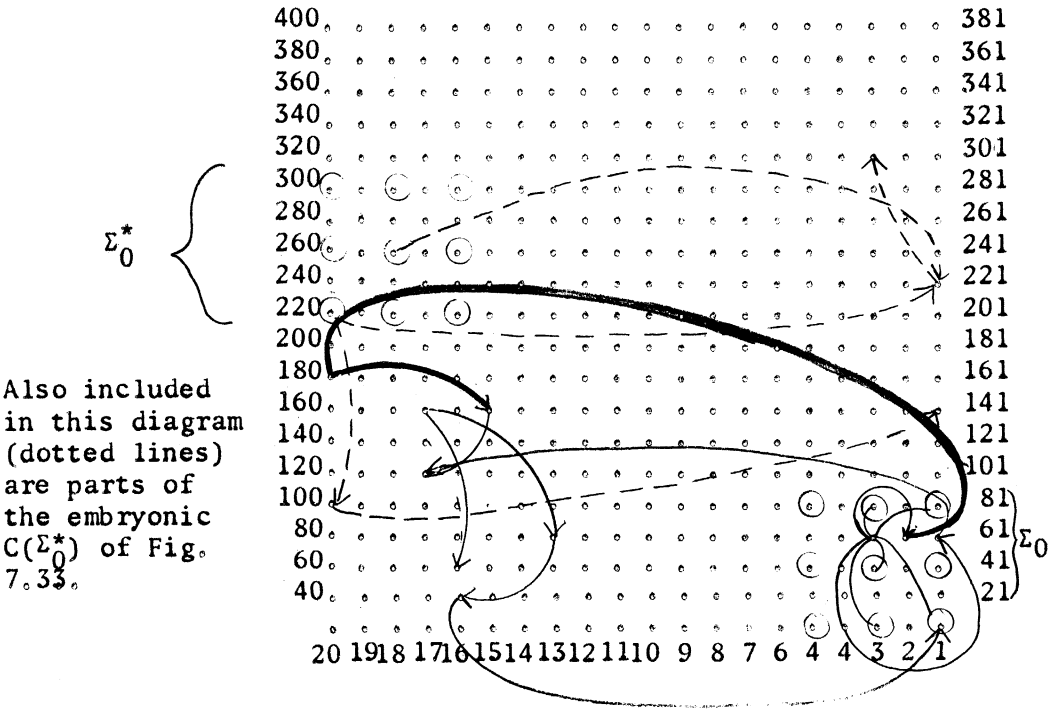

Also included in this diagram (dotted lines) are parts of the embryonic $C(\Sigma_0^*)$ of Fig. 7.33.

Some of the branching within these two branches has been omitted to make the diagram legible. The synapses Σ_τ to $\Sigma_{\tau+1}$ are all maximal (i.e. +8.0) except Σ_{-1} to Σ_0 which is +3.0 having increased from ≈ 0. The synapse-value from neuron $1 \in \Sigma_0$ to neuron $36 \in \Sigma_{-1}$ has decreased to $\approx$. This is typical of the "back" connections from Σ_τ to $\Sigma_{\tau-1}$.

Figure 7.33. Fragments of an Embryonic $C(\Sigma_0^*)$.

Several parts of what appear to be an evolving $C(\Sigma_0^*)$ are shown. (Overlapping neurons are not shown unless part of a path). Notice the fragment of a path from Σ_5^* to Σ_6^*. The synapse-levels from neurons of Σ_τ^* to $\Sigma_{\tau+1}^*$ are shown above the corresponding arrows. Parts of these paths are shown in Fig. 7.32 (dotted lines).

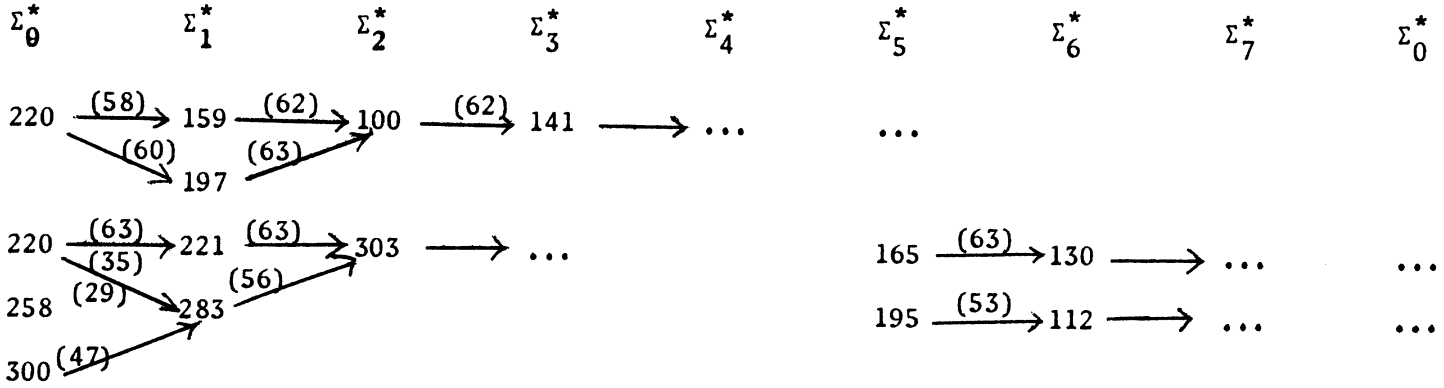

Figure 7.34. Development of Cross-Inhibiting Connections Between $C(\Sigma_0)$ and (the partial) $C(\Sigma_0^*)$.

The arrangement in this figure is the following. In (a), the neurons of $C(\Sigma_0^*)$ are arranged in order according to the successor Σ_t^* in which they fall. Opposite each receiving neuron of $C(\Sigma_0^*)$ is the neuron of $C(\Sigma_0)$ which transmits to it. The synapse-values of this connection at t = 4000 and t = 4350 are given at the right. Similarly for (b). Perusal of the changes in the synapse-values does not show a strong downward trend. Nonetheless, a slight trend is present and the connections tend to remain negative (inhibitory). Given the extremely short interval over which the experiment was performed, this is perhaps the best that could be obtained. Incidentally, recalling the discussion of Chapter 4, it is probably not desirable that all the interconnections to become negative, since some positive ones may assist the revival of one cell-assembly as the other becomes fatigued.

(a) Connections from $C(\Sigma_0)$ and $C(\Sigma_0^*)$.

Receiving Neurons of $C(\Sigma_0^*)$		Transmitting Neurons of $C(\Sigma_0)$	Synapse-Values t = 4000	t = 4350
Σ_0^*	220	180 ε Σ_3	-8.00	-7.75
		155 ε Σ_4	+3.25	+7.25
Σ_1^*	159	62 ε Σ_2	+0.50	+0.25
		144 ε Σ_1	-8.50	-8.50
		155 ε Σ_4	0.00	-0.75
		157 ε Σ_4	1.50	-2.25
Σ_2^*	100	36 ε Σ_6	-1.25	-1.00
		61 ε Σ_2	0.00	-0.25
		62 ε Σ_2	-0.50	-0.75
		155 ε Σ_4	-2.75	-3.00
		157 ε Σ_4	-0.75	-0.50
		180 ε Σ_3	-2.25	-0.75
		144 ε Σ_1	-2.25	-2.50
Σ_3^*	141	62 ε Σ_2	-0.25	-0.75
		157 ε Σ_4	+0.50	+0.75
		117 ε Σ_5	0.00	0.00

Figure 7.34 (continued)

(b) Connections from $C(\Sigma_0^*)$ to $C(\Sigma_0)$.

Receiving Neurons of $C(\Sigma_0)$		Transmitting Neurons of $C(\Sigma_0^*)$	Synapse-Values t = 4000	t = 4350
Σ_0		... None ...		
Σ_1	63	159 ε Σ_1^*	+1.75	+1.00
	63	100 ε Σ_2^*	-0.25	-0.25
	63	141 ε Σ_3^*	-3.00	-2.50
	144	100 ε Σ_2^*	+1.25	+1.75
	144	159 ε Σ_1^*	+0.25	-0.25
	144	220 ε Σ_0	-0.50	-0.75
Σ_2	61	100 ε Σ_2^*	+0.50	+0.00
	62	141 ε Σ_3^*	-3.00	-2.75
	62	159 ε Σ_1^*	+0.50	+0.75
Σ_3	56	159 ε Σ_1^*	-2.25	-2.00
	180	197 ε Σ_1^*	0.00	+0.25
Σ_4	157	100 ε Σ_2^*	-2.00	-2.25
		159 ε Σ_1^*	-1.25	-1.25
		197 ε Σ_1^*	-1.50	0.00
Σ_5	117	141 ε Σ_3^*	-2.25	-1.50
	117	197 ε Σ_3^*	-1.00	-1.00
Σ_6	36	100 ε Σ_2^*	-0.75	-1.25

7.5.5 Conclusions

A structural characterization of the formation and development of cell-assemblies has been given in terms of the model. Behind this formation is the synapse-level change law, expressed in the model in terms of the probabilities $U(\lambda)$ and $D(\lambda)$ and the balancing equation relating these quantities and F_b:

$$\frac{D(\lambda)}{U(\lambda) + D(\lambda)} = \frac{F_b}{N} = f_b = \frac{1}{\hat{r}_q} .$$

The experiments bear out the fact that Hebb's law (as expressed in the model) solely is responsible for the structural changes giving rise to the cycles $C(\Sigma_0)$ and $C(\Sigma_0^*)$ and to the trend toward cross-inhibition between $C(\Sigma_0)$ and $C(\Sigma_0^*)$. No other mechanism of the model can account for these empirically observed phenomena.

By no means does the author claim that all has been done as originally planned or hoped. Many things remain. For example, development of a threshold curve-fatigue curve calculus analogous to that of Chapter 4 for $V(r)$, improving the Boolean relations of Chapter 4 to yield more readily estimates of P_k^*, a study of dynamic relationships between cycles $C(\Sigma_0)$ and $C(\Sigma_0^*)$, etc. However, the following have been done:

(1) a basic stability calculus relating N, ρ, and $V(r)$ was developed and tested empirically (Chapters 4 and 6);

(2) this calculus was modified to include the presence of negative (inhibitory) connections (Chapters 4 and 6);

(3) closed cycles $C(\Sigma_0)$ were formed (Chapter 7);

(4) partial formation of a possible cross-inhibitory pair of cell-assemblies $C(\Sigma_0)$ and $C(\Sigma_0^*)$ was effected (Chapter 7).

It is hoped that these will form the basis of more extensive work in the future involving much larger and more complex networks using the more versatile computers emerging today.

APPENDIX: A NOTE ON THE GENERATION OF CONNECTION SCHEMES

1. Random Number Generation

In the approximation to the urmodel (Chapter 4, Section 4.2.1), a number n is drawn at random from the unit interval. To effect this in the model, a pseudo-random number generation is used. The qualifier "pseudo" suggests that, in fact, the output of the generator is not truly random. However, the validity of all the arguments in Chapter 4 concerning the number of connections received by a neuron $i \in \mathcal{N}$ from subset $M \subset \mathcal{N}$ stems back to the uniform randomness generated by the connection assignment schemes of Section 4.2.1. Consequently, some evidence will be advanced in the next section to show that the generator used in this study was adequate, the effects of non-randomness being essentially negligible.

To the best of the author's knowledge, all contemporary random number generators used on digital computers are defective in some sense or another:

(a) some produce all zeros after a certain number of samplings (e.g., the "mid-square" method, see Greenberger [8], reference 9);

(b) some cycle after a large number of samplings (e.g., the power residue method);

(c) some leave gaps or sets over which no sample points can ever occur (e.g., some forms of the power residue method, again see Greenberger [8]);

(d) there may be correlations of different orders among successive samples of a sampling sequence; etc.

The generator used in this study is definitely defective in the sense of (b), though apparently not in the sense of (c). It is of the form

$$\mathcal{G} : n_{i+1} \equiv (n_i m) \text{ modulo } 2^{35}, \quad i = 1, 2, 3, \ldots$$

where $m = 5^{15}$ and n_i is the i-th number sampled.

Clearly, this generator is not random at all; however, it has a large period and the modulo 2^{35} reduction scrambles the digits of n_i somewhat in the fashion of the spin of a roulette wheel — a type of "random" shift is obtained. Although, as observed by Greenberger [8], there exist examples of this general type of generator having defect (c), it appears that this specific one is free of it (Crichton [3]). Moreover, this $\mathcal{G}$, like Greenberger's example, has the enormous advantage of being implented by a very short and rapid subroutine on the IBM 7090.

In any case — in agreement with Greenberger — the guiding principle in favor of selecting the generator $\mathcal{G}$ is:

(1) the period of $\mathcal{G}$ is essentially infinite;

(2) it appears reasonably free of defects like (c);

(3) it requires little computer storage and is fast;

(4) it appears to fulfill the requirements of the problem at hand.

The next section will be devoted to showing the validity of (4) for this study. Consequently, the $\mathcal{G}$ above is adequate.

There exists a relatively substantial volume of literature on random-number generation, including some that specify very sophisticated tests for measuring the degree of randomness of any particular generator. No one test, however, appears to be sufficient and one is forced to rely on criteria such as (4) above to judge the merit of any one particular generator.

2. Tests of Distributions

As mentioned in the preceding section, the specific generator used in this study was

$\mathcal{J}$: $n_{i+1} \equiv (n_i \cdot 5^{15})$ modulo 2^{35}, $i = 1, 2, 3, \ldots$.

For a given n_1, an entire sequence $\mathcal{S} = \{n_i\}_{i=1}^{\infty}$ is determined. n_1 is called the random starter of the sequence $\mathcal{S}$. For different choices of n_1 (relatively prime to 5^{15}), different sequences $\mathcal{S}$ result, hence different connection schemes for $\mathcal{N}$ (given fixed $N = \mathcal{R}$, ρ). This is all right, provided these different schemes possess the same statistics. Here "the same statistics" was taken to mean that the distributions pass the χ^2-test (of a sampled population against a theoretical population with known mean) for reasonable levels of significance.

Let N_K be the expected number of neurons of $\mathcal{N}$ receving exactly K connections (from $\mathcal{N}$). Then, for fixed ρ,

$$N_K = p_K N, \quad K = 0, 1, 2, \ldots ,$$

where p_K is the probability that a neuron of $\mathcal{N}$ receive exactly K connections from $\mathcal{N}$:

$$p_K = e^{-\rho} \frac{\rho^K}{K!}, \quad K = 0, 1, 2, \ldots .$$

For the given ρ, N, let a connection-scheme be generated by $\mathcal{J}$ and the algorithm (Figure 4.3) of Chapter 4. Let N_K^* be the actual count of neurons of $\mathcal{N}$ receiving exactly K connections from $\mathcal{N}$. The χ^2-test will be applied now to the theoretical distribution $\{N_K\}_{K=0}^{\infty}$ and the actual, $\{N_K^*\}_{K=0}^{K_{max}}$. The sample size is N, the sample mean ρ^* is given by

$$\rho^* = \frac{1}{N} \sum_{k=1}^{K_{max}} K N_K^* ,$$

and the population mean by

$$\frac{1}{N} \sum_{K=0}^{\infty} K\, N_K = \frac{1}{N} \sum_{k=0}^{\infty} K p_K N$$

$$= \sum_{K=0}^{\infty} K p_K$$

$$= \sum_{K=0}^{\infty} K \frac{\rho^K}{K!} e^{-\rho}$$

$$= \rho \sum_{K=0}^{\infty} \frac{K-1}{(K-1)} e^{-\rho}$$

$$= \rho,$$

as it should.

The results of some typical calculations are given in Tables 1 and 2 below (uniform random distribution case). In these tables, N_r^* represents the actual count in the r-th class interval, $p_r(\rho)$, the theoretical frequency that the random variable lie in that interval.

It is clearly a trivial modification of the above reasoning to test the distribution of connections received by a neuron of $\mathfrak{N}$ from some subset $A \subseteq \mathfrak{N}$ (uniform random case only): merely replace ρ by

$$\lambda = \frac{\rho \overline{\overline{A}}}{N}$$

and proceed as before. Typical results of such a calculation are given in Table 3.

There only remains the inherently less tractable case of distance-bias distributions. Here again, the same basic tests of Tables 1 and 2 apply with appropriate modifications, the test of Table 3 being considerably more difficult. For all practical purposes, however, it is sufficient to test the distribution of connections within a desk C_R. This was done by the usual "Petri plate" technique of imposing a cellular grid over $\mathfrak{N}$, sufficiently fine, then counting the number, N_K^*, of cells, in the neighborhood of a fixed neuron, that transmit exactly K connections to the neuron, then comparing this number with the theoretical N_K by means of the χ^2-test. An example of this procedure is shown in Figure 1 and Table 4 below.

A glance at these tables shows that the hypothesis: "the actual distributions are approximately Poisson (with the respective means)" is acceptable at a level of significance usually in the 70-90% range. Considering the

relatively crude generator used, this is quite acceptable.

Figure 1. "Petri-Plate" Sample of Connections in a Neighborhood C_R.

The network of Figure 6.28 (Experiment 9) was used: N = 400, ρ = 55, R = 6, $\overline{\overline{C}}_R \cong \pi R^2 \cong 113$. A typical neighborhood is shown with the neurons transmitting to the receiving neuron (at the center) encircled. The grid used to count the N_K^*'s is shown.

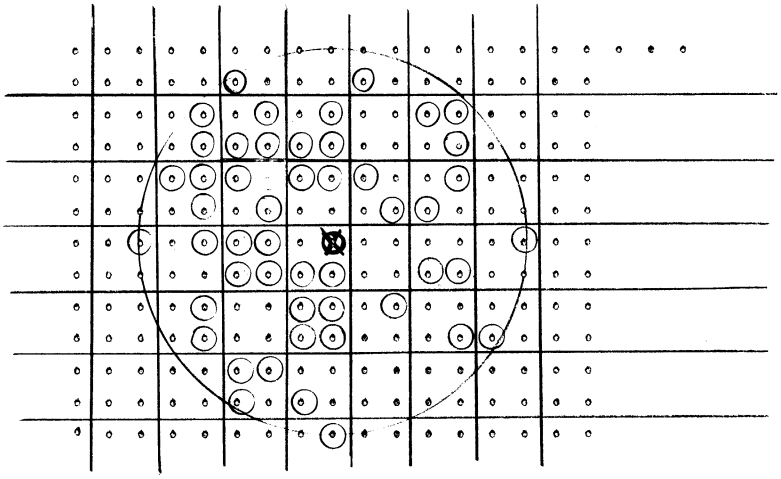

Table 1. χ^2-Test Applied to a Network (Uniform Random Case).

N_r, N_r^*, $p_r(\rho)$ are as defined in the text. N = 400, ρ = 6, $u_r = N_r^* - N_r$. The values of χ^2 were obtained from standard tables.[1]

K	r	N_r^*	N_r	u_r	u_r^2/N_2
0,1,2	1	30	24.3	5.7	1.345
3	2	38	34.9	3.1	0.275
4	3	52	52.5	-0.5	0.005
5	4	67	63.0	4.0	0.254
6	5	60	63.0	-3.0	0.143
7	6	54	54.0	0.0	0
8	7	35	40.5	-5.5	0.746
9	8	18	26.9	-8.9	2.940
10	9	21	16.2	4.8	1.420
11	10	17	16.1	0.9	0.051

m = 9 (degrees of freedom) $\qquad \chi^2 = \dfrac{u_r^2}{N_2} = 7.179$

This satisfies the χ^2-criterion at the 70% level (nine degrees of freedom).

[1] See, for example, Burington, R. S., and May, D. C., Handbook of Probability and Statistics with Tables, Handbook Publishers, Inc., Sandusky, Ohio, Table XIV.

Table 2. χ^2-Test Applied to a Network (Uniform Random Case).

The same network was used as in Table 1, except that a different random starter n_1 was used. This was one of the worst cases sampled, the error perhaps stemming from the counts N_r^* which were made by hand.

K	r	N_r^*	N_r	u_r	u_r^2/N_r
0,1,2	1	13	6.8	6.2	5.650
3	2	18	17.5	0.5	0.014
4	3	29	34.9	-5.9	0.996
5	4	60	52.5	7.5	1.070
6	5	60	63.0	-3.0	0.143
7	6	72	63.0	9.0	1.280
8	7	51	54.0	-3.0	0.166
9	8	35	45.0	-5.5	0.751
10	9	19	26.9	-7.9	2.310
11	10	17	16.2	0.8	0.039
12	11	18	16.1	1.9	0.224

m = 10 (degrees of freedom) χ^2 = 12.643

This satisfies the χ^2-criterion at the 20% level (ten degrees of freedom).

Table 3. X^2-Tests Applied to Subsets of $\mathfrak{N}$.

In the tables below, N_K^* is the count of neruons of $\mathfrak{N}$ receiving exactly K connections from $A \subseteq \mathfrak{N}$ with A = 20 for several values of ρ.

$\rho = 12, \lambda = 0.6$

	K	r	N_r^*	N_r	u_r	u_r^2/N_r	
	0	1	240	219.0	21.0	2.00	
	1	2	118	113.2	4.8	0.20	The χ^2-criterion is satisfied at the 30% level.
	2	3	32	39.5	-7.5	1.40	
≧	3	4	10	9.3	0.7	0.05	

m = 3 (degrees of freedom) χ^2 = 3.65

$\rho = 6, \lambda = 0.3$

	0	1	300	296.0	4	0.054	
	1	2	83	89.0	-6	0.320	The χ^2-criterion is satisfied at the 70% level.
≧	2	3	17	15.0	2	0.270	

m = 2 (degrees of freedom) χ^2 = 0.644

$\rho = 6, \lambda = 0.3$ (different n_1)

	0	1	314	296.0	18	1.09	
	1	2	70	89.0	-19	4.06	The χ^2-criterion is satisfied at the 5% level. The network used was the same as that of Table 2 above.
≧	2	3	16	15.0	1	0.07	

Table 4. χ^2-Test Applied to the C_R of Figure 1.

Let N_r^* be the number of squares falling in the r-th class interval, the corresponding theoretical N_r is given by $N_r = p_r(\lambda)N$, N = the number of squares, $p_r(\lambda)$ the theoretical frequence that the random variable lie in the r-th class interval. Here λ is given by $(\rho/\overline{C}_R)\cdot 4 = 2.0$.

	K	r	N_r^*	N_r	u_r	u_r^2/N_r
	0	1	4	3.8	0.2	.01
	1	2	6.3	7.6	-1.3	0.22
	2	3	5.5	7.6	-1.1	0.16
$\geq$	3	4	9.0	9.05	-0.05	0
	m = 3					$\chi^2 = 0.39$

This satisfies the χ^2-criterion (three degrees of freedom) at the 90% significance level.

BIBLIOGRAPHY

1. Burns, B. D., The Mammalian Cerebral Cortex, London, Edward Arnold Ltd. (1958).

2. Crichton, J. W., "The Principles of Living Beings: An Exploratory Essay," Doctoral Dissertation, The University of Michigan, Ann Arbor, Michigan, 1964.

3. _____, unpublished personal communication (1966).

4. _____, and Finley, Jr., M. R., "Programmed Simulation of Nerve Net" (letter to J. H. Holland) (1961).

5. _____, and Holland, J. H., "A New Method of Simulating the Central Nervous System Using an Automatic Computer," Technical Memorandum 2144-1195-M, The University of Michigan, March 1959.

6. Eccles, J. C., The Neurophysiological Basis of Mind, Oxford, Clarendon Press (1953).

7. Finley, Jr., M. R., "Experimental Study of Neural Networks by Means of a Digital Computer Simulation" in Research in Theory of Adaptive Systems, Interim Engineering Report, The University of Michigan, January 1965.

8. Greenberger, Martin, "Method in Randomness" in Communications of the Association for Computing Machinery, Vol. 8, No. 3, March 1966, pp. 177-179.

9. Hebb, D. O., The Organization of Behavior, New York, John Wiley and Sons, Inc. (1949).

10. Milner, P. M., "The Cell Assembly: Mark II" in Psych. Review, 64, 4 (1957), pp. 242-252.

11. Rochester, N., Holland, J. H., Haibt, L. H., and Duda, W. L., "Tests on a Cell-Assembly Theory of Action of the Brain Using a Large Digital Computer" in Transactions on Information Theory, IRE, IT-2, No. 2.

12. Sharpless, S. K., and Halpern, L. M., "The Electrical Excitability of Chronically Isolated Cortex Studied by Means of Permanently Implanted Electrodes" in Electroencelph. Clin. Neurophysiol., 14 (1962), pp. 244-255.

ERRATA

Page	Line	Correction
1	11	Delete the period after "behavior" and insert: "(but see page 4, paragraph 2)."
3	6 up	"assemply" should read "assembly"
5	9	"inter-cellular" should read "intra-cellular"
6	9 up	"dendritic branching" should read "few dendrites"
7	10	"unknow" should read "unknown"
9	4 & 5	Place to the right of equations: "(symmsetric form of Hebb's postulate)"
12	12	"assemply" should read "assembly"
20	11 up	"$\lambda_j i(t)$" should read "$\lambda_{ji}(t)$"
20	8 up	"change up" should read "increase"
20	7 up	"change down" should read "decrease in"
21	2	"models of Hebb's synapse-growth law." should read "models of a symmetric form of Hebb's synapse-growth law."
21	4	"connection m_{ji} ..." should read "connection, m_{ji} ..."
22	6 up	"product" should read "sum"
28	8 up	"change up of" should read "increase in"
28	6 up	"change down" should read "decrease"
33	7	"change" should read "increase"
33	8	"change down" should read "decrease"
43	9 up	"down" should read "up"

ERRATA (Concluded)

Page	Line	Correction
47	6	"intervenining" should read "intervening"
48	2	"stable-steady-stable" should read "stable-steady-state"
60	14	"[d]" should read "ρ[d]"
66	8	"in ." should read "in $\mathcal{M}$."
68	4 up	"fata:" should read "fatal"
69	5 up	"at, now" should read "at t and"
71	8 up	Insert | before "$r = 0, 1, \ldots, r_q\}$"
95	3	"surpress" should read "suppress"
99	5 up	"Eudidean" should read "Euclidean"
104	2	"Eudidean" should read "Euclidean"
125	4	"tranma" should read "trauma"
263	3 up	"reuslts" should read "results"
265	1	"forth" should read "fourth"